The Pennsylvania State University

The Graduate School

Eberly College of Science

# PHOSPHOPROTEOMIC ANALYSIS OF RIBOSOMAL PROTEINS: IMPLICATIONS IN TRANSLATION AND APOPTOSIS

A Dissertation in

Biochemistry, Microbiology, and Molecular Biology

by

Jennifer Lynn Miller



Submitted in Partial Fulfillment
of the Requirements
for the Degree of

Doctor of Philosophy

May 2009

The dissertation of Jennifer Lynn Miller was reviewed and approved* by the following:

Emine C. Koc
Assistant Professor Biochemistry and Molecular Biology
Dissertation Advisor
Chair of Committee

Robert A. Schlegel
Professor of Biochemistry and Molecular Biology

Wendy Hanna-Rose
Assistant Professor Biochemistry and Molecular Biology

Ming Tien
Professor of Biochemistry

Erin D. Sheets
Assistant Professor of Chemistry

Richard J. Frisque
Professor of Molecular Virology
Head of the Department of Biochemistry and Molecular Biology

*Signatures are on file in the Graduate School.

## ABSTRACT

Mammalian mitochondrial ribosomes synthesize thirteen proteins that are essential for oxidative phosphorylation. Besides having a major role in ATP synthesis, mitochondria also contribute to biochemical processes coordinating apoptosis, mitochondrial diseases, and aging in eukaryotic cells. This unique class of ribosomes is protein-rich and distinct from cytoplasmic ribosomes. However, mitochondrial ribosomes (55S) share a significant homology to bacterial ribosomes (70S), particularly in size, the general mechanism of translation, and ribosomal protein content. Due to the overall resemblance between the two systems and the earlier reports of post-translational modifications, we investigated how phosphorylation of ribosomal proteins from bacteria and mitochondria regulates translation and other acquired roles. Identification of twenty-four phosphorylated 70S and 55S ribosomal proteins as well as the potential endogenous kinase was achieved using 2D-gel electrophoresis and tandem mass spectrometry. Specific detection of phosphorylation was performed by [$\gamma$-$^{32}$P] ATP-labeling, ProQ staining, or the use of phospho-specific antibodies. Many of the phosphorylated proteins are located at the polypeptide exit tunnel, mRNA binding path, and the sarcin-ricin loop of the ribosome, implying the functional role of this post-translational modification in translation. By immobilized metal affinity and strong cation exchange chromatography, enrichment of phosphopeptides resulted in the mapping of phosphorylation sites that were evolutionarily conserved and correlated to ribosomal function. Moreover, we have demonstrated, in the presence of *in vitro* phosphorylation, the inhibition of protein synthesis by mitochondrial kinases PKA, PKCδ, and Abl Tyr kinase. From these phosphoproteomic analyses of 70S and 55S ribosomal proteins, a mitochondrial specific protein DAP3 and the conserved L7/L12 protein were chosen for functional studies. Death Associated Protein 3 (DAP3), also referred to as mitochondrial ribosomal protein S29 (MRPS29), is a GTP-binding apoptotic small subunit protein. DAP3 is phosphorylated at Ser215 or Thr216, Ser220, Ser251 or Ser252, and Ser280. Interestingly, most of the phosphorylation sites are dispersed around the GTP-binding motifs and may alter protein conformation and activity. Site-directed mutagenesis studies on selected phosphorylation sites were performed to determine the effect of phosphorylation on cell viability and PARP cleavage as an indication of caspase

activation. On the other hand, L7/L12, a large subunit protein, is essential for translation by binding and stimulating several GTPases. *E. coli* L7/L12 is phosphorylated at Ser15, Ser33, and Thr52. Sites of phosphorylation are strategically located at different functional domains of the protein, inducing conformational changes to the stalk. Site-directed mutagenesis studies coupled to *in vitro* translation assays were performed, stimulating or inhibiting protein synthesis due to the charge repulsion of neighboring acidic residues in various arrangements. In addition, we detected bovine mitochondrial ribosomal L12 to be phosphorylated as determined by 2D-gel analysis and the use of phospho-specific antibodies. Overall, these proteomic studies identified novel phosphorylated targets and demonstrated the importance of post-translational modifications to translation and apoptosis by maintaining the delicate balance between these two opposing processes in the cell.

## TABLE OF CONTENTS

## LIST OF FIGURES

## LIST OF TABLES

## ABBREVIATIONS

| | |
|---|---|
| 2D | two-dimensional |
| 5S | rRNA of the large subunit of the bacterial ribosome |
| 12S | rRNA of the small subunit of the mitochondrial ribosome |
| 16S | rRNA of the large subunit of the mitochondrial ribosome<br>rRNA of the small subunit of the bacterial ribosome |
| 23S | rRNA of the large subunit of the bacterial ribosome |
| 28S | small subunit of the mitochondrial ribosome |
| 30S | small subunit of the bacterial ribosome |
| 39S | large subunit of the mitochondrial ribosome |
| 50S | large subunit of the bacterial ribosome |
| 55S | intact mitochondrial ribosomes |
| 70S | intact bacterial ribosomes |
| Å | angstroms |
| aa-tRNA | aminoacyl tRNA |
| Abl Tyr | Abl protein tyrosine kinase |
| ADP | adenosine diphosphate |
| AIF | apoptosis inducing factor |
| AKAPs | A-kinase anchor proteins |
| Akt | protein kinase B |
| Apaf1 | apoptosis protease activating factor 1 |
| A site | aminoacyl site for tRNA |
| ATP | adenosine triphosphate |
| ATP6 | ATP synthase subunit 6 |
| ATP8 | ATP synthase subunit 8 |
| bp | base pair |
| BCKD | branched chain α ketoacid dehydrogenase |
| BCKDP | branched chain α ketoacid dehydrogenase phosphatase |
| capLC-ESI | capillary liquid chromatography nanoelectrospray ionization |
| CDK11 | cyclin dependent kinase 11 |
| CID | collision-induced dissociation |
| CKI | casein kinase I |
| CKII | casein kinase II |
| Complex I | NADH dehydrogenase |
| Complex II | succinate dehydrogenase |
| Complex III | ubiquinol cytochrome c oxidoreductase |
| Complex IV | cytochrome c oxidase |
| Complex V | ATP synthase |
| COX1 | cytochrome c oxidase subunit 1 |
| COX2 | cytochrome c oxidase subunit 2 |
| COX3 | cytochrome c oxidase subunit 3 |
| CP | central protuberance |
| Csk | COOH-terminal SRC kinase |
| CTD | C-terminal domain |
| cyro-EM | cyro-electron microscopy |

| | |
|---|---|
| CYTB | subunit of ubiquinol cytochrome c oxidoreductase |
| DAP3 | death associated protein 3 |
| DCA | dichloroacetate |
| DMPK | dystrophia myotonica protein kinase |
| dta | data dependent acquisition |
| DTT | dithiothreitol |
| EF-G | bacterial elongation factor G |
| EF-Ts | bacterial elongation factor Ts |
| EF-Tu | bacterial elongation factor Tu |
| $EF\text{-}G_{mt}$ | mitochondrial elongation factor G |
| $EF\text{-}Tu_{mt}$ | mitochondrial elongation factor Tu |
| EGFR | epidermal growth factor receptor |
| ELK | eukaryotic like protein kinase |
| ERK | extracellular signal regulated kinase |
| E site | exit site for tRNA |
| ETL | exit tunnel lid |
| Fgr | Gardner-Rasheed feline sarcoma |
| fMet | formylated methionine |
| Fyn | protein tyrosine kinase |
| GAR | GTPase activating region |
| GC/MS | gas chromatography/mass spectrometry |
| GEF | guanine nucleotide exchange factor |
| Glu | glutamic acid |
| GSK3β | glycogen synthase kinase 3 beta |
| hNOA1 | human nitric oxide associated protein 1 |
| Hsp60 | heat shock protein 60 |
| IB | immunoblot |
| IF-1 | bacterial initiation factor 1 |
| IF-2 | bacterial initiation factor 2 |
| $IF\text{-}2_{mt}$ | mitochondrial initiation factor 2 |
| IF-3 | bacterial initiation factor 3 |
| $IF\text{-}3_{mt}$ | mitochondrial initiation factor 3 |
| IMAC | immobilized metal affinity chromatography |
| Immuno-EM | immnoelectron microscopy |
| IPG | immobilized pH gradient |
| JNK | c-Jun N-terminal kinase |
| kDa | kilo daltons |
| L8 | L10 and L7/L12 |
| LKB1 | serine-threonine kinase |
| LTQ | linear trap |
| Lyn | protein tyrosine kinase |
| MAPK | mitogen-activated protein kinase |
| MDa | mega daltons |
| MEK | MAPK/ERK kinase |
| mgf | Mascot generic file |
| mgt | mitochondrial triangular gate-like structure |

| | |
|---|---|
| MPK-1 | MAP kinase phosphatase-1 |
| mRNA | messenger RNA |
| MRP | mitochondrial ribosomal protein |
| MS | mass spectrometry |
| MS/MS | tandem mass spectrometry |
| mTOR | mammalian target of rapamcyin |
| ND1 | NADH dehydrogenase subunit 1 |
| ND2 | NADH dehydrogenase subunit 2 |
| ND3 | NADH dehydrogenase subunit 3 |
| ND4 | NADH dehydrogenase subunit 4 |
| ND4L | NADH dehydrogenase subunit 4L |
| ND5 | NADH dehydrogenase subunit 5 |
| ND6 | NADH dehydrogenase subunit 6 |
| NEPHGE | non-equilibrium pH gradient electrophoresis |
| NIH | National Institutes of Health |
| nt | nucleotides |
| NTD | N-terminal domain |
| PAGE | polyacrylamide gel electrophoresis |
| PAK5 | p21-activated kinase 5 |
| PAS | polypeptide-accessible site |
| PARP | poly ADP ribose polymerase |
| PCTAIRE2 | related to cell division cycle 2 serine/threonine kinases |
| PDB | protein data bank |
| PDCD9 | programmed cell death protein 9 |
| PDK | pyruvate dehydrogenase kinase |
| PDP | pyruvate dehydrogenase phosphatase |
| PES | polypeptide exit site |
| PINK1 | PTEN-induced putative kinase 1 |
| PKA | cAMP-dependent protein kinase |
| PKCδ | protein kinase C delta |
| pmol | pico moles |
| PMSF | phenylmethylsulfonyl fluoride |
| poly U | polyphenylalanine |
| PP1 | protein phosphatase 1 |
| PP2A | protein phosphatase 2A |
| PP2Cγ | protein phosphatase 2C gamma |
| P site | peptidyl site for tRNA |
| PTC | peptidyl transferase site |
| PTP1D | protein tyrosine phosphatase 1D |
| PTPMT1 | protein tyrosine phosphatase mitochondrial 1 |
| PVDF | polyvinylidene fluoride |
| RAF1 | proto-oncogene serine/threonine kinase |
| RF | release factor |
| RIP3 | receptor-interacting protein 3 |
| ROS | reactive oxygen species |
| rRNA | ribosomal RNA |

| | |
|---|---|
| SAPK3 | stress-activated protein kinase 3 |
| SCX | strong cation exchange chromatography |
| SD | standard deviation |
| SDS | sodium dodecyl sulfate |
| Ser | serine |
| SHP-2 | Src homology phosphatase 2 |
| SLE | systemic lupus erythematosus |
| Src | steroid receptor co-activator |
| SRL | sarcin-ricin loop |
| SRP | signal recognition particle |
| STS | staurosporine |
| Thr | threonine |
| TIM50 | translocase of the inner membrane 50 |
| tRNA | transfer RNA |
| Tyr | tyrosine |
| UV | ultraviolet |
| WT | wild-type |
| Xcorr | cross correlation score |

## ACKNOWLEDGEMENTS

First, I would like to thank my advisor, Dr. Emine Koc, for her patience and understanding throughout my dissertation work. She is a wonderful role model for a woman scientist. Second, I would like to thank Dr. Hasan Koc, for the many hours spent running my LC-MS/MS samples for protein identification and mapping of phosphorylated residues. To the Koc Lab, both past and present members, your help, support, advice, and most importantly friendship allowed me to persevere through times of frustration and reach my ultimate goal. I would like to thank my dissertation committee for their constant support and guidance during my time at Penn State. Finally, I would like to thank my family and fiancée, Seungkyu, for seeing me through this journey and loving me every step of the way.

# CHAPTER 1

# Introduction

## 1.1 Mitochondria

Mitochondria are the powerhouses of the cell, because they produce about 90% of the energy in a eukaryotic cell (Wallace 1997). In addition to this specialized function, mitochondria are critical for signaling and apoptosis (Butow and Avadhani 2004; Eskes et al. 2000; Goldenthal and Marin-Garcia 2004; Zoratti and Szabò 1995). More recently, mitochondria have become the focus in studies of lifespan and caloric restriction, given they produce an abundance of reactive oxygen species (ROS) and accumulation of mutations in the mitochondrial DNA results in a variety of diseases (Amara et al. 2007; Ahm et al. 2008; Kussmaul and Hirst 2006; Wallace 1992; Zangarelli et al. 2006). These functions can be attributed to the complexity of the organelle and the diversity of proteins housed within its compartments.

According to the endosymbiotic theory, mitochondria originally descended from ancient bacteria and are a membrane-enclosed dynamic organelle, which can be subdivided into four sections (Margulis 1981). The outer membrane is a phospholipid bilayer, which is permeable to ions, ATP, ADP, nutrients, and other small molecules (Perkins et al. 1997). The inter-membrane space, is a narrow region between the two membranes where several apoptotic factors are stored including cytochrome c, apoptosis inducing factor (AIF), endonuclease G, and others (Jiang and Wang 2004). The inner membrane houses the five oligomeric complexes of oxidative phosphorylation. The matrix, the innermost chamber, consists of invaginations called cristae which increase the surface area within the mitochondria (Perkins et al. 1997). This chamber contains the ribosomes, a circular genome, and enzymes involved in many biochemical pathways including the citric acid cycle, the urea cycle, and heme synthesis.

Typically, there are 200-2000 mitochondria in a eukaryotic cell, while two to ten copies of the mitochondrial genome are found in a single mitochondrion (Shuster et al.

1988; Wiesner et al. 1992). Figure 1.1 depicts the mitochondrial genome, which is inherited from the mother and is double-stranded, circular, and about 16.5 kb in size (Anderson et al. 1981). Interestingly, mitochondrial DNA encodes thirty-seven genes, specifically thirteen proteins of the respiratory chain complex (cytochrome b, ND1, ND2, ND3, ND4, ND4L, ND5, ND6, COXI, COXII, COXIII, ATP6, ATP8), 22 tRNAs, and 2 rRNAs (12S and 16S) (Anderson et al. 1981). The DNA consists of a heavy and light strand, as determined by their buoyant densities in alkaline cesium chloride gradients (Clayton 1982). Twelve proteins and both rRNAs are transcribed from the heavy strand, while ND6 is transcribed from the light strand (Bonawitz et al. 2006). In this tightly packed genome, the D-loop region serves as the center for regulation. Many mutations in the mitochondrial genome result in deafness, neurodegenerative diseases, muscle weakness, and are linked to diabetes and cancer as well (Wallace 1992; Brandon et al. 2006).

Eukaryotic cells contain two types of ribosomes, cytoplasmic ribosomes found in the cytosol and mitochondrial ribosomes located within the mitochondria. The cytoplasmic ribosomes are responsible for all the proteins synthesized in a cell except for the thirteen hydrophobic components of the electron transport chain and ATP synthase encoded in the mitochondrial genome, which are located within the inner membrane of the mitochondria and are essential for ATP production. Remarkably, mitochondrial ribosomes resemble bacterial ribosomes in terms of structural features of the small and large subunits, ribosomal protein content, and mechanism of protein synthesis, specifically the translational machinery. Due to these similarities, as well as our broad knowledge and characterization of the bacterial system, it is hypothesized that each system could be regulated in a similar manner by post-translational modifications, particularly phosphorylation. Therefore, it is important to stress the structural and functional features of the bacterial ribosome.

## 1.2 Structural Features of Bacterial Ribosomes

Ribosomes are large ribonucleoprotein particles composed of RNA and protein. Specifically, prokaryotic ribosomes contain more RNA (67%) compared to protein (33%)

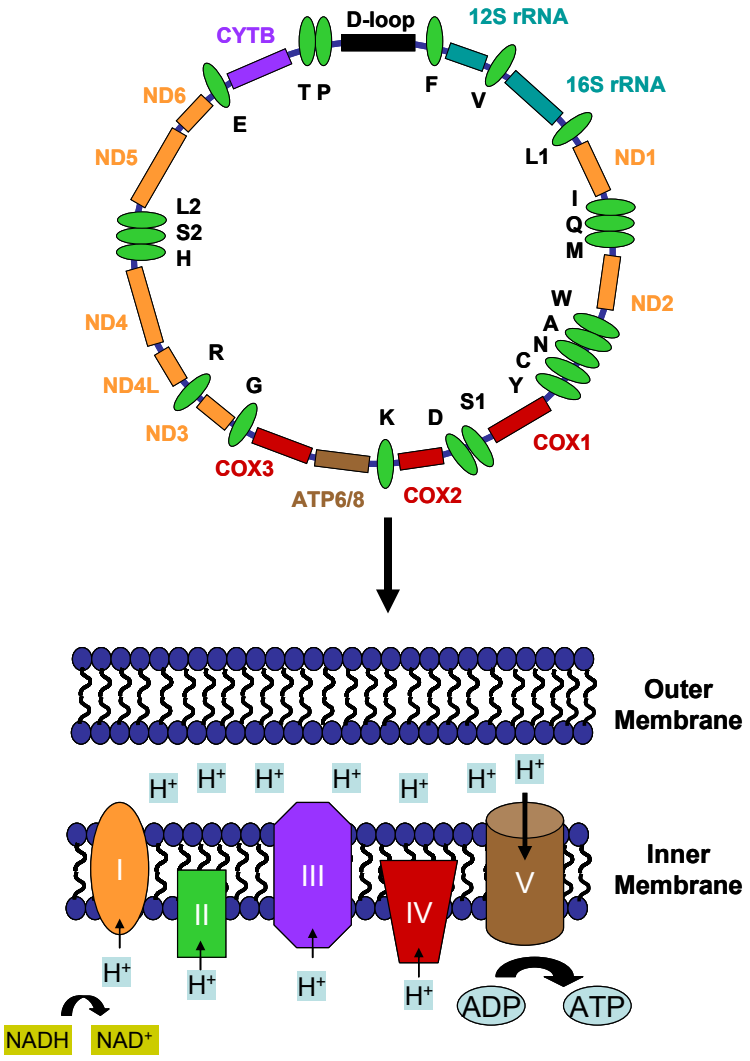


**Figure 1.1. The circular mitochondrial genome encodes subunits of electron transport chain complexes.** The genome is 16, 569 bp and very compact containing one regulatory region called the D-loop labeled in black. The green ovals represent the 22 tRNA genes labeled in black. Particularly, serine and leucine each have two tRNAs. The small (12S) and large (16S) subunit rRNAs are highlighted in light blue. The genome encodes thirteen proteins, seven subunits of Complex I/NADH dehydrogenase (ND1, ND2, ND3, ND4, ND4L, ND5, ND6) shown in orange, one subunit of Complex III/Ubiquinol cytochrome c oxidoreductase (cytochrome b) shown in purple, three subunits of Complex IV/Cytochrome c oxidase (COXI, COX II, COX III) shown in red, and two subunits of Complex V/ATP synthase (ATP6 and ATP 8) shown in brown. The complexes needed for electron transport are located in the inner mitochondrial membrane. Protons are pumped out of the matrix creating a gradient to drive the conversion of ADP to ATP providing fuel for the cell. This figure was adapted from (Wallace 1999; Ojala et al. 1980).

(Ban et al. 2000). Sedimenting as a 70S particle that is 2.3 MDa in size, the ribosome consists of a small subunit (30S) and a large subunit (50S) (Table 1.1). The two subunits are held together by intersubunit bridges of RNA-RNA, protein-protein, or RNA-protein (Yusupov et al. 2001). The small subunit is responsible for binding and decoding mRNAs in addition to helping the large subunit in the translocation process (Carter et al. 2000; Carter et al. 2001). The 30S subunit encompasses a 16S rRNA and twenty-one ribosomal proteins, S1-S21 (Wittmann-Liebold 1985). The large subunit carries the peptidyl transferase activity that catalyzes peptide bond formation (Nissen et al. 2000). The 50S subunit of bacterial ribosomes has two rRNAs (5S and 23S) and thirty-three ribosomal proteins, L1-L36 (Wittmann-Liebold 1985). In particular, L7/L12 is the same protein except that L7 is the N-terminal acetylated form of the protein, while L8 can be described as L10 in complex with L7/L12.

### 1.2.1 Small Subunit of the Bacterial Ribosome

The 30S subunit is defined by three distinct regions: the head, platform, and body segments (Table 1.2 and Figure 1.2). The mRNA binding proteins of the small subunit can be classified as primary, secondary, or tertiary based on the order of assembly into the subunit and the extent of their interactions with the rRNA (Mizushima and Nomura 1970; Held et al. 1974). Eight proteins are located in the head of the 30S subunit, S2, S3, S7, S9, S10, S13, S14, and S19 which interact with the 3' domain of the 16S rRNA (Wimberly et al. 2000). S7 is primary, while S9, S13, and S19 are secondary, and S2, S3, S10, S14 are tertiary RNA binding proteins. One unique feature of the head is the presence of a beak-like structure composed of both RNA and protein (Wimberly et al. 2000). The platform consists of six ribosomal proteins, S6, S8, S11, S15, S18, and S21 each associating with the central domain of the 16S rRNA (Wimberly et al. 2000). In this cluster there are two of each classification of RNA binding proteins, S8 and S15 are primary, S6 and S18 are secondary, and S11 and S21 are tertiary. Finally, the body of the small subunit houses six more ribosomal proteins, S4, S5, S12, S16, S17, and S20, which are linked to the 5' domain of the 16S rRNA (Wimberly et al. 2000). Three primary RNA binding proteins are present in this group specifically S4, S17, and S20, while S5, S12, and S16 are secondary binding proteins.

**TABLE 1.1 – Comparison of mammalian mitochondrial and bacterial ribosomes**

| Features | Prokaryotic | Mitochondrial |
|---|---|---|
| Size | 2.3 MDa | 2.7 MDa |
| Intact Ribosome | 70S | 55S |
| Small Subunit | 30S | 28S |
| Large Subunit | 50S | 39S |
| Small Subunit Proteins | 21 | 29 |
| Large Subunit Proteins | 33 | 48 |
| Percentage of Protein | 33% | 67% |
| rRNA of Small Subunit | 16S (1542 nt) | 12S (950 nt) |
| rRNA of Large Subunit | 23S (2904 nt) | 16S (1560 nt) |
| | 5S (120 nt) | |
| Percentage of rRNA | 67% | 33% |

**TABLE 1.2 – List of mitochondrial ribosomal proteins with their bacterial homologs**

| 28S Proteins | 30S Proteins | New Class | 39S Proteins | 50S Proteins | New Class |
|---|---|---|---|---|---|
| Not detected | S1 | MRPS22 | MRPL1 | L1 | MRPL37 |
| MRPS2 | S2 | MRPS23 | MRPL2 | L2 | MRPL38 |
| Not detected | S3 | MRPS24 | MRP-L3 | L3 | MRPL39 |
| Not detected | S4 | MRPS25 | MRPL4 | L4 | MRPL40 |
| MRPS5 | S5 | MRPS26 | Not detected | L5 | MRPL41 |
| MRPS6 | S6 | MRPS27 | Not detected | L6 | MRPL42 |
| MRPS7 | S7 | MRPS28 | MRPL7/L12 | L7/L12 | MRPL43 |
| Not detected | S8 | MRPS29 | MRPL9 | L9 | MRPL44 |
| MRPS9 | S9 | MRPS30 | MRPL10 | L10 | MRPL45 |
| MRPS10 | S10 | MRPS31 | MRPL11 | L11 | MRPL46 |
| MRPS11 | S11 | MRPS32 | MRPL13 | L13 | MRPL47 |
| MRP-S12 | S12 | MRPS33 | MRPL14 | L14 | MRPL48 |
| Not detected | S13 | MRPS34 | MRPL15 | L15 | MRPL49 |
| MRPS14 | S14 | MRPS35 | MRPL16 | L16 | MRPL50 |
| MRPS15 | S15 | MRPS36 | MRPL17 | L17 | MRPL51 |
| MRPS16 | S16 | | MRPL18 | L18 | MRPL52 |
| MRPS17 | S17 | | MRPL19 | L19 | MRPL53 |
| MRPS18-1 | S18 | | MRPL20 | L20 | MRPL54 |
| MRPS18-2 | | | MRPL21 | L21 | MRPL55 |
| MRPS18-3 | | | MRPL22 | L22 | MRPL56 |
| Not detected | S19 | | MRPL23 | L23 | |
| Not detected | S20 | | MRPL24 | L24 | |
| MRPS21 | S21 | | Not detected | L25 | |
| | | | MRPL27 | L27 | |
| | | | MRPL28 | L28 | |
| | | | Not detected | L29 | |
| | | | MRPL30 | L30 | |
| | | | Not detected | L31 | |
| | | | MRPL32 | L32 | |
| | | | MRPL33 | L33 | |
| | | | MRPL34 | L34 | |
| | | | MRPL35 | L35 | |
| | | | MRPL36 | L36 | |

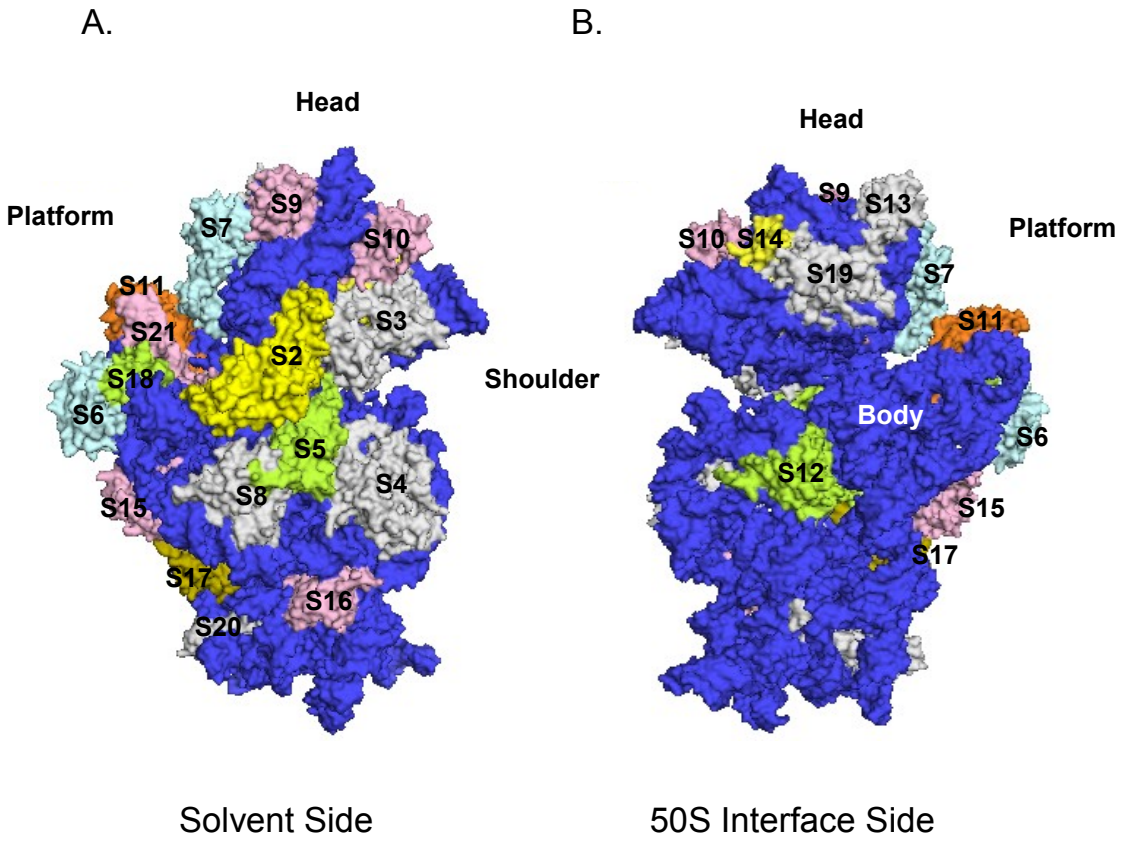


**Figure 1.2 – 3D-Models of the *E. coli* ribosomal subunits displaying the location of the ribosomal proteins.** The ribosomal proteins with homologs in mitochondria are highlighted in different colors, while gray represents ribosomal proteins only found in bacteria, and blue is the rRNA. Coordinates of the *E. coli* 30S subunit and 50S subunit were obtained from the Protein Data Bank (Acc. # 2AW7 and 2AW4). (A) The 30S subunit is illustrated from the solvent side, while (B) represents a view of the small subunit from the 50S interface.

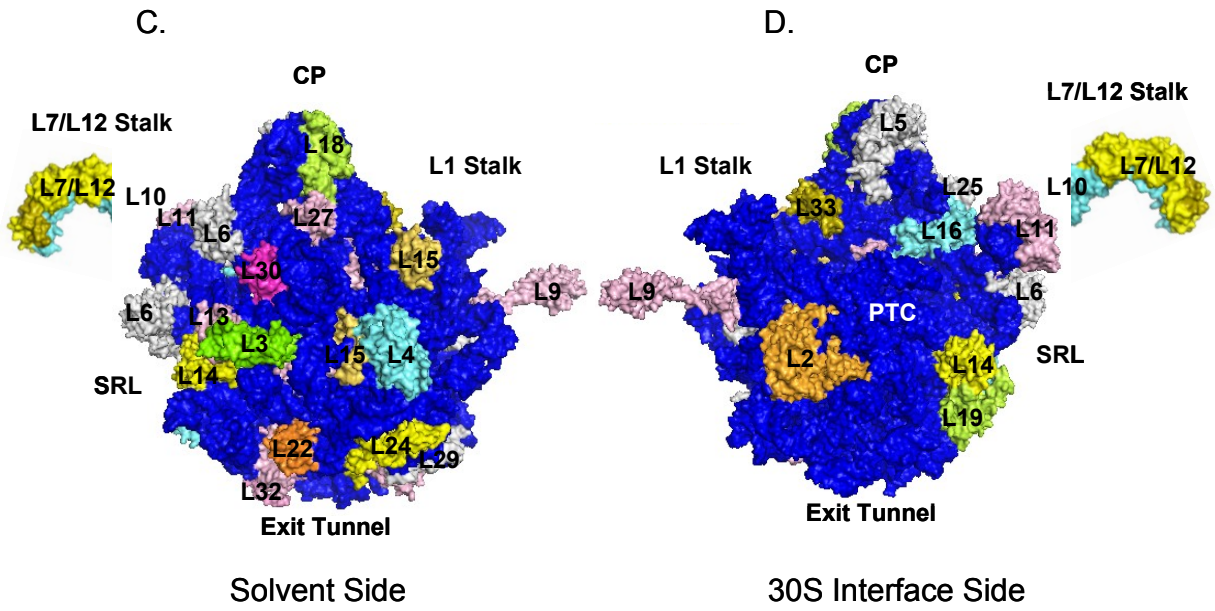


(C) Representation of the 50S subunit from the solvent side, while (D) is a view of the large subunit from the 30S interface. Specific regions denoted are peptidyl transferase center (PTC), central protuberance (CP), sarcin-ricin loop (SRL), and the ribosomal proteins were labeled in the model generated by PyMOL software (DeLano 2002).

The small subunit proteins can be classified into categories based on binding to the mRNA or to the tRNAs in the A (aminoacyl), P (peptidyl), and E (exit) sites on the ribosome. S1, S7, and S11 are primarily responsible for tethering the mRNA to the ribosome. S1 is a very large ribosomal protein containing multiple repeats of the oligonucleotide binding fold similar to initiation factor 1 (IF-1) (Subramanian 1983). S7 and S11 are also in contact with the E site tRNA and may assist in ejecting the tRNA from the ribosome (Carter et al. 2000). S18 and S21 are known to bind to the Shine-Dalgarno sequence of the mRNA in the pre-initiation complex, yet in the post-initiation complex S2 interacts with the message (Yusupova et al. 2006). Additionally, S3, S4, and S5 form part of the mRNA binding path and associate with the 3' end of the message (Dontsova et al. 1992; Yusupova et al. 2001). S9 has a C-terminal tail which is in close proximity to the peptidyl tRNA and controls P site specificity during translation as does S13 (Noller et al. 2005). S12 functions in tRNA decoding at the A site relative to the wobble base (third codon) coordinating the magnesium ion (Brodersen and Nissen 2005).

### 1.2.2 Large Subunit of the Bacterial Ribosome

The large subunit designated as the 50S can be dissected into six prominent areas of functional significance (Table 1.2 and Figure 1.2). The L1 stalk directly across from the L7/L12 stalk houses the L1 protein which is an RNA binding protein and as predicted the stalk is primarily composed of domain V of the 23S rRNA (Yusupov et al. 2001). One possible function is to eject the tRNA from the E site, while the L1 stalk must shift from a closed to an open conformation with respect to the central protuberance (Korostelev et al. 2006; Selmer et al. 2006). The central protuberance of the ribosome, located in between the L1 and L7/L12 stalks consists of L5, L18, L25, and the 5S rRNA (Ban et al. 2000). L5 is known to interact with two small subunit proteins S13 and S19, while L18 is near the signal recognition particle (SRP) binding path and assists in complexing the 5S rRNA to the 23S rRNA (Bloemink and Moore 1999; Schaffitzel et al. 2006). Another key feature of the 50S subunit is the L7/L12 stalk, containing L10 which anchors L7/L12 to the ribosome and four to six copies of the flexible L7/L12 protein depending upon the bacteria. It is sometimes called GAR for GTPase activating region, because it enhances the activity of at least four GTPases (Helgstrand et al. 2007). The C-

terminal domain of L7/L12 can span a volume of 45 Å given the mobility of the linker region, which could influence the recruitment of different factors needed for protein synthesis (Diaconu et al. 2005). L11 is a neighbor to L10 on the ribosome having a role in factor binding and in termination of translation (Van Dyke et al. 2002; Datta et al. 2005). The sarcin-ricin loop (domain VI) of the 23S rRNA is positioned directly below the L7/L12 stalk and is also important for factor binding, containing L3 and L13. L13 is a component of active sub-ribosomal particles composed of both of the 50S subunit rRNAs, while L3 is positioned close to the catalytic site of the ribosome (Bischof et al. 1995; Khaitovich et al. 1999). The peptidyl transferase site is a rRNA center, therefore the ribosome is referred to as a ribozyme, yet many of the ribosomal proteins have long extensions acting as tails which reach into the vicinity of the active site including L2 and L16 (Ban et al. 2000). Finally, the polypeptide exit tunnel of bacterial ribosomes is surrounded by domains I and III of the 23S rRNA as well as L4, L22, L23, L24, and L29 (Nissen et al. 2000). L22 is partially responsible for giving the tunnel its Teflon-like property, while L23 is capable of interacting with both trigger factor and SRP (Nissen et al. 2000; Beckmann et al. 2001).

## 1.3 Structural Features of Mitochondrial Ribosomes

The 55S mammalian mitochondrial ribosome (2.71 MDa) was found to be larger in size but more porous in comparison to the 70S bacterial ribosome (Patel et al. 2001). Moreover, the intersubunit space is similar to cytoplasmic ribosomes yet in a more open conformation (Sharma et al. 2003). Mammalian mitochondria are protein-rich (67%) with the majority of the ribosomal proteins in clusters in the periphery and relatively larger in size than their bacterial counterparts (Table 1.1) (Matthews et al. 1982; Sharma et al. 2003). The two subunits are held together by fifteen intersubunit bridges dominated by protein-protein bridges and much fewer RNA-RNA bridges, as the proteins may have acquired additional functions (Sharma et al. 2003). On the other hand, the two rRNAs (33%) have distinct segments which are severely truncated, compensated by the heavier ribosomal proteins (Matthews et al. 1982; Sharma et al. 2003).

### 1.3.1 Small Subunit of the Mitochondrial Ribosome

The intact 55S ribosome can be subdivided into a small subunit (28S) and a large subunit (39S) as depicted in Figure 1.3 (Hamilton and O'Brien 1974). The 28S subunit contains a single rRNA (12S) and twenty-nine proteins (Koc et al. 2001b; Suzuki et al. 2001a). Fourteen mitochondrial ribosomal proteins (MRPs) of the small subunit have bacterial homologs including: MRPS2, MRPS5, MRPS6, MRPS7, MRPS9, MRPS10, MRPS11, MRPS12, MRPS14, MRPS15, MRPS16, MRPS17, MRPS18, and MRPS21, while the remaining represent new class proteins specifically, MRPS22 through MRPS36 (Koc et al. 2001b) (Figure 1.2 and Table 1.2). Interestingly, in mitochondria, there are three variants of the S18 protein (MRPS18-1, MRPS18-2, MRPS18-3) and it is believed each ribosome contains one variant in the 28S subunit resulting in a heterogeneous population of ribosomes (Koc et al. 2001b). However, there are no mitochondrial homologs to seven of the prokaryotic ribosomal proteins including S1, S3, S4, S8, S13, S19, and S20 (Koc et al. 2001b).

Overall the small subunit proteins with prokaryotic homologs tend to be located in the core of the ribosome, while the new mitochondrial specific proteins are tentatively assigned to the periphery of the 28S subunit as the exact locations are unknown. Structurally, the key features of the small subunit are conserved including the head, platform, and body regions. Mitochondrial small subunit proteins located in the head region are MRPS2, MRPS7, MRPS9, MRPS10, and MRPS14, interacting with the 3' domain of the 12S rRNA (Koc et al. 2001a). MRPS6, MRPS11, MRPS15, MRPS18, and MRPS21 are positioned in the platform region and associate with the central domain of the 12S rRNA creating the P-site on the ribosome (Koc et al. 2001a). Finally, the body is comprised of four ribosomal proteins including MRPS5, MRPS12, MRPS16, and MRPS17 which are linked to the 5' domain of the 12S rRNA (Koc et al. 2001a). However, the mitochondrial small subunit contains protein-rich patches referred to as the lower body lobe and the beak lobe of the head as most of the proteins are 4-25 kDa larger than their bacterial homologs (Sharma et al. 2003). One unique feature of the mitochondrial small subunit is the triangular gate-like structure called the mRNA gate (mgt) covering part of the mRNA entry site and an extension of MRPS2 as shown in

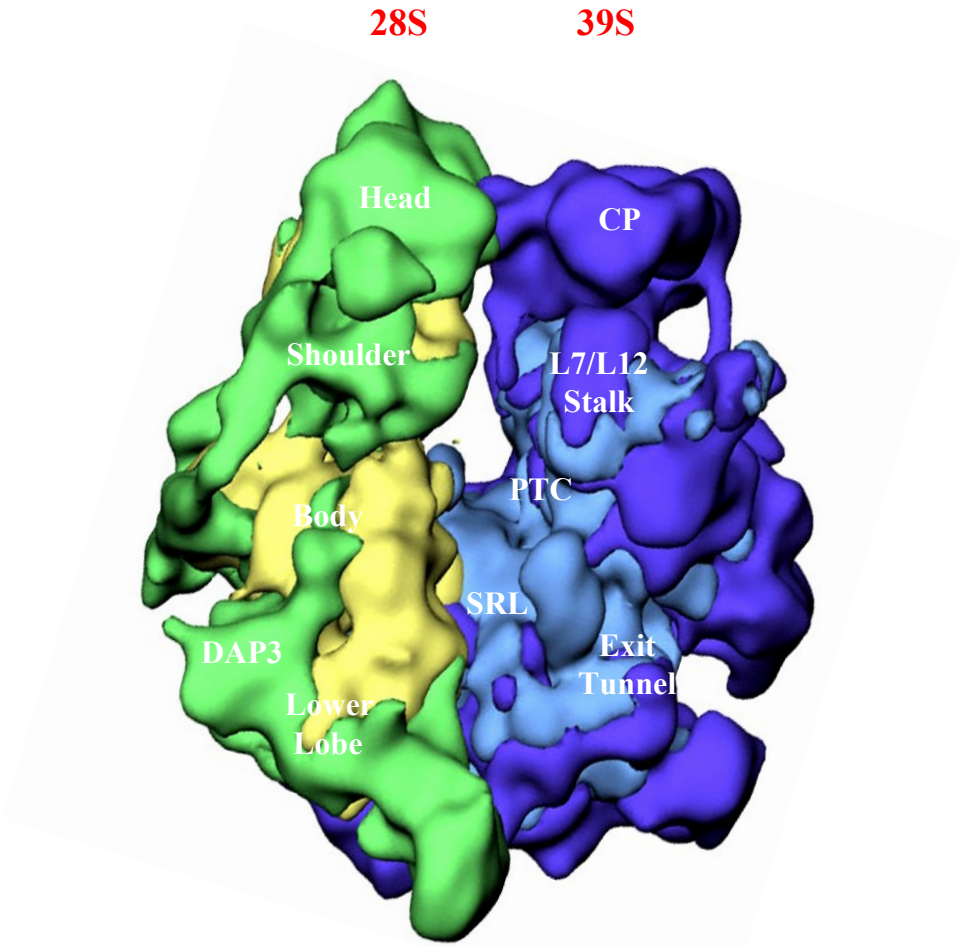


**Figure 1.3. The 13.5 Å cryo-EM structure of the 55S mammalian mitochondrial ribosome.** The small (28S) subunit is on the left in yellow and green, while the large (39S) subunit is on the right in light and dark blue. The core of the ribosome shown in yellow and light blue, represent ribosomal proteins that are conserved in bacteria. On the other hand, the green and dark blue portions in the periphery represent mitochondrial specific ribosomal proteins. SRL denotes the sarcin-ricin loop, PTC is the peptidyl transferase site, while CP is the central protuberance of the large subunit. This figure was adapted from (Sharma et al. 2003).

Figure 1.4 (Sharma et al. 2003). Typically, the mRNA channel in bacteria is comprised of S3, S4, and S5; however, mitochondrial ribosomes do not have homologs for S3 and S4, therefore mitochondrial specific proteins must serve as replacements (Koc et al. 2001b. It is speculated this gate may be a way to regulate translation initiation and recognize the mRNAs, given their lack of any characteristic features at the 5' end (Sharma et al. 2003).

### 1.3.2 Large Subunit of the Mitochondrial Ribosome

The 39S subunit consists of a single rRNA (16S) and forty-eight proteins (Koc et al. 2001c; Suzuki et al. 2001b) Of the mitochondrial 39S proteins, twenty-eight have prokaryotic homologs particularly, MRPL1, MRPL2, MRPL3, MRPL4, MRPL7/L12, MRPL9, MRPL10, MRPL11, MRPL13, MRPL14, MRPL15, MRPL16, MRPL17, MRPL18, MRPL19, MRPL20, MRPL21, MRPL22, MRPL23, MRPL24, MRPL27, MRPL28, MRPL30, MRPL32, MRPL33, MRPL34, MRPL35, MRPL36 as shown in Figure 1.2 and Table 1.2 (Koc et al. 2001c). Because mitochondria are protein-rich, the remaining twenty ribosomal proteins (MRPL37 to MRPL56) are again mitochondrial specific with most having an unknown function and location on the ribosome (Koc et al. 2001c). Only five ribosomal proteins from bacteria do not have mitochondrial homologs, L5, L6, L25, L29, and L31 (Koc et al. 2001c).

Structural investigations have verified the three classic features of the 39S subunit including the central protuberance, the L1 stalk, and the L12 stalk are each larger than their bacterial counterparts, while the porous periphery is packed with mitochondrial specific proteins (Sharma et al. 2003). The central protuberance contains L5, L18, L25, and the 5S rRNA in the bacterial ribosome, yet only MRPL18 has been identified in mitochondria (Koc et al. 2001c). The central protuberance is twice as large in mitochondria and contains a large subunit handle, which is protein-rich and may have evolved to assume the necessary role of the 5S rRNA as well as a P site finger generating a tight connection to the mitochondrial tRNA in contrast to the E site (Sharma et al. 2003). The L12 stalk is a very dynamic and unusual characteristic of the ribosome, consisting of L10 and multiple copies of the L12 protein, although the exact number is

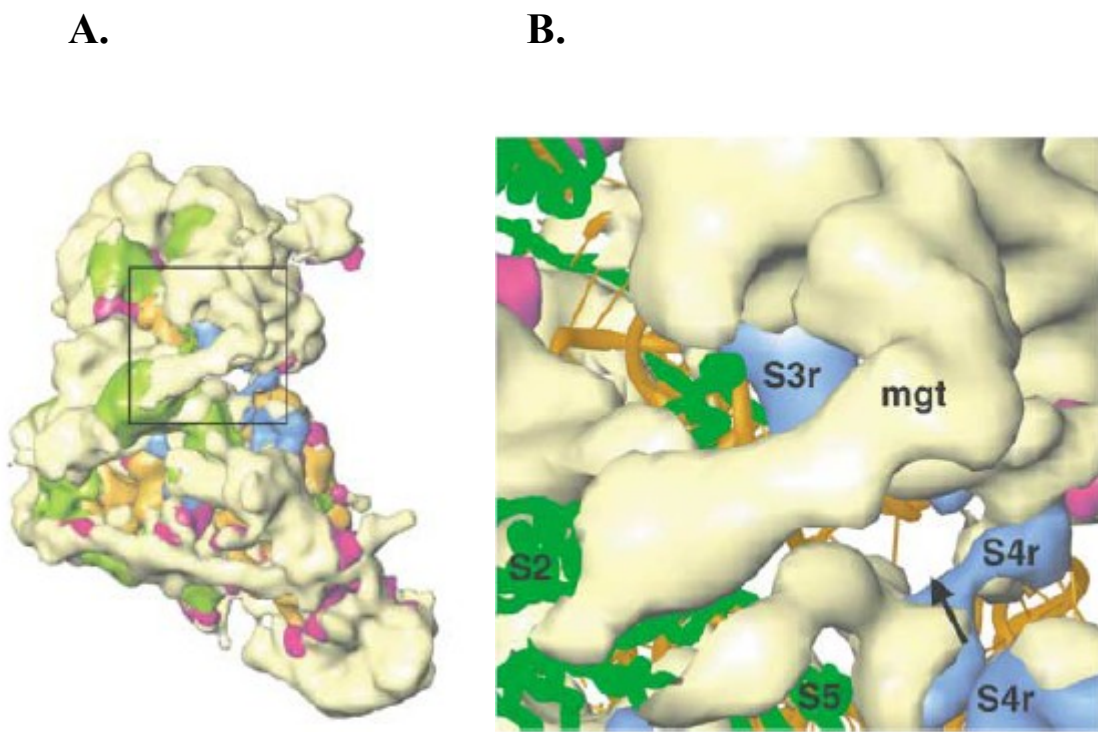


**Figure 1.4. Stereo representation of the detailed topography of the mRNA entry site.** Side view of the 28S subunit at the mRNA entry site was shown in A, and the mRNA entry site was enlarged in B. The site is composed principally of proteins and is partially covered by a triangular gate-like structure (mgt), which is composed of mitoribosome-specific proteins in yellow. The conserved small subunit proteins in green S2 and S5 and mitoribosome-specific protein masses are in blue that replace bacterial protein S3 and segments of protein S4 are identified with the suffix r. The arrow points to the mRNA entry site. Reprinted from *Cell*, 115, Sharma et al., Structure of the Mammalian Mitochondrial Ribosome Reveals an Expanded Functional Role for Its Component Proteins, 97-108, Copyright © 2003, with permission from Elsevier.

unknown in mitochondria and the presence of the acetylated form (L7) is uncertain. The sarcin-ricin loop (SRL) is conserved below the L12 stalk and contains MRPL3 and MRPL13 (Koc et al. 2001c). The peptide exit tunnel in the mitochondrial ribosome actually appears to have two exit sites (Figure 1.5). One site is 63 Å away from the peptidyl transferase center and is referred to as the polypeptide accessible site, while the traditional exit site is 88 Å away, possibly serving different routes based on the selection of chaperones needed to correctly fold the protein for insertion into the inner membrane (Sharma et al. 2003). The conventional exit does contain a lid-like structure called the exit tunnel lid, which may assist in controlling the release of the newly synthesized protein. The exit tunnel is surrounded by MRPL22, MRPL23, and MRPL24, each with bacterial homologs, while L29 is missing in this structure, though compensated by another large protein (Sharma et al. 2003). Finally, it is worth noting the location of L6 and L31 do not appear to be offset by mitochondrial specific proteins (Sharma et al. 2003).

### 1.3.3 Additional Functions of Mitochondrial Ribosomal Proteins

In mitochondria, some ribosomal proteins have acquired additional functions beyond translation, linking this organelle to apoptosis, cancer and disease states, as well as the aging process and virus integration. For example, MRPS29, also known as DAP3, MRPS30, MRPL37, and MRPL41 apoptotic proteins from the small and large subunits respectively (Kissil et al. 1995; Koc et al. 2001d; Levshenkova et al. 2004; Chintharlapalli et al. 2005). MRPS34 was shown to interact with the human homolog of *Drosophila* discs large tumor suppressor protein (hDLG) prior to entry into the mitochondria (Ogawa et al. 2003). MRPS31 also known as Imogen 38 is considered an auto-antigen recognized by T cells in type I diabetes, while a mutation in the MRPS22 gene was identified causing antenatal mitochondrial disease, as the patient displayed low levels of the 12S rRNA and a reduction in the activity of the respiratory chain complexes (Arden et al. 1996; Saada et al. 2007). MRPL47 in *C. elegans* was found to increase the lifespan of worms, but at the expense of reduced oxygen consumption and a lower ATP content (Lee et al. 2003). Recently, MRPS18-2, one of the three variants of the S18 protein in mammalian mitochondria, was identified to be a binding partner of EBNA-6

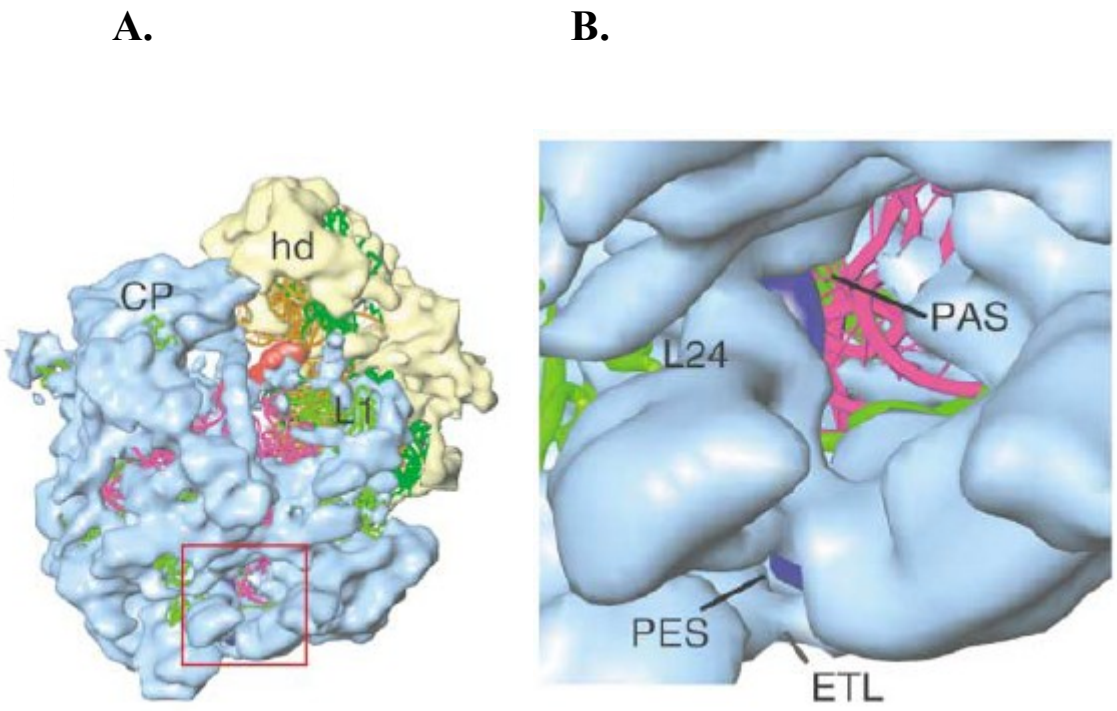


**Figure 1.5. Stereo representation of the topography of the two putative sites of polypeptide exit in the large subunit of the mitoribosome.** A view of the 39S subunit at the polypeptide exit tunnel was shown in A, and the exit site was enlarged in B. The large subunit shown from the L1 protein side reveals a large opening (PAS) in the tunnel before the PES. A model of an α-helical polypeptide chain in dark blue is used to delineate the polypeptide exit tunnel. Landmarks: PAS, polypeptide-accessible site; ETL, exit tunnel lid; PES, polypeptide exit site. Segments of the large subunit proteins in green present in the immediate vicinity are identified. Reprinted from *Cell*, 115, Sharma et al., Structure of the Mammalian Mitochondrial Ribosome Reveals an Expanded Functional Role for Its Component Proteins, 97-108, Copyright © 2003, with permission from Elsevier.

(Kashuba et al. 2008). This interaction promotes free E2F1 to enter the cell cycle at S-phase, allowing the virus to transform the host cell (Kashuba et al. 2008). Therefore, as new roles are assigned to this dynamic organelle, it is relevant to clearly identify the function of these mitochondrial ribosomal proteins.

## 1.4 Translation in Bacteria and Mammalian Mitochondria

Besides the structural similarities between bacterial and mitochondrial ribosomes, they also share common factors needed for the initiation and elongation steps of protein synthesis. First, the ribosome must scan the mRNA to determine where to begin translating. In bacteria, the ribosome recognizes a poly-purine motif in the mRNA called the Shine-Dalgarno sequence, while for cytoplasmic ribosomes a 5' cap acts as scaffold to build the initiation complex. However, mitochondrial mRNAs have neither of these recognition motifs and translation begins close to the 5' end of the mRNA, which is very compact containing almost no 5' and 3' UTRs and only a short poly A tail (Montoya et al. 1981; Anderson et al. 1982).

Translation as depicted in Figure 1.6 begins with all three initiation factors bound to the small subunit. IF-3 is released and IF-2, a GTPase promotes the binding of the small subunit to the initiator tRNA, formylated methionine (fMet) positioned in the P site. The large subunit is now free to bind to the small subunit, creating the intact 70S ribosome and both IF-1 and IF-2 are dissociated from the small subunit. The initiation phase is complete and the elongation phase can begin, which generates a growing polypeptide chain. A ternary complex is formed consisting of EF-Tu, GTP, and the tRNA coding for a specific amino acid which is brought to the A site of the ribosome. After hydrolyzing GTP, EF-Tu is released, and peptide bond formation is catalyzed by the large subunit. EF-G, a GTPase is responsible for the translocation of tRNAs and mRNA exposing a new codon at the A site. This process continues until a stop codon is read in the mRNA message resulting in the recruitment of release factors and stimulating the hydrolysis of the polypeptide from the ribosome. The protein is folded into the proper conformation by chaperones and as for mitochondria is inserted into the inner membrane.

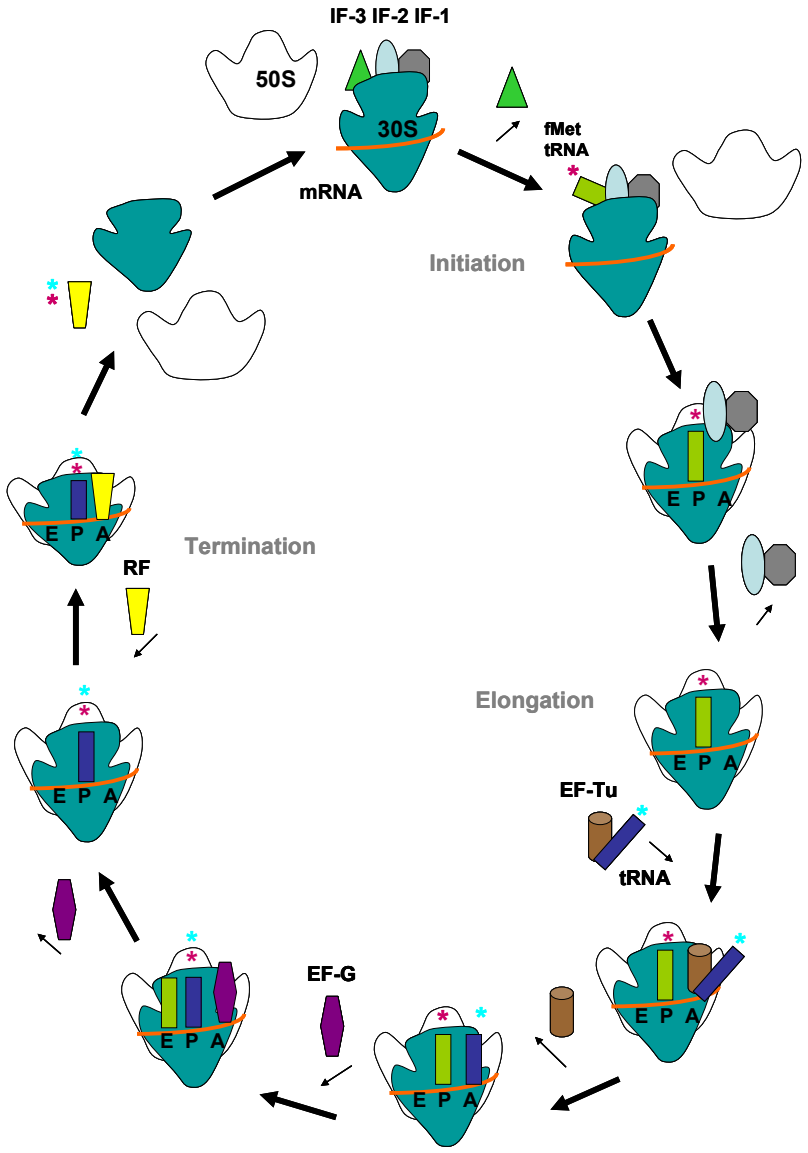


**Figure 1.6. A schematic of protein synthesis as observed in bacterial ribosomes.** Translation can be subdivided into three stages, initiation, elongation, and termination. Details of each step are given in the text. The large and small subunits are shown in white and aqua, respectively. The initiation factors, IF-1, IF-2, and IF-3 are highlighted in gray, pale blue, and green while the mRNA is in orange and the fMet-tRNA is lime colored. The elongation factors, EF-Tu and EF-G are shown in brown and purple respectively, while the new tRNA is dark blue. The elongation phase will continue until a stop codon is read in the mRNA message. The release factor (RF) is depicted in yellow at the termination stage of protein synthesis and the ribosomes are dissociated for another round of translation. The pink and cyan asterisks represent the first methionine and next amino acid added to the growing polypeptide chain. The A, P, and E sites correspond to aminoacyl, peptidyl, and exit sites on the ribosome. This figure was adapted from (Berk and Cate 2007).

### 1.4.1 Prokaryotic and Mitochondrial Initiation Factors

Prokaryotes use three initiation factors (IF-1, IF-2, IF-3) for the first phase of protein synthesis. IF-1 is the smallest bacterial initiation factor of only 8.2 kDa, yet highly conserved in archaeal and eukaryotes. This factor acts to maintain the fidelity of the initiation process by ensuring only the initiator tRNA, docks to the P site (Moazed et al. 1995). Furthermore, it is speculated IF-1 could be essential for cell viability as if depleted slow growth was observed and the formation of short polysomes (Cummings and Hershey 1994). IF-2, a GTPase, is most conserved at its C-terminal end, and has three different isoforms (Laursen et al. 2002). The ratio of the three isoforms is approximately the same under optimal growth conditions, yet in response to cold shock the two smaller isoforms dominant (Sacerdot et al. 1992). Specific functions correlating with this initiation factor are having an affinity for the initiatior tRNA and promoting subunit association (Choi et al. 1998; Pestova et al. 2000). However, this translation factor also serves as a chaperone for protein folding and assists in translating leaderless messages (Caldas et al. 2000; Grill et al. 2000). IF-3 is composed of two structural domains connected by a linker that varies in length and is critical for function (Fortier et al. 1994; Kycia et al. 1995; de Cock et al. 1999). This translation factor prevents formation of the 70S ribosome by binding to the 30S subunit, therefore blocking the ability for the 50S subunit to associate with the small subunit (Sacerdot et al. 1996). Another possible function is in recycling of the ribosomal subunits (Karimi et al. 1999).

Interestingly, only homologs for IF-$2_{mt}$ and IF-$3_{mt}$ have been identified in mitochondria (Liao and Spremulli 1990; 1991; Koc and Spremulli 2002). It is speculated IF-$2_{mt}$ may compensate for the lack of IF-1 by the increase in size and inserted functional domain (Gaur et al. 2008). IF-$2_{mt}$ is ~85 kDa in size, a GTPase, and a monomeric protein. This factor preferentially promotes the binding of the initiator tRNA to the 28S subunit compared to its affinity for Met-tRNA (Spencer and Spremulli 2004). On the other hand, IF-$3_{mt}$ is less conserved and has extensions at both the N-terminal and C-terminal domain (Koc and Spremulli 2002). The general function of this translation factor is dissociating the intact 55S ribosome into its individual subunits creating a pool of 28S and 39S for IF-$2_{mt}$ binding (Koc and Spremulli 2002).

### 1.4.2 Prokaryotic and Mitochondrial Elongation Factors

The elongation step of protein synthesis requires two main factors, EF-Tu and EF-G, which are also present in mitochondria (Cai et al. 2000a; b). Particularly, the N-terminal domain of EF-Tu contains the guanine nucleotide binding site and GTPase activity, while all three domains of the protein interact with the aa-tRNA (Wiborg et al. 1994). Each EF-Tu functions in a similar manner except for two distinct differences. First *E. coli* EF-Tu readily binds guanine nucleotides, while EF-$Tu_{mt}$ has a low affinity for the same nucleotides (Schwartzbach and Spremulli 1991). Second, EF-$Tu_{mt}$ can form a ternary complex with bacterial or mitochondrial aa-tRNAs and anchor them to the A site, while *E. coli* EF-Tu can only bind mitochondrial aa-tRNAs but is incapable of delivering them to the A site ((Kumazawa et al. 1991).

EF-G, which is responsible for the translocation step of protein synthesis, can be subdivided into five domains (Czworkowski et al. 1994). Domain I also called the G domain possesses the catalytic site for GTP hydrolysis, while domains III-V are critical for the translocation process (Martemyanov and Gudkov 2000; Savelsbergh et al. 2000). EF-$G_{mt}$ was initially purified in 1990 from bovine liver, yet not fully characterized until 2004 (Chung and Spremulli 1990; Bhargava et al. 2004). EF-$G_{mt}$ is fully functional on both mitochondrial and bacterial ribosomes, however *E. coli* EF-G is only active in prokaryotic ribosomes unless the L7/L12 stalk is replaced (Eberly et al. 1985; Bhargava et al. 2004; Terasaki et al. 2004).

## 1.5 Phosphorylation of Ribosomal Proteins

Phosphorylation of mitochondrial proteins is one of the most important post-translational modifications implicated in signal transduction and disease states within this organelle (Salvi et al. 2005; Hopper et al. 2006; Gottlieb 2007). In fact, there are at least twenty-five kinases and eight phosphatases which have been localized to the mitochondria and could be responsible for reversible phosphorylation as shown in Table 1.3 (Horbinski and Chu 2005; Salvi et al. 2005). Since mitochondrial ribosomes are responsible for translating some of the essential components in oxidative phosphorylation, it is plausible to suggest regulation of this process by its end product, ATP. Many of the

**TABLE 1.3 – Kinases and phosphatases localized to the mitochondria[a]**

| Kinases | Location Within | Phosphatases | Location Within |
|---|---|---|---|
| Src | Inter-membrane Space | MKP-1 | Outer Membrane |
| | Inner Membrane | PTP1D | Outer Membrane |
| Lyn | Inter-membrane Space | PTPMT1 | Inner Membrane |
| | Inner Membrane | SHP-2 | Inter-membrane Space |
| Fyn | Inter-membrane Space | | Inner Membrane |
| | Inner Membrane | TIM50 | Inner Membrane |
| Csk | Inter-membrane Space | PP1 | Outer Membrane |
| | Inner Membrane | PP2A | Outer Membrane |
| Fgr | Inter-membrane Space | PP2Cγ | Unknown |
| | Inner Membrane | PDPs | Matrix |
| Abl | Unknown | BCKDP | Matrix |
| EGFR | Inner Membrane | | |
| RAF1 | Outer Membrane | | |
| RIP3 | Unknown | | |
| MEK | Outer Membrane | | |
| PAK5 | Outer Membrane | | |
| CKI | Outer Membrane | | |
| GSK3β | Unknown | | |
| ERK | Outer Membrane | | |
| | Inter-membrane Space | | |
| CKII | Unknown | | |
| JNK | Outer Membrane | | |
| SAPK3 | Outer Membrane | | |
| CDK11 | Outer Membrane | | |
| PCTAIRE2 | Unknown | | |
| PKA | Outer Membrane | | |
| | Matrix | | |
| Akt | Inner Membrane | | |
| | Matrix | | |
| PKC | Outer Membrane | | |
| | Inner Membrane | | |
| DMPK | Unknown | | |
| PINK1 | Unknown | | |
| mTOR | Outer Membrane | | |
| PDK | Matrix | | |
| BCKDK | Matrix | | |

[a]Adapted from Pagliarini and Dixon 2006.

respiratory chain complexes are known to be phosphorylated including at least five of the subunits of Complex I and two subunits of ATP synthase (Struglics et al. 1998; Palmisano et al. 2007). In addition, both the mitochondrial and bacterial EF-Tu, part of the translational machinery, were detected as phosphorylated (Lippmann 1993; He et al. 2001). In comparison, regulation of bacterial ribosomes by phosphorylation has already been demonstrated several times. In two early *in vitro* phosphorylation studies of *E. coli* and *Streptomyces collinus* ribosomes, the ribosomal proteins phosphorylated by a cAMP dependent protein kinase from rabbit skeletal muscle and a protein kinase associated with the ribosomes, which cross-reacted with a PKC antibody were identified, respectively (Traugh and Traut 1972; Mikulik et al. 2001). *E. coli* ribosomal proteins S4, S9, S18, S19, L2, L3, L5, L7/L12, L10, and L33 were phosphorylated by the protein kinase from rabbit skeletal muscle at their Ser and Thr residues (Traugh and Traut 1972) and *S. collinus* ribosomal proteins S3, S4, S12, S13, S14, S18, L2, L7/L12, L16, L17, and L23 were determined to be Ser and Thr phosphorylated by the protein kinase associated with the ribosomes (Mikulik et al. 2001). The *in vitro* phosphorylation of ribosomal proteins was found to change the conformation or substrate binding sites in the ribosome and led to a 50% loss of activity in protein synthesis (Traugh and Traut 1972; Mikulik and Janda 1997; Mikulik et al. 2001). In a recent high-throughput analysis of the steady-state phosphoproteome of *E. coli,* ribosomal proteins S7, L7/L12, L16, L19, and L28 were detected as phosphorylated (Macek et al. 2008). Moreover, phosphorylation of L7/L12 and L18 in *Thermus thermophilus* and *Bacillus stearothermophilus* was reported previously (Bloemink and Moore 1999; Ilag et al. 2005). Therefore, with this background knowledge of phosphorylation, two ribosomal proteins, DAP3 and L7/L12, were chosen for detailed functional studies addressing the significance of phosphorylation in apoptosis and translation.

## 1.6 Phosphorylation of Apoptotic Mitochondrial Ribosomal Protein - DAP3

Four mammalian mitochondrial ribosomal proteins (MRPs), two from each subunit, have been demonstrated to be involved in apoptotic signaling pathways (Kissil et al. 1999; Koc et al. 2001d; Miyazaki and Reed 2001; Levshenkova et al. 2004;

Chintharlapalli et al. 2005). Apoptosis, otherwise known as programmed cell death, is a very important cellular process with regard to development, aging, cancer, and neurological diseases. Mitochondria play a crucial role in the intrinsic pathway, whereby a death stimulus such as oxidative stress or chemical induction triggers the release of cytochrome c from the inter-membrane space (Hengartner 2000). Next, cytochrome c interacts with Apaf1 (apoptosis protease activating factor 1) which leads to an activated caspase 9 and formation of the apoptosome (Hengartner 2000). Caspase 3 is cleaved and activated which sparks a cascade of reactions eventually leading to DNA fragmentation and death of the cell (Hengartner 2000).

### 1.6.1 Identification and History of DAP3

One of these apoptotic mitochondrial ribosomal proteins, MRPS29, more commonly known as DAP3 (death associated protein 3), was first identified as a positive mediator of interferon-γ induced cell death through a functional screen of HeLa cells transfected with an antisense cDNA library (Kissil et al. 1995). DAP3 also promotes apoptosis that is induced by tumor necrosis factor α and Fas as observed by structure-function studies (Kissil et al. 1999). However, DAP3 protects ataxia telangiectasia (genetic neurodegenerative disease) cells from apoptosis induced by ionizing radiation and streptonigrin, a metal-dependent antibiotic having anti-tumor activity (Henning 1993). In addition, a study using glioma cells having an induced motility phenotype found DAP3 to be overexpressed and the cells became resistant to apoptosis by the topoisomerase inhibitor, camptothecin (Mariani et al. 2001). Interestingly, DAP3 interacts with hNOA1 (human nitric oxide associated protein 1) and knockdown of this protein made cells more resistant to interferon-γ and staurosporine, a non-selective protein kinase inhibitor (Tang et al. 2008).

Although originally identified as an apoptotic protein, DAP3 also has a second function, being the only GTP-binding protein found in the small subunit of the mammalian and yeast mitochondrial ribosomes (Denslow et al. 1991; Koc et al. 2001b; Saveanu et al. 2001). The presence of this protein accounts for the high specific GTP-binding affinity of small subunits of mitochondrial ribosomes (Denslow et al. 1991).

Immuno-EM studies have localized DAP3 to the base of the lower lobe of the small subunit on the solvent side of the ribosome (O'Brien T et al. 2005), but its exact function in protein synthesis is still unknown. In yeast, DAP3 is required for mitochondrial DNA synthesis and respiration, suggesting this protein has a role in translation (Berger et al. 2000). Furthermore, DAP3 appears to have an impact on mitochondrial physiology as overexpression of the protein results in mitochondrial fragmentation, while DAP3 deficiency in mice is lethal *in utero* with abnormal, shrunken mitochondria (Mukamel and Kimchi 2004; Kim et al. 2007).

### 1.6.2 Post-Translational Modifications of DAP3

DAP3, a ribosomal protein found to be both pro-apoptotic and anti-apoptotic, could be regulated at the post-translational level (Figure 1.7). Post-translational modifications such as prenylation and phosphorylation are a common regulatory theme for proteins involved in apoptosis and cancer. For example, Ras, a proto-oncogene, is modified by farnesyl transferase, which adds a prenyl group to the C-terminal end of the protein (Kato et al. 1992). This lipid modification increases the hydrophobicity of the Ras protein and allows for its localization to the intracellular surface of the cellular membrane to function in oncogenic signal transduction. BIM, when phosphorylated by ERK/MAPK inhibits its pro-apoptotic ability, while phosphorylation of BIM by JNK favors cell death (Lei and Davis 2003; Harada et al. 2004). BAD is able to be phosphorylated by a serine-threonine kinase called Akt and this leads to the inability to promote apoptosis (del Peso et al. 1997). Therefore, it is not surprising that DAP3-induced apoptosis may also be regulated at the post-translational level, which serves as a molecular switch.

Human DAP3 consists of 398 amino acid residues, while the mature form is 380 residues long and 43.6 kDa in mass (Koc et al. 2001d). There are several functionally relevant motifs in the DAP3 sequence as highlighted in Figure 1.7. This ribosomal protein is localized to the mitochondria by a mitochondrial signal sequence at its N-terminal domain consisting of approximately the first seventeen residues (Mukamel and Kimchi 2004). One unique characteristic is that DAP3 is a GTP-binding protein and the three conserved motifs are apparent in the amino acid sequence (Denslow et al. 1991).

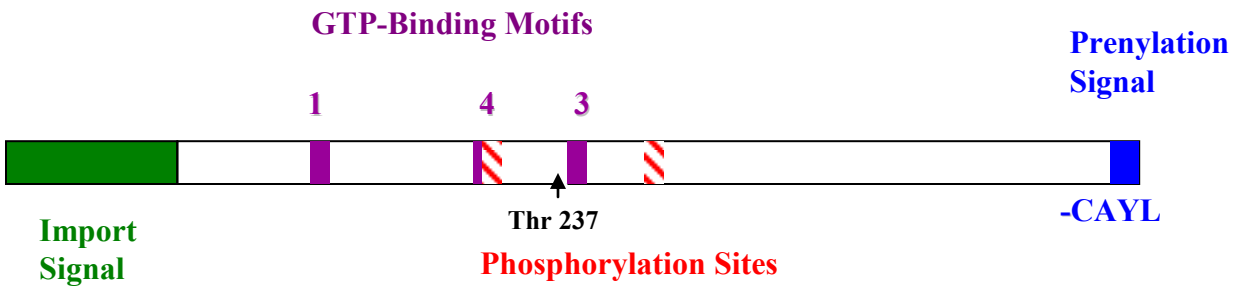


**Figure 1.7. GTP-binding motifs and predicted post-translational modification sites in DAP3.** The mitochondrial localization signal consisting of the first seventeen amino acids is in green. The three conserved GTP-binding motifs are highlighted in purple. Motif #1 is the P-loop region (GEKGTGKTLS), motif #3 (DAVG) is directly after the Thr237, a residue phosphorylated by Akt (Miyazaki et al. 2004), and motif #4 (NKRE) is important for guanine nucleotide specificity. The predicted cAMP and cGMP dependent phosphorylation sites are shown in red. Lastly, the putative prenylation signal (CAYL) at the C-terminus of the protein, which could possibly anchor DAP3 to the inner mitochondrial membrane, is in blue.

The first motif is the P-loop region (GEKGTGKTLS), which is required for apoptosis induction (Kissil et al. 1999). DAVG represents motif three, while motif four (NKRE) is just upstream and is important for guanine nucleotide specificity (Koc et al. 2001d). In addition, it is possible that MRPS27, a protein found in the small subunit of the mitochondrial ribosome, could serve as the guanine nucleotide exchange factor (GEF) for DAP3 because the protein contains one of the conserved recognition sequences (Koc et al. 2001a; Koc et al. 2001d).

A second feature is the putative prenylation site at the C-terminal end (CAYL) where C-terminal deletions have been shown to hinder apoptosis induction in 293 HEK cells (Kissil et al. 1999; Koc et al. 2001d). This lipid modification could follow the CAAX motif where A is either an aliphatic or aromatic amino acid and X is typically leucine. Geranylgeranyltransferase I would then be able to add a twenty carbon geranylgeranyl group to the cysteine residue. Such a modification could play a role in DAP3's ability to induce apoptosis as the geranylgeranyl group would make the protein more hydrophobic and may anchor it to the inner membrane of the mitochondria. It has already been shown that under normal conditions DAP3 is not prenylated as seen from GC/MS studies (Koc et al. 2001d). However, possible prenylation of DAP3 could disturb the membrane structure, which eventually might trigger the opening of the mitochondrial permeability transition pore during apoptosis.

The final distinguishing characteristic of DAP3 is the presence of numerous cAMP and cGMP dependent phosphorylation sites (Koc et al. 2001d). Phosphorylation of DAP3 could serve as a molecular switch, impacting protein synthesis as well as apoptosis and mitochondrial physiology. A previous study has shown that DAP3 can be phosphorylated at Thr237 by Akt (also known as protein kinase B) resulting in the suppression of anoikis, which is cell death caused by the detachment of adherent epithelial cells from the extracellular matrix (Miyazaki et al. 2004). Furthermore, mutating the phosphorylated residue resulted in an increased level of cell death as the survival kinase could no longer phosphorylate the site (Miyazaki et al. 2004). Recently,

the interaction of DAP3 with the serine-threonine kinase LKB1 and role of this kinase in DAP3-induced apoptosis have been studied in osteosarcoma cells (Takeda et al. 2007).

## 1.7 Phosphorylation of the L7/L12 Stalk

The large subunit of the ribosome is partially responsible for translocation along the mRNA in addition to catalyzing peptide bond formation, given the intrinsic peptidyl transferase activity (Nissen et al. 2000; Carter et al. 2001; Bacher et al. 2005). One unique structure of the large subunit is the L7/L12 stalk (L7 is the acetylated form of the protein). This highly flexible portion of the ribosome is conserved between prokaryotes and eukaryotes. The stalk referred to as the L8 complex in prokaryotes consists of a single copy of L10 and two dimers of L7/L12 for most bacteria or three dimers for some thermophiles and archaea (Ilag et al. 2005; Maki et al. 2007). In eukaryotes, the nomenclature for the stalk is the P complex, whereby P0 is L10 and P1/P2 are the L7/L12 proteins.

### 1.7.1 Structural Implications of the L7/L12 Stalk

Many studies have focused on this acidic ribosomal protein, attempting to capture the elusive structure by X-ray crystallography and cryo-electron microscopy (cryo-EM) to comprehend its complex nature and functional significance as observed in Figure 1.8 (Matadeen et al. 1999; Montesano-Roditis et al. 2001; Diaconu et al. 2005). Observing the 50S subunit of *E. coli* at 7.5 Å led to the remarkable finding of identifying the second L7/L12 dimer and therefore the entire L8 complex (Matadeen et al. 1999). Furthermore, by nanogold labeling and difference mapping the correct placement of *E. coli* L7/L12 on the 70S ribosome was deciphered, and it was suggested that conformational changes might occur during elongation (Montesano-Roditis et al. 2001). More recently, the structure of L10 in complex with three L7/L12 dimers was elucidated in *Thermotoga maritima* and resulted in better explanations for how L7/L12 played a role in factor binding and GTPase activation (Diaconu et al. 2005).

This structural information refined the image of L7/L12 and allowed for the dissection of more intricate details, specifically each functional domain. The N-terminal

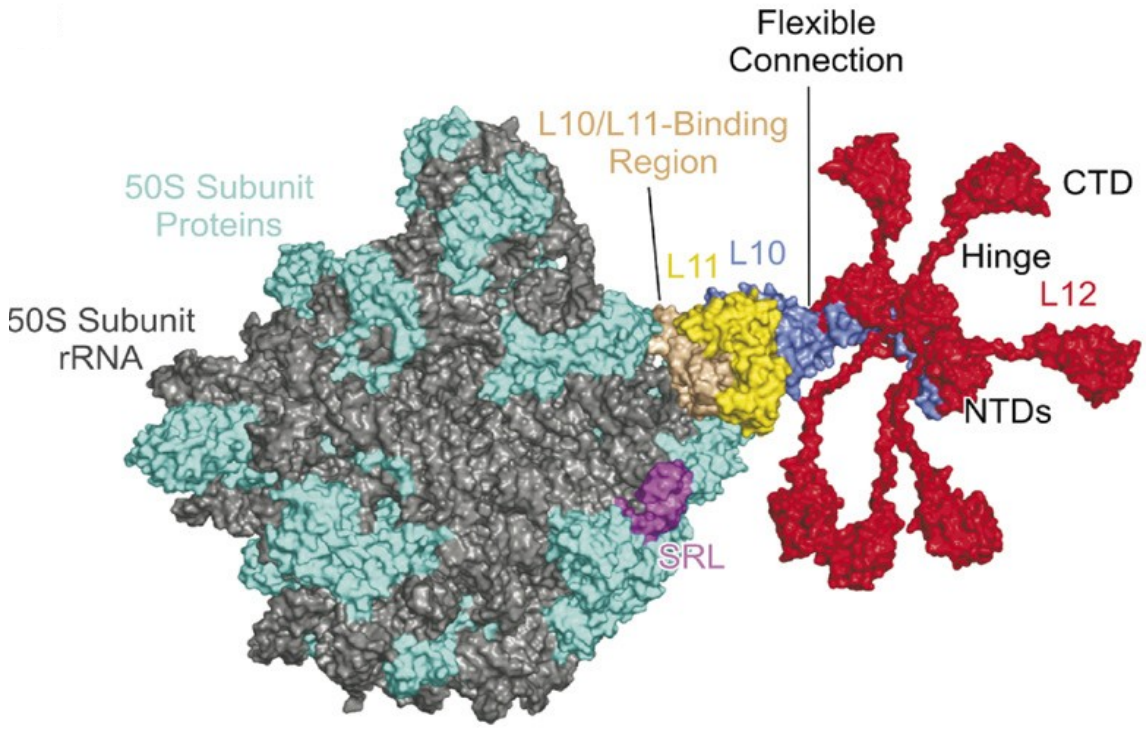


**Figure 1.8. Model of the L7/L12 stalk based on cryo-EM and X-ray structures.** Depicted is the large (50S) subunit of *T. maritima*. The large subunit ribosomal proteins and rRNA are in aqua and gray, respectively. On the right is the ribosomal protein L11 (yellow) and the L7/L12 stalk, which is composed of L10 (blue) and six copies of L7/L12 (red). Labeled in black are the three functional domains of L7/L12, the N-terminal domain which binds to L10, the long flexible hinge region, and the C-terminal domain which binds different GTPases. SRL is the sarcin-ricin loop of the large subunit. The PDB #s used to create this figure are 1MMS, 1RQU, and 1S72. Reprinted from *Cell*, 121, Diaconu et al., Structural Basis for the Function of the Ribosomal L7/12 Stalk in Factor Binding and GTPase Activation, 991-1004, Copyright © 2005, with permission from Elsevier.

domain is responsible for dimer formation and anchors L7/L12 to the ribosome by interacting with the C-terminal end of L10 (Gudkov and Behlke 1978). This C-terminal segment is critical for binding multiple GTPases by stimulating their activity and in essence promoting the synthesis of new polypeptides. Interestingly, *T. thermophilus* has a 2.5-fold higher elongation factor G (EF-G)-dependent GTPase activity compared to *E. coli* resulting from helix α6 within the C-terminal domain (Miyoshi et al. 2009). By mutagenesis, sites at the C-terminal region of L7/L12 were linked to EF-G binding and its timely dissociation from the ribosome (Savelsbergh et al. 2005). In addition, the association of this ribosomal protein to EF-G and EF-Tu catalyzed multiple rounds of GTP hydrolysis by altering the conformation of the G domain (Mohr et al. 2002; Nechifor and Wilson 2007). NMR studies revealed that initiation factor 2 (IF-2) and release factor 3 (RF-3) also have the potential to bind to L7/L12 and all four translational factors dock to several consensus amino acids in the C-terminal domain (Helgstrand et al. 2007). The hinge is described as the elongated, flexible arm connecting the N and C terminal domains together. This segment is necessary for conformational changes supporting the ability to tether different GTPases to the ribosome (Dey et al. 1995).

### 1.7.2 Post-Translational Modifications of L7/L12

With the extensive structural analysis of each functional domain almost complete, the focus shifts to how post-translational modifications of key amino acids can alter the typical function of each domain. In two earlier classic *in vitro* phosphorylation studies in *E. coli* and *Streptomyces collinus* ribosomes, L7/L12 was identified amongst a pool of ribosomal proteins as being phosphorylated at its Ser and Thr residues by a protein kinase from rabbit skeletal muscle and a protein kinase associated with the ribosomes, respectively (Traugh and Traut 1972; Mikulik and Janda 1997; Mikulik et al. 2001). Moreover, in *T. thermophilus*, a thermophile, phosphorylation of L7/L12 was reported on intact ribosomes, but was absent in the stalk complex (Ilag et al. 2005). Implying the phosphorylated form of L7/L12 may be more tightly associated with the ribosome, a recent work found acetylation of L7/L12 at the N-terminus to stabilize and therefore promote an interaction with ribosomal L10 particularly under unfavorable conditions (Ilag et al. 2005; Gordiyenko et al. 2008). Furthermore, in our comprehensive screen to

identify phosphorylated *E. coli* ribosomal proteins by mass spectrometry-based proteomics and in an additional study dissecting phosphorylated residues throughout the *E. coli* proteome during evolution, L7/L12 was detected (Macek et al. 2008; Soung et al. 2009). Not surprisingly, eukaryotic P1/P2 proteins are also phosphorylated both *in vitro* and *in vivo* by casein kinase II at their C-terminal end, which can affect both the level and function of the stalk proteins (Hasler et al. 1991). Interestingly, in the disease systemic lupus erythematosus (SLE) auto-antibodies are generated against the P proteins and phosphorylation could impact the antigenicity of these central ribosomal proteins (Hasler et al. 1991).

### 1.7.3 Identification of L12 in Mitochondria

In comparison, the mitochondrial ribosomal L12 homolog, which is larger in size due to a longer hinge region, has not been studied very extensively. This protein was originally identified as being the product of a delayed early response mRNA, which accumulates in the G1 phase of growth stimulated cells and a truncated version inhibits mitochondrial translation (Marty and Fort 1996). Furthermore, the mRNA for this ribosomal protein is highly expressed in the colon and the lack of mitochondrial activity is connected to tumor formation (Marty et al. 1997). The human gene is located on chromosome 17 at a locus which might serve as a marker for colon cancer (Marty et al. 1997). More recently, MRPL12 was shown to have a role in regulating mitochondrial transcription by directly interacting with the mitochondrial RNA polymerase and creating a feedback loop (Wang et al. 2007). Interestingly, in plant mitochondria there are four differentially expressed forms of L12 varying in molecular weight and pI due to different N-terminal extensions (Delage et al. 2007).

## 1.8 Research Aims

Mammalian mitochondrial ribosomes synthesize thirteen proteins that are essential for oxidative phosphorylation. Besides having a major role in ATP synthesis, mitochondria also contribute to biochemical processes coordinating apoptosis, mitochondrial diseases, and aging in eukaryotic cells. This unique class of ribosomes is protein-rich and distinct from cytoplasmic ribosomes. However, mitochondrial

ribosomes share a significant homology to bacterial ribosomes particularly in size, the general mechanism of translation, and ribosomal protein content. Therefore to better understand how mitochondrial translation is regulated we initially focused our efforts on bacterial ribosomes given the overall resemblance between the two systems. The reports of phosphorylated components of the bacterial and mitochondrial translational machinery, allowed us to hypothesize phosphorylation of bacterial and mitochondrial ribosomal proteins might be one mechanism of regulating translation (Traugh and Traut 1972; Salvi et al. 2005; Hopper et al. 2006; Gottlieb 2007). Phosphorylation could serve as an explanation for the changes in protein-protein as well as protein-RNA interactions observed during the different stages of protein synthesis. Two-dimensional gel electrophoresis of ribosomes coupled to [$\gamma$-$^{32}$P] ATP- labeling and immunoblotting with phospho-specific antibodies were used to detect phosphorylated ribosomal proteins. Gels were stained with a fluorescent dye to capture an image of total protein expression and combined with protein sequence analysis by capillary / liquid chromatography / nanoelectrospray / tandem mass spectrometry (capLC-ESI-MS/MS). Furthermore, the specific Ser, Thr, and Tyr residues were mapped by different enrichment techniques and emphasized the importance of phosphorylation in protein synthesis.

From these analyses, two ribosomal proteins DAP3 and L7/L12 were chosen to characterize how phosphorylation acts as a molecular switch in apoptosis induction and in translation. DAP3, also known as MRPS29, is specific to mitochondria and has been shown to be both a pro-apoptotic and anti-apoptotic protein (Henning 1993; Kissil et al. 1995). We hypothesized phosphorylation may serve as a regulatory mechanism by which DAP3 induces apoptosis. The sites of phosphorylation were mapped by mass spectrometry and site-directed mutagenesis studies on selected Ser and Thr residues investigated the effect of phosphorylation on cell viability and PARP cleavage as indication of caspase activation. Interestingly, the phosphorylated residues are clustered around the GTP-binding motifs and may induce conformational changes to the GTP-binding pocket of DAP3.

L7/L12 is highly conserved phosphoprotein, which in bacteria may be phosphorylated by ELKs (eukaryotic-like protein kinases) discovered by phylogenetic studies (Traugh and Traut 1972; Mikulik and Janda 1997; Ilag et al. 2005; Macek et al. 2008; Perez et al. 2008; Soung et al. 2009). We hypothesized the phosphorylated residues of L7/L12 may be responsible for the hinge rearrangements observed in translation. Initially, the specific phosphorylation sites of *E. coli* L7/L12 were mapped by proteomic techniques. The importance of L7/L12 phosphorylation was demonstrated both *in vitro* and *in vivo* by performing site-directed mutagenesis studies and analyzing the effect of each mutant pair by an *in vitro* translation assay. Furthermore, the homolog of L7/L12 in mitochondria is also phosphorylated and the functional significance of this post-translational modification is beginning to be understood.

## 1.9 References


Ahm, B.H., Kim, H.S., Song, S., Lee, I.H., Liu, J., Vassilopoulos, A., and Deng, C.X. 2008. A role for the mitochondrial deacetylase Sirt3 in regulating energy homeostasis. *Proc. Natl. Acad. Sci. U. S. A.* **105:** 14447-14452.

Amara, C.E., Shankland, E.G., Jubrias, S.A., Marcinek, D.J., Kushmerick, M.J. and Conley, K.E. 2007. Mild mitochondrial uncoupling impacts cellular aging in human muscles in vivo. *Proc. Natl. Acad. Sci. U. S. A.* **104:** 1057-1062.

Anderson, S., Bankier, A.T., Barrell, B.G., de Bruijn, M.H., Coulson, A.R., Drouin, J., Eperon, I.C., Nierlich, D.P., Roe, B.A., Sanger, F., et al. 1981. Sequence and organization of the human mitochondrial genome. *Nature* **290:** 457-465.

Anderson, S., de Brujin, M., Coulson, A., Eperon, I., Sanger, F., and Young, I. 1982. Complete sequence of bovine mitochondrial DNA: Conserved features of the mammalian mitochondrial genome. *J. Mol. Biol.* **156:** 683-717.

Arden, S.D., Roep, B.O., Neophytou, P.I., Usac, E.F., Duinkerken, G., de Vries, R.R., and Hutton, J.C. 1996. Imogen 38: a novel 38-kD islet mitochondrial autoantigen recognized by T cells from a newly diagnosed type 1 diabetic patient. *J. Clin. Invest* **97:** 551-561.

Bacher, J.M., de Crecy-Lagard, V., and Schimmel, P.R. 2005. Inhibited cell growth and protein functional changes from an editing-defective tRNA synthetase. *Proc. Natl. Acad. Sci. U. S. A.* **102:** 1697-1701.

Ban, N., Nissen, P., Hansen, J., Moore, P.B., and Steitz, T.A. 2000. The Complete Atomic Structure of the Large Ribosomal Subunit at 2.4 A Resolution. *Science* **289:** 905-920.

Beckmann, R., Spahn, C.M., Eswar, N., Helmers, J., Penczek, P.A., Sali, A., Frank, J., and Blobel, g. 2001. Architecture of the protein-conducting channel associated with the translating 80S ribosome. *Cell* **107:** 361-372.

Berger, T., Brigl, M., Herrmann, J.M., Vielhauer, V., Luckow, B., Schlondorff, D., and Kretzler, M. 2000. The apoptosis mediator mDAP-3 is a novel member of a conserved family of mitochondrial proteins. *J. Cell Sci.* **113:** 3603-3612.

Berk, V., and Cate, J.H. 2007. Insights into protein biosynthesis from structures of bacterial ribosomes. *Curr. Opin. Struct. Biol.***17:** 302-309.

Bhargava, K., Templeton, P., and Spremulli, L.L. 2004. Expression and characterization of isoform 1 of human mitochondrial elongation factor G. *Protein Expr. Purif.* **37:** 368-376.

Bischof, O., Urlaub, H., Kruft, V., and Wittmann-Liebold, B. 1995. Peptide environment of the peptidyl transferase center from Escherichia coli 70 S ribosomes as determined by thermoaffinity labeling with dihydrospiramycin. *J. Biol. Chem.* **270:** 23060-23064.

Bloemink, M.J., and Moore, P.B. 1999. Phosphorylation of ribosomal protein L18 is required for its folding and binding to 5S rRNA. *Biochemistry* **38:** 13385-13390.

Bonawitz, N.D., Clayton, D.A., and Shadel, G.S. 2006. Initiation and beyond: multiple functions of the human mitochondrial transcription machinery. *Mol. Cell* **24:** 813-825.

Brandon, M., Baldi, P., and Wallace, D.C. 2006. Mitochondrial mutations in cancer. *Oncogene* **25:** 4647-4662.

Brodersen, D.E., and Nissen, P. 2005. The social life of ribosomal proteins. *FEBS J.* **272:** 2098-2108.

Butow, R.A. and Avadhani, N.G. 2004. Mitochondrial signaling: the retrograde response. *Mol. Cell* **14:** 1–15.

Cai, Y.-C., Bullard, J.M., Thompson, N.L., and Spremulli, L.L. 2000a. Interaction of mammalian mitochondrial elongation factor EF-Tu with guanine nucleotides. *Prot. Sci.* **9:** 1791-1800.

Cai, Y.-C., Bullard, J.M., Thompson, N.L., and Spremulli, L.L. 2000b. Interaction of mitochondrial Elongation Factor Tu with aminoacyl-tRNA and Elongation Factor Ts. *J. Biol. Chem.* **275:** 20308-20314.

Caldas, T., Laalami, S., and Richarme, G. 2000. Chaperone properties of bacterial elongation factor EF-G and initiation factor IF2. *J. Biol. Chem.* **275:** 855-860.

Carter, A.P., Clemons, J., Brodersen, D.E., Morgan-Warren, R.J., Hartsch, T., Wimberly, B.T., and Ramakrishnan, V. 2001. Crystal Structure of an Initiation Factor Bound to the 30S Ribosomal Subunit. *Science* **291:** 498-501.

Carter, A.P., Clemons, W.M., Brodersen, D.E., Morgan-Warren, R.J., Wimberly, B.T., and Ramakrishnan, V. 2000. Functional insights from the structure of the 30S ribosomal subunit and its interactions with antibiotics. *Nature* **407:** 340-348.

Chintharlapalli, S.R., Jasti, M., Malladi, S., Parsa, K.V., Ballestero, R.P., and Gonzalez-Garcia, M. 2005. BMRP is a Bcl-2 binding protein that induces apoptosis. *J. Cell. Biochem.* **94:** 611-626.

Choi, S.-K., Lee, J., Zoll, W., Merrick, W., and Dever, T. 1998. Promotion of met-tRNA$^{Met}_i$ binding to Ribosomes by yIF2, a bacterial IF2 homolog in yeast. *Science* **280:** 1757-1760.

Chung, H.K., and Spremulli, L.L. 1990. Purification and characterization of elongation factor G from bovine liver mitochondria. *J. Biol. Chem.* **265:** 21000-21004.

Clayton, D.A. 1982. Replication of animal mitochondrial DNA. *Cell* **28:** 693-705.
Cummings, H., and Hershey, J. 1994. Translation initiation factor IF-1 is essential for cell viability in Escherichia coli. *J. Bact.* **176:** 198-205.

Czworkowski, J., Wang, J., Steitz, T., and Moore, P. 1994. The crystal structure of elongation factor G complexed with GDP at 2.7 A resolution. *EMBO J.* **13:** 3661-3668.

Datta, P.P., Sharma, M.R., Qi, L., Frank, J., and Agrawal, R.K. 2005. Interaction of the G' domain of elongation factor G and the C-terminal domain of ribosomal protein L7/L12 during translocation as revealed by cryo-EM. *Mol. Cell* **20:** 723-731.

de Cock, E., Springer, M., and Dardel, F. 1999. The interdomain linker of Escherichia coli initiation factor IF3: a possible trigger of translation initiation specificity. *Mol. Microbiol.* **32:** 193-202.

del Peso, L., Gonzalez-Garcia, M., Page, C., Herrera, R., and Nunez, G. 1997. Interleukin-3-induced phosphorylation of BAD through the protein kinase Akt. *Science* **278:** 687-689.

Delage, L., Giege, P., Sakamoto, M., and Marechal-Drouard, L. 2007. Four paralogues of RPL12 are differentially associated to ribosome in plant mitochondria. *Biochimie* **89:** 658-668.

DeLano, W.L.T. 2002. The PyMOL Molecular Graphics System. *DeLano Scientific***:** San Carlos, CA, U.S.A.

Denslow, N., Anders, J., and O'Brien, T.W. 1991. Bovine mitochondrial ribosomes possess a high affinity binding site for guanine nucleotides. *J. Biol. Chem.* **266:** 9586-9590.

Dey, D., Oleinikov, A.V., and Traut, R.R. 1995. The hinge region of Escherichia coli ribosomal protein L7/L12 is required for factor binding and GTP hydrolysis. *Biochimie* **77:** 925-930.

Diaconu, M., Kothe, U., Schlunzen, F., Fischer, N., Harms, J.M., Tonevitsky, A.G., Stark, H., Rodnina, M.V., and Wahl, M.C. 2005. Structural basis for the function of the ribosomal L7/12 stalk in factor binding and GTPase activation. *Cell* **121:** 991-1004.

Dontsova, O.A., Rosen, K.V., Bogdanova, S.L., Skripkin, E.A., Kopylov, A.M., and Bogdanov, A.A. 1992. Identification of the Escherichia coli 30S ribosomal subunit protein neighboring mRNA during initiation of translation. *Biochimie* **74:** 363-371.

Eberly, S.L., Locklear, V., and Spremulli, L.L. 1985. Bovine mitochondrial ribosomes. Elongation factor specificity. *J. Biol. Chem.* **260:** 8721-8725.

Eskes, R., Desagher, S., Antonsson, B., Martinou, J.C. 2000. Bid Induces the Oligomerization and Insertion of Bax into the Outer Mitochondrial Membrane. *Mol. Cell. Biol.* **20:** 929-935.

Fortier, P., Schmitter, J., Garcia, C., and Dardel, F. 1994. The N-terminal half of initiation factor 3 is folded as a stable independent domain. *Biochimie* **76:** 376-383.

Gaur, R., Grasso, D., Datta, P.P., Krishna, P.D., Das, G., Spencer, A., Agrawal, R.K., Spremulli, L., and Varshney, U. 2008. A single mammalian mitochondrial translation initiation factor functionally replaces two bacterial factors. *Mol. Cell* **29:** 180-190.

Goldenthal, M.J., and Marin-Garcia, J. 2004. Mitochondrial signaling pathways: a receiver/integrator organelle. *Mol. Cell. Biochem.* **262:** 1-16.

Gordiyenko, Y., Deroo, S., Zhou, M., Videler, H., and Robinson, C.V. 2008. Acetylation of L12 increases interactions in the Escherichia coli ribosomal stalk complex. *J. Mol. Biol.* **380:** 404-414.

Gottlieb, R.A. 2007. Identification of targets of phosphorylation in heart mitochondria. *Methods Mol. Biol.* **357:** 127-137.

Grill, S., Gualerzi, C.O., Londei, P., and Blasi, U. 2000. Selective stimulation of translation of leaderless mRNA by initiation factor 2: evolutionary implications for translation. *EMBO J.* **19:** 4101-4110.

Gudkov, A.T., and Behlke, J. 1978. The N-terminal sequence protein of L7/L 12 is responsible for its dimerization. *Eur. J. Biochem.* **90:** 309-312.

Hamilton, M.G., and O'Brien, T.W. 1974. Ultracentrifugal characterization of the mitochondrial ribosome and subribosomal particles of bovine liver: molecular size and composition. *Biochemistry* **13:** 5400-5403.

Harada, H., Quearry, B., Ruiz-Vela, A., and Korsmeyer, S.J. 2004. Survival factor-induced extracellular signal-regulated kinase phosphorylates BIM, inhibiting its association with BAX and proapoptotic activity. *Proc. Natl. Acad. Sci. U. S. A.* **101:** 15313-15317.

Hasler, P., Brot, N., Weissbach, H., Parnassa, A.P., and Elkon, K.B. 1991. Ribosomal proteins P0, P1, and P2 are phosphorylated by casein kinase II at their conserved carboxyl termini. *J. Biol. Chem.* **266:** 13815-13820.

He, H., Chen, M., Scheffler, N.K., Gibson, B.W., Spremulli, L.L., and Gottlieb, R.A. 2001. Phosphorylation of Mitochondrial Elongation Factor Tu in Ischemic Myocardium: Basis for Chloramphenicol-Mediated Cardioprotection. *Circ. Res.* **89:** 461-467.

Held,W.A., Ballou, B., Mizushima, S., and Nomura, M. 1974. Assembly mapping of 30S ribosomal proteins from Escherichia coli. Further studies. *J. Biol. Chem.* **249:** 3103-3111.

Helgstrand, M., Mandava, C.S., Mulder, F.A., Liljas, A., Sanyal, S., and Akke, M. 2007. The Ribosomal Stalk Binds to Translation Factors IF2, EF-Tu, EF-G and RF3 via a Conserved Region of the L12 C-terminal Domain. *J. Mol. Biol.* **365:** 468-479.

Hengartner, M.O. 2000. The biochemistry of apoptosis. *Nature* **407:** 770-776.

Henning, K.A. 1993. The molecular genetics of human diseases with defective DNA damage processing. In *Genetics*. Stanford University.

Hopper, R.K., Carroll, S., Aponte, A.M., Johnson, D.T., French, S., Shen, R.F., Witzmann, F.A., Harris, R.A., and Balaban, R.S. 2006. Mitochondrial matrix phosphoproteome: effect of extra mitochondrial calcium. *Biochemistry* **45:** 2524-2536.

Horbinski, C., and Chu, C.T. 2005. Kinase signaling cascades in the mitochondrion: a matter of life or death. *Free Radic. Biol. Med.* **38:** 2-11.

Ilag, L.L., Videler, H., McKay, A.R., Sobott, F., Fucini, P., Nierhaus, K.H., and Robinson, C.V. 2005. Heptameric (L12)6/L10 rather than canonical pentameric complexes are found by tandem MS of intact ribosomes from thermophilic bacteria. *Proc. Natl. Acad. Sci. U. S. A.* **102:** 8192-8197.

Jiang, X., and Wang, X. 2004. Cytochrome C-mediated apoptosis. *Annu. Rev. Biochem.* **73:** 87-106.

Karimi, R., Pavlov, M., Buckingham, R., and Ehrenberg, M. 1999. Novel Roles for Classical Factors at the Interface between Translation termination and Initiation. *Mol. Cell* **3:** 601-609.

Kashuba, E., Yurchenko, M., Yenamandra, S.P., Snopok, B., Isaguliants, M., Szekely, L., and Klein, G. 2008. EBV-encoded EBNA-6 binds and targets MRS18-2 to the nucleus, resulting in the disruption of pRb-E2F1 complexes. *Proc. Natl. Acad. Sci. U. S. A.* **105:** 5489-5494.

Kato, K., Cox, A.D., Hisaka, M.M., Graham, S.M., Buss, J.E., and Der, C.J. 1992. Isoprenoid addition to Ras protein is the critical modification for its membrane association and transforming activity. *Proc. Natl. Acad. Sci. U. S. A.* **89:** 6403-6407.

Khaitovich, P., Mankin, A.S., Green, R., Lancaster, L., and Noller, H.F. 1999. Characterization of functionally active subribosomal particles from Thermus aquaticus. *Proc. Natl. Acad. Sci. U. S. A.* **96:** 85-90.

Kim, H.R., Chae, H.J., Thomas, M., Miyazaki, T., Monosov, A., Monosov, E., Krajewska, M., Krajewski, S., and Reed, J.C. 2007. Mammalian dap3 is an essential gene required for mitochondrial homeostasis in vivo and contributing to the extrinsic pathway for apoptosis. *FASEB J.* **21:** 188-196.

Kissil, J.L., Cohen, O., Raveh, T., and Kimchi, A. 1999. Structure-function analysis of an evolutionary conserved protein, DAP3, which mediates TNF-alpha- and Fas-induced cell death. *EMBO J.* **18:** 353-362.

Kissil, J.L., Deiss, L.P., Bayewitch, M., Raveh, T., Khaspekov, G., and Kimchi, A. 1995. Isolation of DAP3, a novel mediator of interferon-gamma-induced cell death. *J. Biol. Chem.* **270:** 27932-27936.

Koc, E.C., Burkhart, W., Blackburn, K., Koc, H., Moseley, A., and Spremulli, L.L. 2001a. Identification of four proteins from the small subunit of the mammalian mitochondrial ribosome using a proteomics approach. *Prot. Sci.* **10:** 471-481.

Koc, E.C., Burkhart, W., Blackburn, K., Moseley, A., and Spremulli, L.L. 2001b. The small subunit of the mammalian mitochondrial ribosome: Identification of the full complement of ribosomal proteins present. *J. Biol. Chem.* **276:** 19363-19374.

Koc, E.C., Burkhart, W., Blackburn, K., Moyer, M.B., Schlatzer, D.M., Moseley, A., and Spremulli, L.L. 2001c. The large subunit of the mammalian mitochondrial ribosome. Analysis of the complement of ribosomal proteins present. *J. Biol. Chem.* **276:** 43958-43969.

Koc, E.C., Ranasinghe, A., Burkhart, W., Blackburn, K., Koc, H., Moseley, A., and L.L., S. 2001d. A new face on apoptosis: Death-associated protein 3 and PDCD9 are mitochondrial ribosomal proteins. *FEBS Lett.* **492:** 166-170.

Koc, E.C., and Spremulli, L.L. 2002. Identification of mammalian mitochondrial translational initiation factor 3 and examination of its role in initiation complex formation with natural mRNAs. *J. Biol. Chem.* **277:** 35541-35549.

Korostelev, A., Trakhanov, S., Laurberg, M., and Noller, H.F. 2006. Crystal structure of a 70S ribosome-tRNA complex reveals functional interactions and rearrangements. *Cell* **126:** 1065-1077.

Kumazawa, Y., Schwartzbach, C., Liao, H.-X., Mizumoto, K., Kaziro, Y., Watanabe, K., and Spremulli, L.L. 1991. Interactions of bovine mitochondrial phenylalanyl-tRNA with ribosomes and elongation factors from mitochondria and bacteria. *Biochim. Biophys. Acta.* **1090:** 167-172.

Kussmaul L, and Hirst, J. 2006. The mechanism of superoxide production by NADH:ubiquinone oxidoreductase (complex I) from bovine heart mitochondria. PNAS **103:** 7607-7612.

Kycia, J., Biou, V., Shu, F., Gerchman, S., Graziano, V., and Ramakrishnan, V. 1995. Prokaryotic translation initiation factor IF3 is an elongated protein consisting of two crystallizable domains. *Biochemistry* **34:** 6183-6187.

Laursen, B.S., de, A.S.S.A., Hedegaard, J., Moreno, J.M., Mortensen, K.K., and Sperling-Petersen, H.U. 2002. Structural requirements of the mRNA for intracistronic translation initiation of the enterobacterial infB gene. *Genes Cells* **7:** 901-910.

Lee, S.S., Lee, R.Y., Fraser, A.G., Kamath, R.S., Ahringer, J., and Ruvkun, G. 2003. A systematic RNAi screen identifies a critical role for mitochondria in C. elegans longevity. *Nat. Genet.* **33:** 40-48.

Lei, K., and Davis, R.J. 2003. JNK phosphorylation of Bim-related members of the Bcl2 family induces Bax-dependent apoptosis. *Proc. Natl. Acad. Sci. U. S. A.* **100:** 2432-2437.

Levshenkova, E.V., Ukraintsev, K.E., Orlova, V.V., Alibaeva, R.A., Kovriga, I.E., Zhugdernamzhilyn, O., and Frolova, E.I. 2004. The structure and specific features of the cDNA expression of the human gene MRPL37. *Bioorg. Khim.* **30:** 499-506.

Liao, H.-X., and Spremulli, L.L. 1990. Identification and initial characterization of translational initiation factor 2 from bovine mitochondria. *J. Biol. Chem.* **265:** 13618-13622.

Liao, H.-X., and Spremulli, L.L. 1991. Initiation of protein synthesis in animal mitochondria: Purification and characterization of translational initiation factor 2. *J. Biol. Chem.* **266:** 20714-20719.

Lippmann, C., Lindschau, C., Vijgenboom, E., Schroder, W., Bosch, L., and Erdmann, V.A. 1993. Prokaryotic elongation factor Tu is phosphorylated in vivo. *J. Biol. Chem.* **268:** 601-607.

Macek, B., Gnad, F., Soufi, B., Kumar, C., Olsen, J.V., Mijakovic, I., and Mann, M. 2008. Phosphoproteome analysis of E. coli reveals evolutionary conservation of bacterial Ser/Thr/Tyr phosphorylation. *Mol. Cell. Proteomics* **7:** 299-307.

Maki, Y., Hashimoto, T., Zhou, M., Naganuma, T., Ohta, J., Nomura, T., Robinson, C.V., and Uchiumi, T. 2007. Three binding sites for stalk protein dimers are generally present in ribosomes from archaeal organism. *J. Biol. Chem.* **282:** 32827-32833.

Margulis, L. 1981. Symbiosis in Cell Evolution. *W.H. Freeman***:** San Francisco, CA.

Mariani, L., Beaudry, C., McDonough, W.S., Hoelzinger, D.B., Kaczmarek, E., Ponce, F., Coons, S.W., Giese, A., Seiler, R.W., and Berens, M.E. 2001. Death-associated protein 3 (Dap-3) is overexpressed in invasive glioblastoma cells in vivo and in glioma cell lines with induced motility phenotype in vitro. *Clin. Cancer Res.* **7:** 2480-2489.

Martemyanov, K.A., and Gudkov, A.T. 2000. Domain III of Elongation Factor G from Thermus thermophilus Is Essential for Induction of GTP Hydrolysis on the Ribosome. *J. Biol. Chem.* **275:** 35820-35824.

Marty, L., and Fort, P. 1996. A delayed-early response nuclear gene encoding MRPL12, the mitochondrial homologue to the bacterial translational regulator L7/L12 protein. *J. Biol. Chem.* **271:** 11468-11476.

Marty, L., Taviaux, S., and Fort, P. 1997. Expression and human chromosomal localization to 17q25 of the growth-regulated gene encoding the mitochondrial ribosomal protein MRPL12. *Genomics* **41:** 453-457.

Matadeen, R., Patwardhan, A., Gowen, B., Orlova, E.V., Pape, T., Cuff, M., Mueller, F., Brimacombe, R., and van Heel, M. 1999. The Escherichia coli large ribosomal subunit at 7.5 A resolution. *Structure* **7:** 1575-1583.

Matthews, D.E., Hessler, R.A., Denslow, N.D., Edwards, J.S., and O'Brien, T.W. 1982. Protein composition of the bovine mitochondrial ribosome. *J. Biol. Chem.* **257:** 8788-8794.

Mikulik, K., and Janda, I. 1997. Protein kinase associated with ribosomes phosphorylates ribosomal proteins of Streptomyces collinus. *Biochem. Biophys. Res. Commun.* **238:** 370-376.

Mikulik, K., Suchan, P., and Bobek, J. 2001. Changes in ribosome function induced by protein kinase associated with ribosomes of Streptomyces collinus producing kirromycin. *Biochem. Biophys. Res. Commun.* **289:** 434-443.

Miyazaki, T., and Reed, J.C. 2001. A GTP-binding adapter protein couples TRAIL receptors to apoptosis-inducing proteins. *Nat Immunol* **2:** 493-500.

Miyazaki, T., Shen, M., Fujikura, D., Tosa, N., Kon, S., Uede, T., and Reed, J.C. 2004. Functional role of death associated protein 3 (DAP3) in anoikis. *J. Biol. Chem.* **279:** 44667-44672.

Miyoshi, T., Nomura, T., and Uchiumi, T. 2009. Engineering and Characterization of the Ribosomal L10-L12 Stalk Complex: A structural element responsible for high turnover of the elongation factor G-dependent GTPase. *J. Biol. Chem.* **284:** 85-92.

Mizushima, S., and Nomura, M. 1970. Assembly mapping of 30 S ribosomal proteins from Escherichia coli. *Nature* **226:** 1214.

Moazed, D., Samaha, R.R., Gualerzi, C., and Noller, H.F. 1995. Specific protection of 16 S rRNA by translational initiation factors. *J. Mol. Biol.* **248:** 207-210.

Mohr, D., Wintermeyer, W., and Rodnina, M.V. 2002. GTPase activation of elongation factors Tu and G on the ribosome. *Biochemistry* **41:** 12520-12528.

Montesano-Roditis, L., Glitz, D.G., Traut, R.R., and Stewart, P.L. 2001. Cryo-electron Microscopic Localization of Protein L7/L12 within the Escherichia coli 70 S Ribosome by Difference Mapping and Nanogold Labeling. *J. Biol. Chem.* **276:** 14117-14123.

Montoya, J., Ojala, D., and Attardi, G. 1981. Distinctive features of the 5'-terminal sequences of the human mitochondrial mRNAs. *Nature* **290:** 465-470.

Mukamel, Z., and Kimchi, A. 2004. Death-associated protein 3 localizes to the mitochondria and is involved in the process of mitochondrial fragmentation during cell death. *J. Biol. Chem.* **279:** 36732-36738.

Nechifor, R., and Wilson, K.S. 2007. Crosslinking of translation factor EF-G to proteins of the bacterial ribosome before and after translocation. *J. Mol. Biol.* **368:** 1412-1425.

Nissen, P., Hansen, J., Ban, N., Moore, P.B., and Steitz, T.A. 2000. The structural basis of ribosome activity in peptide bond synthesis. *Science* **289:** 920-930.

Noller, H.F., Hoang, L., and Fredrick, K. 2005. The 30S ribosomal P site: a function of 16S rRNA. *FEBS Lett.* **579:** 855-858.

O'Brien T, W., O'Brien B, J., and Norman, R.A. 2005. Nuclear MRP genes and mitochondrial disease. *Gene* **354:** 147-151.

Ogawa, F., Adachi, S., Kohu, K., Shige, K., and Akiyama, T. 2003. Binding of the human homolog of the Drosophila discs large tumor suppressor protein to the mitochondrial ribosomal protein MRP-S34. *Biochem. Biophys. Res. Commun.* **300:** 789-792.

Ojala, D., Merkel, C., Gelfand, R., and Attardi, G. 1980. The tRNA genes punctuate the reading of genetic information in human mitochondrial DNA. *Cell* **22:** 393-403.

Pagliarini, D.J., and Dixon, J.E. 2006. Mitochondrial modulation: reversible phosphorylation takes center stage? *Trends Biochem. Sci.* **31:** 26-34.

Palmisano, G., Sardanelli, A.M., Signorile, A., Papa, S., and Larsen, M.R. 2007. The phosphorylation pattern of bovine heart complex I subunits. *Proteomics* **7:** 1575-1583.

Patel, V.B., Cunningham, C.C., and Hantgan, R.R. 2001. Physiochemical Properties of Rat Liver Mitochondrial Ribosomes. *J. Biol. Chem.* **276:** 6739-6746.

Perez, J., Castaneda-Garcia, A., Jenke-Kodama, H., Muller, R., and Munoz-Dorado, J. 2008. Eukaryotic-like protein kinases in the prokaryotes and the myxobacterial kinome. **105:** *Proc. Natl. Acad. Sci. U. S. A.*15950-15955.

Perkins, G., Renken, C., Martone, M.E., Young, S.J., Ellisman, M., and Frey, T. 1997. Electron tomography of neuronal mitochondria: three-dimensional structure and organization of cristae and membrane contacts. *J. Struct. Biol.* **119:** 260-272.

Pestova, T.V., Lomakin, I.B., Lee, J.H., Choi, S.K., Dever, T.E., and Hellen, C.U. 2000. The joining of ribosomal subunits in eukaryotes requires eIF5B. *Nature* **403:** 332-335.

Saada, A., Shaag, A., Arnon, S., Dolfin, T., Miller, C., Fuchs-Telem, D., Lombes, A., and Elpeleg, O. 2007. Antenatal mitochondrial disease caused by mitochondrial ribosomal protein (MRPS22) mutation. *J. Med. Genet.* **44:** 784-786.

Sacerdot, C., Chiaruttini, C., Engst, K., Graffe, M., Milet, M., Mathy, N., and Springer, M. 1996. The role of the AUU initiation codon in the negative feedback regulation of the gene for translation initiation factor IF3 in *Escherichia coli*. *Mol. Micro.* **21:** 331-346.

Sacerdot, C., Vachon, G., Laalami, S., Morel-Deville, F., Cenatiempo, Y., and Grunberg-Manago, M. 1992. Both forms of translational initiation factor IF-2 ($\alpha$ and $\beta$) are required for maximal growth of *Escherichia coli*. *J. Mol. Biol.* **225:** 67-80.

Salvi, M., Brunati, A.M., and Toninello, A. 2005. Tyrosine phosphorylation in mitochondria: a new frontier in mitochondrial signaling. *Free Radic. Biol. Med.* **38:**1267-1277.

Saveanu, C., Fromont-Racine, M., Harington, A., Ricard, F., Namane, A., and Jacquier, A. 2001. Identification of 12 New Yeast Mitochondrial Ribosomal Proteins Including 6 That Have No Prokaryotic Homologues. *J. Biol. Chem.* **276:** 15861-15867.

Savelsbergh, A., Matassova, N.B., Rodnina, M.V., and Wintermeyer, W. 2000. Role of domains 4 and 5 in elongation factor G functions on the ribosome. *J. Mol. Biol.* **300:** 951-961.

Savelsbergh, A., Mohr, D., Kothe, U., Wintermeyer, W., and Rodnina, M.V. 2005. Control of phosphate release from elongation factor G by ribosomal protein L7/12. *EMBO J.* **24:** 4316-4323.

Schaffitzel, C., Oswald, M., Berger, I., Ishikawa, T., Abrahams, J.P., Koerten, H.K., Koning, R.I., and Ban, N. 2006. Structure of the E. coli signal recognition particle bound to a translating ribosome. *Nature* **444:** 503-506.

Schwartzbach, C., and Spremulli, L.L. 1991. Interaction of animal mitochondrial EF-Tu:EF-Ts with aminoacyl-tRNA, guanine nucleotides and ribosomes. *J. Biol. Chem.* **266:** 16324-16330.

Selmer, M., Dunham, C.M., Murphy, F.V.t., Weixlbaumer, A., Petry, S., Kelley, A.C., Weir, J.R., and Ramakrishnan, V. 2006. Structure of the 70S ribosome complexed with mRNA and tRNA. *Science* **313:** 1935-1942.

Sharma, M.R., Koc, E.C., Datta, P.P., Booth, T.M., Spremulli, L.L., and Agrawal, R.K. 2003. Structure of the mammalian mitochondrial ribosome reveals an expanded functional role for its component proteins. *Cell* **115:** 97-108.

Shuster, R.C., Rubenstein, A.J., and Wallace, D.C. 1988. Mitochondrial DNA in anucleate human blood cells. *Biochem. Biophys. Res. Commun.* **155:** 1360-1365.

Soung, G.Y., Miller, J.L., Koc, H., and Koc, E.C. 2009. Comprehensive analysis of phosphorylation sites in *E. coli* ribosomal proteins. *(in revision)*.

Spencer, A.C., and Spremulli, L.L. 2004. Interaction of mitochondrial initiation factor 2 with mitochondrial fMet-tRNA. *Nucleic Acids Res.* **32:** 5464-5470.

Struglics, A., Fredlund, K.M., Moller, I.M., and Allen, J.F. 1998. Two subunits of the F0F1-ATPase are phosphorylated in the inner mitochondrial membrane. *Biochem. Biophys. Res. Commun.* **243:** 664-668.

Subramanian, A.R. 1983. Structure and functions of ribosomal protein S1. *Prog. Nucleic Acid Res. Mol. Biol.* **28:** 101-142.

Suzuki, T., Terasaki, M., Takemoto-Hori, C., Hanada, T., Ueda, T., Wada, A., and Watanabe, K. 2001a. Proteomic Analysis of the Mammalian Mitochondrial Ribosome. Identification of protein components in the 28S small subunit. *J. Biol. Chem.* **276:** 33181-33195.

Suzuki, T., Terasaki, M., Takemoto-Hori, C., Hanada, T., Ueda, T., Wada, A., and Watanabe, K. 2001b. Structural compensation for the deficit of rRNA with proteins in the mammalian mitochondrial ribosome. Systematic analysis of protein components of the large ribosomal subunit from mammalian mitochondria. *J. Biol. Chem.* **276:** 21724-21736.

Takeda, S., Iwai, A., Nakashima, M., Fujikura, D., Chiba, S., Li, H.M., Uehara, J., Kawaguchi, S., Kaya, M., Nagoya, S., et al. 2007. LKB1 is crucial for TRAIL-mediated apoptosis induction in osteosarcoma. *Anticancer Res.* **27:** 761-768.

Tang, T., Zheng, B., Chen, S.H., Murphy, A.N., Kudlicka, K., Zhou, H., and Farquhar, M.G. 2008. hNOA1 interacts with complex I and DAP3 and regulates mitochondrial respiration and apoptosis. *J. Biol. Chem.* **284:** 5414-5424.

Terasaki, M., Suzuki, T., Hanada, T., and Watanabe, K. 2004. Functional compatibility of elongation factors between mammalian mitochondrial and bacterial ribosomes: characterization of GTPase activity and translation elongation by hybrid ribosomes bearing heterologous L7/12 proteins. *J. Mol. Biol.* **336:** 331-342.

Traugh, J.A., and Traut, R.R. 1972. Phosphorylation of ribosomal proteins of Escherichia coli by protein kinase from rabbit skeletal muscle. *Biochemistry* **11:** 2503-2509.

Van Dyke, N., Xu, W., and Murgola, E.J. 2002. Limitation of ribosomal protein L11 availability in vivo affects translation termination. *J. Mol. Biol.* **319:** 329-339.

Wallace, D. 1992. Diseases of the mitochondrial DNA. *Ann. Rev. Biochem.* **61:** 1175-1212.

Wallace, D.C. 1997. Mitochondrial DNA in aging and disease. *Sci. Am.* **277:** 40-47.

Wallace, D.C. 1999. Mitochondrial diseases in man and mouse. *Science* **283:**1482–88.

Wang, Z., Cotney, J., and Shadel, G.S. 2007. Human mitochondrial ribosomal protein MRPL12 interacts directly with mitochondrial RNA polymerase to modulate mitochondrial gene expression. *J. Biol. Chem.* **282:** 12610-12618.

Wiborg, O., Andersen, C., Knudsen, C., Kristensen, T., and Clark, B. 1994. Towards an understanding of structure-function relationships of elongation factor Tu. *Biotechnol. Appl. Biochem.* **19:** 3-15.

Wiesner, R.J., Ruegg, J.C., and Morano, I. 1992. Counting target molecules by exponential polymerase chain reaction: copy number of mitochondrial DNA in rat tissues. *Biochem. Biophys. Res. Commun.* **183:** 553-559.

Wimberly, B.T., Brodersen, D.E., Clemons, W.M., Jr, Morgan-Warren, R.J., Carter, A.P., Vonrhein, C., Hartsch, T., and Ramakrishnan, V. 2000. Structure of the 30S ribosomal subunit. *Nature* **407:** 327-339.

Wittmann-Liebold, B. 1985. Ribosomal proteins. In *Structure, function and genetics of ribosomes*. (eds. B. Hardesty, and G. Kramer), pp. 326-361. Springer-Verlag, New York.

Yusupov, M.M., Yusupova, G.Z., Baucom, A., Lieberman, K., Earnest, T.N., Cate, J.H.D., and Noller, H.F. 2001. Crystal Structure of the Ribosome at 5.5 A Resolution. *Science* **292:** 883-896.

Yusupova, G., Jenner, L., Rees, B., Moras, D., and Yusupov, M. 2006. Structural basis for messenger RNA movement on the ribosome. *Nature* **444:** 391-394.

Yusupova, G.Z., Yusupov, M.M., Cate, J.H., and Noller, H.F. 2001. The Path of Messenger RNA through the Ribosome. *Cell* **106:** 233-241.

Zangarelli, A., Chanseaume, E., Morio, B., Brugère, C., Mosoni, L., Rousset, P., Giraudet, C., Patrac, V., Gachon, P., Boirie, Y., Walrand, S. 2006. Synergistic effects of caloric restriction with maintained protein intake on skeletal muscle performance in 21-month-old rats: a mitochondria-mediated pathway. *FASEB J.* **20:** 2439-2450.

Zoratti, M., and Szabò, I. 1995. The mitochondrial permeability transition. *Biochim. Biophys. Acta.* **1241:** 139-176.

# CHAPTER 2

## Phosphorylated proteins of the mammalian mitochondrial ribosome: implications in protein synthesis and apoptosis

### 2.1 Rationale

Having developed the biochemical and proteomic techniques needed to identify phosphorylated ribosomal proteins in bacteria and map the residues by enrichment, a comparative study in bovine mitochondria was performed. The ribosomes from both systems share many properties including the overall structure of the small and large subunits, ribosomal protein content, and mechanism of translation. In mammalian mitochondria, the purpose of the ribosomes is to translate the thirteen hydrophobic protein products, which are subunits of the respiratory chain complexes required for ATP production. When the ATP levels in the cell are high, it is not necessary to keep producing energy and shutting down the translation of mitochondrial ribosomes is one way of controlling this process creating a negative feedback loop. Therefore, we hypothesize regulation of mitochondrial ribosomes by phosphorylation as a plausible mechanism coupled to the fact there have been multiple accounts of phosphorylation reported in bacterial ribosomes (Traugh and Traut 1972; Mikulik et al. 2001; Macek et al. 2008). We believe some of the conformational changes as well as the shifts in protein-protein and protein-RNA interactions observed during the different stages of protein synthesis could be mediated by phosphorylation.

Three different approaches were employed to detected phosphorylated mitochondrial ribosomal proteins given the low abundance and complexity. Specifically bovine mitochondrial ribosomes were separated by 2D-gel electrophoresis in conjunction to immunoblotting with phospho-specific antibodies, staining with ProQ Diamond phospho dye, or incubating the ribosomes with [$\gamma$-$^{32}$P] ATP. These techniques were reproducible and consistently identified a similar set of phosphorylated mitochondrial

ribosomal proteins. The initial mapping studies have been conducted identifying many putative phosphorylation sites. In addition to the proteomic work presented, we were interested in identifying candidate kinases responsible for endogenously phosphorylating the mitochondrial ribosomes. To address this question, commercial kinases localized to the mitochondria were tested in *in vitro* phosphorylation reactions, to determine if the kinase could phosphorylate mitochondrial ribosomal proteins. A second approach was to fractionate a mitochondrial lysate by strong cation exchange chromatography (SCX) to enrich for mitochondrial kinases. Together, the data from both methods serve as a foundation for more directed studies focusing on the endogenous kinase associated with mitochondrial ribosomes.

## 2.2 Abstract

Mitochondria are the powerhouses of cells, yet they also are involved in biochemical processes coordinating apoptosis, mitochondrial diseases, and aging in eukaryotic cells. Several phosphorylated components of the mitochondrial translation system have been implicated in some of these processes and disease states. However, there is still very limited knowledge on phosphorylation of mitochondrial ribosomal proteins and their role(s) in ribosome function. In this study, we have employed a combination of 2D-gel electrophoresis and mass spectrometry to analyze the mammalian mitochondrial ribosome for phosphorylation and identified the potential endogenous kinase associated with the ribosome responsible for the phosphorylation of twenty-four ribosomal proteins. Individual putative phosphorylation sites were mapped for each mitochondrial ribosomal protein by immobilized metal affinity chromatography (IMAC) and strong cation exchange chromatography (SCX) coupled to mass spectrometry. Moreover, we have demonstrated the phosphorylation and inhibition of protein synthesis *in vitro* by mitochondrial kinases PKA, PKCδ, and Abl Tyr kinase. Therefore, this study should serve as the framework for future studies addressing the regulation mechanisms of mitochondrial translation machinery responsible for the synthesis of thirteen essential proteins of oxidative phosphorylation.

## 2.3 Introduction

Mitochondria, according to the endosymbiotic theory, originally descended from ancient bacteria and became very specialized in producing the majority of the cell's energy in the form of ATP and earning its title as "powerhouse of the cell". To support oxidative phosphorylation, mitochondria contain their own unique ribosomes for the sole purpose of translating thirteen proteins, which are encoded by ~16.5 kb mitochondrial genome and located in the inner membrane to form the oligomeric complexes of oxidative phosphorylation.

The 55S mammalian mitochondrial ribosome primarily consists of proteins and contains about 67% protein and 33% RNA while the ratio is reversed in bacterial ribosomes (Pietromonaco et al. 1991; O'Brien 2002; Sharma et al. 2003). The small subunit (28S) is composed of a 12S rRNA and twenty-nine proteins while the large subunit (39S) consists of a 16S rRNA and forty-eight proteins (Hamilton and O'Brien 1974; Koc et al. 2001a; Koc et al. 2001b). The traditional roles of the small and large ribosomal subunits include binding and decoding mRNAs as well as catalysis of the peptide bond formation (Nissen et al. 2000; Carter et al. 2001; Yusupov et al. 2001; Yusupova et al. 2001). In mitochondria, however, some of the ribosomal proteins have acquired additional functions, linking this organelle to apoptosis, cancer and disease states, as well as the aging process and virus integration (Ogawa et al. 2003; Kashuba et al. 2008). For example, the small subunit proteins DAP3 (MRPS29) and MRPS30, and the large subunit proteins MRPL37 and MRPL41 are apoptotic proteins (Kissil et al. 1995; Koc et al. 2001c; Levshenkova et al. 2004; Chintharlapalli et al. 2005). Moreover, siRNA knockout of MRPL47 in *C. elegans* was found to increase the lifespan of worms at the expense of reduced oxygen consumption and ATP content (Lee et al. 2003). Therefore, as new roles are assigned to this dynamic organelle and ribosomes, it is essential to identify the function of mitochondrial ribosomal proteins and study how post-translational modifications might regulate protein synthesis and these new functions.

Phosphorylation of mitochondrial proteins is one of the most important post-translational modifications implicated in signal transduction and disease states within this

organelle (Salvi et al. 2005; Hopper et al. 2006; Gottlieb 2007). Because mitochondrial ribosomes are responsible for translating some of the essential components in oxidative phosphorylation, it is plausible to suggest regulation of this process by its end product, ATP. In fact, mitochondrial translation elongation factor, mtEF-Tu, becomes phosphorylated and causes inhibition of protein synthesis in ischemic myocardium (He et al. 2001). Similarly, components of the bacterial translational machinery are also known to be regulated by phosphorylation. Bacterial ribosomal proteins from *Escherichia coli* and *Streptomyces collinus* are phosphorylated by a protein kinase from rabbit skeletal muscle and a protein kinase associated with the ribosomes, respectively, which led to a 50% reduction in protein synthesis (Traugh and Traut 1972; Mikulik and Janda 1997; Mikulik et al. 2001; Macek et al. 2008). In a recent analysis of *E. coli* ribosomal proteins, we have identified and mapped additional phosphorylated proteins and revealed the significance of this post-translational modification in protein synthesis as summarized in Table 2.1 (Soung et al. 2009). Moreover, we mapped the phosphorylation sites in apoptotic mitochondrial ribosomal protein DAP3 (MRPS29) and determined the role of specific Ser and Thr phosphorylation sites in cell viability and PARP cleavage (Miller et al. 2008).

In this study, we identified phosphorylated bovine mitochondrial ribosomal proteins and a potential endogenous kinase responsible for this post-translational modification through the use of biochemical techniques and mass spectrometry. Of the seventy-seven proteins on the 55S mitochondrial ribosome, twenty-four are phosphorylated and the specific Ser, Thr, and Tyr residues were mapped by different enrichment approaches. Seven of them were small subunit proteins MRPS7, MRPS9, MRPS11, MRPS16, MRPS18-2, MRPS23, MRPS29 and seventeen were large subunit proteins MRPL1, MRPL2, MRPL3, MRPL9, MRPL10, MRPL11, MRPL13, MRPL15, MRPL18, MRPL22, MRPL24, MRPL27, MRPL28, MRPL40, MRPL43, MRPL45, and MRPL49. More interestingly, many of these bacterial homologs are also phosphorylated in *E. coli* as determined in our recent report (Soung et al. 2009). Furthermore, effects of ribosomal protein phosphorylation by additional mitochondrial kinases, PKA, PKCδ and Abl Tyr kinase, were evaluated in poly-U directed *in vitro* translation assays.

## 2.4 Results and Discussion

### 2.4.1 Phosphorylated Proteins of Bovine 55S Mitochondrial Ribosome

Mammalian mitochondrial 55S ribosomes are composed of two rRNA components and seventy-seven proteins (Koc et al. 2001a; Koc et al. 2001b). We identified twenty-four of the ribosomal proteins as phosphorylated at steady-state using 2D-gel and mass spectrometric analyses of mitochondrial ribosomes (Tables 2.2 and 2.3). Due to the abundance of basic amino acids in mitochondrial ribosomal proteins, purified 55S ribosome samples were first separated on 2D-NEPHGE (non-equilibrium pH gradient electrophoresis) gels and transferred to PVDF membranes for immunoblotting analysis with phospho-specific antibodies. Then, phosphorylated protein spots detected in blots were compared to a Sypro Ruby stained gel for total protein content and the corresponding proteins were excised and digested with trypsin for protein identification by mass spectrometry using locally maintained Swiss-Prot and mitochondrial protein databases (Figure 2.1A).

In this analysis, twenty mammalian mitochondrial ribosomal proteins; MRPS7, MRPS9, MRPS11, MRPS16, MRPS18-2, MRPS29, MRPL1, MRPL2, MRPL3, MRPL9, MRPL10, MRPL13, MRPL15, MRPL22, MRPL24, MRPL28, MRPL40, MRPL43, MRPL45, and MRPL49, were phosphorylated at Ser and/or Thr residues (Figure 2.1B and Table 2.3). However, only ten phosphoproteins from mitochondrial ribosomes were identified as Tyr phosphorylated including: MRPS7, MRPS18-2, MRPL2 MRPL9, MRPL10, MRPL15, MRPL22, MRPL24, MRPL45, and MRPL49 (Figure 2.1C and Table 2.3). In summary, the majority of the mitochondrial ribosomal proteins were phosphorylated at Ser and Thr residues, while less than half are phosphorylated at their Tyr residues, complementing our recent phosphoproteomic analysis of *E. coli* ribosomal proteins (Soung et al. 2009).

To support the results obtained from immunoblotting analyses and identify additional phosphoproteins of mitochondrial ribosomes, two other methods were performed. First, 2D-gels of ribosomal proteins were stained with a phospho-specific

**TABLE 2.1 – Phosphorylated proteins of *E. coli* ribosomes detected by immunoblotting and LC-MS/MS analyses[a]**

| Protein | pI | MW | Phosphosites | Detection | Function |
|---|---|---|---|---|---|
| S3 | 10.27 | 25.9 | Ser, Thr, Tyr | IB/MS | mRNA binding to ribosomes |
| S4 | 10.05 | 23.5 | Ser, Thr, Tyr | IB/MS | mRNA binding/Functional mutations |
| S5 | 10.11 | 17.5 | Ser, Thr, Tyr | IB/MS | mRNA binding/Functional mutations |
| S7 | 10.30 | 17.6 | Ser, Thr, Tyr | IB/MS | mRNA and tRNA binding at E site |
| S9 | 10.94 | 14.9 | Ser, Thr, Tyr | IB/MS | Interaction with P site tRNA |
| S11 | 11.33 | 13.8 | Ser, Thr | IB/MS | mRNA and tRNA binding at E site |
| S12 | 10.88 | 13.7 | Ser, Thr, Tyr | IB/MS | tRNA decoding at A site |
| S13 | 10.78 | 13.1 | Ser, Thr | MS | Subunit joining |
| S18 | 10.60 | 8.9 | Ser, Thr, Tyr | MS | mRNA binding to ribosomes |
| S21 | 11.15 | 8.5 | Tyr | IB/MS | mRNA binding to ribosomes |
| L2 | 10.93 | 29.9 | Ser, Thr | IB/MS | Required for peptidyl transferase |
| L3 | 9.90 | 22.2 | Ser, Thr | IB/MS | Required for peptidyl transferase |
| L4 | 9.72 | 22.1 | Ser, Thr, Tyr | IB/MS | Lines peptide exit tunnel |
| L5 | 9.49 | 20.3 | Tyr | IB/MS | Interaction with P site tRNA |
| L7/L12 | 4.60 | 12.2 | Ser, Thr | MS | Factor-binding stalk |
| L9 | 6.17 | 15.8 | Ser, Thr, Tyr | IB/MS | |
| L11 | 9.64 | 14.9 | Ser, Thr | IB/MS | Factor-binding |
| L13 | 9.91 | 16.0 | Thr, Tyr | IB/MS | |
| L15 | 11.18 | 15.0 | Tyr | IB/MS | |
| L16 | 11.22 | 15.3 | Tyr | IB/MS | A site tRNA binding |
| L19 | 10.57 | 13.3 | Ser, Thr, Tyr | IB/MS | Subunit joining |
| L20 | 11.47 | 13.5 | Ser, Tyr | IB/MS | |
| L22 | 10.23 | 12.2 | Ser, Thr, Tyr | IB/MS | Lines peptide exit tunnel |
| L23 | 9.94 | 11.2 | Ser, Thr | IB/MS | Interacts with chaperones and SRP |
| L24 | 10.21 | 11.3 | Ser, Thr | IB/MS | Interacts with chaperones and SRP |

[a]Adapted from Brodersen and Nissen 2005. IB; immunoblotting, MS; mass spectrometry.

**TABLE 2.2 – Characteristics of phosphorylated bovine mitochondrial ribosomal proteins**

| Protein | pI | Size (kDa) | Subunit | Phospho Sites[a] | *E. coli* Phosphorylated Homolog[b] |
|---|---|---|---|---|---|
| MRPS7 | 9.95 | 27.9 | 28S | T59, T63, Y64, T189 | Yes (S53, S56, S82, T83, Y84, S114, S124, Y153) |
| MRPS9 | 9.35 | 45.2 | 28S | S68, Y69, T70, T109, Y110, S114, S157, Y158, S160, T278, S290, S354, T357 | No |
| MRPS11 | 10.50 | 20.8 | 28S | T127, T133 | Yes (S16, S25, S54, S57, T58, T110, T113) |
| MRPS16 | 9.69 | 15.1 | 28S | Not detected | No |
| MRPS18-2 | 9.27 | 29.2 | 28S | Not detected | Yes (Y31, T33, S35) |
| MRPS23 | 8.90 | 21.6 | 28S | S58, T60, S151, S153, S158, T160 | No |
| MRPS29 | 9.31 | 45.6 | 28S | S214, T215, S219, S250, S251, S279 | No |
| MRPL1 | 9.03 | 36.6 | 39S | Y122, T126, T130, T181 | Yes (S40) |
| MRPL2 | 11.45 | 33.3 | 39S | T55, S56, T73, T74, T224 | Yes (T190) |
| MRPL3 | 9.45 | 38.6 | 39S | S66, T146, T151, S153 | Yes (T16, S21, T25) |
| MRPL9 | 10.04 | 30.0 | 39S | Not detected | No |

| | | | | | |
|---|---|---|---|---|---|
| MRPL10 | 9.83 | 29.3 | 39S | S105, S138, S170, T184, S187 | Yes (S147) |
| MRPL11 | 9.88 | 20.8 | 39S | Not detected | No |
| MRPL13 | 9.35 | 20.6 | 39S | Not detected | Yes (Y16, Y43, T44, T49, Y52) |
| MRPL15 | 10.15 | 33.7 | 39S | Y94, S98 | No |
| MRPL18 | 9.74 | 20.4 | 39S | Not detected | Yes (S45, S52, T53) |
| MRPL22 | 9.87 | 24.2 | 39S | S96 | Yes (T37, Y38, T39, T100, S101, T104) |
| MRPL24 | 9.47 | 24.8 | 39S | T177, S178 | No |
| MRPL27 | 10.19 | 16.0 | 39S | Y90 | No |
| MRPL28 | 9.21 | 30.0 | 39S | Y91 | Yes (T7) |
| [c]MRPL40 | 8.75 | 48.0 | 39S | S138, S210, T211, T212 | No |
| MRPL43 | 10.12 | 17.7 | 39S | T52, S88 | No |
| MRPL45 | 9.31 | 35.2 | 39S | S200, S201, T204 | No |
| MRPL49 | 9.65 | 19.3 | 39S | S41 | No |

[a]Putative phosphorylation sites. [b]Paper in revision (Soung et al. 2009). [c]Also known as MRPL37.

**TABLE 2.3 – Screening for phosphorylated proteins of bovine mitochondrial ribosomes by 2D-Gel electrophoresis coupled to LC-MS/MS analysis**

| | Immunoblotting Analysis | | | | |
|---|---|---|---|---|---|
| **Proteins** | **Ser** | **Thr** | **Tyr** | **ProQ** | **$^{32}$P** |
| MRPS7 | X | X | X | X | X |
| MRPS9 | X | | | | |
| MRPS11 | X | X | | X | X |
| MRPS16 | X | X | | | |
| MRPS18-2 | X | X | X | | X |
| MRPS23 | | | | | X |
| MRPS29 | X | | | | |
| MRPL1 | X | X | | X | |
| MRPL2 | X | X | X | | |
| MRPL3 | X | | | | X |
| MRPL9 | X | X | X | X | X |
| MRPL10 | X | X | X | X | X |
| MRPL11 | | | | | X |
| MRPL13 | X | X | | | |
| MRPL15 | X | X | X | | X |
| MRPL18 | | | | | X |
| MRPL22 | X | X | X | X | X |
| MRPL24 | X | X | X | X | X |
| MRPL27 | | | | | X |
| MRPL28 | X | | | | X |
| [a]MRPL40 | X | X | | X | X |
| MRPL43 | X | X | | | |
| MRPL45 | X | X | X | X | X |
| MRPL49 | X | X | X | X | X |

[a]Also known as MRPL37.

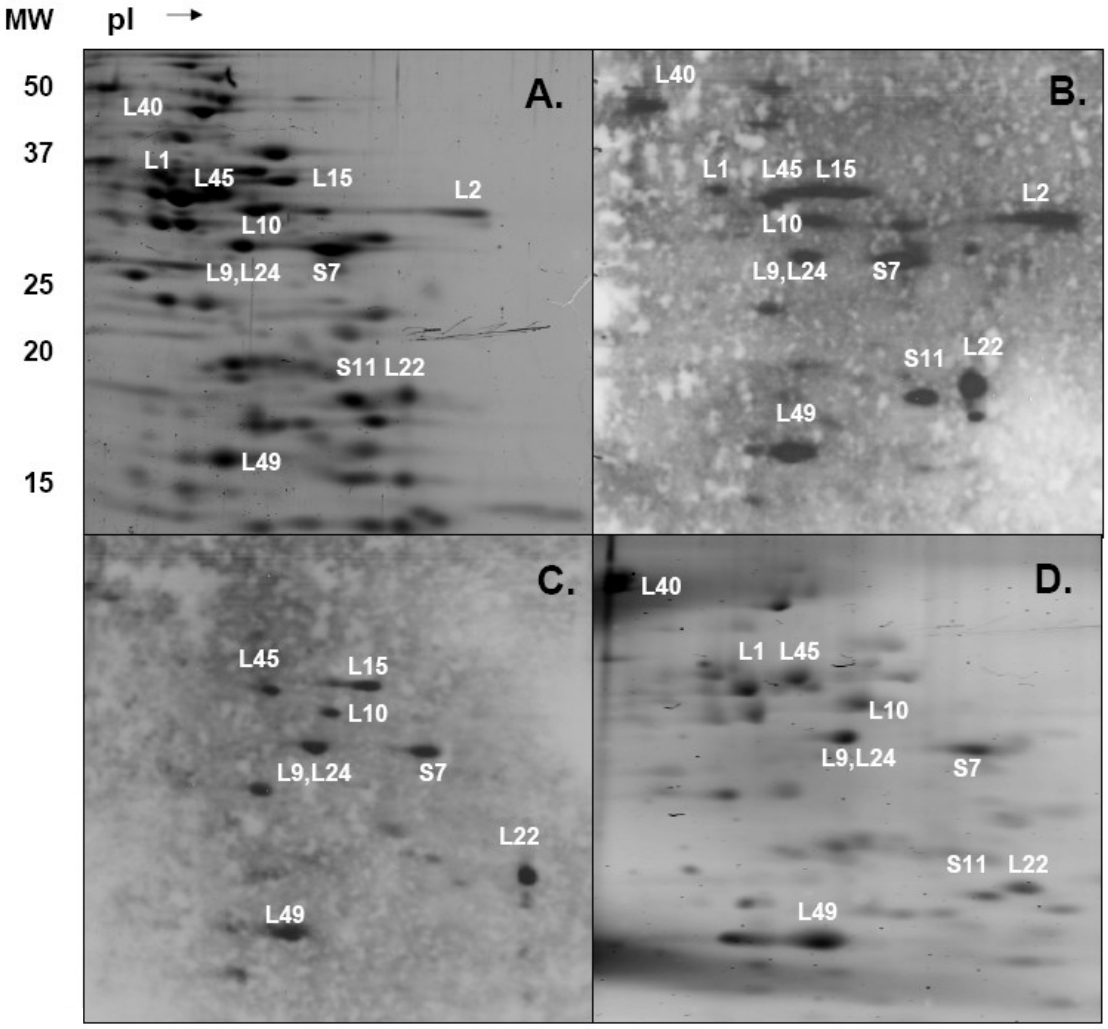


**Figure 2.1 – Two-dimensional gel analysis of phosphorylated mitochondrial ribosomal proteins.** Approximately, 1.8 $A_{260}$ units of bovine mitochondrial ribosomes were separated on non-equilibrium pH gradient electrophoresis (NEPHGE) gels using pI 3-10 and 8-10 ampholytes. The phosphorylated proteins were excised, digested with trypsin, and analyzed by LC-MS/MS for potential phosphorylation sites using an ion trap mass spectrometer. (A) SYPRO Ruby stained gel of the intact 55S bovine mitochondrial ribosomes. (B and C) Immunoblots of 55S ribosomes using anti-phosphoserine and anti-phosphotyrosine antibodies, respectively. Not all of the phosphorylated proteins identified by mass spectrometry are labeled in these 2D-gels. (D) ProQ Diamond phosphoprotein stained gel of intact 55S mitochondrial ribosomes visualized at 532 nm.

fluorescent dye, Pro-Q Diamond, and ten phosphorylated ribosomal proteins, MRPS7, MRPS11, MRPL1, MRPL9, MRPL10, MRPL22, MRPL24, MRPL40, MRPL45, and MRPL49 were identified from the tryptic digests of the 2D-gel spots with a strong fluorescent signal (Figure 2.1D and Table 2.3). Secondly, we incubated the mitochondrial ribosomes with [$\gamma$-$^{32}$P] ATP (Figure 2.2). In this *in vitro* phosphorylation assay, the majority of phosphoproteins identified in immunoblotting analyses were also detected to be phosphorylated by a trace amount of endogenous kinase(s) associated with the mitochondrial ribosomes. A total of seventeen phosphorylated mitochondrial ribosomal proteins, MRPS7, MRPS11, MRPS18-2, MRPS23, MRPL3, MRPL9, MRPL10, MRPL11, MRPL15, MRPL18, MRPL22, MRPL24, MRPL27, MRPL28, MRPL40, MRPL45, and MRPL49, were identified by in-gel tryptic digests of the Coomassie stained 2D-gel spots corresponding to radio-labeled spots (Figure 2.2 and Table 2.3).

### 2.4.2 Mapping the Phosphorylation Sites of Bovine 55S Mitochondrial Ribosome

Though non-equilibrium pH gradient electrophoresis (NEPHGE) is a powerful tool for identifying 55S phosphorylated proteins, few phosphorylated peptides were detected in the analyses. In general, multiple explanations can be attributed to this result. First, mitochondrial ribosomal proteins are very low abundant proteins resulting in the lack of sequence coverage due to the low recovery of different peptides from in-gel digestions. Therefore, it is crucial to obtain a sufficient amount of ribosomes for proteomic analyses addressing post-translational modifications. Second, these ribosomal proteins have a high frequency of lysine and arginine residues present in their amino acid sequences. Trypsin, though the most efficient protease for digestions, cleaves at the C-terminal end of lysine and arginine residues, reducing the number of peptides detected by the mass spectrometer and therefore increasing the probability of missing a phosphorylation site. Third, in the mitochondria, ribosomal proteins are continuously being phosphorylated by kinases and dephosphorylated by phosphatases, as this is a reversible modification. In addition, the ribosomal protein may only be phosphorylated at a particular stage of translation as there are many different conformational changes of the ribosome during protein synthesis. Therefore, the chances of obtaining the

phosphorylated form of the protein are greatly reduced, coupled to the fact the loss of phosphorylation may occur during the digest or MS analysis. On the other hand, the unmodified form of the protein is dominant and tryptic digestions will yield many unmodified peptides detected by the instrument, which will preferentially fragment these peptides.

Therefore, to enhance the probability of detecting phosphorylated peptides of ribosomal proteins from bovine mitochondria, two enrichment methods were employed, immobilized metal affinity chromatography (IMAC) and strong cation exchange chromatography (SCX). Initially, one-dimensional SDS-PAGE coupled to tryptic in-gel and in-solution digests of gradient purified 55S ribosomes were performed before enrichment. IMAC is based on the principle that phosphorylated peptides with anionic phosphate groups have a strong affinity for polyvalent metal cations such as gallium and iron under acidic conditions (Liebler 2002). However, these peptides are eluted from the column under basic conditions while selectively discriminating against acidic peptides. The second method chosen for enrichment was SCX, where peptides are eluted in order of increasing positive charge. Phosphopeptides, whose positive charge is reduced by addition of the negatively charged phosphate moiety, are expected to elute earlier than the rest of the peptides. Given the sensitivity level of the ion trap mass spectrometer, which is capable of multiple rounds of fragmentation, the increased sequence coverage, and enrichment strategies additional phosphorylated peptides were recovered, yielding putative phosphorylation sites. Each phosphorylated peptide had to meet stringent criteria including a Mascot score of at least 45 and a Sequest Xcorr coefficient cutoff of >1.5, 2.0, and 2.5 for +1, +2, +3 charged peptides respectively (Table 2.4). Furthermore, validation was performed using a mitochondrial protein database and the Swiss-Prot database. However, more analysis of 55S ribosomes is needed to identify all the Ser, Thr, and Tyr residues that are modified by phosphorylation.

### 2.4.3 Determining the Effect of Phosphorylation on Mitochondrial Translation

Having identified twenty-four phosphorylated ribosomal proteins in bovine mitochondria out of seventy-seven ribosomal proteins, it was concluded ~30% are

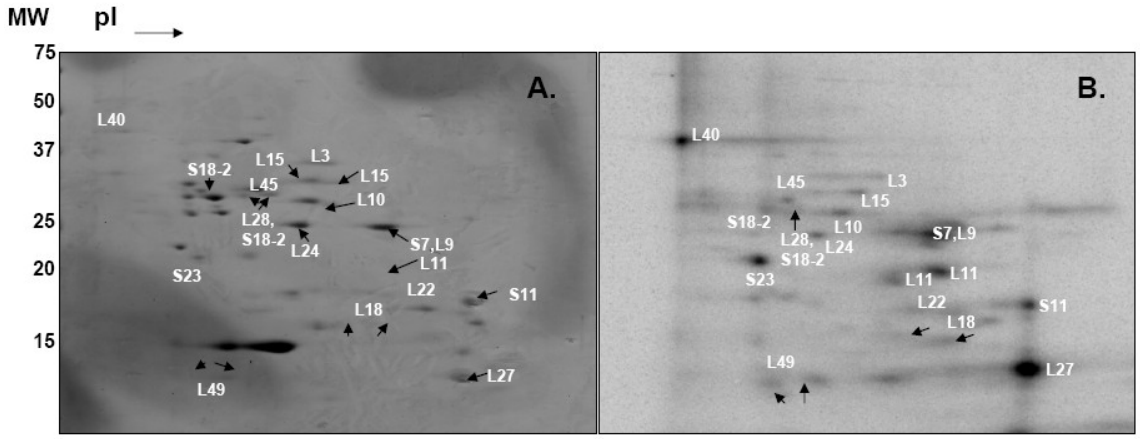


**Figure 2.2 – Two-dimensional gel analysis of *in vitro* phosphorylated mitochondrial ribosomal proteins using [$\gamma$-$^{32}$P] ATP.** Bovine mitochondrial ribosomes (1.8 $A_{260}$ units) were incubated in the presence of 50 μCi [$\gamma$-$^{32}$P] ATP for 1 hr at 30 °C and separated on NEPHGE gels using pI 3-10 and 8-10 ampholytes. The phosphorylated proteins were excised, digested with trypsin, and analyzed by LC-MS/MS for potential phosphorylation sites using an ion trap mass spectrometer. (A) Coomassie Blue stained gel and (B) Phosphor-image of intact 55S mitochondrial ribosomes. Not all of the phosphorylated proteins identified by mass spectrometry are labeled in these 2D-gels.

**TABLE 2.4 – Sequence coverage of phosphoproteins from bovine mitochondrial ribosomes**

| Protein | Accession # | # of Peptides | % Coverage |
|---|---|---|---|
| MRPS7 | Q3T040 | 8 | 49% |
| MRPS9 | Q58DQ5 | 12 | 45% |
| MRPS11 | P82911 | 6 | 33% |
| MRPS16 | P82915 | 2 | 13% |
| MRPS18-2 | P82918 | 3 | 19% |
| MRPS23 | Q2NL27 | 10 | 82% |
| MRPS29 | P82922 | 12 | 37% |
| MRPL1 | NP_001095314 | 6 | 26% |
| MRPL2 | Q2TA12 | 6 | 27% |
| MRPL3 | Q3ZBX6 | 6 | 30% |
| MRPL9 | Q2TBK2 | 7 | 38% |
| MRPL10 | Q3MHY7 | 5 | 40% |
| MRPL11 | Q2YDI0 | 4 | 35% |
| MRPL13 | Q3SYS1 | 5 | 32% |
| MRPL15 | Q0VC21 | 5 | 23% |
| MRPL18 | Q3ZBR7 | 5 | 40% |
| MRPL22 | Q3SZX5 | 5 | 28% |
| MRPL24 | Q3SYS0 | 6 | 42% |
| MRPL27 | Q32PC3 | 3 | 33% |
| MRPL28 | Q2HJJ1 | 3 | 14% |
| [a]MRPL40 | NP_001076869 | 8 | 22% |
| MRPL43 | Q95KE5 | 5 | 31% |
| MRPL45 | Q3T142 | 9 | 30% |
| MRPL49 | Q5EA71 | 6 | 43% |

[a]Also known as MRPL37.

modified. We hypothesized that this post-translational modification might affect the translation and provide a built in feedback loop to control ATP production. Phosphorylation could therefore be one of the regulatory mechanisms of protein synthesis in mammalian mitochondria. Likewise, it had already been shown that phosphorylating the bacterial ribosomes reduced the translation significantly by ~50% (Mikulik and Janda 1997; Mikulik et al. 2001). To determine the extent of phosphorylation, mitochondrial ribosomes were incubated in the presence of [$\gamma$-$^{32}$P] ATP alone and with various purified kinases known to be localized to the mitochondria such as PKA, PKCδ, and Abl protein Tyr kinase (Figure 2.3A). Due to the presence of endogenous kinases associated with mitochondrial ribosomes, a low level of phosphorylation was detected under steady-state conditions, yet the phosphorylation pattern intensified with the addition of commercial kinases (Figure 2.3A). For this reason, these kinases may serve as candidates endogenously phosphorylating the mitochondrial ribosomes *in vivo*. For example, cAMP-dependent protein kinase (PKA), a Ser/Thr kinase associates with A-kinase anchoring proteins (AKAPs), which allows for PKA to localize to the mitochondrial matrix (Chen et al. 2004). Recently, a comparative analysis of wild-type and cAMP deathless S49 lymphoma cells, indicated PKA-stimulated apoptosis occurs by way of the mitochondria (Zhang et al. 2008). In fact, PKA appeared to phosphorylate many of the ribosomal proteins in *in vitro* assays and the banding pattern resembled the control lane with only ribosomes and [$\gamma$-$^{32}$P] ATP implying the phosphorylation of the same proteins in the ribosome (Figure 2.3A). We have also demonstrated the phosphorylation of recombinant MRPS29 (also known as DAP3) at its highly conserved Ser and Thr residues by PKA and PKCδ *in vitro* (Miller et al. 2008). Lastly, as expected fewer mitochondrial ribosomal proteins were Tyr phosphorylated in comparison to our immunoblotting results shown in Figures 2.1C and 2.3A, yet Abl protein Tyr kinase has been shown to translocate to the mitochondria upon endoplasmic reticulum stress-induced apoptosis and in response to necrotic cell death caused by oxidative stress (Ito et al. 2001; Kumar et al. 2001).

Having observed the phosphorylation of mitochondrial ribosomal proteins with these kinases, poly-U directed *in vitro* translation assays were performed to test the role

of phosphorylation on protein synthesis. In these assays, prior to translation, ribosomes were phosphorylated by the addition of kinases and ATP *in vitro*. Upon addition of ATP and phosphorylation buffer as a control; inhibition of 6-7% was detected and this observation was in agreement with the extent of phosphorylation under steady-state conditions (Figure 2.3). However, in the presence of PKA and Abl protein Tyr kinase there was a significant inhibition, ~30%, in translation (Figure 2.3B). Furthermore, phosphorylation by PKCδ had no significant effect on translation and was comparable to the control assay performed in the presence of ATP (Figures 2.3). In conclusion, modification of the Ser, Thr, and Tyr residues of mitochondrial ribosomal proteins is a mechanism by which translation can be temporarily impaired so as not to exhaust the mitochondria and to compensate for the excess ATP produced.

### 2.4.4 Identification of Potential Endogenous Kinases Associated with the Mitochondrial Ribosomes

Our proteomic analysis thus far has resulted in the identification of phosphorylated small and large subunit mitochondrial ribosomal proteins and by enrichment strategies allowed for some putative phosphorylation sites to be mapped. Furthermore phosphorylation of mitochondrial ribosomes has a similar effect as on bacterial ribosomes, hindering protein synthesis. However, we were still missing one critical piece of data that is which kinase is responsible for phosphorylating the mitochondrial ribosomes. Bacterial ribosomes have been shown to be phosphorylated by a cAMP dependent protein kinase from rabbit skeletal muscle and a protein kinase associated with the ribosomes, which cross-reacted with a PKC antibody (Traugh and Traut 1972; Mikulik et al. 2001). Interestingly, in our *in vitro* phosphorylation reactions PKA, PKCδ, and Abl protein Tyr kinase each could phosphorylate the mitochondrial ribosomes as observed in Figure 2.3A and serve as possible candidates for the endogenous phosphorylation.

To pursue this investigation further instead of incubating the ribosomes in the presence of commercial kinases, we decided to isolate fractions with enriched kinase

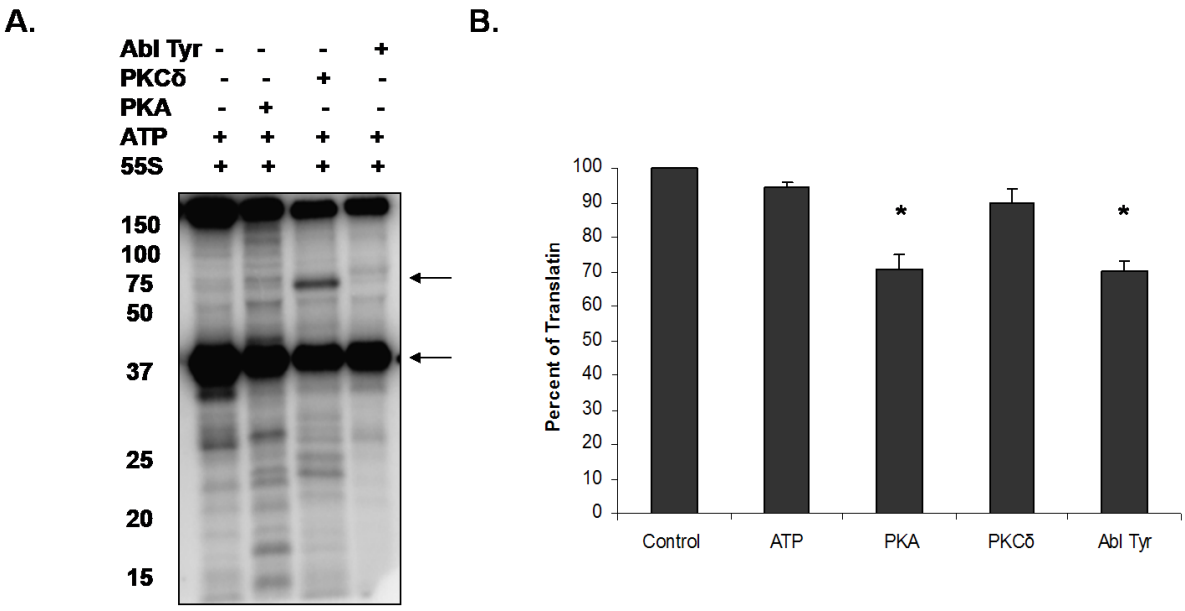


**Figure 2.3 – Mitochondrial ribosomes were phosphorylated in the presence of endogenous and commercial kinases to determine the effect on mitochondrial translation.** Approximately, 0.4 $A_{260}$ units of mitochondrial ribosomes were incubated with 5 µCi [$\gamma$-$^{32}$P] ATP and 2500 U of cAMP-dependent protein kinase (PKA) the catalytic subunit, 48 ng of protein kinase C delta (PKCδ), and 100 U of Abl protein Tyr kinase at 30 °C for 1 hr. The ribosome in the presence of the kinase buffer served as the control. (A) The ribosomal samples were run on an SDS-PAGE gel, fixed, dried, and visualized by phosphor-imaging. The upper arrow indicates PKCδ and the lower arrow is highlighting the phosphorylation of pyruvate dehydrogenase subunits. (B) After phosphorylating the ribosome with different kinases, poly (U)-directed polymerization assays were conducted. Shown is the mean ± SD of three independent experiments. *, $P < 0.05$.

activity from a bovine mitochondrial lysate. In this approach, bovine mitoplasts containing only the inner membrane and matrix portions of the mitochondria, as the outer membrane was removed by digitonin treatment, were lysed in a low salt buffer with sucrose and 1% Triton X-100. After centrifugation of the unbroken mitochondria, the supernatant was dialyzed to remove the sucrose and loaded onto a strong cation exchange (SCX) column containing SP Sepharose resin. After washing the column with low salt buffer, fractions were collected by increasing the salt concentration in a stepwise manner. Individual fractions were tested in *in vitro* phosphorylation reactions with [$\gamma$-$^{32}$P] ATP using different mitochondrial recombinant proteins. As shown in Figure 2.4A, MRPL10, MRPL11, and MRPS18-2 are clearly recognized and phosphorylated by the endogenous kinase present in our enriched bovine mitochondrial lysate. The additional phosphorylated protein bands detected by phosphor-imaging are higher molecular weight proteins, which could be phosphorylated subunits of pyruvate dehydrogenase or kinases which are autophosphorylated.

To identify the putative kinase phosphorylating the ribosomes, a large SDS-PAGE gel was run and selected protein bands were excised, digested with trypsin, and analyzed by mass spectrometry. Three potential kinases were identified including branched chain α-ketoacid dehydrogenase kinase (BCKD kinase), PTEN-induced putative kinase 1 (PINK1), and pyruvate dehydrogenase kinase (PDK). BCKD kinase is a metabolic enzyme that catalyzes the decarboxylation of branched chain α-ketoacids, while PINK1 is associated with oxidative stress and Parkinson's disease (Deng 2005; Pridgeon 2007). PDK is another metabolic enzyme which phosphorylates pyruvate dehydrogenase, the enzyme responsible for the conversion of pyruvate to acetyl CoA. Of the three candidates, we decided to study PDK in more detail as the kinase has been well-characterized. Upon phosphorylation of the E1 subunit of pyruvate dehydrogenase at three different serine residues, the enzyme is inactivated, preventing the generation of acetyl CoA needed for the citric acid cycle and shutting down oxidative phosphorylation in the mitochondria (Holness and Sugden 2003). Therefore, given the presence of PDK in the mitochondria needed to regulate biochemical reactions and its close vicinity to the ribosomes, again a link can be drawn whereby this kinase may phosphorylate the

mitochondrial ribosomes and inhibit translation. In addition, a known weak inhibitor of PDK, sodium dichloroacetate (DCA), was readily available to test in *in vitro* dephosphorylation reactions. In Figure 2.4B, as the concentration of inhibitor was increased more dephosphorylation was evident for MRPS18-2 compared to the control without sodium dichloroacetate. Upon ImageQuant analysis of the signals, a 30% decrease in the intensity of MRPS18-2 signal was obtained when the highest concentration of inhibitor was added to the reaction. Therefore, this data supports the notion that PDK could be one of the kinases responsible for the phosphorylation of mitochondrial ribosomes.

### 2.4.5 Summary

A kinase associated with the ribosomes phosphorylated twenty-four mitochondrial ribosomal proteins, which were confidently detected by three different complementary approaches; specifically seven proteins from the 28S subunit and seventeen proteins from the 39S subunit were consistently identified in the LC-MS/MS analyses. Eighteen bovine mitochondrial ribosomal proteins have *E. coli* homologs, particularly five from the small subunit and thirteen from the large subunit, while the remaining six represent mitochondrial specific proteins. Location of the phosphorylated mitochondrial ribosomal proteins with bacterial homologs was modeled using coordinates for the crystal structure of *E. coli* at 3.5 Å as shown in Figure 2.5 (Schuwirth et al. 2005). As seen in the model, phosphorylated proteins were mainly located in the functional sides of the ribosome such as the mRNA binding path, the peptide exit tunnel, and the sarcin-ricin loop (SRL) region of the ribosome. More interestingly, based on our recent study, eleven of these proteins have phosphorylated *E. coli* ribosomal protein homologs implying a conserved role(s) for phosphorylation in protein synthesis (Soung et al. 2009). Moreover, as first noted for bacterial protein synthesis, our data also suggests that phosphorylation of ribosomal proteins inhibits mitochondrial translation possibly by inducing conformational or structural changes which may alter protein-protein or protein-RNA interactions during different stages of translation. Therefore, given the functional significance of phosphorylation in the bacterial and mitochondrial translation systems, each phosphorylated mitochondrial ribosomal protein with its mapped Ser, Thr, and Tyr

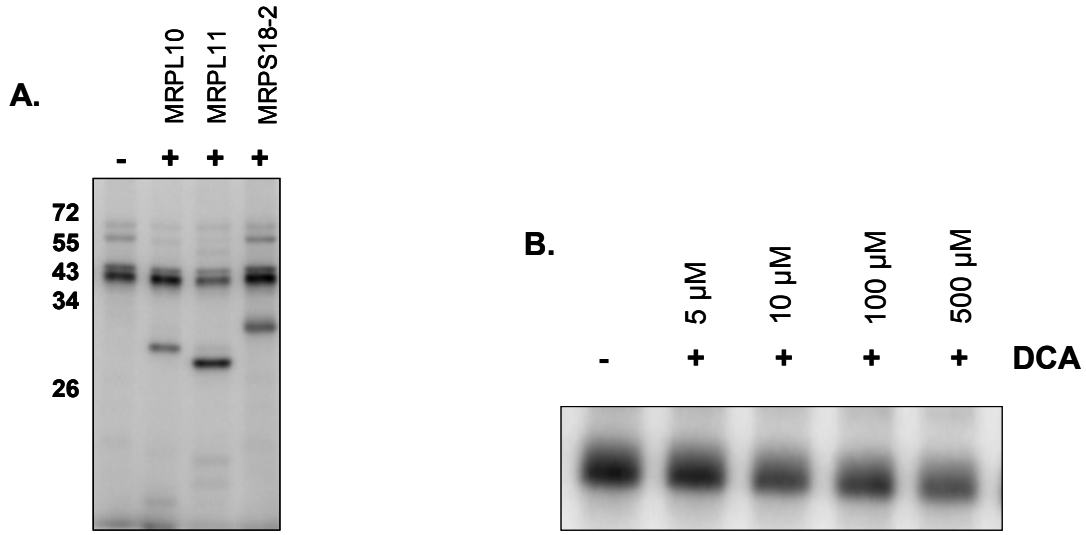


**Figure 2.4 – *In vitro* phosphorylation of recombinant mitochondrial ribosomal proteins by an endogenous kinase associated with the ribosomes and dephosphorylation by sodium dichloroacetate.** (A) An enriched bovine mitochondrial lysate containing endogenous kinases was incubated with 2.5 µCi [$\gamma$-$^{32}$P] ATP in the absence or presence of 0.3 µg of recombinant MRPL10, MRPL11, and MRPS18-2 for 1 hr at 30 °C. The samples were run on an SDS-PAGE gel, fixed, dried, and visualized by phosphor-imaging. (B) An enriched bovine mitochondrial lysate was incubated for 1 hr at 30 °C in the presence of 2.5 µCi [$\gamma$-$^{32}$P] ATP, 0.3 µg MRPS18-2, and different concentrations (5 µM, 10 µM, 100 µM, 500 µM) of sodium dichloroacetate (DCA), an inhibitor of pyruvate dehydrogenase kinase. The samples were processed as described above. ImageQuant was used to estimate the percentage of dephosphorylation of MRPS18-2 after increasing the inhibitor concentration.

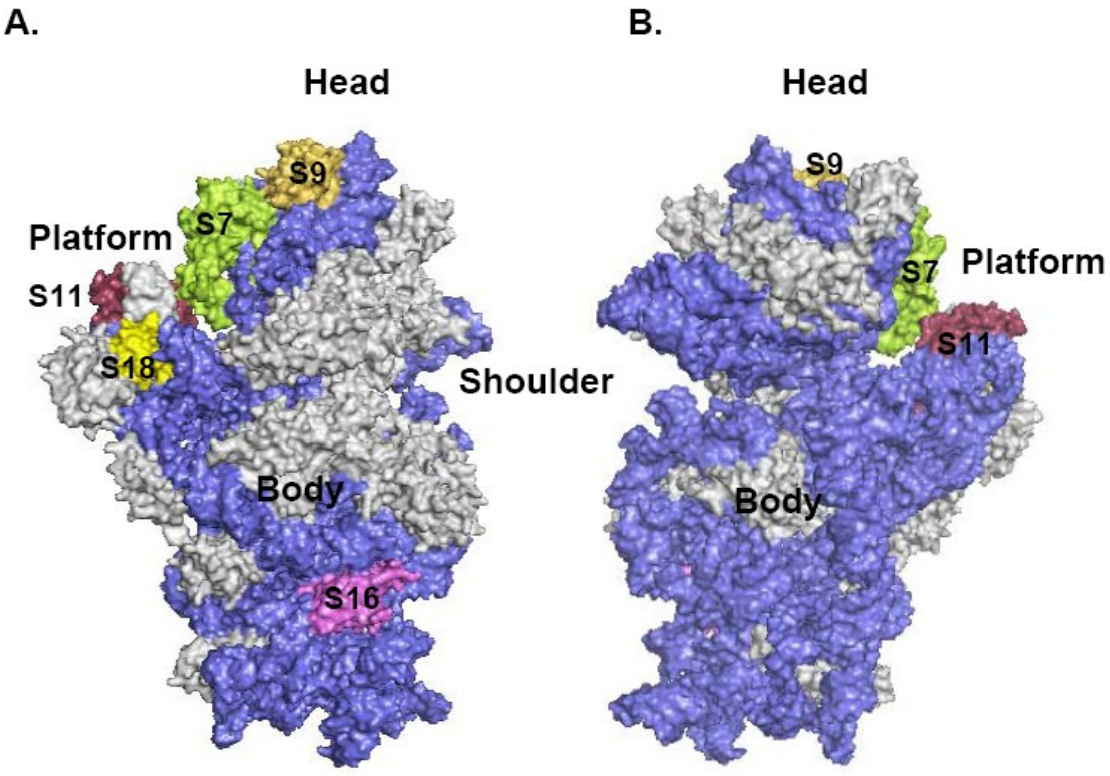


**Figure 2.5 – 3D-Models of the *E. coli* ribosomal subunits displaying the location of phosphorylated mitochondrial ribosomal proteins.** The phosphorylated ribosomal proteins are highlighted in different colors, while gray represents unphosphorylated ribosomal proteins, and blue is the rRNA. Coordinates of the *E. coli* 30S subunit and 50S subunit were obtained from the Protein Data Bank (Acc. # 2AW7 and 2AW4). (A) The 30S subunit is illustrated from the solvent side, while (B) represents a view of the small subunit from the 50S interface.

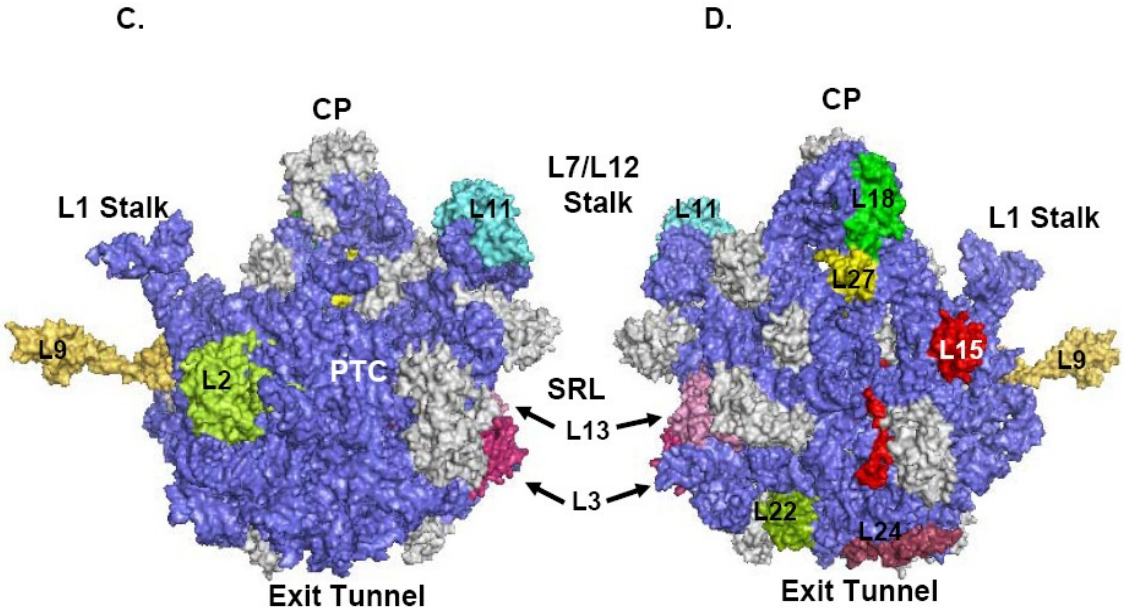


(C) Representation of the 50S subunit from the 30S interface, while (D) is a view of the large subunit from the solvent side. Specific regions, peptidyl transferase center (PTC), central protuberance (CP), sarcin-ricin loop (SRL), L1 and L7/L12 stalks, exit tunnel, and the phosphorylated ribosomal proteins were labeled in the model generated by PyMOL software (DeLano 2002).

residues will be discussed in detail emphasizing their roles in protein synthesis and newly acquired functions in apoptosis and disease.

### 2.4.6 Phosphorylated Bovine Mitochondrial 28S Subunit Proteins with *E. coli* Homologs

***MRPS7*** – In bacteria, S7 is located in the head region of the small subunit and interacts with both mRNA and tRNA throughout the translation process (Cate et al. 1999; Wimberly et al. 2000; Yusupov et al. 2001; Yusupova et al. 2001). Structural studies have demonstrated that the head of the 30S subunit undergoes conformational changes during subunit association, binding of aminoacyl-tRNA or factors, and translocation (Brodersen et al.; Agrawal et al. 1999; Agrawal et al. 2000; Carter et al. 2001; Yusupov et al. 2001; Valle et al. 2003). In addition, this protein is a primary rRNA binding protein and is responsible for proper folding of the 3' major domain of the 16S rRNA, which serves as a docking site for additional ribosomal proteins (Robert and Brakier-Gingras 2001). In this study, MRPS7 was confidently identified as a phosphorylated protein in all three 2D-gel analyses with almost 50% sequence coverage and is highly phosphorylated at Ser, Thr, and Tyr residues (Tables 2.2, 2.3, 2.4). As seen in the alignment of mitochondrial and bacterial S7 homologs from several different species, homology between bacterial and mitochondrial proteins is significant and *E. coli* S7 is also phosphorylated at Ser, Thr, and Tyr residues (Soung et al. 2009). Particularly, four sites were mapped including Thr59, Thr63, Tyr64, and Thr189, of which Thr59 and Tyr64 are highly predicted to be phosphorylated by the NetPhos software. Since S7 is located in the mRNA and tRNA binding path in the small subunit, phosphorylation of this protein might be involved in translocation of these substrates during translation.

***MRPS9*** – In an earlier study, *E. coli* ribosomal S9 was shown to be phosphorylated at Ser and Thr residues by a protein kinase from rabbit skeletal muscle (Traugh and Traut 1972). Similarly we have also detected phosphorylation of MRPS9 at Ser residues by immunoblotting (Table 2.3). Bacterial S9 is located on the back of the head region of the 30S subunit and its extended C-terminal tail enters into the P site of the small subunit

(Figure 2.5) (Wimberly et al. 2000; Yusupov et al. 2001; Hoang et al. 2004; Noller et al. 2005). There are several Lys and Arg residues that make up the C-terminal tail of S9 and promote interactions with the phosphate backbone of the anticodon stem-loop tRNA and control P site specificity during initiation (Noller et al. 2005). In addition to the basic C-terminal tail, there are also highly conserved Thr and Ser residues in the C-terminal tail of the mitochondrial S9 proteins and phosphorylation of these residues would alter the charge on the S9-tail and result in modulating the interaction between this protein and the tRNA. Incidentally, by enrichment and MS analysis we have identified four phosphorylated residues close to the C-terminal tail including Thr278, Ser290, Ser354, and Thr357, each are highly conserved in mitochondria and in some cases bacteria too. Figure 2.6 denotes the spectrum of a doubly-charged phosphorylated peptide of MRPS9 containing Ser354 as the mapped residue. The remaining phosphorylation sites are clustered at the N-terminal and middle regions of the protein and Ser68 has a high probability of being phosphorylated.

***MRPS11*** – Bacterial homolog of S11 is located in the platform region of the small subunit and is known to interact with both mRNA and tRNA during protein synthesis (Figure 2.5) (Robert and Brakier-Gingras 2003). The platform of the 30S subunit undergoes conformational changes during translation as observed in structural studies of bacterial ribosomes, which may promote an interaction at the E site between S7 and S11 (Agrawal et al. 2000; Carter et al. 2001; Yusupov et al. 2001; Robert and Brakier-Gingras 2003; Noller et al. 2005). MRPS11 was detected to be phosphorylated by ProQ Diamond phospho dye, after incubation with [$\gamma$-$^{32}$P] ATP, and immunoblotting with anti-phosphoserine and anti-phosphothreonine (Figure 2.1B and D, Table 2.3). However, phosphorylation of MRPS11 just by the addition of [$\gamma$-$^{32}$P] ATP suggests that this protein was specifically phosphorylated by a kinase associated with the mitochondrial ribosomes (Figure 2.2). Furthermore, its bacterial homolog is phosphorylated primarily at Ser and Thr residues, especially Thr58 of *E. coli* is positioned in a loop region spanning between the N-terminal tail and helix1, where S11 and S7 interact at the Shine Dalgarno binding path (Table 2.2) (Robert and Brakier-Gingras 2003; Soung et al. 2009). Interestingly, Thr58 is conserved in mitochondria (Thr127) and archaeal S11 homologs, whereby the

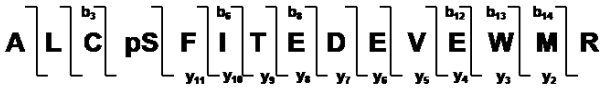


A.

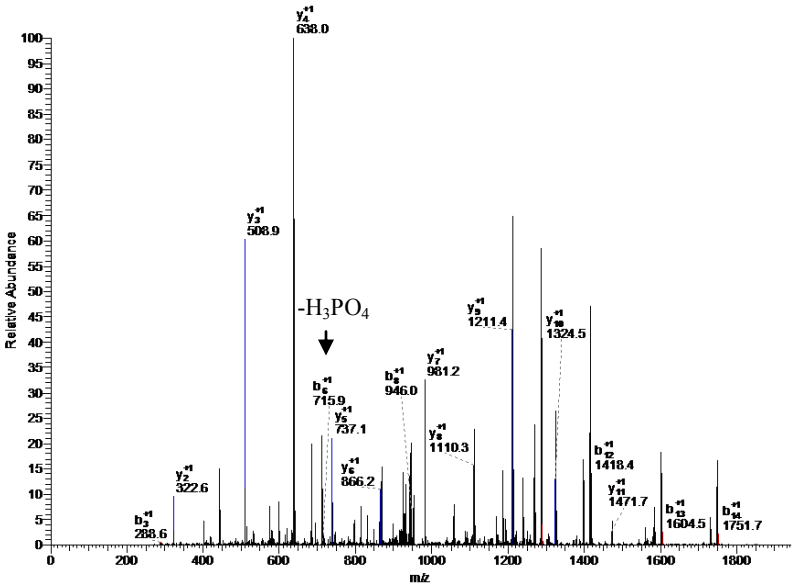


B.

```
                                                                                                  *
RMS9_DOG          299 YLLYFPVTQDREQLMFPFHFLDRLGKHDTTCTVSGGGRSSQAGAIRLAVARALCSFVTEE
RMS9_BOVINE       300 YLLYFPVTQDREQLMFPFHFLDRLGKHDVTCTVSGGGRSSQAGAIRLAMSRALCSFITED
RMS9_HUMAN        300 YQLYFPITQDREQLMFPFHFVDRLGKHDVTCTVSGGGRSAQAGAIRLAMAKALCSFVTED
RMS9_MOUSE        211 YLIYFPITQDREQLMFPFHFLDRLERHDVTCTVSGGGRSAQAGAIRLAMARALCSFVTED
RMS9_CHICKEN      281 ILRYFPVLQDREQLLFPFQFLDRVGKHDAICTVSGGGRSSQAGAIRLATAKALRSFVTET
RS9_THET8          33 FNEYFQGLVRAVAALEPLRAVDALGHFDAYITVRGGGKSGQIDAIKLGIARALVQYN-PD
RS9_ECOLI          35 LEQYFGRETARMVVRQPLELVDMVEKLDLYITVKGGGISGQAGAIRHGITRALMEYD-ES
```

**Figure 2.6 - MS/MS spectrum and alignment of a phosphorylated peptide from MRPS9.** (A) The ion trap mass spectrometer was used to analyze each of the tryptic digests of MRPS9 and a CID MS/MS spectrum of the doubly-charged phosphorylated MRPS9 peptide ALC**p**SFITEDEVEWMR (peptide mass 1927.03, charge 2+) with an Xcorr value of 2.99 was presented. (B) The alignment of S9 from mammalian and bacterial protein sequences including dog (XP_531774), bovine (Q58DQ5), human (P82933), mouse (Q9D7N3), chicken (XP_416921), *T. thermophilus* (P80374), and *E. coli* (P0A7X3) which was created with CLUSTALW program in Biology Workbench and the results are displayed in BOXSHADE. The asterisk indicates the serine residue which is phosphorylated and highly conserved in MRPS9.

additional negative charge may weaken the association with helix1 or trigger conformational changes in S11 hindering its interaction with S7. This post-translational modification could also have a role in protein-RNA interactions needed for a functionally competent ribosome.

***MRPS16*** – This phosphoprotein of only 15.1 kDa was once again detected in the immunoblotting analysis with phospho-specific antibodies; however, the bacterial form was not detected to be phosphorylated in our recent analysis (Tables 2.1, 2.2, 2.3) (Soung et al. 2009). As displayed in Figure 2.5, *E. coli* S16 is located in a narrow cleft in the body of the 30S subunit, interacting with the 5' domain of 16S rRNA (Persson et al. 1995). This protein is required for assembly of the small ribosomal subunit both in mitochondria and bacteria but appears to have a minor if any role in translation (Held et al. 1974; Miller et al. 2004). Of medical relevance, a nonsense mutation (Arg111Stop) in the human MRPS16 gene resulted in a severe reduction in the level of 12S rRNA as well as decreased activity for Complex I and IV (Miller et al. 2004). Upon further examination, it was discovered this mutation prevented the assembly of MRPS11 into the ribosome and yielded a non-functional 28S subunit (Emdadul Haque et al. 2008). There are a few conserved Ser and Thr residues particularly at the C-terminal end of this phosphoprotein near this Arg residue, yet it was not possible to identify them due to the size of the protein and its basic characteristics. Therefore, phosphorylation of this C-terminal tail can be essential for the assembly process and incorporation of MRPS11 into a functional 28S subunit.

***MRPS18-2*** – In mitochondria, there are three variants of the S18 protein and it is believed each ribosome contains one variant in the 28S subunit resulting in a heterogeneous population of ribosomes (Koc et al. 2001a). Positioned in the platform region shown in Figure 2.5, bacterial S18 associates with the 5' ends and the Shine-Dalgarno helix, which is attributed to proper initiation complex formation (Nowotny and Nierhaus 1988; Stade et al. 1989; Brandt and Gualerzi 1992; Jagannathan and Culver 2003). In contrast, mitochondrial mRNAs consistently do not possess a Shine-Dalgarno sequence or 5' and 3' untranslated regions, but instead contain a triangular structure

which partially covers the mRNA entry site (Sharma et al. 2003). Both the *S. collinus* and *E. coli* homolog were previously reported to be Ser and Thr phosphorylated by a protein kinase from rabbit skeletal muscle or a kinase associated with the ribosomes, respectively (Traugh and Traut 1972; Mikulik and Janda 1997; Mikulik et al. 2001). Furthermore, it is known bacterial S18 is phosphorylated at the N-terminal and Ser35 in *E. coli* is conserved in mitochondria as a Thr residue. This post-translational modification could act as a switch locking and unlocking the initiation complex on the 30S subunit (Table 2.2). Of the three variants, MRPS18-1 is the closest relative to the prokaryotic S18, while we only detected MRPS18-2, the largest variant as phosphorylated after incubation with [$\gamma$-$^{32}$P] ATP and immnuoblotting analysis possibly due to their small sizes (Tables 2.3). Similar to its bacterial counterpart, MRPS18-2 was predicted to be phosphorylated at Ser, Thr, and Tyr residues and may regulate the mRNA binding during initation complex formation and protein-protein interactions with S15 and S6 (Agalarov et al. 2000).

### 2.4.7 Phosphorylated Bovine Mitochondrial 39S Subunit Proteins with *E. coli* Homologs

***MRPL1*** – This mitochondrial ribosomal protein of almost 37 kDa has a phosphorylated homolog in *E. coli* (Tables 2.1 and 2.2). Detected in several of the 2D-gel analyses, the protein is a unique feature of the large subunit forming a noticeable protuberance (Table 2.3 and Figure 2.5) (Nikulin et al. 2003). Bacterial L1 is able to bind directly to the 23S rRNA and mRNA by recognizing the same structural motif and though not essential, ribosomal activity was significantly reduced by 40-60% in the absence of L1, hinting at a role in the elongation process (Subramanian and Dabbs 1980; Nevskaya et al. 2006). In addition, structural studies indicated L1 could be associated with the release and disposal of deacylated tRNA from the E site (Nikulin et al. 2003). Finally, this protein regulates the L11-L1 operon (Dean and Nomura 1980). Specifically, *E. coli* Tyr21, located at the junction of the N-terminal helix α1 and α2 is critical for 23S rRNA binding and Thr217, one of the residues responsible for rRNA and mRNA recognition are both highly conserved in mitochondria and may indeed be phosphorylated in MRPL1 (Tables 2.1 and

2.2) (Nevskaya et al. 2006). However, in our phosphoproteomic analysis, we mapped different sites including three Thr residues Thr126, Thr130, and Thr181 as well as one Tyr residue at position 122, each conserved and may also be functionally significant.

***MRPL2*** – Bacterial L2 is a primary RNA binding protein important for peptidyl transferase activity and located at the intersubunit interface of the large subunit as shown in Figure 2.5 (Willumeit et al. 2001). It is essential for the association of the small and large subunits and plays a role in the binding of tRNA to the A and P sites (Diedrich et al. 2000). L2 has a horseshoe configuration clamping domains of the 23S rRNA into the proper orientation, while the middle region includes two RNA-binding motifs (Brennan.L.E. et al. 1999). Bacterial L2 from *E. coli* and *S. collinus* was phosphorylated at Ser and Thr residues by either a protein kinase from rabbit skeletal muscle or a kinase associated with the ribosomes, respectively (Traugh and Traut 1972; Mikulik and Janda 1997; Mikulik et al. 2001). Mitochondrial ribosomal L2 is a very basic protein and phosphorylated at Ser, Thr, and Tyr residues as detected in immunoblotting analyses (Tables 2.2 and 2.3). Remarkably, there are multiple evolutionarily conserved amino acids throughout the entire protein sequence which could serve as targets of phosphorylation by a kinase associated with mitochondria. Our initial findings, identified Ser and Thr residues at the N-terminus which most likely would be part of the mitochondrial localization signal, however, Thr224 is conserved and has evolved into a Tyr residue in bacteria. Phosphorylation might perturb rRNA due to charge repulsion, preventing intersubunit association or inhibit peptidyl transferase activity by disengaging the tRNA decreasing the amount of ATP produced.

***MRPL3*** – In our mass spectrometric analysis, MRPL3 was identified with 30% sequence coverage and phosphorylation status was detected by 2D-gel immunoblotting with a phosphoserine antibody and after incubation with [$\gamma$-$^{32}$P] ATP (Tables 2.3 and 2.4). Not surprisingly, *E. coli* ribosomal L3 had previously been mentioned as a phosphoprotein, whereby a protein kinase from rabbit skeletal muscle could access and phosphorylate its Ser and Thr residues (Tables 2.1 and 2.2) (Traugh and Traut 1972). Bacterial L3 is one of the ribosomal proteins responsible for arranging the sarcrin-ricin loop (SRL)

particularly domain VI of the 23S rRNA for factor binding (Figure 2.5) (Ban et al. 2000; Yusupov et al. 2001). We had mapped a few phosphorylation sites at the N-terminal domain of *E. coli* L3, which are partially conserved in mitochondria (Ser66) and might also be phosphorylated affecting protein interactions at the sarcin-ricin loop (Table 2.2) (Soung et al. 2009). Furthermore, Thr146, Thr151, and Ser153 found in the middle segment of MRPL3 might induce conformational changes in the 16S rRNA and disrupt peptide bond formation.

***MRPL9*** – L9 is located directly below the L1 stalk protuberance in the 50S subunit as depicted in Figure 2.5 (Cate et al. 1999; Yusupov et al. 2001). It is capable of binding to the 23S rRNA and has the ability to control the degree of hopping that occurs during protein synthesis (Marquardt et al. 1979). Hopping refers to the episodes when the peptidyl-tRNA slips and pairs with a non-overlapping codon (Herr et al. 2001). In designing experiments, gene 60 mRNA from the bacteriophage T4 was used and demonstrated under ordinary circumstances the ribosome will hop over a fifty nucleotide gap during translation (Herbst et al. 1994). From our proteomic analysis, MRPL9 was discovered in each of the three different 2D-gel analyses with either L24 or S7, given the similarity in pI and molecular weight, yet does not appear to have a phosphorylated homolog in bacteria (Tables 2.2 and 2.3). We found seven peptides for this phosphoprotein, resulting in almost 40% sequence coverage yet phosphorylated peptides remained elusive (Table 2.4). Several conserved Ser, Thr, and Tyr residues are evident from the amino acid sequence and if phosphorylated may act as a regulatory mechanism controlling this unique hopping function in mitochondria.

***MRPL10*** – A single L10 in conjunction with multiple copies of L7/L12 are referred to as the L8 protein complex in bacteria (Uchiumi et al. 1999). Specifically, the N-terminal domain of L7/L12 binds to the C-terminal end of L10, docking this flexible protein to the large subunit of the ribosome (Figure 2.5) (Uchiumi et al. 1999). From an earlier report analyzing *E. coli* phosphorylated ribosomal proteins, L10 was found to be Ser and Thr phosphorylated by a protein kinase from rabbit skeletal muscle (Table 2.2) (Traugh and Traut 1972). Based on our 2D-gel analysis, MRPL10 was identified in each of the

immunoblots with phospho-specific antibodies in addition to being observed in the ProQ phospho gel and after incubation with [$\gamma$-$^{32}$P] ATP (Table 2.3). Again, many of the Ser and Thr residues found in mitochondrial and bacterial homologs are conserved and phosphorylation of these residues may influence the binding ability of MRPL10 as the N-terminal domain is responsible for attaching to the large subunit and L7/L12 dimers. For example, Ser187 is present throughout the mitochondrial sequences, but converted to a Thr residue in *T. thermophilus*. Ser105, which is also conserved within most mitochondrial sequences and is a Thr residue in *E. coli* besides having a high probability of being phosphorylated by a kinase associated with the ribosomes.

***MRPL11*** – Another critical ribosomal protein, bacterial L11 is in close proximity to L10 and the L7/L12 stalk near the factor binding site on the 50S subunit (Figure 2.5) (Datta et al. 2005). L11 is a central player in translation termination favoring UAG-dependent termination by release factor 1 (RF1), while ribosomes stripped of L11 prefer UGA-dependent termination by release factor 2 (RF2) (Van Dyke et al. 2002). Furthermore, the N-terminal domain (residues 1-72) of L11 is required for stringent factor stimulation, when the ribosome stalls (Kavran and Steitz 2007). This domain is very flexible and attached to a linker region (residues 73-75). Upon factor binding, the N-terminal domain swings in towards the large subunit and this domain moves away from the subunit due to conformational changes stimulated by the GTP hydrolysis (Garcia-Marcos et al. 2007; Kavran and Steitz 2007; Harms et al. 2008). MRPL11 was only detected after incubation with [$\gamma$-$^{32}$P] ATP and does not have a phosphorylated bacterial homolog (Tables 2.1, 2.2, 2.3). In L11 homologs from many bacteria and mitochondria, there are evolutionarily conserved Ser and Thr residues that might be involved in interactions of L11 with the translation factors and the large subunit rRNA and proteins. Changes in phosphorylation status of these residues could impact protein-protein and protein-rRNA interactions, and specifically act as a pivot point when the flexible N-terminal domain changes conformation upon factor binding.

***MRPL13*** – With peptide coverage of just over 30%, MRPL13 was identified in the immunoblotting to be Ser and Thr phosphorylated at steady-state conditions (Tables 2.3

and 2.4). The bacterial homolog of MRPL13 was present in active sub-ribosomal particles and is primarily phosphorylated at Thr and Tyr residues (Tables 2.1 and 2.2) (Khaitovich et al. 1999; Soung et al. 2009). Bacterial L13 is oriented to interact with at least four ribosomal proteins including L3 and L6 near the factor binding site (SRL) as well as L20 and L21 at the opposite end (Figure 2.5) (Ban et al. 2000). Therefore, phosphorylation of MRPL13 can be implicated in having a role in scaffold formation in the SRL region and factor binding to the ribosome. Unfortunately, we were unable to map any phosphorylation sites for this protein, yet Tyr16 and Tyr43 of *E. coli* L13 are conserved in mitochondria and could be candidate sites for mitochondrial ribosomal L13.

***MRPL15*** – This ribosomal protein is located beneath the L1 protuberance stalk as shown in Figure 2.5 and studies with L15 have shown that this protein is capable of interacting with over ten proteins in the large subunit assembly process (Lieberman and Noller 1998). Specifically, bacterial L15 functions during the late stages of assembly, but is not required (Franceschi and Nierhaus 1990). However, the presence of L15 tends to accelerate the formation of active ribosome particles (Franceschi and Nierhaus 1990). MRPL15, a highly basic protein, was detected in immunoblotting analyses in addition to after incubating with [$\gamma$-$^{32}$P] ATP (Tables 2.2 and 2.3). Though the bacterial homolog is not phosphorylated, there are numerous conserved residues which may serve as potential candidates for phosphorylation by a kinase associated with the ribosomes. Specifically, Tyr94 and Ser98 were detected as phosphorylated, which may be important for mediating protein-protein interactions in the assembly process of the 39S as well as governing the rate of assembly, which can directly affect protein synthesis in mitochondria.

***MRPL18*** – As located in Figure 2.5, bacterial L18 is necessary for translation and cell viability as concluded from *in vitro* and *in vivo* studies (Bloemink and Moore 1999; Korepanov et al. 2007). This large subunit protein is known to be phosphorylated and the modification facilitates 5S rRNA binding to the 23S rRNA as demonstrated by Bloemink and Moore, yet mitochondrial ribosomes do not have a 5S rRNA (Bloemink and Moore 1999). The *E. coli* homolog is Ser and Thr phosphorylated, while we only detected MRPL18 in the 2D-gel after incubation with [$\gamma$-$^{32}$P] ATP (Tables 2.1, 2.2, 2.3).

Particularly, Ser52 and Thr53 of *E. coli* are conserved in mitochondria and may also be phosphorylated by an endogenous mitochondrial kinase (Soung et al. 2009). Therefore this common post-translational modification can be implicated in protein-RNA interactions, yet the nature of the association might be different due to the lack of the 5S rRNA.

***MRPL22*** – MRPL22, just over 24 kDa in size, was found in all the 2D-gel analyses of phosphorylated mitochondrial ribosomal proteins (Tables 2.2 and 2.3). Phosphorylation of Ser, Thr, and Tyr residues were mapped in our phosphoproteomic analysis of *E. coli* ribosomal proteins (Tables 2.1 and 2.2) (Soung et al. 2009). Bacterial L22 lines the peptide exit tunnel of the large subunit and forms the narrowest portion of the channel with L4 (Ban et al. 2000). L22 is a core protein associating with all six domains of the 23S rRNA (Ban et al. 2000). Furthermore, a deletion of Met82-Lys83-Arg84 in bacterial L22 leads to erythromycin resistance inhibiting peptide chain elongation (Davydova et al. 2002). Several Ser, Thr, and Tyr residues are clustered in close proximity to the conserved Lys83-Arg84 in bacteria resulting in erythromycin resistance. We identified Ser96 as phosphorylated, a highly conserved residue, however, *E. coli* Thr37, Thr39, and Thr100 are also partially conserved in mitochondrial sequences. Furthermore, phosphorylation of MRPL22 can be responsible for altering interactions with L4 and 16S rRNA acting as a mechanism to regulate the nascent polypeptide release from the exit tunnel.

***MRPL24*** – This mitochondrial ribosomal protein yielded several different peptides from the tryptic digests with a sequence coverage of over 40% (Table 2.4). Identified from the immunoblotting screens as well as ProQ phosphoprotein staining and after incubation with [$\gamma$-$^{32}$P] ATP, the protein appears to be highly phosphorylated (Table 2.3). Two highly conserved phosphorylation sites at the C-terminal end, predicted by the NetPhos software were detected, specifically Thr177 and Ser178. L24 is also located at the end of the peptide exit tunnel as displayed in Figure 2.5 and is capable of interacting with chaperones and the signal recognition particle (SRP) in bacteria (Kramer et al. 2002; Ullers et al. 2003). As an initiator protein, it functions in assembling the 50S subunit

needed for protein synthesis (Nowotny and Nierhaus 1982; Schlunzen et al. 2005; Schuwirth et al. 2005). Therefore phosphorylation at various residues might induce conformational changes during the assembly process or alter protein interactions with neighboring chaperones near the exit tunnel.

***MRPL27*** – Bacterial L27 is positioned at the base of the central protuberance and is tightly linked to the peptidyl transferase center of the 50S subunit (Figure 2.5) (Lotti et al. 1987; Maguire et al. 2005). Deletion of this ribosomal protein leads to severe growth defects and the flexible N-terminal domain is believed to associate with the peptidyl transferase center (Lotti et al. 1987; Maguire et al. 2005). This small mitochondrial ribosomal protein gave a strong signal with [$\gamma$-$^{32}$P] ATP and upon viewing the protein sequence several conserved residues stand out as possible targets for phosphorylation including the mapped residue Tyr90 (Tables 2.2 and 2.3). Post-translational modifications can be implicated in rearranging the 16S rRNA or affecting the ability to place the tRNA at the proper position needed for translation to occur.

***MRPL28*** – L28 is a neighbor of L15 and may have a role in ribosome assembly based on mutations in the operon encoding L28 (Figure 2.5) (Maguire et al. 2005). The *E. coli* homolog of MRPL28 is about three times shorter in length compared to its counterpart and acts as a secondary rRNA binding protein (Table 2.2) (Koc et al. 2001b). In mitochondria, the reduction in the 16S rRNA can be compensated by the increase in length and phosphorylation could be attributed to conformational changes in protein-RNA or protein-protein interactions affecting the assembly process. *E. coli* ribosomal L28 is phosphorylated at only Thr7 and from this current phosphoproteomic analysis MRPL28 was identified in the immunoblotting with a phosphoserine antibody, yet we mapped a conserved Tyr91, which has a significant probability of being phosphorylated by an endogenous mitochondrial kinase (Tables 2.2 and 2.3) (Macek et al. 2008). Furthermore, MRPL28 and MRPS18-2 were found in the same spot after incubation with [$\gamma$-$^{32}$P] ATP, given the pIs and molecular weights are almost identical (Tables 2.2 and 2.3). Of medical interest, MRPL28 was identified as a human melanoma-associated

antigen and the phosphorylation status of this protein may be important for an extra ribosomal function of this protein (Robbins et al. 1995).

### 2.4.8 Phosphorylated Bovine Mitochondrial 28S and 39S Subunit Proteins without *E. coli* Homologs

***MRPS23, MRPL43, MRPL45, and MRPL49*** – This cluster of four mitochondrial ribosomal proteins were detected in multiple 2D-gel analyses, had at least at 30% sequence coverage, and are predominantly Ser and Thr phosphorylated (Tables 2.2, 2.3, 2.4). MRPS23 has three Ser residues at positions 58, 151, and 153 which are predicted to be phosphorylated, yet the protein sequence in the region has only limited conservation in mitochondria. The site for MRPL49, Ser41, is also a strong candidate as a target for an endogenous mitochondrial kinase. Overall, the amino acid sequences for these new class proteins indicate some of the mapped Ser and Thr residues are conserved, yet it is not possible to predict the significance of phosphorylation in structural or functional terms as the location on the ribosome is unknown without a bacterial homolog.

***MRPS29 and MRPL40*** – Two apoptotic proteins, MRPS29 from the 28S subunit and MRPL40 from the 39S subunit were identified in our phosphoproteomic screen of mammalian mitochondrial ribosomal proteins. MRPS29 known as DAP3 (Death Associated Protein 3) is an apoptotic protein with a controversial history and even has a homolog in *Leishmania tarentolae* (Kissil et al. 1995; Maslov et al. 2007). DAP3 has been implicated in mitochondrial physiology as DAP3 deficiency is lethal in mice, while the overexpression results in mitochondrial fragmentation (Mukamel and Kimchi 2004; Kim et al. 2007). Furthermore, it is the only GTP-binding protein on the ribosome and has been localized to the base of the lower lobe of the 28S subunit by immunoelectron microscopy (Miyazaki and Reed 2001; O'Brien T et al. 2005). In a recent study, we have shown phosphorylation of bovine ribosomal DAP3 at several highly conserved Ser and Thr residues using a combination of 2D-gel analysis and mass spectrometry and role of these residues in induction of apoptosis (Miller et al. 2008). MRPS29 was detected when probing with anti-phosphoserine and has many conserved Ser residues throughout its

protein sequence particularly clustering around the specific GTP-binding motifs (Tables 2.2 and 2.3). In addition, two earlier studies reported the importance of DAP3 phosphorylation by Akt kinase in suppression of anoikis and by LKB1, a Ser/Thr kinase, in induction of apoptosis in cells ectopically expressing DAP3 (Miyazaki et al. 2004; Takeda et al. 2007).

Mitochondrial ribosomal protein L40 also known as MRPL37 was identified from immunoblotting with phospho-specific antibodies as well after incubation with [$\gamma$-$^{32}$P] ATP and staining with ProQ phosphoprotein dye (Tables 2.2 and 2.3). Having mapped two Ser and Thr phosphorylation sites, Ser138 is highly likely to be modified by a kinase and overall MRPL40 shows sequence similarity to another apoptotic protein MRPS30 (PDCD9) from the small subunit (Koc et al. 2001c; Levshenkova et al. 2004). Increased expression was observed in lung tumor cells compared to normal cells, as the gene may be activated in transformed cells (Levshenkova et al. 2004). Therefore, this finding allows us to hypothesize that phosphorylation may act as a molecular switch in the stimulation or progression of apoptosis. In addition, gradually more evidence is accumulating that the mitochondrial ribosomal proteins are involved in cell death pathways, with at least two being phosphoproteins, and disease states suggesting conformational and/or functional changes of the ribosome occurs as a result of this post-translational modification.

## 2.5 Conclusion

As we reported for bacterial ribosomes (Soung et al. 2009), mammalian mitochondrial ribosomes are also phosphorylated at Ser, Thr, and Tyr residues by an endogenous kinase associated with the ribosome and the majority of the sites mapped are highly conserved or predicted to be phosphorylated by the NetPhos software. *In vitro* phosphorylation of ribosomal proteins by mitochondrial kinases PKA, PKCδ, and Abl Tyr kinase inhibited protein synthesis. Findings reported in this study suggest that phosphorylation plays a significant role in mitochondrial protein synthesis and physiology. Our study should be followed by site-directed mutagenesis analyses to

specifically determine the role of each modified site in protein synthesis and possibly in signal transduction and disease states.

## 2.6 Materials and Methods

### 2.6.1 Preparation of 55S Bovine Mitochondrial Ribosomes

Preparation of mitochondrial ribosomes starting from 4 kg of bovine liver was adapted from previously described methods (Matthews et al. 1982; Spremulli 2007). To preserve protein phosphorylation, phosphatase inhibitors (2 mM imizadole, 1 mM sodium orthovanadate, 1.15 mM sodium molybdate, 1 mM sodium fluoride, and 4 mM sodium tartrate dehydrate) were added during the ribosome purification. Ribosomes separated in sucrose gradients were either pelleted by ultracentrifugation or concentrated using a Microcon Ultracel YM-10 centrifugal unit (Millipore Corp.) for further analysis.

### 2.6.2 NEPHGE Electrophoresis and Phosphoprotein Staining of Mitochondrial Ribosomes

Approximately 1.8 $A_{260}$ units of purified ribosome sample was acetone precipitated and the pellet was resuspended in lysis buffer consisting of 9.8 M urea, 2% (w/v) NP-40, 2% ampholytes pI 3-10 and 8-10, and 100 mM DTT. The samples were loaded on NEPHGE (non-equilibrium pH gradient electrophoresis) tube gels and equilibrated in buffer containing 60 mM Tris-HCl pH 6.8, 2% SDS, 100 mM DTT, and 10% glycerol (Cahill et al. 1995). The second dimension gels, usually 14%, were transferred to PVDF membranes and probed with the following primary antibodies: monoclonal anti-phosphoserine at a 1:5000 dilution (Sigma-Aldrich Inc., Product # B 7911), monoclonal anti-phosphothreonine at a 1:10000 (Sigma-Aldrich Inc., Product # B 7661) or monoclonal anti-phosphotyrosine at a 1:5000 dilution (Sigma-Aldrich Inc., Product # P 4110). The membranes were developed using the SuperSignal West Femto Max Sensitivity Substrate (Pierce Biochemicals Inc.) according to the protocol provided by the manufacturer. For further confirmation of protein phosphorylation, gels were

stained with the ProQ Diamond phosphoprotein dye (Molecular Probes) and visualized by a laser scanner at an excitation wavelength of 532 nm.

### 2.6.3 *In vitro* Phosphorylation and Dephosphorylation of 55S Mitochondrial Ribosomes

Mitochondrial ribosomes (1.8 $A_{260}$ units) were incubated with 50 μCi [$\gamma$-$^{32}$P] ATP and 200 μM cold ATP at 30 °C for 1 hr. The ribosomal proteins were separated by two-dimensional NEPHGE gels, fixed in 20% methanol/7% acetic acid, and visualized by phosphor-imaging (Amersham Biosciences Inc.).

*In vitro* phosphorylation reactions were also performed in the absence or presence of commercial kinases. In this case, 0.4 $A_{260}$ units of mitochondrial ribosomes were incubated with 5 μCi [$\gamma$-$^{32}$P] ATP and 200 μM cold ATP, 2500 U of cAMP-dependent protein kinase (PKA) the catalytic subunit (New England BioLabs, Product # P6000S), 48 ng of protein kinase C delta (PKCδ) (Sigma-Aldrich Inc., Product # P 8538), and 100 U of Abl protein Tyr kinase (New England BioLabs, Product # P6050S) at 30 °C for 1 hr. The conditions for each phosphorylation assay were adapted from the protocols provided by the manufacturers. The ribosomal proteins were separated on an SDS-PAGE gel and visualized by phosphor-imaging (Amersham Biosciences Inc.) or used directly in the poly (U)-directed *in vitro* translation reactions.

Finally, *in vitro* phosphorylation reactions were performed with an enriched bovine mitochondrial lysate containing endogenous kinases. In this scenario, 0.3 μg of recombinant MRPL10, MRPL11, and MRPS18-2 were incubated with 100 μM cold ATP and 2.5 μCi [$\gamma$-$^{32}$P] ATP for 1 hr at 30 °C followed by SDS-PAGE and phosphor-imaging (Amersham Biosciences Inc.). Dephosphorylation reactions were setup in a similar manner as described above except different concentrations (5 μM, 10 μM, 100 μM, 500 μM) of sodium dichloroacetate (DCA), an inhibitor of pyruvate dehydrogenase kinase were added. For quantitation of the MRPS18-2 signals in the dephosphorylation reactions, ImageQuant 5.0 (Molecular Dynamics) was used.

### 2.6.4 In-Gel Digestions

The phosphorylated protein spots detected by immunoblotting, [$\gamma$-$^{32}$P] ATP - labeling, and ProQ Diamond phosphoprotein stain were excised from a SYPRO Ruby (Molecular Probes) or Coomassie Blue stained gel diced into tiny pieces, and transferred to a microcentrifuge tube. Gel samples were destained with 200 mM ammonium bicarbonate pH 8 in 50% acetontrile and vortexed for 10 min. This process was repeated if necessary until the gel pieces were clear in color. Next, the samples were dehydrated with acetonitrile and allowed to dry for 30 min. Trypsin was freshly diluted in 25 mM ammonium bicarbonate, added to the gel pieces, and incubated overnight at 37 °C. The next morning, the extract is transferred to an autosampler vial insert and the gel samples are sonicated in 50% acetonitrile with 5% formic acid for 30 min. This extract was combined with the first and together are dried using the SpeedVac. Once the volume was reduced to 5-10 µl they were reconstituted in 0.1% formic acid for LC-MS/MS analysis.

### 2.6.5 Enrichment of Phosphorylated Peptides of Mitochondrial Ribosomes

The PhosphoProfile I phosphopeptide enrichment kit (Sigma-Aldrich Inc.) was used for enrichment of phosphorylated peptides of bovine mitochondrial ribosomes. The protocol provided in the kit was followed to enrich the phosphopeptides obtained from in-solution tryptic digestions of intact 55S mitochondrial ribosomes (approximately 3.6 $A_{260}$ units). Briefly, the digested protein sample was acidified with glacial acetic acid to a final concentration of 250 mM and loaded on the gallium silica spin column (Sigma-Aldrich Inc.). The column was washed twice with 50 mM acetic acid in 10% acetonitrile and eluted with 0.4 M $NH_4OH$ in 20% acetonitrile. The eluate was dried by SpeedVac and reconstituted in 0.1% formic acid for the LC-MS/MS analysis.

The second method of enrichment was strong cation exchange chromatography (SCX) using a BioBasic SCX column (2.1 x 250 mm, 5 micron, 300 Å, ThermoFinnigan Co.). Initially, 55S bovine mitochondrial samples were incubated with 10 µg of RNAse A at 37 °C for 1 h. Prior to in-solution trypsin digestion, the ribosome sample was denatured in 6 M Guanidine HCl and processed through a C4 reverse-phase trap cartridge (Michrom Bioresources, Inc.) to concentrate, desalt, and remove degraded RNA.

Following the sample clean up, the eluate was dried in a speed vac and resuspended in 30 µl of 25 mM $NH_4HCO_3$ for trypsin digestion, which was added directly to the sample solution at 1:50 ratio and incubated at 37 °C overnight. After in-solution trypsin digestion, peptides were eluted with a gradient of 5 mM phosphate (pH 2.7), 25% acetonitrile (Mobile phase A) and 5 mM phosphate (pH 2.7), 25% acetonitrile, 350 mM KCl (Mobile phase B). The gradient started with a hold at 0% B for 5 min. It was ramped to 15% B in 20 min, then quickly to 80% B in 5 min, and held there for 5 min. The column was equilibrated at 0% B for 15 min prior to next injection. Absorbance over the range of 200 to 300 nm was measured and absorbance at 210 nm was plotted. Fractions (600 µl) were collected throughout for 30 min. Early fractions, which are expected to be enriched in phosphopeptides, were reduced to 20 µl using a SpeedVac. The SCX fractions were online desalted and analyzed by LC-MS/MS.

### 2.6.6 Mass Spectrometric Analysis of Phosphorylated Proteins of Mitochondrial Ribosomes

Tryptic peptides obtained from in-gel digestions were analyzed by a capillary liquid chromatography - nanoelectrospray ionization - tandem mass spectrometry (LC-MS/MS) for protein identification. Tandem MS spectra obtained by fragmenting a peptide by collision-induced dissociation (CID) was acquired using the LC-MS/MS system that consisted of a Surveyor HPLC pump, a Surveyor Micro AS autosampler, and an LTQ linear ion trap mass spectrometer (ThermoFinnigan). The acquired spectra were evaluated using Xcalibur 2.0 and Bioworks 3.2 softwares. The raw CID tandem MS spectra were also converted to Mascot generic files (.mgf) using the extract msn software (ThermoFinnigan). The .dta and .mgf files were submitted to a site-licensed Sequest and Mascot (version 2.2) search engines to search against in-house generated sequences of 55S proteins, all known mitochondrial proteins, and proteins in the Swiss-Prot database. Database searches were performed with cysteine carbamidomethylation as a fixed modification. The variable modifications were methionine oxidation (+16 Da) and phosphorylation (+80 Da) of Ser, Thr, and Tyr residues and loss of water (-18 Da) from Ser and Thr due to beta elimination during loss of the phosphate moiety. Up to two

missed cleavages were allowed for the protease of choice. Peptide mass tolerance and fragment mass tolerance were set to 3 and 2 Da, respectively.

Mascot and Sequest are similar search engines to analyze data obtained from the mass spectrometer. Mascot uses the MOWSE algorithm, which is based on comparing the *m/z* (mass/charge) values of the peptides in the experimental sample to the *m/z* values of peptides in a given database digested with a specified enzyme (Liebler 2002). The algorithm takes into account larger proteins giving rise to more peptides and that smaller peptides may match more often to *m/z* values in the database. In addition, the Mascot software can provide a statistical analysis of the data and considers the probability of peptide matches being random events compared to true identities (Liebler 2002). The Sequest software was designed in a similar manner to Mascot, whereby the experimental and theoretical MS/MS spectrum are compared and an Xcorr (cross correlation score) is calculated (Liebler 2002). The candidate peptide ranked as #1 in the database is assigned the highest Xcorr value. Typically, longer well-matched peptides receive a higher Xcorr value than shorter peptides.

### 2.6.7 Polymerization Assays

Poly (U)-directed *in vitro* translation reactions contained 50 mM Tris-HCl pH 7.8, 1 mM dithiothreitol, 0.1 mM spermine, 40 mM KCl, 8.5 mM $MgCl_2$, 2.5 mM phosphoenolpyruvate, 0.18 U pyruvate kinase, 0.5 mM GTP, 50 U RNasin Plus, 12.5 µg/mL poly (U), 26.4 pmol [$^{14}$C]-Phe-tRNA, 0.25 µM EF-$Tu_{mt}$, 1 µg EF-$G_{mt}$, and 0.4 $A_{260}$ units of mitochondrial ribosomes. The reaction mixture was incubated at 37 °C for 30 min and terminated by the addition of cold 5% trichloroacetic acid followed by incubation at 90 °C for 10 min. The precipitate was collected on nitrocellulose filter membranes and the incorporation of [$^{14}$C]-Phe was quantified using a liquid scintillation counter. Results were analyzed using the two-tailed unpaired t test. Values of *$P<0.05$ were considered statistically significant.

### 2.6.8 Enrichment and Identification of Bovine Mitochondrial Kinases

Mitoplasts from bovine liver were ground with mortar/pestle and lysed in .26 M sucrose, 50 mM KCl, 15 mM $MgCl_2$, 20 mM HEPES pH 7.6, 1 mM EDTA, 0.05 mM spermine, 0.05 mM spermidine, 1% Triton X-100, as well as protease and phosphatase inhibitors. The lysate was incubated at 4 °C for 20 min followed by centrifugation at 15,000 rpm for 45 min at 4 °C. The supernatant was dialyzed in 50 mM KCl, 5 mM $MgCl_2$, 20 mM HEPES pH 7.6, 1 mM EDTA, and 10% glycerol at 4 °C. Afterwards the sample was loaded onto an SCX column using SP Sepharose Fast Flow resin (Amersham Biosciences Inc.), washed twice with 50 mM KCl, 5 mM $MgCl_2$, 20 mM HEPES pH 7.6, 1 mM EDTA, and eluted in a stepwise manner up to 1.5 M KCl. Each wash and elution contained protease and phosphatase inhibitors. Aliquots were taken and tested for the presence of kinase activity by incubating with recombinant mitochondrial proteins (MRPL10, MRPL11, MRPS18-2) and [$\gamma$-$^{32}$P] ATP as described earlier. Individual fractions were then acetone precipitated and run on a large 10% SDS-PAGE to separate the higher molecular weight proteins, where the kinases are most abundant and in-gel digests with trypsin were performed for MS analysis.

## 2.7 References


Agalarov, S.C., Sridhar, P.G., Funke, P.M., Stout, C.D., and Williamson, J.R. 2000. Structure of the S15,S6,S18-rRNA complex: assembly of the 30S ribosome central domain. *Science* **288:** 107-113.

Agrawal, R.K., Heagle, A.B., Penczek, P., Grassucci, R.A., and Frank, J. 1999. EF-G-dependent GTP hydrolysis induces translocation accompanied by large conformational changes in the 70S ribosome. *Nat. Struct. Biol.* **6:** 643-647.

Agrawal, R.K., Spahn, C.M., Penczek, P., Grassucci, R.A., Nierhaus, K.H., and Frank, J. 2000. Visualization of tRNA movements on the Escherichia coli 70S ribosome during the elongation cycle. *J. Cell Biol.* **150:** 447-460.

Ban, N., Nissen, P., Hansen, J., Moore, P.B., and Steitz, T.A. 2000. The Complete Atomic Structure of the Large Ribosomal Subunit at 2.4 A Resolution. *Science* **289:** 905-920.

Bloemink, M.J., and Moore, P.B. 1999. Phosphorylation of ribosomal protein L18 is required for its folding and binding to 5S rRNA. *Biochemistry* **38:** 13385-13390.

Brandt, R., and Gualerzi, C.O. 1992. Ribosomal localization of the mRNA in the 30S initiation complex as revealed by UV crosslinking. *FEBS Lett.* **311:** 199-202.

Brennan.L.E., Nakagawa.J., Egger.D., Bienz.K., and Moroni.C. 1999. Characterisation and mitochondrial localisation of AUH, an AU-specific RNA-binding enoyl-CoA hydratase. *Gene* **228:** 85-91.

Brodersen, D.E., Clemons, W.M., Jr., Carter, A.P., Wimberly, B.T., and Ramakrishnan, V. Crystal structure of the 30 S ribosomal subunit from Thermus thermophilus: structure of the proteins and their interactions with 16 S RNA. 2002. *J. Mol. Biol.* **316:** 725-768.

Brodersen, D.E. and Nissen, P. 2005. The social life of ribosomal proteins. *FEBS J.* **272:** 2098-2108.

Cahill, A., Baio, D., and Cunningham, C. 1995. Isolation and characterization of rat liver mitochondrial ribosomes. *Anal. Biochem.* **232:** 47-55.

Carter, A.P., Clemons, J., Brodersen, D.E., Morgan-Warren, R.J., Hartsch, T., Wimberly, B.T., and Ramakrishnan, V. 2001. Crystal Structure of an Initiation Factor Bound to the 30S Ribosomal Subunit. *Science* **291:** 498-501.

Cate, J.H., Yusupov, M.M., Yusupova, G.Z., Earnest, T.N., and Noller, H.F. 1999. X-ray crystal structures of 70S ribosome functional complexes. *Science* **285:** 2095-2104.

Chen, R., Fearnley, I.M., Palmer, D.N., and Walker, J.E. 2004. Lysine 43 is trimethylated in subunit C from bovine mitochondrial ATP synthase and in storage bodies associated with batten disease. *J. Biol. Chem.* **279:** 21883-21887.

Chintharlapalli, S.R., Jasti, M., Malladi, S., Parsa, K.V., Ballestero, R.P., and Gonzalez-Garcia, M. 2005. BMRP is a Bcl-2 binding protein that induces apoptosis. *J. Cell Biochem.* **94:** 611-626.

Datta, P.P., Sharma, M.R., Qi, L., Frank, J., and Agrawal, R.K. 2005. Interaction of the G' domain of elongation factor G and the C-terminal domain of ribosomal protein L7/L12 during translocation as revealed by cryo-EM. *Mol. Cell* **20:** 723-731.

Davydova, N., Streltsov, V., Wilce, M., Liljas, A., and Garber, M. 2002. L22 ribosomal protein and effect of its mutation on ribosome resistance to erythromycin. *J. Mol. Biol.* **322:** 635-644.

Dean, D., and Nomura, M. 1980. Feedback regulation of ribosomal protein gene expression in Escherichia coli. *Proc. Natl. Acad. Sci. U. S. A.* **77:** 3590-3594.

DeLano, W.L.T. 2002. The PyMOL Molecular Graphics System. *DeLano Scientific***:** San Carlos, CA, U.S.A.

Deng, H., Jankovic, J., Guo, Y., Xie, W., and Le, W. 2005. Small interfering RNA targeting the PINK1 induces apoptosis in dopaminergic cells SH-SY5Y. *Biochem. Biophys. Res. Commun.* **337:** 1133-1138.

Diedrich, G., Spahn, C.M., Stelzl, U., Schafer, M.A., Wooten, T., Bochkariov, D.E., Cooperman, B.S., Traut, R.R., and Nierhaus, K.H. 2000. Ribosomal protein L2 is involved in the association of the ribosomal subunits, tRNA binding to A and P sites and peptidyl transfer. *EMBO J.* **19:** 5241-5250.

Emdadul Haque, M., Grasso, D., Miller, C., Spremulli, L.L., and Saada, A. 2008. The effect of mutated mitochondrial ribosomal proteins S16 and S22 on the assembly of the small and large ribosomal subunits in human mitochondria. *Mitochondrion* **8:** 254-261.

Franceschi, F.J., and Nierhaus, K.H. 1990. Ribosomal proteins L15 and L16 are mere late assembly proteins of the large ribosomal subunit. Analysis of an Escherichia coli mutant lacking L15. *J. Biol. Chem.* **265:** 16676-16682.

Garcia-Marcos, A., Morreale, A., Guarinos, E., Briones, E., Remacha, M., Ortiz, A.R., and Ballesta, J.P. 2007. In vivo assembling of bacterial ribosomal protein L11 into yeast ribosomes makes the particles sensitive to the prokaryotic specific antibiotic thiostrepton. *Nucleic Acids Res.* **35:** 7109-7117.

Gottlieb, R.A. 2007. Identification of targets of phosphorylation in heart mitochondria. *Methods Mol. Biol.* **357:** 127-137.

Hamilton, M.G., and O'Brien, T.W. 1974. Ultracentrifugal characterization of the mitochondrial ribosome and subribosomal particles of bovine liver: molecular size and composition. *Biochemistry* **13:** 5400-5403.

Harms, J.M., Wilson, D.N., Schluenzen, F., Connell, S.R., Stachelhaus, T., Zaborowska, Z., Spahn, C.M., and Fucini, P. 2008. Translational regulation via L11: molecular switches on the ribosome turned on and off by thiostrepton and micrococcin. *Mol. Cell* **30:** 26-38.

He, H., Chen, M., Scheffler, N.K., Gibson, B.W., Spremulli, L.L., and Gottlieb, R.A. 2001. Phosphorylation of Mitochondrial Elongation Factor Tu in Ischemic Myocardium: Basis for Chloramphenicol-Mediated Cardioprotection. *Circ. Res.* **89:** 461-467.

Held, W.A., Ballou, B., Mizushima, S., and Nomura, M. 1974. Assembly mapping of 30 S ribosomal proteins from Escherichia coli. Further studies. *J. Biol. Chem.* **249:** 3103-3111.

Herbst, K.L., Nichols, L.M., Gesteland, R.F., and Weiss, R.B. 1994. A mutation in ribosomal protein L9 affects ribosomal hopping during translation of gene 60 from bacteriophage T4. *Proc. Natl. Acad. Sci. U. S. A.* **91:** 12525-12529.

Herr, A.J., Nelson, C.C., Wills, N.M., Gesteland, R.F., and Atkins, J.F. 2001. Analysis of the roles of tRNA structure, ribosomal protein L9, and the bacteriophage T4 gene 60 bypassing signals during ribosome slippage on mRNA. *J. Mol. Biol.* **309:** 1029-1048.

Hoang, L., Fredrick, K., and Noller, H.F. 2004. Creating ribosomes with an all-RNA 30S subunit P site. *Proc. Natl. Acad. Sci. U. S. A.* **101:** 12439-12443.

Holness, M.J., and Sugden, M.C. 2003. Regulation of pyruvate dehydrogenase complex activity by reversible phosphorylation. *Biochem. Soc. Trans.* **31:** 1143-1151.

Hopper, R.K., Carroll, S., Aponte, A.M., Johnson, D.T., French, S., Shen, R.F., Witzmann, F.A., Harris, R.A., and Balaban, R.S. 2006. Mitochondrial matrix phosphoproteome: effect of extra mitochondrial calcium. *Biochemistry* **45:** 2524-2536.

Ito, Y., Pandey, P., Mishra, N., Kumar, S., Narula, N., Kharbanda, S., Saxena, S., and Kufe, D. 2001. Targeting of the c-Abl Tyrosine Kinase to Mitochondria in Endoplasmic Reticulum Stress-Induced Apoptosis. *Mol. Cell. Biol.* **21:** 6233-6242.

Jagannathan, I., and Culver, G.M. 2003. Assembly of the central domain of the 30S ribosomal subunit: roles for the primary binding ribosomal proteins S15 and S8. *J. Mol. Biol.* **330:** 373-383.

Kashuba, E., Yurchenko, M., Yenamandra, S.P., Snopok, B., Isaguliants, M., Szekely, L., and Klein, G. 2008. EBV-encoded EBNA-6 binds and targets MRS18-2 to the nucleus, resulting in the disruption of pRb-E2F1 complexes. *Proc. Natl. Acad. Sci. U. S. A.* **105:** 5489-5494.

Kavran, J.M., and Steitz, T.A. 2007. Structure of the base of the L7/L12 stalk of the Haloarcula marismortui large ribosomal subunit: analysis of L11 movements. *J. Mol. Biol.* **371:** 1047-1059.

Khaitovich, P., Mankin, A.S., Green, R., Lancaster, L., and Noller, H.F. 1999. Characterization of functionally active subribosomal particles from Thermus aquaticus. *Proc. Natl. Acad. Sci. U. S. A.* **96:** 85-90.

Kim, H.R., Chae, H.J., Thomas, M., Miyazaki, T., Monosov, A., Monosov, E., Krajewska, M., Krajewski, S., and Reed, J.C. 2007. Mammalian dap3 is an essential gene required for mitochondrial homeostasis in vivo and contributing to the extrinsic pathway for apoptosis. *FASEB J.* **21:** 188-196.

Kissil, J.L., Deiss, L.P., Bayewitch, M., Raveh, T., Khaspekov, G., and Kimchi, A. 1995. Isolation of DAP3, a novel mediator of interferon-gamma-induced cell death. *J. Biol. Chem.* **270:** 27932-27936.

Koc, E.C., Burkhart, W., Blackburn, K., Moseley, A., and Spremulli, L.L. 2001a. The small subunit of the mammalian mitochondrial ribosome: Identification of the full complement of ribosomal proteins present. *J. Biol. Chem.* **276:** 19363-19374.

Koc, E.C., Burkhart, W., Blackburn, K., Schlatzer, D.M., Moseley, A., and Spremulli, L.L. 2001b. The large subunit of the mammalian mitochondrial ribosome: Analysis of the complement of ribosomal protein present. *J. Biol. Chem.* **276:** 43958-43969.

Koc, E.C., Ranasinghe, A., Burkhart, W., Blackburn, K., Koc, H., Moseley, A., and L.L., S. 2001c. A new face on apoptosis: Death-associated protein 3 and PDCD9 are mitochondrial ribosomal proteins. *FEBS Lett.* **492:** 166-170.

Korepanov, A.P., Gongadze, G.M., Garber, M.B., Court, D.L., and Bubunenko, M.G. 2007. Importance of the 5 S rRNA-binding ribosomal proteins for cell viability and translation in Escherichia coli. *J. Mol. Biol.* **366:** 1199-1208.

Kramer, G., Rauch, T., Rist, W., Vorderwulbecke, S., Patzelt, H., Schulze-Specking, A., Ban, N., Deuerling, E., and Bukau, B. 2002. L23 protein functions as a chaperone docking site on the ribosome. *Nature* **419:** 171-174.

Kumar, S., Bharti, A., Mishra, N.C., Raina, D., Kharbanda, S., Saxena, S., and Kufe, D. 2001. Targeting of the c-Abl tyrosine kinase to mitochondria in the necrotic cell death response to oxidative stress. *J. Biol. Chem.* **276:** 17281-17285.

Lee, S.S., Lee, R.Y., Fraser, A.G., Kamath, R.S., Ahringer, J., and Ruvkun, G. 2003. A systematic RNAi screen identifies a critical role for mitochondria in C. elegans longevity. *Nat. Genet.* **33:** 40-48.

Levshenkova, E.V., Ukraintsev, K.E., Orlova, V.V., Alibaeva, R.A., Kovriga, I.E., Zhugdernamzhilyn, O., and Frolova, E.I. 2004. The structure and specific features of the cDNA expression of the human gene MRPL37. *Bioorg. Khim.* **30:** 499-506.

Lieberman, K.R., and Noller, H.F. 1998. Ribosomal protein L15 as a probe of 50 S ribosomal subunit structure. *J. Mol. Biol.* **284:** 1367-1378.

Liebler, D.C. 2002. Introduction to Proteomics: Tools for the New Biology. *Humana Press***:** Totowa, NJ, U.S.A.

Lotti, M., Stoffler-Meilicke, M., and Stoffler, G. 1987. Localization of ribosomal protein L27 at the peptidyl transferase centre of the 50 S subunit, as determined by immuno-electron microscopy. *Mol. Gen. Genet.* **210:** 498-503.

Macek, B., Gnad, F., Soufi, B., Kumar, C., Olsen, J.V., Mijakovic, I., and Mann, M. 2008. Phosphoproteome analysis of E. coli reveals evolutionary conservation of bacterial Ser/Thr/Tyr phosphorylation. *Mol. Cell. Proteomics* **7:** 299-307.

Maguire, B.A., Beniaminov, A.D., Ramu, H., Mankin, A.S., and Zimmermann, R.A. 2005. A protein component at the heart of an RNA machine: the importance of protein l27 for the function of the bacterial ribosome. *Mol. Cell* **20:** 427-435.

Marquardt, O., Roth, H.E., Wystup, G., and Nierhaus, K.H. 1979. Binding of Escherichia coli ribosomal proteins to 23S RNA under reconstitution conditions for the 50S subunit. *Nucleic Acids Res.* **6:** 3641-3650.

Maslov, D.A., Spremulli, L.L., Sharma, M.R., Bhargava, K., Grasso, D., Falick, A.M., Agrawal, R.K., Parker, C.E., and Simpson, L. 2007. Proteomics and electron microscopic characterization of the unusual mitochondrial ribosome-related 45S complex in Leishmania tarentolae. *Mol. Biochem. Parasitol.* **152:** 203-212.

Matthews, D.E., Hessler, R.A., Denslow, N.D., Edwards, J.S., and O'Brien, T.W. 1982. Protein composition of the bovine mitochondrial ribosome. *J. Biol. Chem.* **257:** 8788-8794.

Mikulik, K., and Janda, I. 1997. Protein kinase associated with ribosomes phosphorylates ribosomal proteins of Streptomyces collinus. *Biochem. Biophys. Res. Commun.* **238:** 370-376.

Mikulik, K., Suchan, P., and Bobek, J. 2001. Changes in ribosome function induced by protein kinase associated with ribosomes of Streptomyces collinus producing kirromycin. *Biochem. Biophys. Res. Commun.* **289:** 434-443.

Miller, C., Saada, A., Shaul, N., Shabtai, N., Ben-Shalom, E., Shaag, A., Hershkovitz, E., and Elpeleg, O. 2004. Defective mitochondrial translation caused by a ribosomal protein (MRPS16) mutation. *Ann. Neurol.* **56:** 734-738.

Miller, J.L., Koc, H., and Koc, E.C. 2008. Identification of phosphorylation sites in mammalian mitochondrial ribosomal protein DAP3. *Protein Sci.* **17:** 251-260.

Miyazaki, T., and Reed, J.C. 2001. A GTP-binding adapter protein couples TRAIL receptors to apoptosis-inducing proteins. *Nat. Immunol.* **2:** 493-500.

Miyazaki, T., Shen, M., Fujikura, D., Tosa, N., Kon, S., Uede, T., and Reed, J.C. 2004. Functional role of death associated protein 3 (DAP3) in anoikis. *J. Biol. Chem.* **279:** 44667-44672.

Mukamel, Z., and Kimchi, A. 2004. Death-associated protein 3 localizes to the mitochondria and is involved in the process of mitochondrial fragmentation during cell death. *J. Biol. Chem.* **279:** 36732-36738.

Nevskaya, N., Tishchenko, S., Volchkov, S., Kljashtorny, V., Nikonova, E., Nikonov, O., Nikulin, A., Kohrer, C., Piendl, W., Zimmermann, R., et al. 2006. New insights into the interaction of ribosomal protein L1 with RNA. *J. Mol. Biol.* **355:** 747-759.

Nikulin, A., Eliseikina, I., Tishchenko, S., Nevskaya, N., Davydova, N., Platonova, O., Piendl, W., Selmer, M., Liljas, A., Drygin, D., et al. 2003. Structure of the L1 protuberance in the ribosome. *Nat. Struct. Biol.* **10:** 104-108.

Nissen, P., Hansen, J., Ban, N., Moore, P.B., and Steitz, T.A. 2000. The Structural Basis of Ribosome Activity in Peptide Bond Synthesis. *Science* **289:** 920-930.

Noller, H.F., Hoang, L., and Fredrick, K. 2005. The 30S ribosomal P site: a function of 16S rRNA. *FEBS Lett.* **579:** 855-858.

Nowotny, V., and Nierhaus, K.H. 1982. Initiator proteins for the assembly of the 50S subunit from Escherichia coli ribosomes. *Proc. Natl. Acad. Sci. U. S. A.* **79:** 7238-7242.

Nowotny, V., and Nierhaus, K.H. 1988. Assembly of the 30S subunit from Escherichia coli ribosomes occurs via two assembly domains which are initiated by S4 and S7. *Biochemistry* **27:** 7051-7055.

O'Brien T, W., O'Brien B, J., and Norman, R.A. 2005. Nuclear MRP genes and mitochondrial disease. *Gene* **354:** 147-151.

O'Brien, T.W. 2002. Evolution of a protein-rich mitochondrial ribosome: implications for human genetic disease. *Gene* **286:** 73-79.

Ogawa, F., Adachi, S., Kohu, K., Shige, K., and Akiyama, T. 2003. Binding of the human homolog of the Drosophila discs large tumor suppressor protein to the mitochondrial ribosomal protein MRP-S34. *Biochem. Biophys. Res. Commun.* **300:** 789-792.

Persson, B.C., Bylund, G.O., Berg, D.E., and Wikstrom, P.M. 1995. Functional analysis of the ffh-trmD region of the Escherichia coli chromosome by using reverse genetics. *J. Bacteriol.* **177:** 5554-5560.

Pietromonaco, S., Denslow, N., and O'Brien, T.W. 1991. Proteins of mammalian mitochondrial ribosomes. *Biochimie* **73:** 827-836.

Pridgeon, J.W., Olzmann, J. A., Chin, L.S., and Li, L. 2007. PINK1 protects against oxidative stress by phosphorylating mitochondrial chaperone TRAP1. *PLoS Biol.* **5:** e172.

Robbins, P.F., el-Gamil, M., Li, Y.F., Topalian, S.L., Rivoltini, L., Sakaguchi, K., Appella, E., Kawakami, Y., and Rosenberg, S.A. 1995. Cloning of a new gene encoding an antigen recognized by melanoma-specific HLA-A24-restricted tumor-infiltrating lymphocytes. *J. Immunol.* **154:** 5944-5950.

Robert, F., and Brakier-Gingras, L. 2001. Ribosomal protein S7 from Escherichia coli uses the same determinants to bind 16S ribosomal RNA and its messenger RNA. *Nucleic Acids Res.* **29:** 677-682.

Robert, F., and Brakier-Gingras, L. 2003. A functional interaction between ribosomal proteins S7 and S11 within the bacterial ribosome. *J. Biol. Chem.* **278:** 44913-44920.

Salvi, M., Brunati, A.M., and Toninello, A. 2005. Tyrosine phosphorylation in mitochondria: a new frontier in mitochondrial signaling. *Free Radic. Biol. Med.* **38:** 1267-1277.

Schlunzen, F., Wilson, D.N., Tian, P., Harms, J.M., McInnes, S.J., Hansen, H.A., Albrecht, R., Buerger, J., Wilbanks, S.M., and Fucini, P. 2005. The binding mode of the trigger factor on the ribosome: implications for protein folding and SRP interaction. *Structure* **13:** 1685-1694.

Schuwirth, B.S., Borovinskaya, M.A., Hau, C.W., Zhang, W., Vila-Sanjurjo, A., Holton, J.M., and Cate, J.H. 2005. Structures of the bacterial ribosome at 3.5 A resolution. *Science* **310:** 827-834.

Sharma, M.R., Koc, E.C., Datta, P.P., Booth, T.M., Spremulli, L.L., and Agrawal, R.K. 2003. Structure of the mammalian mitochondrial ribosome reveals an expanded functional role for its component proteins. *Cell* **115:** 97-108.

Soung, G.Y., Miller, J.L., Koc, H., and Koc, E.C. 2009. Comprehensive analysis of phosphorylation sites in *E. coli* ribosomal proteins. *(in revision)*.

Spremulli, L.L. 2007. Large-scale isolation of mitochondrial ribosomes from mammalian tissues. *Methods Mol. Biol.* **372:** 265-275.

Stade, K., Rinke-Appel, J., and Brimacombe, R. 1989. Site-directed cross-linking of mRNA analogues to the Escherichia coli ribosome; identification of 30S ribosomal components that can be cross- linked to the mRNA at various points 5' with respect to the decoding site. *Nucleic Acids Res.* **17:** 9889-9908.

Subramanian, A.R., and Dabbs, E.R. 1980. Functional studies on ribosomes lacking protein L1 from mutant Escherichia coli. *Eur. J. Biochem.* **112:** 425-430.

Takeda, S., Iwai, A., Nakashima, M., Fujikura, D., Chiba, S., Li, H.M., Uehara, J., Kawaguchi, S., Kaya, M., Nagoya, S., et al. 2007. LKB1 is crucial for TRAIL-mediated apoptosis induction in osteosarcoma. *Anticancer Res.* **27:** 761-768.

Traugh, J.A., and Traut, R.R. 1972. Phosphorylation of ribosomal proteins of Escherichia coli by protein kinase from rabbit skeletal muscle. *Biochemistry* **11:** 2503-2509.

Uchiumi, T., Hori, K., Nomura, T., and Hachimori, A. 1999. Replacement of L7/L12.L10 protein complex in Escherichia coli ribosomes with the eukaryotic counterpart changes the specificity of elongation factor binding. *J. Biol. Chem.* **274:** 27578-27582.

Ullers, R.S., Houben, E.N., Raine, A., ten Hagen-Jongman, C.M., Ehrenberg, M., Brunner, J., Oudega, B., Harms, N., and Luirink, J. 2003. Interplay of signal recognition particle and trigger factor at L23 near the nascent chain exit site on the Escherichia coli ribosome. *J. Cell Biol.* **161:** 679-684.

Valle, M., Zavialov, A., Sengupta, J., Rawat, U., Ehrenberg, M., and Frank, J. 2003. Locking and unlocking of ribosomal motions. *Cell* **114:** 123-134.

Van Dyke, N., Xu, W., and Murgola, E.J. 2002. Limitation of ribosomal protein L11 availability in vivo affects translation termination. *J. Mol. Biol.* **319:** 329-339.

Willumeit, R., Forthmann, S., Beckmann, J., Diedrich, G., Ratering, R., Stuhrmann, H.B., and Nierhaus, K.H. 2001. Localization of the protein L2 in the 50 S subunit and the 70 S E. coli ribosome. *J. Mol. Biol.* **305:** 167-177.

Wimberly, B.T., Brodersen, D.E., Clemons, W.M., Jr, Morgan-Warren, R.J., Carter, A.P., Vonrhein, C., Hartsch, T., and Ramakrishnan, V. 2000. Structure of the 30S ribosomal subunit. *Nature* **407:** 327-339.

Yusupov, M.M., Yusupova, G.Z., Baucom, A., Lieberman, K., Earnest, T.N., Cate, J.H.D., and Noller, H.F. 2001. Crystal Structure of the Ribosome at 5.5 A Resolution. *Science* **292:** 883-896.

Yusupova, G.Z., Yusupov, M.M., Cate, J.H., and Noller, H.F. 2001. The Path of Messenger RNA through the Ribosome. *Cell* **106:** 233-241.

Zhang, L., Zambon, A.C., Vranizan, K., Pothula, K., Conklin, B.R., and Insel, P.A. 2008. Gene expression signatures of cAMP/protein kinase A (PKA)-promoted, mitochondrial-dependent apoptosis. Comparative analysis of wild-type and cAMP-deathless S49 lymphoma cells. *J. Biol. Chem.* **283:** 4304-4313.

# CHAPTER 3

# Identification of phosphorylation sites in mammalian mitochondrial ribosomal protein DAP3

## 3.1 Rationale

Death Associated Protein 3 (DAP3) also known as MRPS29 is a well characterized apoptotic protein that was identified as one of the mitochondrial ribosomal proteins without a bacterial homolog (Kissil et al. 1999; Koc et al. 2001c; Miyazaki and Reed 2001). DAP3 is localized to the base of the lower lobe of the small subunit; however, its function in translation is unclear (O'Brien T et al. 2005). In addition to the fact the phosphorylated residues identified were highly conserved within the mitochondria, two reports implicated DAP3 in association with LKB1 and Akt, Ser/Thr kinases (Miyazaki et al. 2004; Takeda et al. 2007). Therefore, DAP3 was chosen for further functional studies as we hypothesized phosphorylation might be a molecular switch responsible for the regulation of DAP3-induced apoptosis, which can be readily tested by different experiments examining cell death. In this study, the phosphorylation sites were mutated to alanine residues and after overexpressing each construct in cell lines, two methods were chosen to assess the ability for wild-type and mutant DAP3 to induce apoptosis. Western blots were performed using cleaved PARP (poly ADP-ribose polymerase) as a marker for apoptosis. When PARP is cleaved by an activated caspase 3, the protein no longer can assist in DNA repair. The second method addressed cell viability by directly measuring the activity of mitochondrial dehydrogenases in living cells. Together this data should support our hypothesis, in addition to identifying other kinases localized to the mitochondria, which may endogenously phosphorylate DAP3.

## 3.2 Abstract

Mammalian mitochondrial ribosomes synthesize thirteen proteins that are essential for oxidative phosphorylation. In addition to their role in protein synthesis, some

of the mitochondrial ribosomal proteins have acquired functions in other cellular processes such as apoptosis. Death Associated Protein 3 (DAP3), also referred to as mitochondrial ribosomal protein S29 (MRPS29), is a GTP-binding apoptotic protein located in the small subunit of the ribosome. Previous studies have shown that phosphorylation is one of the most likely regulatory mechanisms for DAP3 function in apoptosis and maybe in protein synthesis; however, no phosphorylation sites were identified. In this study, we have investigated the phosphorylation status of ribosomal DAP3 and mapped the phosphorylation sites by tandem mass spectrometry. Mitochondrial ribosomal DAP3 is phosphorylated at Ser215 or Thr216, Ser220, Ser251 or Ser252, and Ser280. In addition, phosphorylation of recombinant DAP3 by protein kinase A and protein kinase Cδ at residues that are endogenously phosphorylated in ribosomal DAP3 suggests both of these kinases as potential candidates responsible for the *in vivo* phosphorylation of DAP3 in mammalian mitochondria. Interestingly, the majority of the phosphorylation sites detected in our study are clustered around the highly conserved GTP-binding motifs, which may affect the protein conformation and activity. Site-directed mutagenesis studies on selected phosphorylation sites were performed to determine the effect of phosphorylation on cell viability and PARP cleavage as indication of caspase activation. Overall our findings suggest DAP3, a mitochondrial ribosomal small subunit protein, is a novel phosphorylated target.

## 3.3 Introduction

Mitochondria are the powerhouses of eukaryotic cells, generating most of the ATP through oxidative phosphorylation. Although 13 mitochondrially-encoded proteins are essential for this process and survival of eukaryotic cells, the mitochondrial translational system responsible for the synthesis of these proteins is one of the least understood systems. Proteomic studies of mitochondrial ribosomes have indicated that some of the ribosomal proteins have acquired unique functions in addition to their essential role in protein synthesis (Koc et al. 2001a; Koc et al. 2001b; Koc et al. 2001c; Sharma et al. 2003; O'Brien T et al. 2005). Several mammalian mitochondrial ribosomal proteins (MRPs) are involved in apoptotic signaling pathways (Kissil et al. 1999; Koc et al. 2001c; Miyazaki and Reed 2001; Chintharlapalli et al. 2005; Levshenkova et al.

2004). One of these, MRPS29, more commonly known as DAP3, was first identified as a positive mediator of interferon-γ induced cell death through a functional screen of HeLa cells transfected with an antisense cDNA library (Kissil et al. 1995). Although it is historically linked to cell death, DAP3 is the only GTP-binding protein found in the small subunit of the mammalian and yeast mitochondrial ribosomes (Denslow et al. 1991; Koc et al. 2001a; Saveanu et al. 2001). The presence of this protein accounts for the high specific GTP-binding affinity of small subunits of mitochondrial ribosomes (Denslow et al. 1991). Immuno-EM studies have localized DAP3 to the base of the lower lobe of the small subunit on the solvent side of the ribosome (O'Brien T et al. 2005), but its role in protein synthesis is still unknown. In yeast, DAP3 is required for mitochondrial DNA synthesis and respiration (Berger et al. 2000). This observation indicates that DAP3 plays a role in protein synthesis, which is required for the maintenance of mitochondrial DNA in yeast. Furthermore, a theme connecting DAP3 to mitochondrial physiology is gaining support as DAP3 deficiency in mice is lethal *in utero* and the observed embryos had abnormal, shrunken mitochondria (Kim et al. 2007).

Mitochondria are highly dynamic and phosphorylation of Ser, Thr, or Tyr residues represents a possible regulatory mechanism employed in this organelle. A large number of phosphorylated mitochondrial proteins have been reported including subunits of Complex I and V, heat shock proteins, apoptotic proteins, and enzymes of the citric acid cycle (Liu et al. 2003; Schulenberg et al. 2003; Taylor et al. 2003; Salvi et al. 2005; Hopper et al. 2006). To better understand the mechanism behind the variety of roles that DAP3 plays within the mitochondria, we hypothesized that the function of ribosomal DAP3 can be partially controlled by phosphorylation. Phosphorylation of DAP3 could serve as a molecular switch, impacting protein synthesis as well as apoptosis and mitochondrial physiology. A previous study has shown that DAP3 can be phosphorylated at Thr237 by Akt resulting in the suppression of anoikis; and mutating this residue resulted in an increased level of cell death as the survival kinase could no longer phosphorylate the site (Miyazaki et al. 2004). Recently, the interaction of DAP3 with the Ser/Thr kinase LKB1 and role of this kinase in DAP3-induced apoptosis have been studied in osteosarcoma cells (Takeda et al. 2007).

To expand on these initial studies, we used mass spectrometry-based proteomics to identify and map the specific phosphorylation sites on ribosomal DAP3 and *in vitro* phosphorylation sites of recombinant DAP3 using several different kinases localized to the mitochondria. By way of phosphorylated amino acid specific antibodies and tandem mass spectrometry, we provide evidence for phosphorylation of mitochondrial ribosomal DAP3 isolated from bovine mitochondrial 55S ribosomes. Moreover, selected phosphorylated residues were evaluated for their effect on cell viability and caspase activation detected by the DNA single strand repair enzyme poly (ADP-ribose) polymerase (PARP) cleavage. Our findings suggest that phosphorylation is one of the mechanisms modulating the function of ribosomal DAP3 in the progression of apoptosis in mitochondria.

## 3.4 Results

### 3.4.1 DAP3 is Phosphorylated on 55S Mitochondrial Ribosomes

To determine the phosphorylation status of DAP3, crude mitochondrial ribosomes were isolated from bovine liver using previously described methods (Matthews et al. 1982) and fractionated into intact 55S mitochondrial ribosomes. Mammalian mitochondrial ribosomes contain 77 known proteins, of which 29 are in the small subunit and 48 are in the large subunit (O'Brien et al. 1999; O'Brien et al. 2000; Koc et al. 2001a; Koc et al. 2001b; Suzuki et al. 2001a; Suzuki et al. 2001b). The proteins of the 55S ribosomes were separated by using non-equilibrium pH gradient electrophoresis (NEPHGE) tube gels rather than the commonly used immobilized pH gradient (IPG) strips due to the abundance of basic amino acids in the ribosomal protein sequences (Cahill et al. 1995). SDS-PAGE separation was used as the second dimension and the proteins were located by staining with SYPRO Ruby, for total protein content (Figure 3.1A). Bovine DAP3 migrates in the 37-50 kDa region and the exact location of the DAP3 protein was determined by immunoblotting and mass spectrometric identification of the 2D-gel spots as shown by an arrow in Figure 3.1. The pattern of DAP3 obtained from this analysis showed the characteristic trailing towards a more acidic pI expected for

a phosphorylated protein (Figure 3.1B). Furthermore, the sample was probed with anti-phosphoserine antibody and DAP3 is serine phosphorylated as noted in Figure 3.1C.

In addition, purified 55S ribosome preparations were analyzed by both in-solution digests of the whole ribosomal protein mixture, the shotgun approach, and in-gel digests of the 1D-gel separated proteins to improve the peptide coverage and, as a result, the likelihood of detecting more phosphopeptides. Despite having greater than 70% sequence coverage of the DAP3 protein by using these various approaches, only one phosphorylated peptide was detected for DAP3, amongst the more common unphosphorylated form of the peptide. This is not surprising because proteins are constantly cycling between the phosphorylated and unphosphorylated state. In addition, just a small fraction of the DAP3 copies present may be phosphorylated at a given time depending on the stage of translation and conformation of the ribosome, making it much more difficult to capture the phosphorylated DAP3. Therefore, we employed phosphopeptide enrichment of the intact 55S ribosomes by immobilized metal affinity chromatography (IMAC) based on selective binding of phosphopeptides to gallium. This enrichment strategy allowed us to detect additional peptides, which increased the sequence coverage and identification of two new DAP3 phosphopeptides containing multiple phosphorylation sites (Table 3.1).

Tandem MS spectra generated by fragmentation of peptides by collision-induced dissociation (CID) were used for both detection and mapping of phosphorylation sites. The spectra matching to phosphopeptides were each carefully validated for overall data quality and signal-to-noise of peaks matching to expected *m/z* values in addition to applying the Sequest Xcorr coefficient cutoff of >1.5, 2.0, and 2.5 for +1, +2, +3 charged peptides respectively. Interestingly, the majority of the phosphorylation sites identified in the bovine DAP3 sequence had been predicted to be phosphorylated using the NetPhos prediction tool including Ser215, Thr216, Ser220, Ser252, and Ser280 (Table 3.1). Furthermore, most of the phosphorylation sites are located in close proximity to GTP-binding motifs found in the DAP3 sequence except Ser280 (Figure 3.2A). Therefore, as a comparison the three-dimensional structure of the human Ras-21 was modeled in the

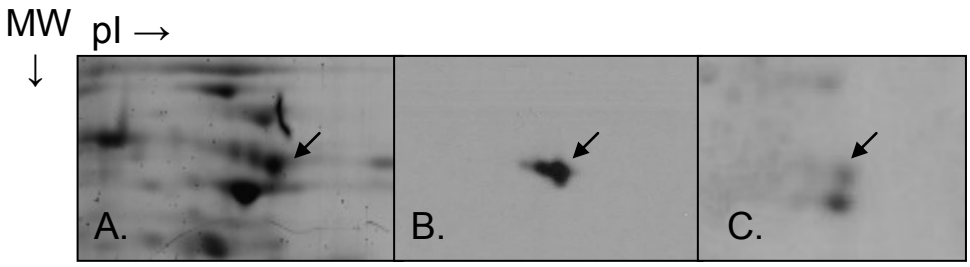


D.


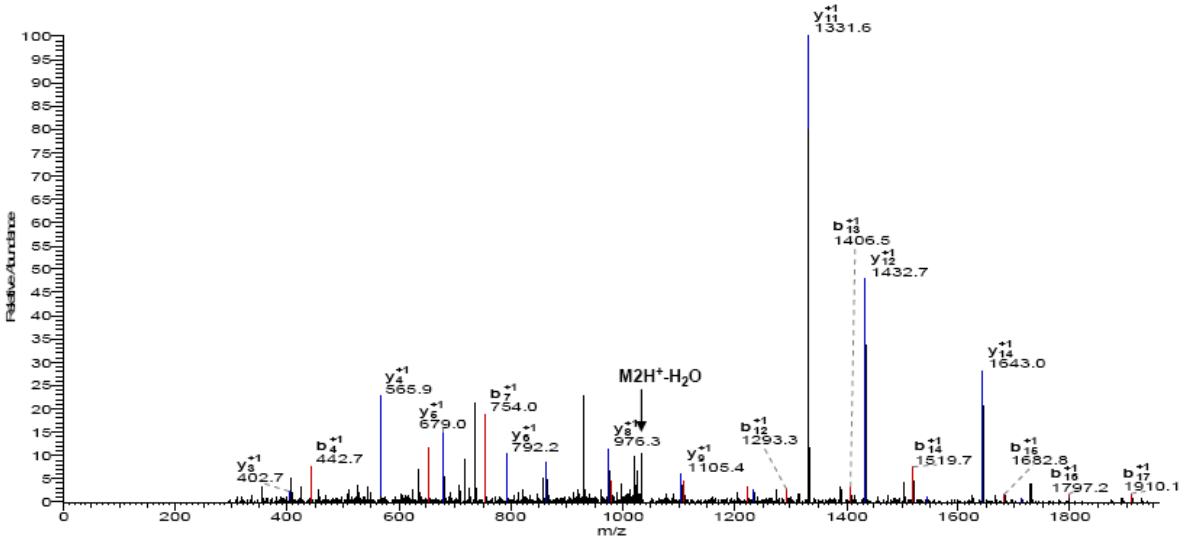


**Figure 3.1. Phosphorylated DAP3 was detected in 55S bovine mitochondrial ribosomes by immunoblotting and mass spectrometry.** Bovine mitochondrial ribosomal proteins (1.8 $A_{260}$ units) were separated on 2D-NEPHGE gels; the DAP3 protein was excised, digested with trypsin, and analyzed by LC/MS/MS for potential phosphorylation sites using an ion trap mass spectrometer. A) SYPRO Ruby stained gel for total protein content, B and C) Western blot analysis of the 55S bovine mitochondrial ribosomes using anti-DAP3 and anti-phosphoserine antibodies, respectively. The arrow indicates the location of DAP3 on the gel or Western blot. D) CID MS/MS spectrum for doubly-charged phosphorylated peptide EDK**p**SPITPEELALIYNLR (peptide mass 2084.4, charge 2+).

**TABLE 3.1** – ***In vivo*** **and** ***in vitro*** **phosphorylation sites of DAP3 detected and mapped by MS/MS analyses**

| Kinase | | Tryptic Phosphorylated Peptides | Phosphorylated Residue(s) | Peptide Mass and Charge | Xcorr[a] |
|---|---|---|---|---|---|
| *In vivo*[b] | 213-232 | RE**p**(ST)EKG**p**SPLAEVVEQGIMR[c] | S215 or T216, S220 | 2295.2, 3+ | 47[d] |
| | 250-257 | Q**p**(SS)LGVFR | S251 or S252 | 876.4, 1+ | 2.02,2.08 |
| | 277-294 | EDK**p**SPITPEELALIYNLR | S280 | 2084.4, 2+ | 4.67 |
| PKA[e] | 30-46 | Q**p**SIAAHLDNQVPVESPR | S31 | 1844.2, 2+ | 5.01 |
| | 176-189 | QRFDQPLEA**p**(ST)WLK | S185 or T186 | 1702.4, 2+ | 2.53,2.87 |
| | 219-232 | G**p**SPLGEVVEQGITR | S220 | 1426.1, 2+ | 3.52 |
| PKCδ[e] | 30-46 | Q**p**SIAAHLDNQVPVESPR | S31 | 1844.2, 2+ | 4.92 |
| | 178-189 | FDQPLEA**p**(ST)WLK | S185 or T186 | 1514.9, 2+ | 3.74,3.62 |
| | 235-245 | NA**p**TDAVGIVLK | T237 | 1181.6, 2+ | 3.70 |
| | 277-294 | EDK**p**SPIAPEELALVHNLR | S280 | 2014.7, 3+ | 5.59 |

[a]Xcorr coefficient cutoff of >1.5, 2.0, and 2.5 for +1, +2, +3 charged peptides
[b]Peptides obtained from bovine mitochondrial ribosomal DAP3
[c]Oxidiation of methionine
[d]Mascot score
[e]Peptides obtained from *in vitro* phosphorylated recombinant human DAP3

GTP-bound configuration to illustrate relative conformations of GTP-binding motifs, G1-G5 in Figure 3.2B (Pai et al. 1990). Interestingly, eight of the phosphorylated residues are found in the vicinity of the GTP-binding motifs. For example, Ser215, Thr216, and Ser220 are evolutionarily conserved and located after G4 motif (NKRE). Similarly, the peptide score for phosphorylation of Ser251 was very close to the score for Ser252; therefore, phosphorylation of Ser251 and Ser252 were not distinguishable (Table 3.1). Both of these residues are positioned just a short distance after G3 motif implying their possible role in forming the GTP-binding pocket (Figure 3.2A-B). The other phosphorylation site determined was Ser280 and this residue is highly conserved and predicted to be phosphorylated. The tandem mass spectrum of the phosphorylated peptide containing the Ser280 phosphorylation is shown in Fig.uren3.1D indicating a neutral loss of a water (-18 Da) molecule that is known to occur as a result of loss of the phosphate moiety from the Ser280 through β-elimination. One additional potential phosphorylation site, Thr237, was also identified in our analysis, but with a lower MASCOT score and/or Sequest Xcorr coefficient.

### 3.4.2 Ectopically Expressed DAP3 is Serine and Threonine Phosphorylated in HEK293T Cells

To further support the *in vivo* phosphorylation analysis of DAP3, we decided to study DAP3 in cell culture as experiments connecting phosphorylation status and apoptosis induction together can be more readily performed in this system. Initially, DAP3 was cloned into the mammalian expression vector, pcDNA, to express the protein in HEK293T (human embryonic kidney) cells, because these cells have a high transfection efficiency. In Figure 3.3A-B, cell lysates were probed with an anti-DAP3 antibody to ensure the protein was being overexpressed in HEK293T cells. From the figure, human DAP3 is clearly overexpressed about 2-3 fold compared to the cells transfected with the control vector, pcDNA. Furthermore, the protein is localized to the mitochondria and can be incorporated into the mitochondrial ribosomes. Therefore the next critical experiment was to determine if the ectopically expressed human DAP3 was phosphorylated as hypothesized because this would provide a reasonable foundation for

A.

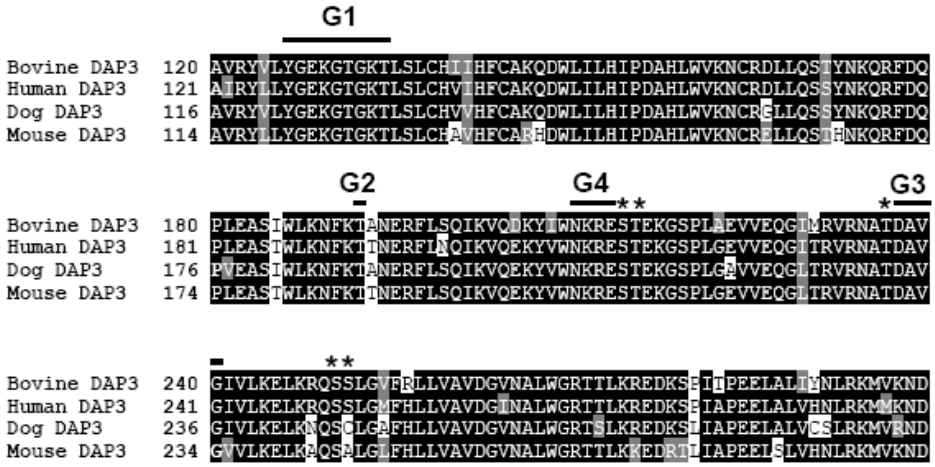


B.

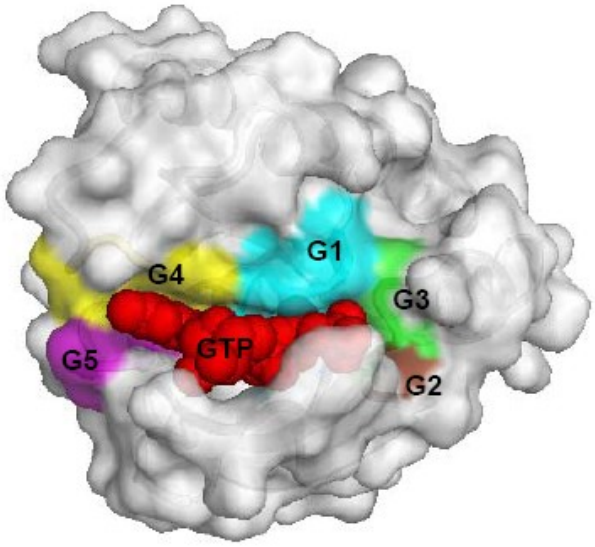


**Figure 3.2. Primary sequence alignment of bovine (Swiss-Prot P82922), human (Swiss-Prot P51398), dog (Gen Bank CK653556 and DR105073), and mouse (Swiss-Prot Q9ER88) DAP3 proteins and the 3D-model of the GTP-binding pocket.** A) The four guanine nucleotide binding motifs are indicated by G1, G2, G3, and G4 with thick lines. Asterisks (*) specify phosphorylation sites found in this proteomic analysis. The alignment was created with CLUSTALW program in Biology Workbench and the results are displayed in BOXSHADE. B) The 3D-model of the human Ras-21 in the GTP-bound configuration was generated by PyMOL (DeLano 2002) using the coordinates obtained from Protein Databank (PDB) entry 5P21 (Pai et al. 1990). The five conserved guanine nucleotide-binding motifs and GTP are labeled as G1-G5 and GTP and colored in cyan, brown, green, yellow, purple and red, respectively.

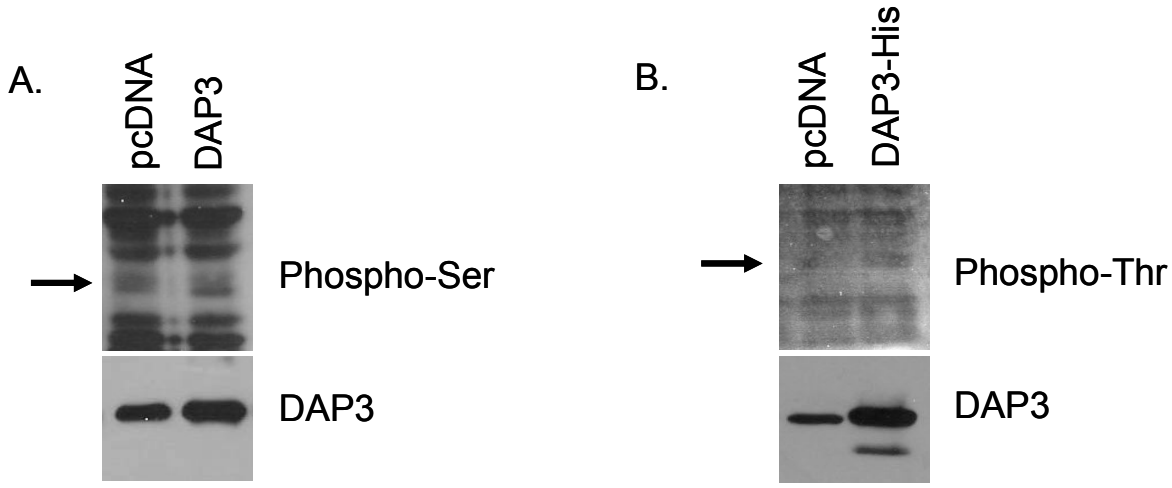


**Figure 3.3. Ectopically expressed DAP3 was detected by phospho-specific antibodies in HEK293T cells.** Approximately 4 x $10^5$ HEK293T cells were transiently transfected with 2-4 μg of plasmid DNA for DAP3, DAP3-His, and the control vector pcDNA. After an incubation of 24-48 h at 37 °C, the cells were collected and lysed. A and B) Each panel is a Western blot probed with anti-phosphoserine, anti-phosphothreonine, and anti-DAP3 using 50 μg of protein. The arrow indicates the location of DAP3 on the Western blot.

later mutating the phosphorylation sites to alanine residues and investigating their role in apoptosis induction. To address this question, immunoblotting was performed with phospho-specific antibodies and as hypothesized, ectopically expressed human DAP3 is phosphorylated at both serine and threonine residues (Figure 3.3A-B). The data is in agreement with the proteomics analysis studying bovine ribosomal DAP3 and can serve as a basis for site-directed mutagenesis work.

### 3.4.3 *In Vitro* Phosphorylation of Recombinant DAP3 by PKA and PKCδ

Web-based tools including Scan ProSite and NetPhos were employed to identify possible kinases, which may serve as candidates to phosphorylate DAP3 *in vivo* and to identify potential serine, threonine, and tyrosine phosphorylation sites in the human DAP3 sequence (Blom et al. 1999). cAMP-dependent protein kinase (PKA) and protein kinase C delta (PKCδ) were chosen as the best candidates to phosphorylate DAP3, as each had predicted sites that corresponded to our *in vivo* data. For example, PKA was predicted to phosphorylate Ser215 and Ser251. This kinase can be localized to the mitochondria through A-kinase anchoring proteins (AKAPs) and its enzyme activity occurs on the matrix side of the inner membrane (Chen et al. 2004). Furthermore, given the consensus motif for PKCδ, Thr216 is a probable target. PKCδ is found within the mitochondria or is translocated there depending on the cell type (Brodie and Blumberg 2003). Overall, the NetPhos prediction results indicated that eight serine, two threonine, and one tyrosine residues were predicted to be phosphorylated with high probability in the human DAP3 sequence.

Human recombinant DAP3 supporting an N-terminal His tag was overexpressed in *E. coli* and purified under native conditions by affinity chromatography using a Ni-NTA column (Figure 3.4A). Phosphorylation reactions carried out with recombinant DAP3 in the presence of various kinases were analyzed by SDS-PAGE followed by ProQ-Diamond phosphoprotein staining. It was clear that DAP3 was phosphorylated by both PKA and PKCδ compared to the untreated recombinant DAP3 used as a control (Figure 3.4B). Since the ProQ-Diamond is not a residue-specific phosphoprotein dye, it was not possible to determine which residue was phosphorylated. To determine the

specific site(s) of phosphorylation by these kinases, LC/MS/MS analyses were performed on the in-gel digests of kinase reaction products. Tandem mass spectrometry analyses revealed phosphorylation of Ser31, Ser185 or Thr186 by both PKA and PKCδ as the CID tandem mass spectra reflected either a neutral loss of phosphoric acid ($M2H^+$-$H_3PO_4$) or water (-18 Da) molecule (Table 3.1). Two additional phosphorylation sites, Thr237 and Ser280, and one additional PKA phosphorylation site, Ser220, were identified in the PKCδ and PKA reactions, respectively (Table 3.1). The spectra used in mapping of these sites are shown in Figure 3.5A-B. These spectra reflected a loss of water (-18 Da) from Ser220 by β-elimination in Figure 5A and an increase of 80 Da in molecular weight of the peptide for Thr237 in Figure 5B. Of interest, neither Ser185 nor Thr237 had been predicted to be phosphorylated, yet each site is evolutionarily conserved. In particular, Thr237 is the same site that was previously phosphorylated by Akt (also known as protein kinase B) suppressing anoikis; however, we were unable to show *in vitro* phosphorylation by this kinase (Figure 3.4C) (Miyazaki et al. 2004). This site precedes GTP-binding G3 motif (DAVG), while Ser185 is upstream of G2 motif (Thr193), once again emphasizing this clustering effect of the phosphorylation sites (Figure 3.2A-B). In addition to the kinases mentioned, we also tested whether the expressed DAP3 was a substrate for the Abl protein tyrosine kinase since Tyr208 was predicted (96%) to be phosphorylated (Figure 3.4C). The ProQ analysis revealed recombinant DAP3 could be a target for this kinase, but we were unable to confidently map any phosphorylated Tyr residues. This was probably because some of the Tyr residues are located in Lys and Arg rich regions and tryptic digestion of DAP3 resulted in peptides that were too small to be detected and phosphorylated residues could potentially be missed. For this reason, proteolytic digestions with Glu C (cleaves at the C-terminal end of glutamic acid) and Lys C (cleaves at the C-terminal end of lysine) were also performed. However, no additional phosphopeptides were detected. Overall, the DAP3 sequence coverage was 84%, 17%, and 32% using trypsin, Glu C, and Lys C, respectively.

### 3.4.4 Effects of DAP3 Mutations on Cell Viability and PARP Cleavage

DAP3 was originally identified as a pro-apoptotic protein; therefore the role of phosphorylated residues on cell viability and PARP cleavage as an indication of caspase

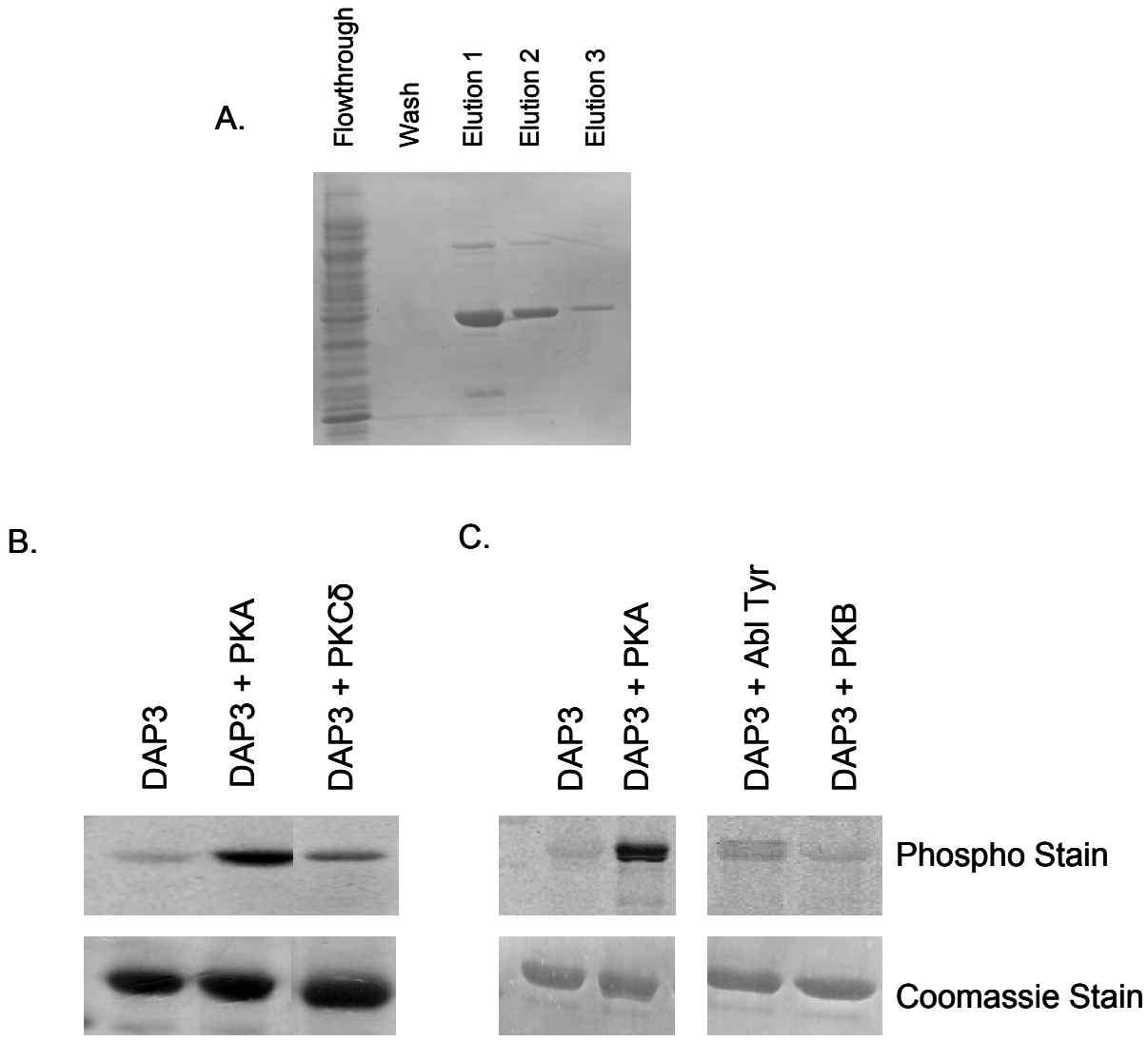


**Figure 3.4. Recombinant DAP3 was phosphorylated *in vitro* and assessed by ProQ Diamond phospho dye.** A) DAP3 carrying an N-terminal His tag was expressed in the BL21-RIL strain of *E. coli* for 5 h at 23 °C, and purified under native conditions by affinity chromatography using the Ni-NTA column. Each fraction was eluted with 250 mM imidazole. *In vitro* phosphorylation reactions consisted of 5 µg of recombinant DAP3 protein, 200 µM cold ATP, and 100 U of Abl protein tyrosine kinase, 20 U of PKB, 2500 U of PKA, or 48 ng of PKCδ. Each reaction was incubated for 1 h at 30 °C, run an SDS-PAGE gel, and stained with the ProQ Diamond Phospho dye. Phosphorylated DAP3 was excised from a Coomassie stained gel, digested with trypsin, Lys C, or Glu C, and analyzed with an ion trap mass spectrometer. B) Overexpressed DAP3 with and without PKA and PKCδ. C) Overexpressed DAP3 with and without PKA, Abl tyrosine kinase, and PKB (also known as Akt).

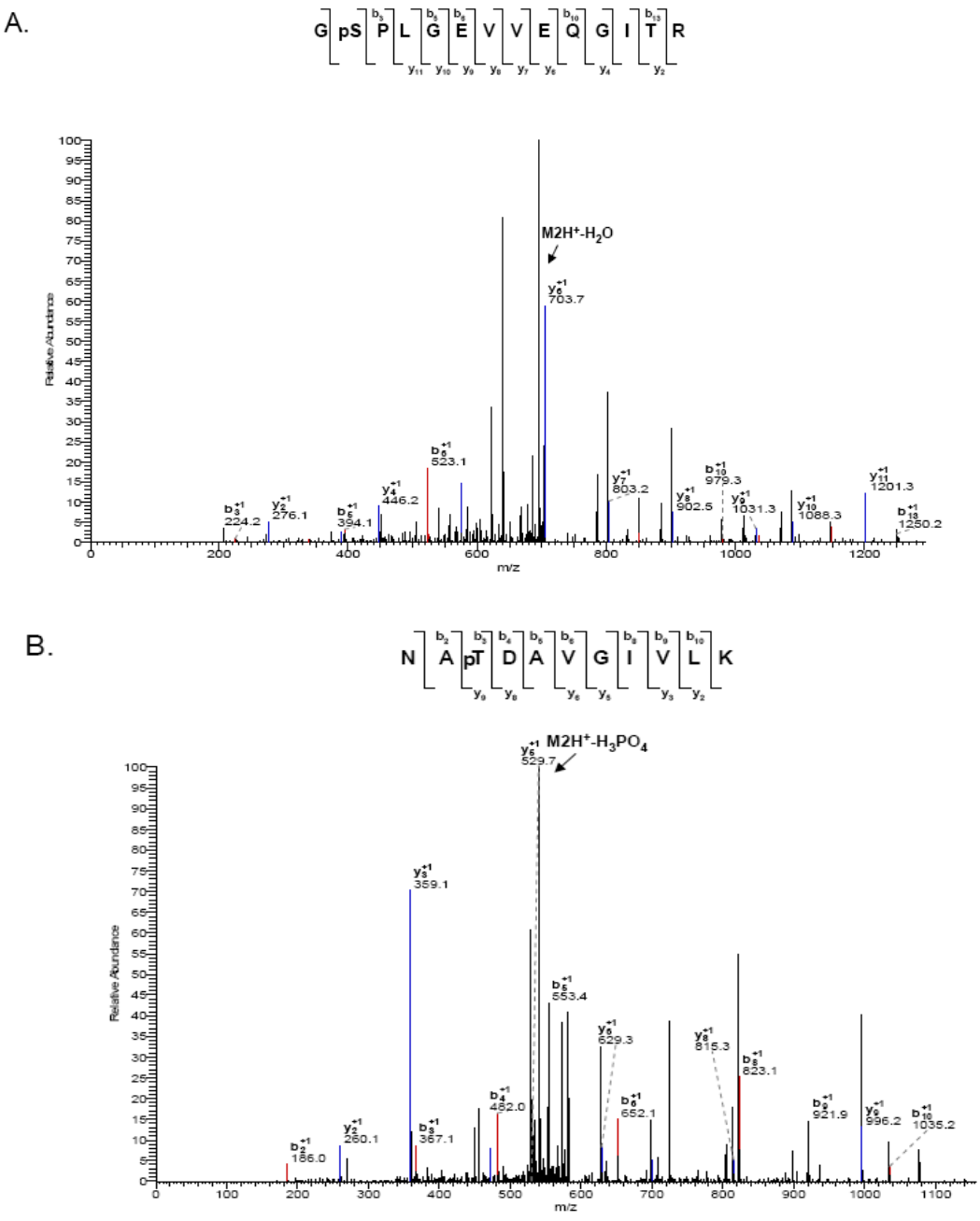


**Figure 3.5. PKA and PKCδ phosphorylated recombinant DAP3 and the modified peptides were identified by mass spectrometry.** CID MS/MS spectra acquired by an ion trap mass spectrometer were used to map the specific sites of phosphorylation by observing a shift of +80 Da in the masses of *b* and *y* ions, which corresponds to an addition of a phosphate group, starting at the site of modification. CID MS/MS spectra for tryptic doubly-charged A) phosphoserine-containing peptide G**p**SPLGEVVEQGITR (peptide mass 1426.1, charge 2+), B) phosphothreonine-containing peptide NA**p**TDAVGIVLK (peptide mass 1181.6, charge 2+).

activation was investigated by site-directed mutagenesis. Residues determined to be phosphorylated and in close proximity to GTP-binding motifs were mutated to alanine residues and mutants were constructed in the mammalian expression vector pcDNA3.1(+). Each was transiently transfected into HEK293T cells to compare the expression levels of the wild-type DAP3, DAP3 mutants, and endogenous DAP3 as obtained from the control vector. In general, the DAP3 constructs were overexpressed 2-fold compared to the endogenous level of DAP3 in HEK293T cells. After the 24 h incubation, the cell viability assay was performed which is based on the cleavage of the tetrazolium salt by mitochondrial dehydrogenases in viable cells. Therefore, these assays are directly related to mitochondrial function of cells transfected with the wild-type and the mutant DAP3 constructs. As seen in Figure 3.6A, the ectopically-expressed DAP3 reduced the cell viability by about 11%, while the expression of S31A and S185A mutants decreased it by 16-17%. In particular, the mutations generated for some of the phosphorylation sites found in ribosome-associated DAP3, namely Ser215, Thr216, Thr237, Ser251, and Ser252, reversed the cell death caused by the wild-type DAP3 (Figure 3.6A). Therefore, these Ser and Thr residues might be critical for induction of apoptosis by ectopic expression of DAP3 in these human cell lines.

In addition to cell viability assays, immunoblotting analysis of PARP cleavage was performed using cell lysates obtained from HEK293T cells transiently transfected with the DAP3 mutants. As observed in Figure 3.6B, wild-type DAP3 and mutant constructs were overexpressing corresponding protein products about 2-fold compared to the endogenous level of DAP3 expression. Probing the same blot for endogenous Hsp60 levels served as a loading control. In normal cells, PARP is involved in DNA repair but, once cleaved by caspase 3, it is inactivated and can serve as a marker for the induction of apoptosis. First a weak signal was observed for cleaved PARP after the transfection with pcDNA alone, yet this was not seen in untransfected cells. Second as indicated in Figure 3.6B, more PARP cleavage was detected in cells expressing exogenous DAP3 compared to cells receiving the control vector alone. Moreover, Ser215, Thr216, Thr237, Ser251, and Ser252 DAP3 mutants reduced the PARP cleavage compared to cells overexpressing wild-type DAP3, while the Ser31 mutant (data not shown) and the Ser185 mutant had

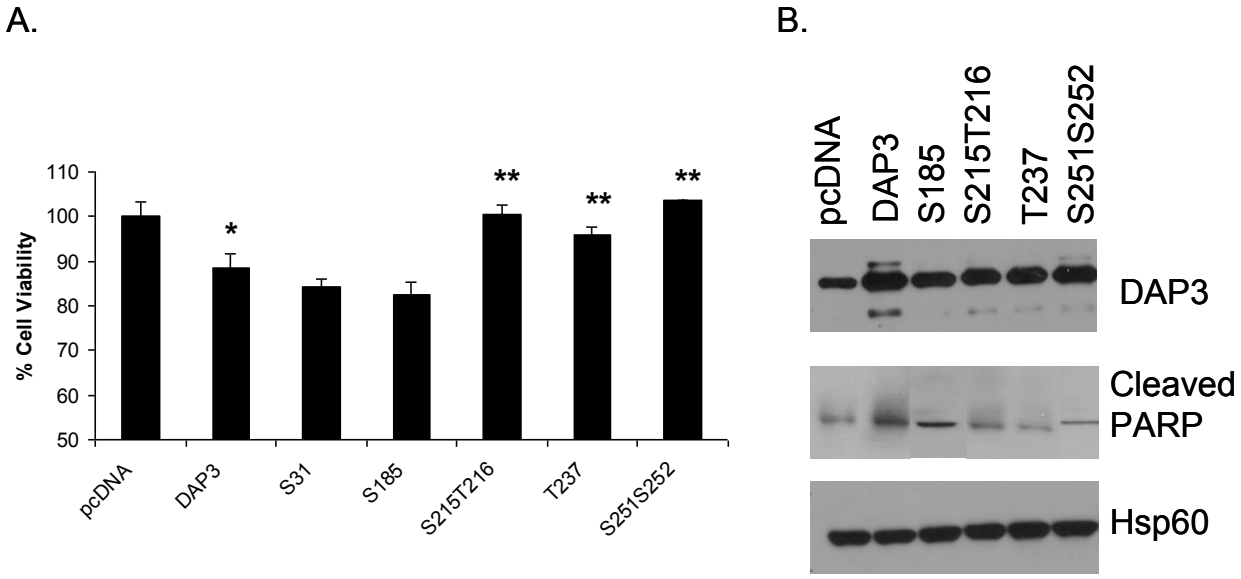


**Figure 3.6. Cell viability and PARP cleavage is assessed in selected DAP3 phosphorylation mutants.** A) HEK293T cells were seeded at 1 x $10^4$ in a 96 well plate and transiently transfected with 0.2 μg of plasmid DNA for each of the DAP3 constructs and the pcDNA control vector. Upon 24 h incubation at 37 °C, the WST-1 reagent was added and the cells were incubated for another 5 h at 37 °C. The reagent is based on the principle that in viable cells, mitochondrial dehydrogenases are active. Shown is the mean ± SD of three experiments. *, $P < 0.05$ for comparing DAP3 to pcDNA; **, $P < 0.05$ for comparing S215T216, T237, S251S252 DAP3 phosphorylation mutants to DAP3. B) HEK293T cells were seeded at 4 x $10^5$ in a 6 well plate and transiently transfected with 2 μg of plasmid DNA for the control vector pcDNA, DAP3, and selected DAP3 phosphorylation mutants. After 24 h incubation at 37 °C, the cells were collected, lysed, and 50 μg of the cell lysate was loaded onto an SDS-PAGE gel. Western blot analyses were performed to detect DAP3 expression, cleaved PARP levels, and Hsp60 levels as a loading control.

comparable levels of PARP cleavage. Findings obtained with these mutants near the GTP-binding motifs 2, 3, and 4 of DAP3 in cell viability assays suggest the importance of the GTP-binding motifs in DAP3-induced apoptosis. Interestingly, Ser31 and Ser185 phosphorylated *in vitro* by PKA and PKCδ were not as effective in modulating apoptotic function of DAP3 as detected in cell viability and PARP cleavage assays.

## 3.5 Discussion

DAP3 has been described as a pro-apoptotic protein promoting apoptosis induced by interferon γ, tumor necrosis factor α, and Fas as observed by structure-function studies (Kissil et al. 1995; Kissil et al. 1999; Mukamel and Kimchi 2004). Further studies, however, demonstrated that the overexpression of DAP3 protects *A. telangiectasia* and glioblastoma cells from ionizing radiation and streptonigrin-induced and camptothecin-induced apoptosis (Henning 1993; Mariani et al. 2001). These two contradictory effects attributed to the overexpression of DAP3 might be controlled by phosphorylation in apoptosis. In fact, phosphorylation of DAP3 by Akt kinase and LKB1, a Ser/Thr kinase, was reported to be important for suppression of anoikis (Miyazaki et al. 2004) and pro-apoptotic function of DAP3 in induction of apoptosis in osteosarcoma cells (Takeda et al. 2007). However, there are no proteomics data available for identification of specific phosphorylated residues of DAP3 as part of the mammalian mitochondrial small subunit and role of these phosphorylation sites in induction of apoptosis. Here, we report the phosphorylation status of mitochondrial ribosomal DAP3 as a component of 55S ribosomes and construct a list of potential kinases known to be translocated into mitochondria, which may be capable of phosphorylating DAP3 *in vivo* and the role of some of the phosphorylation sites in induction of apoptosis.

One of the common features of the phosphorylation sites found in this study is their close proximities to the conserved GTP-binding motifs found in DAP3. Mutation of GTP-binding, specifically the P-loop motif was previously shown to be important for pro-apoptotic activity of DAP3 (Kissil et al. 1999). GTP-binding proteins are constantly switching between GDP and GTP-bound state, triggering the activation of various effectors. In general, guanine nucleotide binding motif G2 is essential for magnesium

coordination; G3 interacts with the magnesium binding site and the γ-phosphate of GTP, while motif G4 is important for recognizing the guanine ring. Especially, DAP3 phosphorylation at residues Ser215, Thr216, Thr237, Ser251, and Ser252 surrounding the G4 and G3 motifs may distort the conformation of the GTP-binding pocket and affect GTP-binding/hydrolysis (Figure 3.2A-B). For this reason, mutations generated at these residues have possibly caused conformational and/or electrostatic changes in the GTP-binding pocket and affected the apoptotic function of DAP3 as demonstrated by PARP cleavage and cell viability assays. On the other hand, mutations at Ser31 and Ser185 did not interfere with pro-apoptotic functions of DAP3 and they have shown decreased cell viability and increased PARP cleavage activity resembling the wild-type DAP3. Therefore, as many other GTP-binding proteins, DAP3 can also be tightly regulated by phosphorylation and mutations at these phosphorylated residues may cause changes in its functions in cells.

Many of the phosphorylated serine and threonine residues found in this study are highly conserved and locations of these residues in various kinase recognition motifs suggest that the DAP3 protein is a substrate for many different kinases. As demonstrated in this study, multiple kinases can phosphorylate the same residue in DAP3, which was evident with the phosphorylation of Ser31, Ser185, Thr186, Thr237, and Ser280 by a kinase endogenously phosphorylating DAP3, PKA and PKCδ. Phosphorylation of the same residue in the DAP3 sequence by different kinases, may also modulate DAP3 function, as some kinases are classified as survival vs. pro-apoptotic. Furthermore, in comparison to other well-known pro-apoptotic proteins DAP3 is rather unique as a component of the mitochondrial ribosome; therefore, one needs to keep in mind that multiple roles attributed to DAP3 in apoptosis might simply be due to changes in the synthesis of thirteen-mitochondrially encoded proteins that are essential for oxidative phosphorylation.

## 3.6 Materials and Methods

### 3.6.1 Purification and *In vitro* Phosphorylation of Recombinant DAP3

Human DAP3 (ATCC #8585718) was cloned into the pET28a vector, supporting an N-terminal His tag, using *Xho I* and *Nde I* as the restriction sites and the following primers:

5' DAP3 – pET28a - GGGAATTCCATATGGCTCGCCAAAGCATTGC
3' DAP3 – pET28a - CCGCTCGAGTTAGAGGTAGGCACAGTGCCGCT

The clone was expressed in the BL21-RIL strain of *E. coli* for 5 h at 23 °C, and purified under native conditions by affinity chromatography using the Ni-NTA column. Each fraction was eluted with 250 mM imidazole. *In vitro* phosphorylation of DAP3 was carried out with kinases cAMP-dependent protein kinase (PKA) the catalytic subunit (New England BioLabs, Product # P6000S), protein kinase C delta (PKCδ) (Sigma-Aldrich Inc., Product # P 8538), protein kinase B (PKB) (New England BioLabs, Product # P8103S), and Abl protein tyrosine kinase (New England BioLabs, Product # P6050S). Approximately 5 µg of recombinant DAP3 protein and 200 µM cold ATP were used in each 20 µl kinase assay containing 100 U of Abl protein tyrosine kinase, 20 U of PKB, 2500 U of PKA, or 48 ng of PKCδ and incubated for 1 h at 30 °C. Overall the reaction conditions were adapted from the protocols provided by the manufacturers. Resulting protein samples were run on SDS-PAGE gels, stained with ProQ Diamond Phosphoprotein Gel Stain (Molecular Probes Inc.), and visualized by a laser scanner at an excitation wavelength of 532 nm. The bands corresponding to DAP3 were excised and in-gel digested with proteases trypsin (cleaves at the C-terminal end of lysine and arginine residues), Lys C (cleaves at the C-terminal end of lysine residues), and Glu C (cleaves at the C-terminal end of glutamic acid) for better coverage. The peptides from in-gel digestion were analyzed by LC/MS/MS for DAP3 identification and mapping of the phosphorylation sites.

### 3.6.2 Isolation and Detection of Phosphorylated Mitochondrial Ribosomal DAP3

Preparation of mitochondrial ribosomes starting from 4 kg of bovine liver using a flow-thru tissue homogenizer was adapted from a previously described method (Matthews et al. 1982). In order to preserve phosphorylation status of ribosomal proteins, phosphatase inhibitors (2 mM imizadole, 1 mM sodium orthovanadate, 1.15 mM sodium molybdate, 1 mM sodium fluoride, and 4 mM sodium tartrate dehydrate) were added during the homogenization process. Crude ribosomes were loaded onto a 10-30% sucrose gradient and fractionated to isolate intact 55S ribosomes. Proteins in the fractions were either pelleted by ultracentrifugation or concentrated using a Microcon Ultracel YM-10 centrifugal unit (Millipore Corp.) and precipitated with acetone. The resulting pellet (approximately 1.8 $A_{260}$ units) was resuspended in lysis buffer consisting of 9.8 M urea, 2% (w/v) NP-40, 2% ampholytes pI 3-10 and 8-10, and 100 mM DTT. The samples were loaded on NEPHGE (non-equilibrium pH gradient electrophoresis) tube gels and equilibrated in buffer containing 60 mM Tris-HCl pH 6.8, 2% SDS, 100 mM DTT, and 10% glycerol (Cahill et al. 1995). The 14% second dimension gel was stained with SYPRO Ruby (Molecular Probes Inc.) or Coomassie Blue for total protein content and the DAP3 gel piece was excised based on Western blot analysis. To complement this, one-dimensional SDS-PAGE and in-solution digestion samples (approximately 1.8 $A_{260}$ units) were also prepared from purified 55S fractions. A C4-reverse phase trap column (Michrom Bioresources Inc.) was used to desalt and to concentrate the above protein samples using the procedure provided by the manufacturer. For the in-solution digests, the eluate was dried in a SpeedVac and resuspended in 25 mM $NH_4HCO_3$ for trypsin digestion, which was added directly to the sample solution at 1:50 ratio and incubated at 37 °C overnight. Peptides obtained from in-gel and in-solution digestions were analyzed by LC/MS/MS and the peptides generated were used for DAP3 identification and mapping of the phosphorylation sites.

### 3.6.3 Enrichment of Phosphorylated Peptides

The PhosphoProfile I phosphopeptide enrichment kit (Sigma-Aldrich Inc.) was used for enrichment of phosphorylated peptides of DAP3. The protocol provided in the kit was followed to enrich the phosphopeptides obtained from in-solution digestion of intact 55S mitochondrial ribosomes (approximately 3.6 $A_{260}$ units). Briefly, the digested

protein sample was acidified with glacial acetic acid to a final concentration of 250 mM and loaded on the gallium silica spin column (Sigma-Aldrich Inc.). The column was washed twice with 50 mM acetic acid in 10% acetonitrile and eluted with 0.4 M $NH_4OH$ in 20% acetonitrile. The eluate was dried by SpeedVac and reconstituted in 0.1% formic acid for the LC/MS/MS analysis.

### 3.6.4 Mass Spectrometric Mapping of DAP3 Phosphorylation Sites

Detection and mapping of phosphorylation sites was achieved by database searching of tandem mass spectra of proteolytic peptides searched against protein databases. Tandem MS spectra obtained by fragmenting a peptide by collision-induced dissociation (CID) were acquired using a capillary liquid chromatography - nanoelectrospray ionization - tandem mass spectrometry (LC/MS/MS) system that consisted of a Surveyor HPLC pump, a Surveyor Micro AS autosampler, and an LTQ linear ion trap mass spectrometer (ThermoFinnigan). The acquired spectra were evaluated using Xcalibur 2.0 and Bioworks 3.2 softwares. The raw CID tandem MS spectra were also converted to Mascot generic files (.mgf) using the extract msn software (ThermoFinnigan). The .dta and .mgf files were submitted to a site-licensed Sequest and Mascot (version 2.2) search engines to search against in-house generated sequences of 55S proteins, all known mitochondrial proteins, and proteins in the Swiss-Prot database. Database searches were performed with cysteine carbamidomethylation as a fixed modification. The variable modifications were methionine oxidation (+16 Da) and phosphorylation (+80 Da) of Ser, Thr, and Tyr residues and loss of water (-18 Da) from Ser and Thr due to β-elimination during loss of the phosphate moiety. Up to 2 missed cleavages were allowed for the protease of choice. Peptide mass tolerance and fragment mass tolerance were set to 3 and 2 Da, respectively. Tandem MS spectra that are matched to phosphorylated peptides were manually evaluated at the raw data level with the consideration of overall data quality, signal-to-noise of matched peaks, and the presence of dominant peaks that did not match to any theoretical *m/z* value.

Mascot and Sequest are similar search engines to analyze data obtained from the mass spectrometer. Mascot uses the MOWSE algorithm, which is based on comparing

the *m/z* (mass/charge) values of the peptides in the experimental sample to the *m/z* values of peptides in a given database digested with a specified enzyme (Liebler 2002). The algorithm takes into account larger proteins giving rise to more peptides and that smaller peptides may match more often to *m/z* values in the database. In addition, the Mascot software can provide a statistical analysis of the data and considers the probability of peptide matches being random events compared to true identities (Liebler 2002). The Sequest software was designed in a similar manner to Mascot, whereby the experimental and theoretical MS/MS spectrum are compared and an Xcorr (cross correlation score) is calculated (Liebler 2002). The candidate peptide ranked as #1 in the database is assigned the highest Xcorr value. Typically, longer well-matched peptides receive a higher Xcorr value than shorter peptides.

### 3.6.5 Site-Directed Mutagenesis and Transient Transfection

DAP3 and DAP3-$His_6$ constructs were cloned into the mammalian vector pcDNA 3.1(+) using *Kpn I* and *Xho I* as the restriction sites and selected phosphorylation sites (Ser31, Ser185, Ser215, Thr216, Thr237, Ser251, Ser252) were mutated to alanine residues using the QuikChange Site-Directed Mutagenesis Kit (Stratagene Inc.). Below is the list of primers used to generate each construct.

5' DAP3 - pcDNA 3.1 (+) - AAACGGGGTACCGAGATGATGCTGAAAGGAATAAC
3' DAP3 - pcDNA 3.1 (+) - CCGCTCGAGTTAGAGGTAGGCACAGTGCCGCT

5' DAP3-$His_6$ - AAACGGGGTACCGAGATGATGCTGAAAGGAATAAC
3' DAP3-$His_6$ - AGATCTCTCGAGTTAATGGTGATGGTGATGATGGAGGTAGGCACAGTGCCG

5' S31A – GGGACCCAGGCTCGCCAAGCCATTGCTGCTCACC
3' S31A – GGTGAGCAGCAATGGCTTGGCGAGCCTGGGTCCC

5' S185A – CCTTTAGAGGCTGCAACCTGGCTGAAG
3' S185A – CTTCAGCCAGGTTGCAGCCTCTAAAGG

5' S215AT216A – GGAATAAGAGAGAAGCCGCTGAGAAAGGGAGTCC
3' S215AT216A – GGACTCCCTTTCTCAGCGGCTTCTCTCTTATTCC

5' T237A – CGGGTGAGGAACGCCGCAGATGCAGTTGG
3' T237A – CCAACTGCATCTGCGGCGTTCCTCACCCG

5’ S251AS252A – GCTAAAGAGGCAAGCTGCTTTGGGTATGTTTCACC
3’ S251AS252A – GGTGAAACATACCCAAAGCAGCTTGCCTCTTTAGC

DNA from each construct was prepared using either the QIA Prep Spin Miniprep Kit (Qiagen Inc.) or the QIAfilter Plasmid Midi Kit (Qiagen Inc.) and further purification was obtained by phenol-chloroform extraction. HEK293T cells (human embryonic kidney cell line) were maintained in DMEM medium supplemented with 10% heat-inactivated FBS, penicillin G, streptomycin, and cultured at 37 °C in a humidified atmosphere containing 5% $CO_2$ and 95% air. HEK293T cells were seeded at 4 x $10^5$ in a 6 well plate and transiently transfected with 2 μg of plasmid DNA using Lipofectamine 2000 (Invitrogen Corp.). Upon 24 h incubation at 37 °C, cells were collected, and lysed in buffer consisting of 50 mM Tris-HCl pH 7.4, 150 mM NaCl, 1 mM EDTA, 1 mM EGTA, 1% NP-40, 0.5% SDS, and a protease and phosphatase inhibitor cocktail for mammalian cells (Sigma-Aldrich Inc.). The protein concentration was determined using the BCA Protein Assay Kit (Pierce Biochemicals Inc.) for Western blot analysis.

### 3.6.6 Pull Down Assay

HEK293T cells were seeded at 4 x $10^5$ in a 6 well plate and transiently transfected with 4 μg of plasmid DNA using Lipofectamine 2000 (Invitrogen Corp.). Upon a 48 h incubation at 37 °C, the cells were collected, and lysed in a buffer consisting of 50 mMTris-HCl pH 7.4, 150 mM NaCl, 1% NP-40, 0.5% SDS, and protease and phosphatase inhibitor cocktails (Sigma-Aldrich Inc.). The whole cell lysate was diluted to 0.125% SDS and incubated overnight at 4 °C with 50 μl of the Ni-NTA beads (Qiagen Inc.). The beads were collected by centrifugation and washed twice with a wash buffer containing 40 mM KC1, 20 mM $MgCl_2$, 20 mM Tris-HCl pH 7.6, 10% glycerol, 7 mM β-mercaptoethanol, 0.125% SDS, and 10 mM imidazole. The beads were eluted three times in elution buffer consisting of 40 mM KC1, 20 mM $MgCl_2$, 20 mM Tris-HCl pH 7.6, 10% glycerol, 7 mM β-mercaptoethanol, 250 mM imidazole, and protease and phosphatase inhibitor cocktails (Sigma-Aldrich Inc.), followed by Western blot analysis.

### 3.6.7 Western Blot Analysis

Protein samples for either one-dimensional or two-dimensional analysis were loaded on SDS-PAGE gels and transferred to a PVDF membrane. The blot was probed with monoclonal anti-DAP3 at a 1:5000 dilution (Transduction Laboratories, Product # 610662), monoclonal anti-Hsp60 at a 1:4000 dilution (Transduction Laboratories, Product # 611562) or polyclonal anti-cleaved PARP at a 1:1000 dilution (Cell Signaling Technology Inc., Product # 9541). The membranes were developed with the SuperSignal West Pico Chemiluminescent Substrate (Pierce Biochemicals Inc.) according to the protocol provided by the manufacturer. To determine the phosphorylation state of DAP3, we probed the blots with monoclonal anti-phosphoserine at a 1:20000 dilution (Sigma-Aldrich Inc., Product # B 7911) and monoclonal anti-phosphothreonine at a 1:10000 dilution (Sigma-Aldrich Inc., Product # B 7661). The membranes were developed using the SuperSignal West Femto Max Sensitivity Substrate (Pierce Biochemicals Inc.) according to the protocol provided by the manufacturer.

### 3.6.8 Cell Viability Assay

HEK293T cells were seeded at 1 x $10^4$ in a 96 well plate and transiently transfected with 0.2 µg of plasmid DNA using Lipofectamine 2000 (Invitrogen Corp.). Upon 24 h incubation at 37 °C, 10 µl of the WST-1 Reagent (Roche Applied Science) was added to each well and incubated at 37 °C for 5 h. The absorbance was read at 450 and 650 nm using a microplate reader. Results were analyzed using the two-tailed unpaired t test. Values of $*P<0.05$ were considered statistically significant.

## 3.7 References

Berger, T., Brigl, M., Herrmann, J.M., Vielhauer, V., Luckow, B., Schlondorff, D., and Kretzler, M. 2000. The apoptosis mediator mDAP-3 is a novel member of a conserved family of mitochondrial proteins. *J. Cell Sci.* **113:** 3603-3612.

Blom, N., Gammeltoft, S., and Brunak, S. 1999. Sequence and structure-based prediction of eukaryotic protein phosphorylation sites. *J. Mol. Biol.* **294:** 1351-1362.

Brodie, C., and Blumberg, P.M. 2003. Regulation of cell apoptosis by protein kinase c delta. *Apoptosis* **8:** 19-27.

Cahill, A., Baio, D., and Cunningham, C. 1995. Isolation and characterization of rat liver mitochondrial ribosomes. *Anal.Biochem.* **232:** 47-55.

Chen, R., Fearnley, I.M., Peak-Chew, S.Y., and Walker, J.E. 2004. The phosphorylation of subunits of complex I from bovine heart mitochondria. *J. Biol. Chem.* **279:** 26036-26045.

Chintharlapalli, S.R., Jasti, M., Malladi, S., Parsa, K.V., Ballestero, R.P., and Gonzalez-Garcia, M. 2005. BMRP is a Bcl-2 binding protein that induces apoptosis. *J. Cell. Biochem.* **94:** 611-626.

DeLano, W.L.T. 2002. The PyMOL Molecular Graphics System. *DeLano Scientific***:** San Carlos, CA, U.S.A.

Denslow, N., Anders, J., and O'Brien, T.W. 1991. Bovine mitochondrial ribosomes possess a high affinity binding site for guanine nucleotides. *J. Biol. Chem.* **266:** 9586-9590.

Henning, K.A. 1993. The molecular genetics of human diseases with defective DNA damage processing. In *Genetics*. Stanford University.

Hopper, R.K., Carroll, S., Aponte, A.M., Johnson, D.T., French, S., Shen, R.F., Witzmann, F.A., Harris, R.A., and Balaban, R.S. 2006. Mitochondrial matrix phosphoproteome: effect of extra mitochondrial calcium. *Biochemistry* **45:** 2524-2536.

Kim, H.R., Chae, H.J., Thomas, M., Miyazaki, T., Monosov, A., Monosov, E., Krajewska,M., Krajewski, S., and Reed, J.C. 2007. Mammalian dap3 is an essential gene required for mitochondrial homeostasis in vivo and contributing to the extrinsic pathway for apoptosis. *FASEB J.* **21:** 188-196.

Kissil, J.L., Cohen, O., Raveh, T., and Kimchi, A. 1999. Structure-function analysis of an evolutionary conserved protein, DAP3, which mediates TNF-alpha- and Fas-induced cell death. *EMBO J.* **18:** 353-362.

Kissil, J.L., Deiss, L.P., Bayewitch, M., Raveh, T., Khaspekov, G., and Kimchi, A. 1995. Isolation of DAP3, a novel mediator of interferon-gamma-induced cell death. *J. Biol. Chem.* **270:** 27932-27936.

Koc, E.C., Burkhart, W., Blackburn, K., Moseley, A., and Spremulli, L.L. 2001a. The small subunit of the mammalian mitochondrial ribosome: Identification of the full complement of ribosomal proteins present. *J. Biol. Chem.* **276:** 19363-19374.

Koc, E.C., Burkhart, W., Blackburn, K., Moyer, M.B., Schlatzer, D.M., Moseley, A., and Spremulli, L.L. 2001b. The large subunit of the mammalian mitochondrial ribosome. Analysis of the complement of ribosomal proteins present. *J. Biol. Chem.* **276:** 43958-43969.

Koc, E.C., Ranasinghe, A., Burkhart, W., Blackburn, K., Koc, H., Moseley, A., and L.L., S. 2001c. A new face on apoptosis: Death-associated protein 3 and PDCD9 are mitochondrial ribosomal proteins. *FEBS Lett.* **492:** 166-170.

Levshenkova, E.V., Ukraintsev, K.E., Orlova, V.V., Alibaeva, R.A., Kovriga, I.E., Zhugdernamzhilyn, O., and Frolova, E.I. 2004. The structure and specific features of the cDNA expression of the human gene *MRPL37*. *Bioorg. Khim.* **30:** 499-506.

Liebler, D.C. 2002. Introduction to Proteomics: Tools for the New Biology. *Humana Press***:** Totowa, NJ, U.S.A.

Liu, J., Chen, J., Dai, Q., and Lee, R.M. 2003. Phospholipid scramblase 3 is the mitochondrial target of protein kinase C delta-induced apoptosis. *Cancer Res.* **63:** 1153-1156.

Mariani, L., Beaudry, C., McDonough, W.S., Hoelzinger, D.B., Kaczmarek, E., Ponce, F., Coons, S.W., Giese, A., Seiler, R.W., and Berens, M.E. 2001. Death-associated protein 3 (Dap-3) is overexpressed in invasive glioblastoma cells in vivo and in glioma cell lines with induced motility phenotype in vitro. *Clin. Cancer Res.* **7:** 2480-2489.

Matthews, D.E., Hessler, R.A., Denslow, N.D., Edwards, J.S., and O'Brien, T.W. 1982. Protein composition of the bovine mitochondrial ribosome. *J. Biol. Chem.* **257:** 8788-8794.

Miyazaki, T., and Reed, J.C. 2001. A GTP-binding adapter protein couples TRAIL receptors to apoptosis-inducing proteins. *Nat. Immunol.* **2:** 493-500.

Miyazaki, T., Shen, M., Fujikura, D., Tosa, N., Kon, S., Uede, T., and Reed, J.C. 2004. Functional role of death associated protein 3 (DAP3) in anoikis. *J. Biol. Chem.* **279:** 44667-44672.

Mukamel, Z., and Kimchi, A. 2004. Death-associated protein 3 localizes to the mitochondria and is involved in the process of mitochondrial fragmentation during cell death. *J. Biol. Chem.* **279:** 36732-36738.

O'Brien, T.W., Fiesler, S., Denslow, N.D., Thiede, B., Wittmann-Liebold, B., Mouge, E., Sylvester, J.E., and Graack, H.-R. 1999. Mammalian mitochondrial ribosomal proteins: Amino acid sequences, characterization and identification of corresponding gene sequences. **274** *J. Biol. Chem.* 36043-36051.

O'Brien, T.W., Liu, J., Sylvester, J., Mourgey, E.B., Fischel-Ghodsian, N., Thiede, B., Wittmann-Liebold, B., and Graack, H.-R. 2000. Mammalian mitochondrial ribosomal proteins (4): Amino acid sequencing, characterization and identification of corresponding gene sequences. *J. Biol. Chem. C* **275:** 18153-18159.

O'Brien T, W., O'Brien B, J., and Norman, R.A. 2005. Nuclear MRP genes and mitochondrial disease. *Gene* **354:** 147-151.

Pai, E., Krengel, U., Petsko, G., Goody, R., Kabsch, W., and Wittinghofer, A. 1990. Refined crystal structure of the triphosphate conformation of H-ras p21 at 1.35 A resolution: implications for the mechanism of GTP hydrolysis. *EMBO J.* **9:** 2351-2359.

Salvi, M., Brunati, A.M., and Toninello, A. 2005. Tyrosine phosphorylation in mitochondria: a new frontier in mitochondrial signaling. *Free Radic. Biol. Med.* **38:** 1267-1277.

Saveanu, C., Fromont-Racine, M., Harington, A., Ricard, F., Namane, A., and Jacquier, A. 2001. Identification of 12 new yeast mitochondrial ribosomal proteins including 6 that have no prokaryotic homologues. *J. Biol. Chem.* **276:** 15861-15867.

Schulenberg, B., Aggeler, R., Beechem, J.M., Capaldi, R.A., and Patton, W.F. 2003. Analysis of steady-state protein phosphorylation in mitochondria using a novel fluorescent phosphosensor dye. *J. Biol. Chem.* **278:** 27251-27255.

Sharma, M.R., Koc, E.C., Datta, P.P., Booth, T.M., Spremulli, L.L., and Agrawal, R.K. 2003. Structure of the mammalian mitochondrial ribosome reveals an expanded functional role for its component proteins. *Cell* **115:** 97-108.

Suzuki, T., Terasaki, M., Takemoto-Hori, C., Hanada, T., Ueda, T., Wada, A., and Watanabe, K. 2001a. Proteomic Analysis of the Mammalian Mitochondrial Ribosome: Identification of Protein Components in the 28S Small Subunit. *J. Biol. Chem.* **276:** 33181-33195.

Suzuki, T., Terasaki, M., Takemoto-Hori, C., Hanada, T., Ueda, T., Wada, A., and Watanabe, K. 2001b. Structural compensation for the deficit of rRNA with proteins in the mammalian mitochondrial ribosome. Systematic analysis of protein components of the large ribosomal subunit from mammalian mitochondria. *J. Biol. Chem.* **276:** 21724-21736.

Takeda, S., Iwai, A., Nakashima, M., Fujikura, D., Chiba, S., Li, H.M., Uehara, J., Kawaguchi, S., Kaya, M., Nagoya, S., et al. 2007. LKB1 is crucial for TRAIL-mediated apoptosis induction in osteosarcoma. *Anticancer Res.* **27:** 761-768.

Taylor, S.W., Fahy, E., Zhang, B., Glenn, G.M., Warnock, D.E., Wiley, S., Murphy, A.N., Gaucher, S.P., Capaldi, R.A., Gibson, B.W., et al. 2003. Characterization of the human heart mitochondrial proteome. *Nat. Biotechnol.* **21:** 281-286.

# CHAPTER 4

## Role of *E. coli* ribosomal L7/L12 phosphorylation in translation

### 4.1 Rationale

Identification of the phosophorylated ribosomal proteins in *E. coli* by mass spectrometry-based proteomics revealed the presence of twenty-four ribosomal proteins in the 70S ribosome. However, the role of each phosphorylation site in ribosomal function and in translation is still missing. For this purpose, we selected a multi-copy protein located at the L7/L12 stalk of the ribosome with highly flexible domains. First, L7/L12 is highly conserved in bacterial, archaeal, and eukaryotic ribosomes recruiting four GTPases at different timepoints during protein synthesis (Itoh and Wittmann-Liebold 1978; Rich and Steitz 1987; Koc et al. 2001; Helgstrand et al. 2007). Second, given the function of L7/L12 is known *in vitro* translation assays can be performed to test the effect of phosphorylation during the elongation process. Finally, prior reports have stated L7/L12 to be phosphorylated confirming the mass spectrometric analysis, yet the specific Ser and Thr sites were not identified (Traugh and Traut 1972; Mikulik and Janda 1997; Mikulik et al. 2001; Ilag et al. 2005). Therefore, we decided to investigate the functional significance of L7/L12 phosphorylation in translation as explained in terms of conformational changes to the different flexible domains of the protein. Initially, the phosphorylated residues were mutated to alanine and the phospho-mimetic glutamic acid. Then two complementary approaches were taken to address this specific aim. One can take advantage of the fact L7/L12 can easily be removed from the 50S subunit by high salt and ethanol treatment (Uchiumi et al. 1999). This strategy allows for the L7/L12 protein to be removed quite efficiently and replaced by a mutant form thereby reconstituting the ribosome for activity assays. The second strategy incorporates the mutant L7/L12 into the 50S subunit upon overexpression maintaining the structural integrity of the ribosome. This approach generates a hybrid ribosome containing predominantly the mutant L7/L12 protein, yet a low percentage of the endogenous form

is still present when testing for ribosomal activity. The goal was to use both methods as supporting evidence for the effect of phosphorylation on bacterial L7/L12 in translation.

## 4.2 Abstract

The L7/L12 stalk is a highly conserved structure of the ribosome from bacteria to eukaryotes and is essential for binding of translation factors during protein synthesis. The stalk also known as the L8 complex in prokaryotes is composed of a single copy of L10 and multiple dimers of L7/L12. The stalk has been characterized as being an acidic phosphoprotein in many different organisms. However, phosphorylated residues have not been identified in previous studies. Here we report phosphorylation of *E. coli* L7/L12 at Ser15, Ser33, and Thr52 as mapped by tandem mass spectrometry. These phosphorylated residues are strategically located at different functional domains of the protein, which may be significant in conformational changes of the stalk. Highly conserved phosphorylated Ser and Thr residues were selected for site-directed mutagenesis of each residue to Ala and Glu to mimic non-phosphorylated and phosphorylated residues, respectively. Effects of these mutations on translation were evaluated by *in vitro* translation assays. The most profound effects on translation were observed in Glu mutants possibly by charge repulsion of neighboring acidic residues in various conformations. Phosphorylation of the mitochondrial homolog of L7/L12, MRPL12, was also determined by 2D-gel electrophoresis and tandem mass spectrometry of the mitochondrial ribosome. Moreover, we have shown phosphorylation of the recombinant MRPL12 by an endogenous mitochondrial kinase. Therefore, our findings suggest that phosphorylation of L7/L12 stalk is a highly conserved regulatory mechanism found in different organisms ranging from bacteria to mammalian mitochondria.

## 4.3 Introduction

Ribosomes are massive particles consisting of protein and RNA that are essential for protein synthesis. These ribonucleoprotein particles are composed of a small subunit (30S) and a large subunit (50S) which forms the 70S ribosome in bacteria. The L7/L12 stalk, a component of the large subunit, is conserved between prokaryotes and eukaryotes

including mitochondrial ribosomes (Itoh and Wittmann-Liebold 1978; Rich and Steitz 1987; Koc et al. 2001). This highly conserved stalk is composed of a copy of L10, and depending on the organism, either two or three dimers of L7/L12 (L7 is the L12 with acetylated N-terminus) (Ilag et al. 2005; Maki et al. 2007).

Current crystallographic studies failed to reveal the structure of the L7/L12 stalk as part of the 50S subunit to comprehend its complex nature and functional significance in translation (Yusupov et al. 2001; Schuwirth et al. 2005). However, translocation of tRNA revealed large conformational changes of the stalk as determined by cryo-EM (Datta et al. 2005). In addition, the crystal structure of the *Thermotoga maritima* L7/L12 stalk revealed the domains of L10 and L7/L12 and possible conformational changes of the stalk in factor binding and GTPase activation (Diaconu et al. 2005). The bacterial L7/L12 protein is arranged into three distinct domains, the N-terminal and C-terminal globular domains connected with a flexible linker region as determined by NMR studies (Bocharov et al. 1996). The N-terminal domain is responsible for dimer formation and anchors L7/L12 to the ribosome by interacting with the C-terminal end of L10 (Gudkov and Behlke 1978). The C-terminal domain is necessary for binding elongation factors EF-Tu and EF-G as well as initiation factor 2 (IF-2) and release factor 3 (RF-3) (Helgstrand et al. 2007). In addition to connecting the N- and C- terminal domains of L7/L12, the linker region is responsible for conformational rearrangements of the two globular domains in tethering different GTPases during translation (Dey et al. 1995). Interestingly, there are three highly conserved Ser and Thr residues located at the critical positions of each domain structure in L7/L12.

Phosphorylation of Ser and Thr was reported for L7/L12 in both *Escherichia coli* and *Streptomyces collinus* ribosomes, by a protein kinase from rabbit skeletal muscle and a protein kinase associated with the ribosomes, respectively (Traugh and Traut 1972; Mikulik and Janda 1997; Mikulik et al. 2001). More recently, in *Thermus thermophilus*, phosphorylation of L7/L12 was reported on intact ribosomes, but was absent in the stalk complex (Ilag et al. 2005). Furthermore, it is speculated that the modified form of L7/L12 may be bound tighter to the large subunit as acetylation of L7/L12 at the N-

terminus stabilized and promoted an interaction with ribosomal L10 particularly under unfavorable conditions (Ilag et al. 2005; Gordiyenko et al. 2008). In addition, its cytoplasmic counterparts have been shown to be phosphorylated by casein kinase II at their C-terminal end, which can affect both the level and function of the stalk proteins (Hasler et al. 1991). Therefore, it can be concluded that phosphorylation is a plausible way of regulating the different functional domains of this multi-copy protein. Moreover, eukaryotic-like protein kinases have been discovered in prokaryotes by phylogenetic studies (Perez et al. 2008).

We hypothesized that phosphorylation is important in regulating the function of L7/L12 in translation and mass spectrometry-based proteomics were used to map the specific Ser and Thr phosphorylation sites of *E. coli* ribosomal L7/L12. Two Ser and one Thr residue were mapped, each highly conserved and evenly distributed amongst the three functional domains of the protein. We demonstrated the importance of phosphorylation both *in vitro* and *in vivo* by performing site-directed mutagenesis studies and analyzing the effect of each mutant pair by the *in vitro* translation assay. Further, we detected MRPL12 to be Ser and Thr phosphorylated by an endogenous kinase associated with the ribosomes using 2D-gel analysis of bovine mitochondrial ribosomes. Overall, phosphorylation can be seen as a mode of regulation for yet another ribosomal protein.

## 4.4 Results

### 4.4.1 *E. coli* L7/L12 is Phosphorylated in 70S Ribosomes

Initially, a comprehensive screen was performed to identify phosphorylated *E. coli* ribosomal proteins of the 70S ribosome by mass spectrometry-based proteomics (Soung et al. 2009). Amongst the many phosphorylated ribosomal proteins identified, the multi-copy L7/L12 protein became the focal point of interest due to earlier accounts of L7/L12 phosphorylation (Traugh and Traut 1972; Mikulik and Janda 1997; Mikulik et al. 2001; Ilag et al. 2005; Soung et al. 2009). To confirm phosphorylation of L7/L12, three different strategies were used. First, control and *E. coli* cells overexpressing L7/L12 were grown in the presence of [$^{32}$P]-orthophosphate for incorporation of [$^{32}$P]-phosphate

into ribosomal proteins. After incorporation of [$^{32}$P] into cells, crude ribosomes were isolated by ultracentrifugation. Ribosomal proteins were separated by SDS-PAGE and visualized by phosphor-imaging. As detected by phosphor-imaging, endogenous and overexpressed L7/L12 were incorporated into the ribosome and the protein bands were phosphorylated (Figure 4.1A). Secondly, phosphorylation of L7/L12 was detected by Western blotting using anti-phospho Ser antibody; however, only phosphorylation of the recombinant L7/L12 was observed due to insufficient transfer of the endogenous L7/L12 to the PVDF membrane (Figure 4.1B). The third strategy was to detect phosphorylation of L7/L12 by staining the SDS-PAGE with a phospho-specific fluorescent dye, ProQ Diamond, and scanning at 532 nm. Collectively, using [$^{32}$P]-labeling and different phospho protein detection methods, we confirmed the phosphorylation of endogenous and overexpressed L7/L12 proteins.

### 4.4.2 Mapping the Phosphorylation Sites of *E. coli* L7/L12 in 70S Ribosomes

Having confirmed the phosphorylation status of L7/L12 in bacterial ribosomes, we proceeded with the mapping of the specific Ser or Thr residues and studying the role of each phosphorylation event in translation. Initially, SDS-PAGE and 2D-NEPHGE (non-equilibrium pH gradient electrophoresis) of *E. coli* ribosomal proteins were run sequentially and protein bands corresponding to the molecular weight and pI of L7/L12 were excised and digested with trypsin. The mass spectrometric analysis yielded few phosphorylated peptides for L7/L12, given the size of the protein, the conformational state of the ribosome during translation, and the chance of losing the phosphate during the in-gel digests or MS analysis. To improve the peptide coverage and, as a consequence, the likelihood of detecting more phosphopeptides, in-solution tryptic digestions of the 70S ribosome preparations were coupled to two different enrichment strategies. First, we used immobilized metal affinity chromatography (IMAC) enrichment, whereby phosphopeptides selectively bind to a metal such as iron or gallium and are eluted from the column under basic conditions. The second method was strong cation exchange (SCX) chromatography, where peptides are eluted in order of increasing positive charge. Phosphopeptides, whose positive charge is reduced by addition of the negatively charged phosphate moiety, are expected to elute earlier than the rest of the

peptides. Using each technique linked to the initial efforts, three phosphorylated peptides were detected for L7/L12 including the following phosphorylation sites, Ser15, Ser33, and Thr52. Tandem-MS spectra generated by fragmentation of peptides by collision-induced dissociation (CID) were used for both recognition and mapping of the phosphorylation sites. The spectra matching to phosphopeptides were each carefully validated for overall data quality and signal-to-noise of peaks matching to expected *m/z* values in addition to applying the stringent Sequest Xcorr coefficient cutoff of >1.5, 2.0, and 2.5 for +1, +2, +3 charged peptides respectively. Figure 4.1C, shows a representative spectrum of a triply-charged peptide containing the phosphorylated Ser15 residue for L7/L12.

### 4.4.3 Reconstitution of the 70S Ribosome with Wild-type and Mutant L7/L12 Proteins

Interestingly, each of the Ser and Thr residues identified in our MS analyses are conserved in a variety of bacteria and bovine mitochondria as well as being positioned at critical functional junctions in the L7/L12 protein (Figure 4.2A-C) (DeLano 2002; Bocharov et al. 2004). After mapping the phosphorylated residues by mass spectrometry, we wanted to determine their role in translation, specifically if these charged residues might induce conformational changes to the hinge region of L7/L12. Our aim was to develop a tightly controlled *in vitro* system by reconstituting the bacterial stalk with each of the mutant versions of the L7/L12 protein to eliminating the contribution from the endogenous protein. In addressing this, *E. coli* ribosomal L7/L12 was cloned into pET28a, a bacterial expression vector with an N-terminal His tag, and point mutations were generated by site-directed mutagenesis. Mutations were to alanine (S15A, S33A, T52A) and to the corresponding phospho-mimetic using glutamic acid (S15E, S33E, T52E), which served as a positive control in our assays. Furthermore, one pair of double mutants, S33A-T52A and S33E-T52E, were also constructed for sites which act as junctions surrounding the flexible domain of L7/L12. Each of these representative mutations should provide direct evidence for the functional relevance of the phosphorylation site as determined by *in vitro* translation assays.

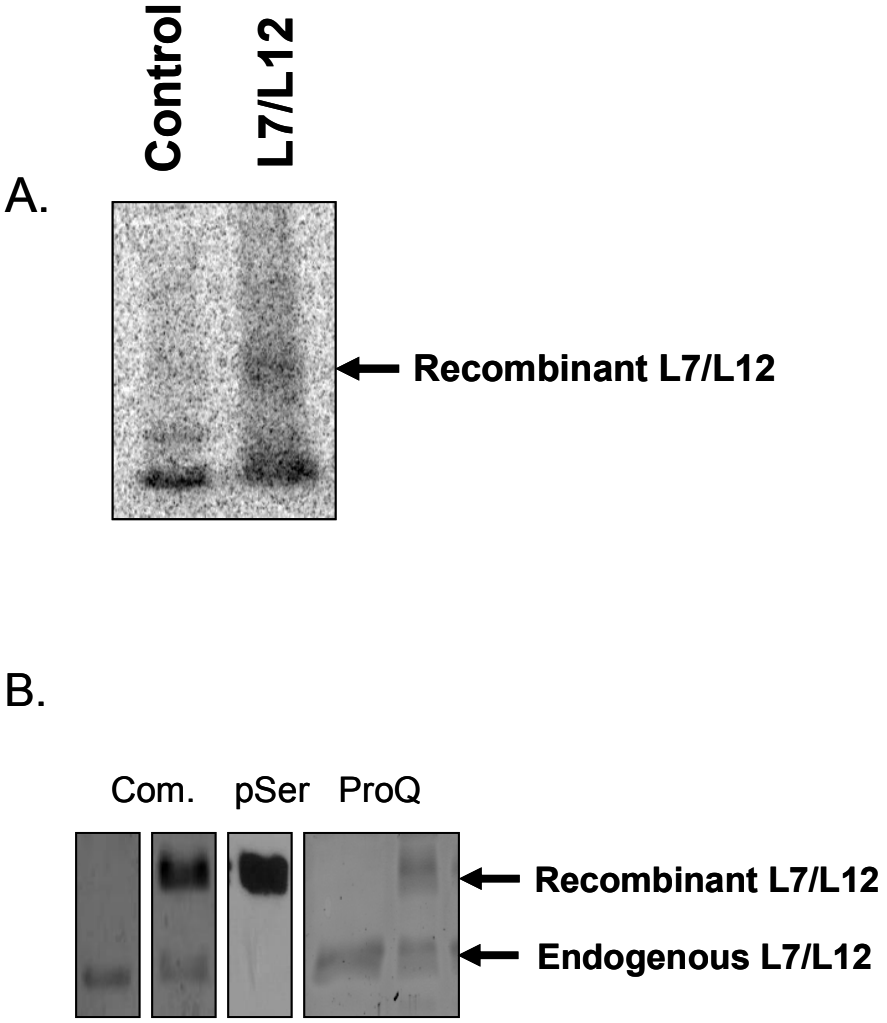


**Figure 4.1. L7/L12 phosphorylation in *E. coli* ribosomes was confirmed by three biochemical methods and mass spectrometry.** A) Control cells and cells overexpressing wild-type ribosomal L7/L12 were grown to an early log phase at 37 °C in LB medium. The cells were labeled with 20 μCi [$^{32}$P]-orthophosphate for 1 hr at 37 °C followed by sonication and isolation of crude ribosomes as described in Materials and Methods. Proteins were analyzed by SDS-PAGE coupled to autoradiography. B) An SDS-PAGE gel stained with Coomassie detecting the endogenous and recombinant L7/L12 as indicated by black arrows. In addition, an immunoblot probed with anti phospho Ser and a gel stained with ProQ phospho dye showing each form of the L7/L12 protein is phosphorylated.

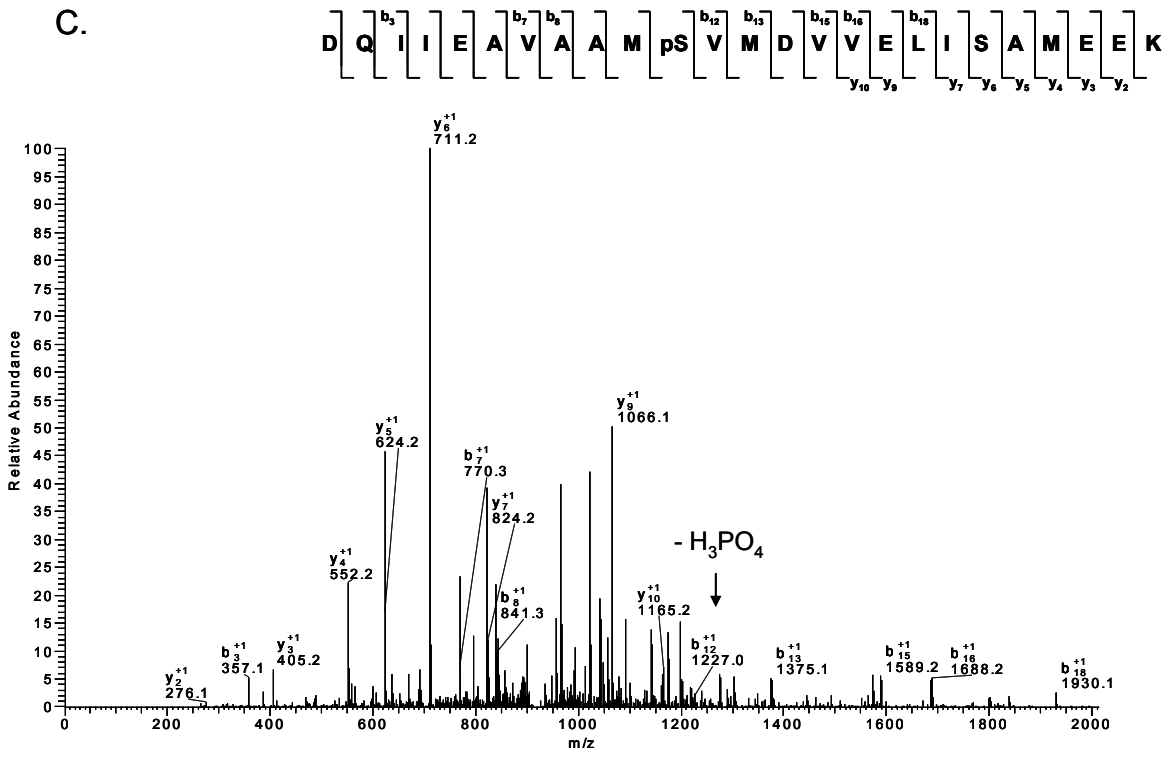


C) The CID MS/MS spectrum for a triply charged phosphorylated peptide of L7/L12, DQIIEAVAAM**p**SVMDVVELISAMEEK, (peptide mass 2755.84, charge 3+) from the ion trap mass spectrometer. Ser15 at the N-terminal domain of the protein was detected as phosphorylated.

A.

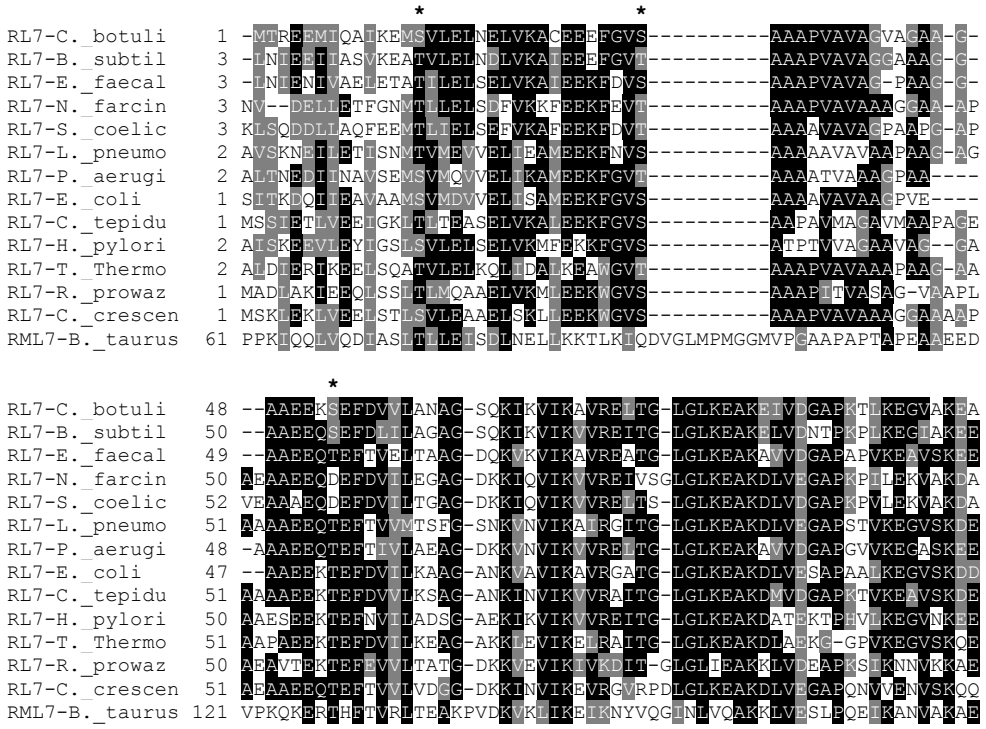


**Figure 4.2. A comparison of bacterial and mitochondrial ribosomal L7/L12 protein sequences with the location of the phosphorylated residues highlighted in the extended and folded hinge conformations.** A) Primary sequence alignment of thirteen bacterial and one mitochondrial L7/L12 protein sequence – *C. botulinum* (EDS76450), *B. subtilis* (P02394), *E. faecalis* (Q830Q8), *N. farcinica* (YP_121327), *S. coelicolor* (P41102), *L. pneumophila* (YP_094365), *P. aeruginosa* (AAG07659), *E. coli* (P0A7K2), *C. tepidum* (Q8KG16), *H. pylori* (P55834), *T. thermophilus* (Q8VVE2), *R. prowazekii* (Q92J87), *C. crescentus* (Q9AAU7), and *B. taurus* (NP_963900). Phosphorylation sites detected in the proteomic analysis are marked with asterisks, while the neighboring glutamic acid residues surround the mapped phosphorylation sites. The alignment was created with the CLUSTALW program in Biology Workbench and the results are displayed in BOXSHADE.

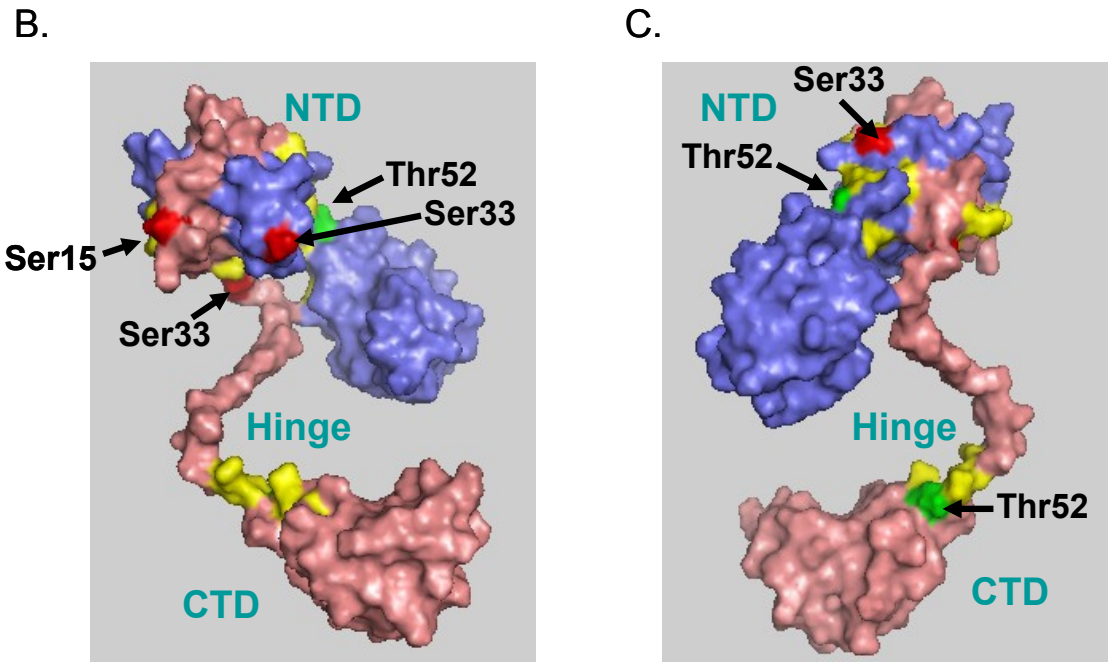


B-C) Different views of the extended and folded conformations of the *E. coli* L7/L12 dimers (pink and blue). The coordinates were obtained from Protein Databank (PDB) entry 1RQU and the image was generated by PyMOL (Bocharov, et al. 2004; DeLano 2002). Labeled in blue are the three segments of the protein, the N-terminal domain (NTD), the flexible hinge region, and the C-terminal domain (CTD). The three phosphorylation sites mapped are colored in red and green, Ser15, Ser33, and Thr52. Glutamic acid residues in near vicinity to the phosphorylation sites are highlighted in yellow.

Wild-type as well as each of the different alanine and glutamic acid mutant L7/L12 proteins and L10 were overexpressed in *E. coli* and purified under native conditions using the affinity of the His tag for Ni-NTA resin. Figure 4.3A depicts each of the purified L7/L12 constructs and L10 after dialysis, indicating that they are free of contaminants and soluble. *E. coli* 70S ribosomes without the stalk were prepared by incubation of ribosomes in a buffer containing 1M ammonium chloride and 50% ethanol. Protein samples obtained from this treatment were separated on a 16% SDS-PAGE and stained by Coomassie Blue (Figure 4.3B). Based on mass spectrometric analysis of the protein bands, the major protein released from the 70S ribosome was L7/L12 protein, while trace amounts of L10 and L11 were also released from the ribosome (Figure 4.3B).

Varying amounts of stripped ribosomes, L10, and L7/L12 were tested to reconstitute an active 70S bacterial ribosome capable of supporting translation. Stripped bacterial ribosomes incubated in the presence of only purified L10 were not active, strengthening the notion that the majority of the L7/L12 had been detached by the high salt and ethanol treatment. However, in the presence of purified L10 and wild-type L7/L12 a significant increase in protein synthesis was measured, partially reviving the inactivated ribosomes and serving as a reference for comparison to the ribosomes with the mutant L7/L12 proteins. We performed reconstitution of hybrid 70S ribosomes using the stripped ribosomes and purified wild-type and mutants of L7/L12 protein and tested for the efficiency of hybrid ribosomes in translation (Figure 4.3C). In these poly-U dependent *in vitro* translation assays, S33A and S33E mutants produced the most significant effect in the levels of phenylalanine synthesized, while the remaining mutants had no significant effect.

### 4.4.4 Incorporation of Wild-type and Mutant L7/L12 Proteins into the *E. coli* Ribosome

In addition to reconstitution of hybrid ribosomes from the purified components, we have taken an alternative approach to test the roles of Ala and Glu acid mutants of L7/L12 on translation. We propose that isolating hybrid ribosomes, which have incorporated the recombinant L7/L12 protein in the cell, under native conditions would

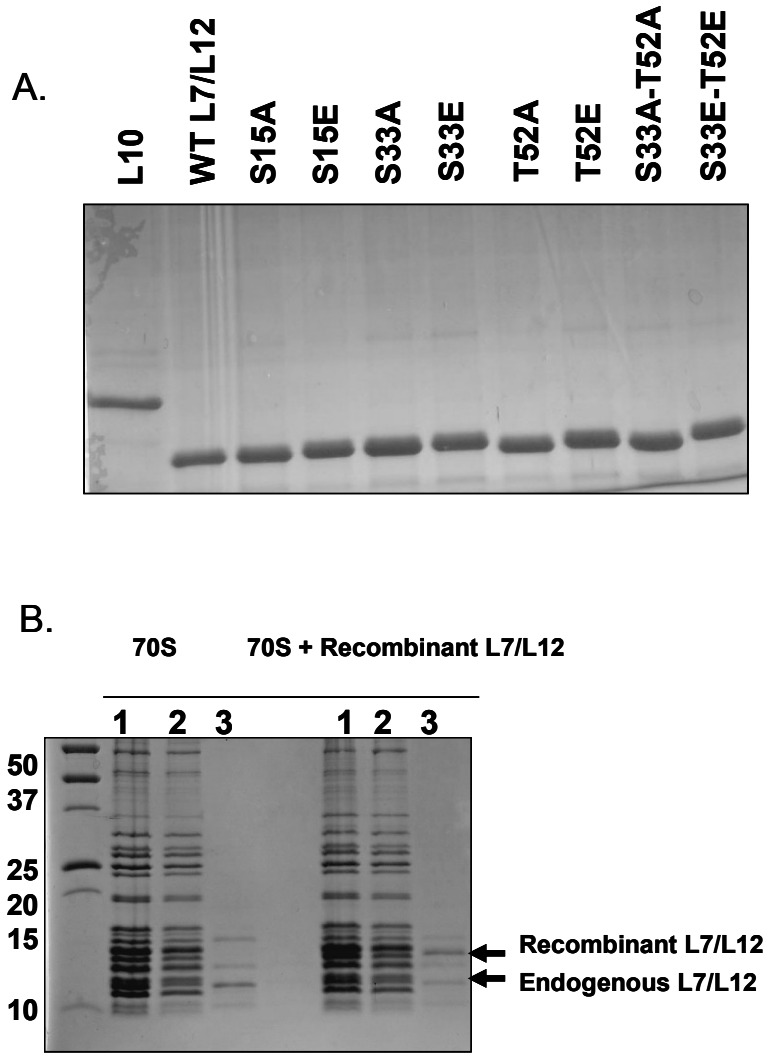


**Figure 4.3. The effect of L7/L12 phosphorylation in translation was analyzed after reconstitution of the ribosome with wild-type and mutant L7/L12 proteins.** A) SDS-PAGE gel stained with Coomassie of the purified L10, wild-type L7/L12, and each of the mutant L7/L12 proteins after dialysis. B) Coomassie stained SDS-PAGE gel of 70S ribosomes and ribosomes overexpressing wild-type L7/L12. Lane 1 and 2 are ribosomes before and after the removal of L7/L12 by high salt and ethanol treatment, while Lane 3 is of the supernatant once the stalk protein was removed. The black arrows point to the endogenous and recombinant forms of the L7/L12 protein.

C.

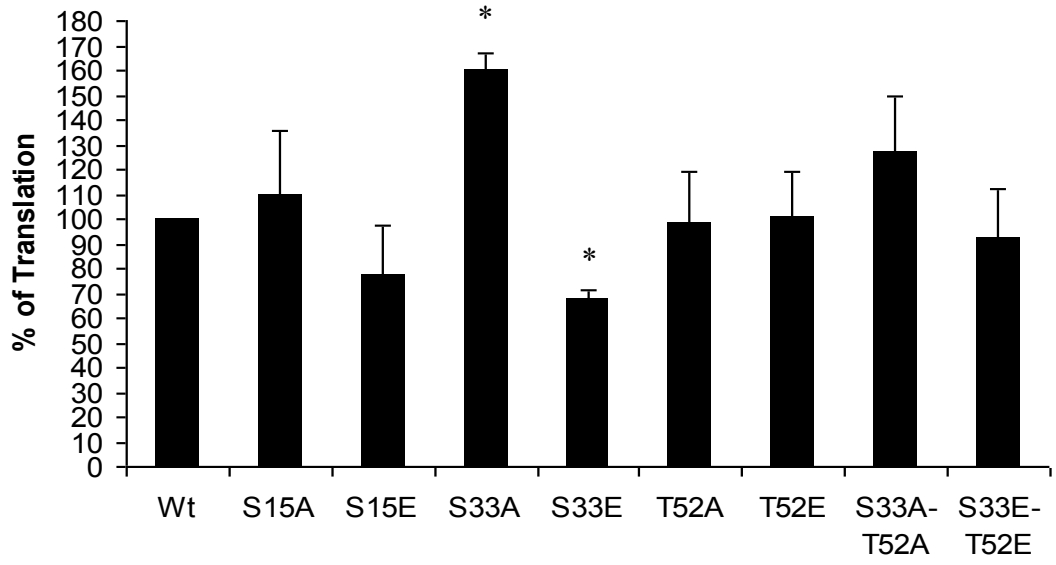


C) *E. coli* ribosomes (11.2 pmol) deficient in L7/L12 were incubated in the presence of recombinant L10 (22.4 pmol) for 10 min at 37 °C. Afterwards, 44.8 pmol of recombinant L7/L12 (wild-type or mutant version) was added and incubated for an additional 10 min at 37 °C. Poly (U)-directed polymerization assays were performed for 15 min at 37 °C with the reconstituted ribosomes. Shown is the mean ± SD of three independent experiments. *****, $P < 0.05$.

allow us to obtain the greatest activity necessary for the *in vitro* translation assays and maintain the structure as well as conformation of the intact 70S ribosome. For this purpose, 70S ribosomes were purified from *E. coli* cells overexpressing wild-type and each mutant L7/L12 pair. To determine the level of incorporation of overexpressed wild-type and mutant L7/L12 proteins into the *E. coli* ribosome, the L7/L12 stalk was stripped by high salt and ethanol using purified 70S ribosomes (Figure 4.3B). In the SDS-PAGE, endogenous L7/L12 is ~12.3kDa in size, while the recombinant wild-type L7/L12 can easily be distinguished by the increase in molecular weight (black arrows). Therefore, the incorporation data was collected by loading equal amounts of the supernatant containing the two different versions of L7/L12 (endogenous and recombinant) on SDS-PAGE gels and staining with Sypro Ruby for ImageQuant analysis. A second choice to quantify the incorporation of the L7/L12 protein (black arrows) into the hybrid ribosomes was by Coomassie staining of equally loaded gradient purified ribosomes (Figure 4.4). By these methods, we were able to confidently compare the endogenous L7/L12 level to the recombinant wild-type and mutant L7/L12 incorporated into the bacterial large subunit. It was concluded that there was a 65-75% incorporation rate for each of the recombinant proteins.

### 4.4.5 *In vitro* Translation Assays with Hybrid *E. coli* Ribosomes

Given the L7/L12 mutant pairs appeared to be incorporated into the ribosome to a similar extent, we first looked at the growth pattern of each mutant L7/L12 protein in comparison to wild-type over a period of time. However, the results were not convincing and quite variable so a more compatible approach was used instead. We tested the ability of the hybrid ribosomes to translate a polypeptide of phenylalanine. Initially, bacterial ribosomes with and without the overexpressed wild-type L7/L12 were tested for their efficiency in translation. No noticeable difference in activity was observed, indicating that the 70S ribosomes with wild-type L7/L12 served as a good standard and reference point to evaluate the translation rate of each of the mutant L7/L12 proteins. *In vitro* translation assays in the presence of saturating (Figure 4.5A) and limiting (Figure 4.5B) amounts of EF-Tu and EF-G were performed to maximize the chances of detecting true differences in polypeptide production. In examining the first pair of mutants, S15A and

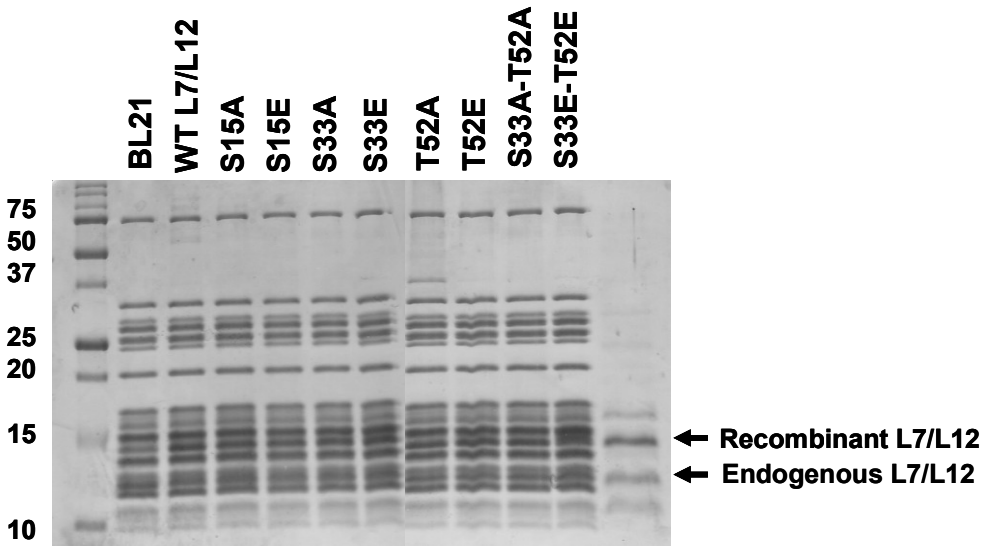


**Figure 4.4. The incorporation of wild-type and mutant L7/L12 proteins into *E. coli* ribosomes was determined.** Coomassie stained SDS-PAGE gel of gradient purified ribosomes (9 pmol) after overexpressing each of the different L7/L12 constructs. The black arrows indicate the endogenous and recombinant versions of the protein. ImageQuant was used to estimate the percentage of incorporation of each recombinant protein tested.

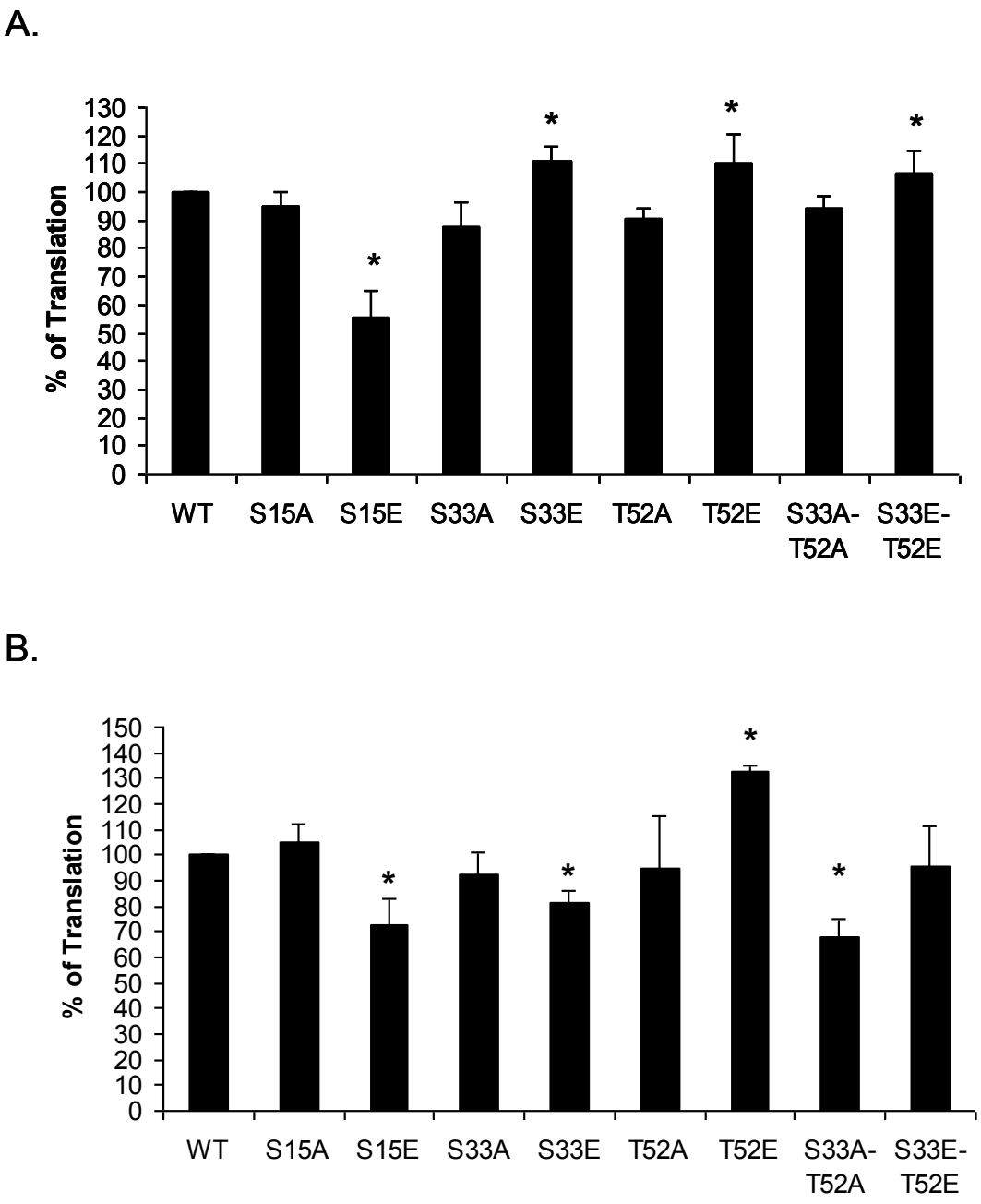


**Figure 4.5. The effect of L7/L12 phosphorylation in hybrid ribosomes was evaluated.** A-B) Poly (U)-directed polymerization assays were performed for 15 min at 37 °C with sucrose gradient purified hybrid ribosomes (11.2 pmol) containing either the wild-type or a mutant form of the L7/L12 protein. The assays were conducted in the presence of saturating (0.65 µg *E. coli* EF-Tu and 1 µg EF-$G_{mt}$) and limiting (0.43 µg *E. coli* EF-Tu and 0.25 µg EF-$G_{mt}$) amounts of elongation factors as observed in A and B respectively. Shown is the mean ± SD of three or four independent experiments. *, $P < 0.05$.

S15E, the mutation to alanine had no significant impact on translation, with values comparable to the wild-type. On the other hand, S15E severely reduced the translation between 30-45% in the presence and absence of saturating quantities of elongation factors. The second pair of mutant L7/L12 proteins, S33A and S33E, is located at the junction between the N-terminal domain and hinge region. When saturating amounts of EF-Tu and EF-G were added to the reaction mixture, S33E stimulated poly (U)-directed polymerization, by an estimate of 10%. However, when the factors were limiting, S33E decreased protein synthesis by about 20% yielding a similar pattern as when the stalk was reconstituted (Figure 4.3C). The Thr52 mutations at the junction between the flexible arm and C-terminal domain control the rotation of the factor binding site of L7/L12. The alanine mutant did not have a significant effect on protein synthesis, while T52E enhanced the reaction by almost 30% in the presence limiting elongation factors (Figure 4.5B). The S33A-T52A mutations only affected the polymerization assay in the absence of saturating elongation factors, by about 35% inhibition, while S33E-T52E maintained the ability to translate as well as the wild-type ribosomes as shown previously by reconstitution (Figures 4.3C). Overall, a consensus trend was observed in the L7/L12 mutant pairs. The alanine mutants showed minimal effect in most instances, while the glutamic acid mutants already having the additional negative charge as would occur if the L7/L12 Ser or Thr residues were phosphorylated, can either promote or inhibit protein synthesis as will be explained structurally in terms of the extended and compact conformations of the L7/L12 dimers.

In addition to the *in vitro* translation assays mentioned, hybrid ribosomes which were overexpressing the wild-type or mutant L7/L12 protein were treated with high salt and ethanol to remove the L7/L12 stalk. After the treatment, the stripped ribosomes were collected by ultracentrifugation and reconstituted with the corresponding recombinant protein according to whichever protein had been overexpressed in those particular ribosomes. The polymerization assays were performed and compared to the wild-type L7/L12 values. In doing these experiments, it became evident that one variable which was difficult to control was whether all the ribosomal preps were being stripped evenly and efficiently, that is removing the same amount of the L7/L12 protein each time. For

example, if more of the L7/L12 protein remained bound to the 50S subunit then adding the recombinant protein upon reconstitution might artificially inflate the level of protein synthesis. Therefore, it was concluded this type of experiment would not show the real effect of the L7/L12 mutant proteins in translation.

### 4.4.6 MRPL12 is Phosphorylated in 55S Mitochondrial Ribosomes

Because L7/L12 is such a functionally significant and highly conserved phosphorylated ribosomal protein in bacteria, archaea, and eukaryotes, we decided to investigate whether the mitochondrial homolog was also phosphorylated in bovine liver. To determine the phosphorylation status of MRPL12, 55S gradient purified mitochondrial ribosomes were isolated using previously described methods (Matthews et al. 1982). Mammalian mitochondrial ribosomes contain seventy-seven proteins, of which forty-eight are in the large subunit. It is still not clear how many copies of MRPL12 are present in the ribosome (Koc et al. 2001; Suzuki et al. 2001). As shown in Figure 4.6A, MRPL12 is Ser and Thr phosphorylated as observed by immunoblotting. In addition, intact 55S ribosomes were separated by 2D-gel electrophoresis and multiple trailing spots with slight changes in molecular weight, which are usually diagnostic for phosphorylation, were identified by mass spectrometry (Figure 4.6B). Finally, *in vitro* phosphorylation assays were performed with recombinant MRPL12 using an enriched mitochondrial lysate containing an endogenous kinase, which modified MRPL12 (Figure 4.6C). Thorough alignment of MRPL12 from different eukaryotes as well as bacterial L7/L12, Thr75, Thr89, Thr128, and Thr194 were predicted as candidate phosphorylation sites, which might be functionally significant.

## 4.5 Discussion

The L7/L12 stalk is an evolutionarily conserved large subunit ribosomal protein having three functional domains. Of the three regions, the highly flexible hinge can be viewed as its trademark and described as a moving arm critical for the efficiency of protein synthesis. In addition, L7/L12 is widely accepted as a multi-copy acidic phosphoprotein (Traugh and Traut 1972; Mikulik and Janda 1997; Mikulik et al. 2001; Ilag et al. 2005). Though many aspects of this protein have sufficiently been

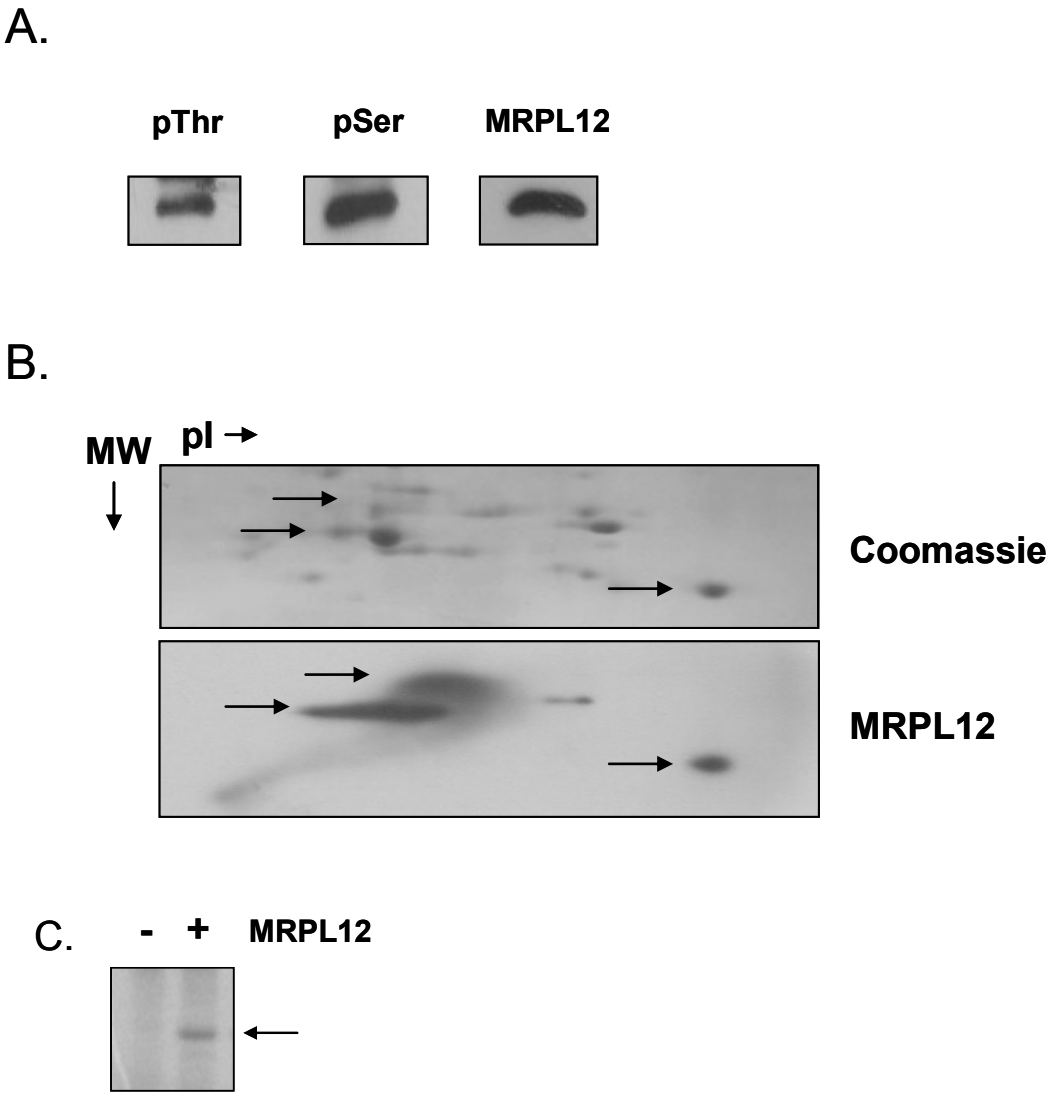


**Figure 4.6. Three different approaches were used to indicate phosphorylation of MRPL12 in 55S bovine mitochondrial ribosomes.** A) Gradient purified bovine mitochondrial ribosomal proteins (5 pmol) were separated on one-dimensional gels and probed with anti phospho Ser, phospho Thr, MRPL12 antibodies, respectively. B) Approximately 35 pmol of 55S ribosomal proteins were separated on 2D-gels and either stained with Coomassie Blue or probed with the anti MRPL12 antibody. The MRPL12 protein spots were excised, digested with trypsin, and analyzed by LC/MS/MS using an ion trap mass spectrometer. The arrows indicate the location of MRPL12 on the gel or immunoblot. C) An enriched bovine mitochondrial lysate containing endogenous kinases was incubated with 2.5 μCi [$\gamma$-$^{32}$P] ATP in the absence or presence of 0.4 μg of recombinant MRPL12 for 1 hr at 30 °C. The samples were loaded on an SDS-PAGE gel and autoradiographed. The arrow points to MRPL12.

characterized, the regulation by post-translational modifications, in particular mapping of the crucial phosphorylation sites, is missing. Therefore, we conducted a comprehensive proteomic analysis to identify phosphorylated ribosomal proteins from *E. coli*, map the phosphorylated residues, and understand the mechanism through which this modification might regulate different steps of bacterial translation (Soung et al. 2009). In doing so, we detected two serines (Ser15 and Ser33) and one threonine (Thr52) residue of L7/L12 to be phosphorylated by mass spectrometry. We also occasionally detected Ser90 in our analyses, but with a much lower Mascot and/or Bioworks score, which coincides with an additional study dissecting phosphorylated residues throughout the *E. coli* proteome during evolution (Macek et al. 2008). However, we decided not to further investigate this residue due to the lack of conservation in bacterial protein sequences.

The bacterial ribosome is composed of approximately two-thirds RNA and can be described as a ribozyme, yet the ribosomal proteins are necessary for proper folding of the rRNA to ensure the specific contacts are maintained for protein synthesis. In general, phosphorylation of ribosomal proteins is known to change the conformation or substrate binding sites of proteins on the ribosome, leading to a 50% reduction in protein synthesis (Traugh and Traut 1972; Mikulik and Janda 1997; Mikulik et al. 2001). In addition, this modification is also speculated to stimulate structural alterations in the mRNA binding path, break inter-subunit contact points, and inhibit tRNA interactions promoting a decrease in the rate of translation (Soung et al. 2009). Yet, in a recent report phosphorylated L7/L12 in *T. thermophilus* is proposed to enhance the association of L7/L12 to the ribosome as was also reported for the role of N-terminal acetylation of L7/L12 under stress conditions (Ilag et al. 2005; Gordiyenko et al. 2008).

The L7/L12 protein exists as dimers in the extended and compact conformation as depicted in Figure 4.2B-C, while structural rearrangements of the hinge induced by phosphorylation may explain the contrasting effects observed in translation (Dey et al. 1998; Wahl et al. 2000; Bocharov et al. 2004). By cross-linking cysteine residues of L7/L12 at both the N and C terminal domains introduced by mutagenesis, it was discovered this stalk protein can interact with 30S and 50S ribosomal proteins (Dey et al.

1998). Specifically, Cys12 and Cys33 associated very strongly with L10, while Cys63, Cys89, and Cys99 at the C-terminal end predominantly bound to L11, representing the folded conformation (Dey et al. 1998). Weaker associations were reported for other 50S ribosomal proteins including L2 and L5 in the peptidyl transferase site, while surprisingly the C-terminal region of L7/L12 was also capable of extending to contact the head of the small subunit (Dey et al. 1998). Another study suggested that, in the same L7/L12 dimer, the orientation can be such that one copy is retracted due to a helical hinge while the other copy has an elongated hinge (Bocharov et al. 2004). This conformational variation can be justified as part of a continuous cycle, specifically once the elongation factors bind to L7/L12 the hinge contracts upon itself, while the release of EF-Tu and EF-G after GTP hydrolysis results in the extended hinge conformation (Bocharov et al. 2004). Therefore, the three phosphorylation sites of L7/L12 at the N-terminal domain and at the junctions of the hinge were mutated to an uncharged residue and to the negatively charged glutamic acid to mimic phosphorylation. These mutations would allow us to study if phosphorylation has a role in regulating the conformational changes during translation.

### 4.5.1 S15A and S15E - N-Terminal Domain L7/L12 Mutations

The helical N-terminal domain of L7/L12 comprising residues 1-36 is essential mainly for dimerization and acting to secure the stalk protein to the 50S subunit by interacting with L10 (Gudkov and Behlke 1978). Our proteomic analysis detected Ser15 as phosphorylated in *E. coli* ribosomes (Figure 4.1C). In examining the crystal structure, Ser15 is 6-7 Å away from Glu49 and Glu50 of the C-terminal domain in the folded conformation (Figure 4.2). We therefore propose that the phosphorylation of Ser15 introduces an additional negative charge and the two residues would repel each other, favoring an extended hinge and weakening the docking site, given that the translation was inhibited in the absence and presence of saturating amounts of elongation factors (Figure 4.5). The unwanted charge would disrupt the N and C terminal interactions, promoting the immediate release of the elongation factors, and inhibiting translation. A similar scenario occurred with S15F, whereby the mutation altered the interaction with Glu96 at the C-terminal end, reducing the translational capability and destabilizing the dimer

(Nomura et al. 2003). On the other hand, S15A remained as active compared to the wild-type L7/L12 since the balance between charges was maintained.

### 4.5.2 S33A and S33E - N-Terminal L7/L12 Junction Mutations

The helical hinge spans residues 37-52 and provides adequate access for IF-2, EF-Tu, EF-G, and RF-3 to bind to the C-terminal end of the stalk by alternating its conformation between a folded and elongated structure (Dey et al. 1998; Wahl et al. 2000; Bocharov et al. 2004). Phosphorylated Ser33 is at the junction between the end of the N-terminal domain and the start of the flexible hinge serving as a pivot point controlling the widespread movement of the arm (Figure 4.2). In the compact model of L7/L12, the localization of this phosphorylated Ser residue is 10-11 Å away from three charged amino acids, Glu27, Glu28, and Lys29 so the vital N and C terminal interface is stabilized. However, in the extended conformation of this bacterial ribosomal protein, Ser33 is 5.5-7 Å from Glu27 and Glu28. The charge repulsion would trigger the outstretched hinge and provide more frequent opportunities to contact the circulating elongation factors driving the synthesis of new polypeptides in the presence of saturating levels of EF-Tu and EF-G (Figure 4.5A). However, upon mutating this junction, the flexibility of the hinge is reduced as observed in the decreased levels of phenylalanine synthesized on the ribosome in the presence of limiting quantities of elongation factors (Figure 4.5B).

### 4.5.3 T52A and T52E – C-Terminal L7/L12 Junction Mutations

The C-terminal end of L7/L12 contains residues 53-120 and is a structural composite of α helices and β sheets. This segment of the stalk protein is well-known for binding multiple GTPases needed for the different stages of translation (Helgstrand et al. 2007). For example, strains of *E. coli* containing either of these two point mutations, G74D or E82K each decreased the level of protein synthesis on the ribosome (Kirsebom et al. 1986). Thr52 is strategically positioned at the opposite end of the hinge region from Ser33, serving as a junction to the beginning of the C-terminal domain (Figure 4.2B-C). This phosphorylation site is surrounded by Glu49 and Glu50 in the folded model or is in close vicinity to Glu53 in the extended form of the dimer. In either arrangement, Thr52

commands the small rotational movements of the C-terminal end of the protein and like charges are best separated. Enhancing the outward stretch of this domain and providing more access to the selection of translational factors would assist in the efficiency of protein synthesis as concluded from the *in vitro* translation assays using different amounts of elongation factors (Figures 4.5A-B). Furthermore, this particular site of phosphorylation is highly conserved in mitochondrial protein sequences and modified to the negatively charged aspartic acid in some bacteria supporting our MS analysis (Figure 4.2A).

### 4.5.4 S33A-T52A and S33E-T52E – L7/L12 Hinge Mutations

The final L7/L12 mutant pair generated was double mutants S33A-T52A and S33E-T52E, which were used to evaluate the ends of the linker region (Figure 4.2). As expected from the crystal structure and the single point mutations, the phospho-mimetic compensated for the kink in the moving arm by enhanced rotational movement of its C-terminal domain, therefore restoring translation to the wild-type standard (Figure 4.5B). However, a slight stimulation in protein synthesis was reported in the presence of saturating EF-Tu and EF-G given that the extended hinge would accommodate for the excess negative charge (Figure 4.5A).

### 4.5.5 Possible Significance of MRPL12 Phosphorylation

Mitochondrial ribosomal protein L12 was originally identified as being the product of a delayed early response mRNA, which accumulates in the G1 phase of growth stimulated cells and a truncated version inhibits mitochondrial translation (Marty and Fort 1996). Furthermore, the mRNA for this ribosomal protein is highly expressed in the colon and it is known that the lack of mitochondrial activity is linked to tumor formation (Marty et al. 1997). The human gene is located on chromosome 17 at a locus which might serve as a marker for colon cancer (Marty et al. 1997). This phosphoprotein is conserved in cytoplasmic and bacterial ribosomes, so it is not surprising to find the mitochondrial homolog to be Ser and Thr phosphorylated by an endogenous kinase associated with the ribosomes (Figure 4.6A and C). Interestingly, in plants there are four differentially expressed forms of MRPL12 varying in molecular weight and pI due to

different N-terminal extensions (Delage et al. 2007), which is reminiscent of our findings from the Coomassie stained 2D-gel of bovine mitochondrial ribosomes supporting the notion of phosphorylation (Figure 4.6B). Another study indicated that MRPL12 has a role in regulating mitochondrial transcription by directly interacting with the mitochondrial RNA polymerase and stimulating the synthesis of mRNA (Wang et al. 2007). Post-translational modifications may serve as a trigger allowing this ribosomal protein to cycle back and forth to maintain a balance between mitochondrial transcription and translation in the cell. In conclusion, phosphorylation is an inherent characteristic of L7/L12, which is one mechanism of regulating this multi-copy ribosomal protein required for translation.

## 4.6 Material and Methods

### 4.6.1 Preparation of *E. coli* Ribosomes

*E. coli* ribosomes from W strain were prepared following a previously described method (Remold-O'Donnell and Thach 1970; Graves et al. 1980). Briefly, *E. coli* cells were grown to an optical density of 0.5 at $A_{600}$. After grinding the cells using alumina in ribosomal Buffer A (20 mM Tris-HCl pH 7.6, 10 mM $MgCl_2$, 1 mM DTT), crude ribosomes were isolated using a differential centrifugation method. The crude ribosomal pellet was resuspended in Ribosomal Buffer B (50 mM Tris-HCl pH 7.6, 20 mM $MgCl_2$, 1 mM DTT, 1 M $NH_4Cl$) and then in Ribosomal Buffer B' (50 mM Tris-HCl pH 7.6, 20 mM $MgCl_2$, 1 mM DTT, 0.5 M $NH_4Cl$) after centrifugation of the suspension at 48,000 rpm in a Beckman 50.2 Ti rotor for 3.5 h at 4 ºC to remove the ribosome associated translational factors. Finally, the high-salt washed ribosomes were resuspended in Ribosomal Buffer C (10 mM Tris-HCl pH 7.6, 10 mM $MgCl_2$, 1 mM DTT, and 50 mM $NH_4Cl$). Crude ribosomes were loaded onto a 10-30% sucrose gradient and fractionated to isolate intact 70S ribosomes. Proteins in the fractions were pelleted by ultracentrifugation for detailed analysis. The ribosome preparations used in in-solution digestions, IMAC, and SCX experiments contained phosphatase and protease inhibitors.

### 4.6.2 *In vivo* $^{32}$P-Orthophosphate Labeling of *E. coli* Ribosomal Proteins

Bacteria were grown to an early log phase at 37 °C in LB medium. The culture was centrifugted and the pellet was resuspended in 20 ml of phosphate-free M9 medium. Isotope, 10 μCi/ml of $^{32}$P-orthophosphate, was added and followed by 1 hr incubation at 37 °C. The cell pellet was resuspended in ribosomal Buffer A and sonicated before the sedimentation of crude ribosomes. Then, the ribosomal proteins were subjected to SDS-PAGE and autoradiography.

### 4.6.3 Phosphopeptide Enrichment of *E. coli* L7/L12

To maximize detection of phosphorylated peptides for L7/L12 in our in-solution digestion of 70S ribosome samples, two different phosphopeptide enrichments were performed. Initially, 263 pmol of *E. coli* 70S ribosomes sample was incubated with 10 μg of RNAse A at 37 °C for 1 h. Prior to in-solution trypsin digestion, the ribosome sample was denatured in 6 M Guanidine HCl and processed through a C4 reverse-phase trap cartridge (Michrom Bioresources, Inc.) to concentrate, desalt, and remove degraded RNA. Following the sample clean up, the eluate was dried in a speed vac and resuspended in 30 μL of 25 mM $NH_4HCO_3$ for trypsin (Sequencing Grade Modified Trypsin, Promega Corporation) digestion, which was added directly to the sample solution at 1:50 ratio and incubated at 37 °C overnight. After in-solution trypsin digestion, phosphorylated tryptic peptides were enriched by IMAC/SwellGel gallium-chelated resin (Phosphopeptide Isolation Kit, Pierce Biochemicals Inc.) according to the protocol provided by the manufacturer or by strong cation exchange chromatography (SCX) using a BioBasic SCX column (2.1 x 250 mm, 5 micron, 300 Å, ThermoFinnigan Co.). Peptides were eluted with a gradient of 5 mM phosphate (pH 2.7), 25% acetonitrile (Mobile phase A) and 5 mM phosphate (pH 2.7), 25% acetonitrile, 350 mM KCl (Mobile phase B). The gradient started with a hold at 0% B for 5 min. It was ramped to 15% B in 20 min, then quickly to 80% B in 5 min, and held there for 5 min. The column was equilibrated at 0% B for 15 min prior to next injection. Absorbance over the range of 200 to 300 nm was measured and absorbance at 210 nm was plotted. Fractions (600 μL) were collected throughout for 30 min. Early fractions, which are expected to be enriched in

phosphopeptides, were reduced to 20 μL using a SpeedVac. The SCX fractions were online desalted and analyzed by LC-MS/MS.

### 4.6.4 Mass Spectrometric Mapping of L7/L12 Phosphorylation Sites

For protein identification by tandem mass spectrometry, tryptic digests were analyzed by LC-MS/MS that consisted of a Surveyor HPLC pump, a Surveyor Micro AS autosampler, and an LTQ linear ion trap mass spectrometer (ThermoFinnigan Co.). Detection and mapping of phosphorylation sites were achieved by database searching of tandem mass spectra of proteolytic peptides against protein databases. Tandem MS spectra obtained by fragmenting a peptide by collision-induced dissociation (CID) were processed and analyzed using Xcalibur 2.0 and Bioworks 3.2 software. The raw CID tandem MS spectra were also converted to Mascot generic files (.mgf) using the extract msn software (ThermoFinnigan Co.). The .dta and .mgf files were submitted to a site-licensed Sequest or Mascot (version 2.2) search engines to search against in-house generated sequences of 70S proteins, all known mitochondrial proteins, and proteins in the Swiss-Prot database. Database searches were performed with cysteine carbamidomethylation as a fixed modification when the cysteines were alkylated by iodoacetamide. The variable modifications were methionine oxidation (+16 Da) and phosphorylation (+80 Da) of Ser, Thr, and Tyr residues and loss of water (-18 Da) from Ser and Thr due to β-elimination during loss of the phosphate moiety. Up to 2 missed cleavages were allowed for the protease of choice. Peptide mass tolerance and fragment mass tolerance were set to 3 and 2 Da, respectively. Tandem MS spectra that are matched to phosphorylated peptides were manually evaluated at the raw data level with the consideration of overall data quality, signal-to-noise of matched peaks, and the presence of dominant peaks that did not match to any theoretical *m/z* value. When Sequest search engine was used, Xcorr coefficient cutoff values of >1.5, 2.0, and 2.5 were applied for +1, +2, +3 charged peptides, respectively.

Mascot and Sequest are similar search engines to analyze data obtained from the mass spectrometer. Mascot uses the MOWSE algorithm, which is based on comparing the *m/z* (mass/charge) values of the peptides in the experimental sample to the *m/z* values

of peptides in a given database digested with a specified enzyme (Liebler 2002). The algorithm takes into account larger proteins giving rise to more peptides and that smaller peptides may match more often to *m/z* values in the database. In addition, the Mascot software can provide a statistical analysis of the data and considers the probability of peptide matches being random events compared to true identities (Liebler 2002). The Sequest software was designed in a similar manner to Mascot, whereby the experimental and theoretical MS/MS spectrum are compared and an Xcorr (cross correlation score) is calculated (Liebler 2002). The candidate peptide ranked as #1 in the database is assigned the highest Xcorr value. Typically, longer well-matched peptides receive a higher Xcorr value than shorter peptides.

### 4.6.5 Purification and Site-Directed Mutagenesis

*E. coli* and human mitochondrial ribosomal L7/L12 were cloned into the pET28a vector while *E. coli* L10 was cloned into the pET26b vector each using *Xho I* and *Nde I* as the restriction sites. Each of the His tag proteins were expressed in the BL21 strain of *E. coli* for 4 h at 25 °C, and purified under native conditions using the Ni-NTA column. The phosphorylation sites of *E. coli* L7/L12 (Ser15, Ser33, Thr52) were mutated to alanine and glutamic acid residues using the QuikChange Site-Directed Mutagenesis Kit (Stratagene Inc.). In addition, S33A-T52A and S33E-T52E double mutants were also constructed for analysis. Each of the mutant His tag L7/L12 proteins were expressed as described above and purified under native conditions using the Ni-NTA column. The recombinant proteins were dialyzed for 3 h at 4 °C in 20 mM Tris-HCl pH 7.5, 10 mM $MgCl_2$, 200 mM $NH_4C1$, 2 mM DTT prior to reconstitution.

### 4.6.6 Removal of L7/L12 from the *E. coli* Ribosome

Stripping the L7/L12 stalk from bacterial ribosomes was performed following a previously described method with a few minor changes (Uchiumi et al. 1999). *E. coli* ribosomes in the extraction buffer (40 mM Tris-HCl pH 7.5, 20 mM $MgCl_2$, 1 M $NH_4C1$, 10 mM BME) were incubated in a water bath for 5 min at 30 °C in a total volume of 2 mL. 1 mL of ethanol (prewarmed to 30 °C) was added to the sample and the incubation continued for another 10 min at 30 °C with oscillation. Then an additional 1 mL of

ethanol (prewarmed to 30 °C) was added and the sample was incubated for a final 5 min at 30 °C with oscillation. The stripped *E. coli* ribosomes were centrifuged at 40,000 rpm for 5 h at 4 °C. The supernatant was collected and the ribosomal pellet was resuspended in 50 mM Tris-HCl pH 7.5, 20 mM $MgCl_2$, 50 mM $NH_4Cl$, 2 mM DTT and used for the reconstitution experiments. SDS-PAGE gels were run to confirm the ribosomes had been stripped and protein bands in the supernatant were identified by mass spectrometry. Primarily L7/L12 with trace amounts of L10 and L11 were detected in the supernatant. Gels were stained with Coomassie Blue or Sypro Ruby (Invitrogen, Inc.) for quantitation and the incorporation of the different L7/L12 constructs into the bacterial ribosome was determined by ImageQuant 5.0 (Molecular Dynamics). In addition, the supernatant was probed with monoclonal anti-phosphoserine at a 1:5000 dilution (Sigma-Aldrich Inc., Product # B 7911) or monoclonal anti-phosphothreonine at a 1:10000 (Sigma-Aldrich Inc., Product # B 7661). The membranes were developed using the SuperSignal West Pico Sensitivity Substrate (Pierce Biochemicals Inc.) following the protocol provided by the manufacturer. Furthermore, the ProQ Diamond Phosphoprotein Gel Stain (Molecular Probes) was used and the proteins were visualized by a laser scanner at an excitation wavelength of 532 nm, as an alternative method to check for phosphorylation.

### 4.6.7 Reconstitution of *E. coli* Ribosomes

Reconstitution of the L7/L12 stalk from bacterial ribosomes was performed following a previously described method with some slight modifications (Griaznova and Traut 2000). Approximately 11.2 pmol of stripped *E. coli* ribosomes was incubated with a 2 fold excess (22.4 pmol) of purified L10 in reconstitution buffer (20 mM Tris-HCl pH 7.5, 10 mM $MgCl_2$, 60 mM $NH_4Cl$, 2 mM DTT) for 10 min at 37 °C in a water bath. Then a 4 fold excess (44.8 pmol) of purified wild-type or mutant L7/L12 in reconstitution buffer was added to the reaction mixture and incubated for another 10 min at 37 °C in a water bath. The samples were centrifuged at 13,000 rpm for 10 min at 4 °C and the supernatant was used in the *in vitro* translation assays.

### 4.6.8 *In vitro* Translation Assays

Reactions (100 µl) contained 50 mM Tris-HCl pH 7.8, 1 mM dithiothreitol, 0.1 mM spermine, 80 mM $NH_4Cl$, 6 mM $MgCl_2$, 2.5 mM phosphoenolpyruvate, 0.18 U pyruvate kinase, 0.5 mM GTP, 25-50 U RNasin Plus, 12.5 µg/mL poly (U), 20 pmol [$^{14}$C]-Phe-tRNA, 0.65 µg *E. coli* EF-Tu, 1 µg EF-$G_{mt}$, and 11.2 pmol of *E. coli* ribosomes. Under limiting conditions, 0.43 µg *E. coli* EF-Tu and 0.25 µg EF-$G_{mt}$ were used in the reactions. The reaction mixture was incubated at 37 °C for 15 min and terminated by the addition of cold 5% trichloroacetic acid followed by incubation at 90 °C for 10 min. The precipitate was collected on nitrocellulose filter membranes and the incorporation of [$^{14}$C]-Phe was quantified using a liquid scintillation counter. Results were analyzed using the two-tailed unpaired t test. Values of *$P<0.05$ were considered statistically significant.

### 4.6.9 Isolation and Detection of Phosphorylated Mitochondrial Ribosomal L12

Preparation of mitochondrial ribosomes starting from 4 kg of bovine liver was adapted from previously described methods (Matthews et al. 1982; Spremulli 2007). To preserve protein phosphorylation, phosphatase inhibitors (2 mM imizadole, 1 mM sodium orthovanadate, 1.15 mM sodium molybdate, 1 mM sodium fluoride, and 4 mM sodium tartrate dehydrate) were added during the ribosome purification. Ribosomes separated on sucrose gradients and pelleted by ultracentrifugation were acetone precipitated for 2D-gel analysis. The resulting pellet (35 pmol) was resuspended in Destreak Rehydration Buffer (Amersham Biosciences Inc.) and loaded into the rehydration tray dropwise. The ReadyStrip IPG Strip ampholytes pI 3-10 (Bio-Rad Laboratories, Inc.) and 7cm in length covered the sample and rehydration occurred overnight. After running the first dimension the strips were equilibrated in 6 M urea, 0.375 M Tris-HCl pH 8.8, 2% SDS, 20% glycerol, and 2% (w/v) DTT for 10 min. Once removed, the strips were equilibrated in a second buffer with the same components described above except with 2.5% (w/v) iodoacetamide. The strips were loaded onto the second dimension SDS-PAGE gel and either stained with Coomassie Blue or transferred to a PVDF membrane probing with a polyclonal anti MRPL12 at a 1:500 dilution (Covance Inc.).

### 4.6.10 *In vitro* Phosphorylation of Recombinant Mitochondrial L12

Mitoplasts from bovine liver were ground with mortar/pestle and lysed in .26 M sucrose, 50 mM KCl, 15 mM $MgCl_2$, 20 mM HEPES pH 7.6, 1 mM EDTA, 0.05 mM spermine, 0.05 mM spermidine, 1% Triton X-100, as well as protease and phosphatase inhibitors. The lysate was incubated at 4 °C for 20 min followed by centrifugation at 15,000 rpm for 45 min at 4 °C. The supernatant was dialyzed in 50 mM KCl, 5 mM $MgCl_2$, 20 mM HEPES pH 7.6, 1 mM EDTA, and 10% glycerol at 4 °C. Afterwards the sample was loaded on an SCX column using SP Sepharose Fast Flow resin (Amersham Biosciences Inc.), washed twice with 50 mM KCl, 5 mM $MgCl_2$, 20 mM HEPES pH 7.6, 1 mM EDTA, and eluted in a stepwise manner to 1.5 M KCl. Each wash and elution contained protease and phosphatase inhibitors. Aliquots were taken and tested for the presence of kinase activity by incubating with and without recombinant L12 (0.4 μg), 100 μM cold ATP, and 2.5 μCi [$\gamma$-$^{32}$P] ATP for 1 hr at 30 °C followed by SDS-PAGE and autoradiography.

## 4.7 References


Bocharov, E., Gudkov, A., and Arseniev, A. 1996. Topology of the secondary structure elements of ribosomal protein L7/L12 from E. coli in solution. *FEBS Lett.* **379:** 291-294.

Bocharov, E.V., Sobol, A.G., Pavlov, K.V., Korzhnev, D.M., Jaravine, V.A., Gudkov, A.T., and Arseniev, A.S. 2004. From structure and dynamics of protein L7/L12 to molecular switching in ribosome. *J. Biol. Chem.* **279:** 17697-17706.

Datta, P.P., Sharma, M.R., Qi, L., Frank, J., and Agrawal, R.K. 2005. Interaction of the G' domain of elongation factor G and the C-terminal domain of ribosomal protein L7/L12 during translocation as revealed by cryo-EM. *Mol. Cell* **20:** 723-731.

Delage, L., Giege, P., Sakamoto, M., and Marechal-Drouard, L. 2007. Four paralogues of RPL12 are differentially associated to ribosome in plant mitochondria. *Biochimie* **89:** 658-668.

DeLano, W.L.T. 2002. The PyMOL Molecular Graphics System. *DeLano Scientific***:** San Carlos, CA, U.S.A.

Dey, D., Bochkariov, D.E., Jokhadze, G.G., and Traut, R.R. 1998. Cross-linking of selected residues in the N- and C-terminal domains of Escherichia coli protein L7/L12 to other ribosomal proteins and the effect of elongation factor Tu. *J. Biol. Chem.* **273:** 1670-1676.

Dey, D., Oleinikov, A.V., and Traut, R.R. 1995. The hinge region of Escherichia coli ribosomal protein L7/L12 is required for factor binding and GTP hydrolysis. *Biochimie* **77:** 925-930.

Diaconu, M., Kothe, U., Schlunzen, F., Fischer, N., Harms, J.M., Tonevitsky, A.G., Stark, H., Rodnina, M.V., and Wahl, M.C. 2005. Structural basis for the function of the ribosomal L7/12 stalk in factor binding and GTPase activation. *Cell* **121:** 991-1004.

Gordiyenko, Y., Deroo, S., Zhou, M., Videler, H., and Robinson, C.V. 2008. Acetylation of L12 increases interactions in the Escherichia coli ribosomal stalk complex. *J. Mol. Biol.* **380:** 404-414.

Graves, M., Breitenberger, C., and Spremulli, L.L. 1980. *Euglena gracilis* chloroplast ribosomes: Improved isolation procedure and comparison of elongation factor specificity with prokaryotic and eukaryotic ribosomes. *Arch. Biochem. Biophys.* **204:** 444-454.

Griaznova, O., and Traut, R.R. 2000. Deletion of C-terminal residues of Escherichia coli ribosomal protein L10 causes the loss of binding of one L7/L12 dimer: ribosomes with one L7/L12 dimer are active. *Biochemistry* **39:** 4075-4081.

Gudkov, A.T., and Behlke, J. 1978. The N-terminal sequence protein of L7/L 12 is responsible for its dimerization. *Eur. J. Biochem.* **90:** 309-312.

Hasler, P., Brot, N., Weissbach, H., Parnassa, A.P., and Elkon, K.B. 1991. Ribosomal proteins P0, P1, and P2 are phosphorylated by casein kinase II at their conserved carboxyl termini. *J. Biol. Chem.* **266:** 13815-13820.

Helgstrand, M., Mandava, C.S., Mulder, F.A., Liljas, A., Sanyal, S., and Akke, M. 2007. The Ribosomal Stalk Binds to Translation Factors IF2, EF-Tu, EF-G and RF3 via a Conserved Region of the L12 C-terminal Domain. *J. Mol. Biol.* **365:** 468-479.

Ilag, L.L., Videler, H., McKay, A.R., Sobott, F., Fucini, P., Nierhaus, K.H., and Robinson, C.V. 2005. Heptameric (L12)6/L10 rather than canonical pentameric complexes are found by tandem MS of intact ribosomes from thermophilic bacteria. *Proc. Natl. Acad. Sci. U. S. A.* **102:** 8192-8197.

Itoh, T., and Wittmann-Liebold, B. 1978. The primary structure of Bacillus subtilis acidic ribosomal protein B-L9 and its comparison with Escherichia coli proteins L7/L12. *FEBS Lett.* **96:** 392-394.

Kirsebom, L.A., Amons, R., and Isaksson, L.A. 1986. Primary structures of mutationally altered ribosomal protein L7/L12 and their effects on cellular growth and translational accuracy. *Eur. J. Biochem.* **156:** 669-675.

Koc, E.C., Burkhart, W., Blackburn, K., Moyer, M.B., Schlatzer, D.M., Moseley, A., and Spremulli, L.L. 2001. The large subunit of the mammalian mitochondrial ribosome. Analysis of the complement of ribosomal proteins present. *J. Biol. Chem.* **276:** 43958-43969.

Liebler, D.C. 2002. Introduction to Proteomics: Tools for the New Biology. *Humana Press***:** Totowa, NJ, U.S.A.

Macek, B., Gnad, F., Soufi, B., Kumar, C., Olsen, J.V., Mijakovic, I., and Mann, M. 2008. Phosphoproteome analysis of E. coli reveals evolutionary conservation of bacterial Ser/Thr/Tyr phosphorylation. *Mol. Cell. Proteomics* **7:** 299-307.

Maki, Y., Hashimoto, T., Zhou, M., Naganuma, T., Ohta, J., Nomura, T., Robinson, C.V., and Uchiumi, T. 2007. Three binding sites for stalk protein dimers are generally present in ribosomes from archaeal organism. *J. Biol. Chem.* **282:** 32827-32833.

Marty, L., and Fort, P. 1996. A delayed-early response nuclear gene encoding MRPL12, the mitochondrial homologue to the bacterial translational regulator L7/L12 protein. *J. Biol. Chem.* **271:** 11468-11476.

Marty, L., Taviaux, S., and Fort, P. 1997. Expression and human chromosomal localization to 17q25 of the growth-regulated gene encoding the mitochondrial ribosomal protein MRPL12. *Genomics* **41:** 453-457.

Matthews, D.E., Hessler, R.A., Denslow, N.D., Edwards, J.S., and O'Brien, T.W. 1982. Protein composition of the bovine mitochondrial ribosome. *J. Biol. Chem.* **257:** 8788-8794.

Mikulik, K., and Janda, I. 1997. Protein kinase associated with ribosomes phosphorylates ribosomal proteins of Streptomyces collinus. *Biochem. Biophys. Res. Commun.* **238:** 370-376.

Mikulik, K., Suchan, P., and Bobek, J. 2001. Changes in ribosome function induced by protein kinase associated with ribosomes of Streptomyces collinus producing kirromycin. *Biochem. Biophys. Res. Commun.* **289:** 434-443.

Nomura, T., Mochizuki, R., Dabbs, E.R., Shimizu, Y., Ueda, T., Hachimori, A., and Uchiumi, T. 2003. A point mutation in ribosomal protein L7/L12 reduces its ability to form a compact dimer structure and to assemble into the GTPase center. *Biochemistry* **42:** 4691-4698.

Perez, J., Castaneda-Garcia, A., Jenke-Kodama, H., Muller, R., and Munoz-Dorado, J. 2008. Eukaryotic-like protein kinases in the prokaryotes and the myxobacterial kinome. *Proc. Natl. Acad. Sci. U. S. A.***105:** 15950-15955.

Remold-O'Donnell, E., and Thach, R.E. 1970. A new method for the purification of initiation factor F2 in high yield, and an estimation of stoichiometry in the binding reaction. *J. Biol. Chem.* **245:** 5737-5742.

Rich, B.E., and Steitz, J.A. 1987. Human acidic ribosomal phosphoproteins P0, P1, and P2: analysis of cDNA clones, in vitro synthesis, and assembly. *Mol. Cell. Biol.* **7:** 4065-4074.

Schuwirth, B.S., Borovinskaya, M.A., Hau, C.W., Zhang, W., Vila-Sanjurjo, A., Holton, J.M., and Cate, J.H. 2005. Structures of the bacterial ribosome at 3.5 A resolution. *Science* **310:** 827-834.

Soung, G.Y., Miller, J.L., Koc, H., and Koc, E.C. 2009. Comprehensive analysis of phosphorylation sites in *E. coli* ribosomal proteins. *(in revision)*.

Spremulli, L.L. 2007. Large-scale isolation of mitochondrial ribosomes from mammalian tissues. *Methods Mol. Biol.* **372:** 265-275.

Suzuki, T., Terasaki, M., Takemoto-Hori, C., Hanada, T., Ueda, T., Wada, A., and Watanabe, K. 2001. Structural compensation for the deficit of rRNA with proteins in the mammalian mitochondrial ribosome. Systematic analysis of protein components of the large ribosomal subunit from mammalian mitochondria. *J. Biol. Chem.* **276:** 21724-21736.

Traugh, J.A., and Traut, R.R. 1972. Phosphorylation of ribosomal proteins of Escherichia coli by protein kinase from rabbit skeletal muscle. *Biochemistry* **11:** 2503-2509.

Uchiumi, T., Hori, K., Nomura, T., and Hachimori, A. 1999. Replacement of L7/L12.L10 protein complex in Escherichia coli ribosomes with the eukaryotic counterpart changes the specificity of elongation factor binding. *J. Biol. Chem.* **274:** 27578-27582.

Wahl, M.C., Bourenkov, G.P., Bartunik, H.D., and Huber, R. 2000. Flexibility, conformational diversity and two dimerization modes in complexes of ribosomal protein L12. *EMBO J.* **19:** 174-186.

Wang, Z., Cotney, J., and Shadel, G.S. 2007. Human mitochondrial ribosomal protein MRPL12 interacts directly with mitochondrial RNA polymerase to modulate mitochondrial gene expression. *J. Biol. Chem.* **282:** 12610-12618.

Yusupov, M.M., Yusupova, G.Z., Baucom, A., Lieberman, K., Earnest, T.N., Cate, J.H.D., and Noller, H.F. 2001. Crystal Structure of the Ribosome at 5.5 A Resolution. *Science* **292:** 883-896.

# CHAPTER 5

## Summary and Future Directions

### 5.1 Phosphoproteomic Analyses

Mitochondria are known to be the powerhouses for cells, generating most of the cellular energy needed to sustain life. However, mitochondria also control death since they are have roles in apoptosis, reactive oxygen species (ROS) production, and disease states. Therefore, it is essential to maintain a delicate balance between these two opposing processes. Given that mitochondrial ribosomes are responsible for translating the subunits of the hydrophobic oligomeric complexes required for oxidative phosphorylation, one mechanism of regulating this intricate process may be through phosphorylation. This is plausible to suggest since ATP is the resulting product of translation. Moreover, there are at least twenty-five kinases and eight phosphatases which have been localized to the mitochondria and could regulate this post-translational modification (Horbinski and Chu 2005; Salvi et al. 2005). Furthermore, phosphorylation is the most common way to regulate many signal transduction pathways in cells.

Earlier reports indicated a number of prokaryotic ribosomal proteins were phosphorylated, yet the sites modified were not discovered (Traugh and Traut 1972; Mikulik and Janda 1997; Macek et al. 2008). Proteomic studies to identify all of the components of the mitochondrial ribosome (55S), which resembles bacterial ribosomes (70S), were only completed in 2001 (Koc et al. 2001a; Koc et al. 2001b; Suzuki et al. 2001b; Suzuki et al. 2001a). Therefore, my dissertation work begins by combining these previous findings and filling in the gaps by focusing on identifying phosphorylated ribosomal proteins in mitochondria as well as in bacteria, due to the striking structural and functional similarities between the systems. 2D-gel electrophoresis and various enrichment strategies are powerful proteomic techniques, which would allow for the detection of such low abundant proteins of the ribosome and map the specific Ser, Thr, and Tyr residues phosphorylated by kinases associated with the ribosomes.

The phosphoproteomic analyses revealed Ser and Thr phosphorylation were more common compared to Tyr phosphorylation, which is not surprising in light of the kinases present. About half of the phosphorylated 55S ribosomal proteins have homologs in prokaryotes that are also modified at their Ser, Thr, or Tyr residues (Soung et al. 2009). This implies the post-translational modification was conserved and may be functionally relevant to the cell. Many of these ribosomal proteins can be grouped into functionally significant corners of the ribosome, especially the mRNA binding path of the small subunit, while in the large subunit the factor binding sites, the polypeptide exit tunnel, and the peptidyl transferase site are each critical for different steps in protein synthesis. Disruption of protein-protein and protein-RNA interactions by phosphorylation at these fundamental regions on the ribosomes might be necessary, yet reversible for cell survival. Therefore, this initial comprehensive study comparing the phosphoproteome of 70S and 55S ribosomes should serve as a template for more directed inquiries of ribosomal proteins and the relationship between their role in protein synthesis and how they are regulated by phosphorylation. This can be accomplished more readily with bacterial ribosomes by site-directed mutagenesis analyses coupled to assays assessing translation or mRNA binding. Valuable information can be extracted by understanding the mechanism by which finite movements are controlled and applied to the pool of available structural data. With this in mind, two ribosomal proteins, L7/L12 and DAP3, were chosen for more detailed functional studies.

## 5.2 L7/L12 Phosphorylation

The L7/L12 stalk composed of L10 and multiple copies of the L7/L12 protein is essential for protein synthesis by stimulating the activity of at least four GTPases needed throughout the translation cycle (Helgstrand et al. 2007). L7/L12 is a highly conserved phosphoprotein from prokaryotes to eukaryotes (Traugh and Traut 1972; Mikulik and Janda 1997; Ilag et al. 2005; Macek et al. 2008; Soung et al. 2009). However, the unanswered question remained, which modified residues are critical to the stalk's functionality. Interestingly, in *E. coli* L7/L12 three highly conserved phosphorylation sites were mapped, each located at a different functional domain of the protein. Ser15 is in the N-terminal domain, which anchors L7/L12 to L10 and the 50S ribosome. Ser33 is

positioned at the beginning of the long flexible hinge region, while Thr52 is at the end close to the C-terminal domain, which binds GTPases. Remarkably, upon viewing the structure of L7/L12 in either a compact or elongated conformation, based on the hinge shape, each of these phosphorylation sites is situated amongst neighboring glutamic acid residues. It is thought once the negative charges are brought into close proximity they would repel each other and L7/L12 would try to adopt a more feasible orientation to compensate for the excess negative charge. Therefore, these three phosphorylation sites govern and control the movement of the linker region impacting polypeptide synthesis, by how well the domains of the protein interact with each other or with the GTPases.

The mitochondrial L12 stalk was also determined to be phosphorylated by a kinase associated with the ribosomes, which interestingly phosphorylates the bacterial version of the protein as well. MRPL12 may be phosphorylated at the same Ser and Thr residues as bacterial L7/L12 based on alignment and structure predictions, strengthening the idea of L7/L12 being a conserved phosphoprotein throughout evolution. Site-directed mutagenesis and functional studies are needed for verification. Originally, identified as a product of a delayed early response mRNA in the mid 1990s, more recently the protein was found to interact with the mitochondrial RNA polymerase stimulating transcription (Marty and Fort 1996; Wang et al. 2007). The tight coupling of the transcription and translation processes is known in yeast mitochondrial and bacterial ribosomes, yet not in mammalian mitochondrial ribosomes. One could speculate phosphorylation might act as a molecular switch allowing the protein to cycle back and forth between associating with the mitochondrial RNA polymerase needed to transcribe the mRNA and being a component of the ribosomal machinery required to translate the message. This hypothesis could be addressed in future studies, by determining if the mitochondrial RNA polymerase binds to the phosphorylated or dephosphorylated form of MRPL12. One last finding, which also requires further investigation, is the detection of MRPL12 at different molecular weights. Two versions of MRPL12 were detected in mammalian mitochondria, which differed by a few amino acids at the N-terminus of the protein (Terasaki et al. 2004). In plants there are four different forms of this protein each varying in mass due to N-terminal extensions, yet each were localized to the mitochondria

(Delage et al. 2007). Though unlike yeast or bacterial L7/L12, it is possible mammalian mitochondrial L12 also exists in different versions, yet the present copy number is unknown.

## 5.3 Phosphorylation of New Class Mitochondrial Ribosomal Proteins

There were six new class phosphorylated ribosomal proteins identified in this high throughput analysis of mitochondrial ribosomes, of which three have proposed roles in apoptosis and cancer. Particularly, MRPS23 and MRPS29 (DAP3) are components of the small subunit, while MRPL40 is a large subunit protein. MRPS29 and MRPL40, two of the four apoptotic mitochondrial ribosomal proteins are phosphorylated, implying this post-translational modification may be a common theme in apoptosis induction (Kissil et al. 1995; Koc et al. 2001c; Levshenkova et al. 2004; Chintharlapalli et al. 2005). Furthermore, it can be hypothesized the number of apoptotic 55S ribosomal proteins may escalate over time, as each of these mitochondrial specific proteins are studied in detail, deciphering their location on the ribosome and functional attributes. One final thought is the possibility that the whole mitochondrial ribosome may undergo structural alterations during this essential cellular process, which could be researched in the future.

One of these apoptotic mitochondrial specific proteins, DAP3, appears to be overexpressed in a wide variety of cancer cells including glioma, osteosarcoma, and in thymoma tissue (Mariani et al. 2001; Sasaki et al. 2004; Takeda et al. 2007). In addition, the protein has a dual function either promoting cell death or inhibiting the process in cancer cells (Kissil et al. 1995; Mariani et al. 2001). To explain the phenomenon of this GTP-binding component of the 28S subunit, it was hypothesized phosphorylation might play a role as a molecular switch in apoptosis induction therefore the sites of phosphorylation were mapped. DAP3 is primarily Ser phosphorylated and the residues are clustered around the GTP-binding motifs, which may distort the conformation of the GTP-binding pocket and affect the ability for DAP3 to induce cell death (Miller et al. 2008). After site-directed mutagenesis analyses coupled to cell viability assays and caspase activation determination, selected residues were classified as regulating the apoptotic function of DAP3 (Miller et al. 2008). The second phosphorylated apoptotic

protein linked to cancer is MRPL40, which shows sequence similarity to MRPS30 an apoptotic small subunit protein (Koc et al. 2001; Levshenkova et al. 2004). Widely expressed in multiple organs of the body, increased expression was observed in lung tumor cells compared to normal cells, as the gene may be activated in transformed cells (Levshenkova et al. 2004). Finally the third new class protein associated with cancer was MRPS23, which has been implicated in uterine cervical cancer having rapid proliferation and invasiveness (Lyng et al. 2006).

This evidence strengthens the idea that all three of these ribosomal proteins may be regulated by phosphorylation and act in a similar manner in different cancers. Therefore, it would be relevant to determine the phosphorylation status of MRPS23, MRPS29, and MRPL40 in a variety of cancers to see if a correlation can be made. A proteomic approach would accommodate an experiment of this nature and may allow for the sites of modification to be mapped. The phosphorylated residues could be compared to the sites detected from my work as if different kinases are present there is an increased chance of phosphorylating alternative Ser, Thr, or Tyr residues given the unique properties of each individual kinase. In the end, a collection of proteins such as these may serve as biomarkers in predicting a specific cancer.

## 5.4 Mitochondrial Kinases

Having identified phosphorylated 55S ribosomal proteins, the kinase responsible for this post-translational modification was still unknown. By enriching a mitochondrial lysate coupled to mass spectrometry, my most recent finding is a putative kinase responsible for endogenously phosphorylating the mitochondrial ribosomal proteins. Pyruvate dehydrogenase kinase (PDK) is a metabolic enzyme which phosphorylates pyruvate dehydrogenase, the enzyme responsible for the conversion of pyruvate to acetyl CoA. Upon phosphorylation of the E1 subunit of pyruvate dehydrogenase at three different Ser residues, the enzyme is inactivated, preventing the generation of acetyl CoA needed for the citric acid cycle and shutting down oxidative phosphorylation in the mitochondria (Holness and Sugden 2003). PDK regulation is based on a feedback mechanism, whereby increasing amounts of ATP and acetyl CoA activate the kinase,

while an abundance of ADP and pyruvate inactivate the enzyme. Given the presence of PDK in the mitochondria needed to regulate biochemical reactions and its close proximity to the ribosomes, it might phosphorylate the mitochondrial ribosomes and inhibit translation as another way of preventing the production of ATP.

The initial groundwork has been laid for identifying this elusive kinase, yet more detailed experiments are needed for confirmation including testing other inhibitors such as lipoic acid and radicicol. In addition, two other kinases repeatedly appeared in the proteomic analysis, branched chain α-ketoacid dehydrogenase kinase (BCKD kinase) and PTEN-induced putative kinase 1 (PINK1). BCKD kinase is another metabolic enzyme that catalyzes the decarboxylation of branched chain α-ketoacids, while PINK1 is associated with oxidative stress and Parkinson's disease (Deng 2005; Pridgeon 2007). Recently, it was shown PINK1 forms a multiprotein complex with the GTPase Miro and the adapter protein Milton, playing a role in mitochondrial trafficking (Weihofen 2009). Each of these kinases may also be potential candidates and therefore should be screened carefully. It is my assumption that multiple kinases may target the ribosomes depending on the conditions of the cell. For example, DAP3 can be phosphorylated by PKA and PKCδ based on my research, in addition to Akt when anoikis was induced or LKB1 in osteosarcoma cells (Miyazaki et al. 2004; Takeda et al. 2007; Miller et al. 2008). Understanding which kinases are interacting with the mitochondrial ribosomal proteins is just as crucial as mapping the residues as with this knowledge you have a more complete picture of protein-protein networking within the mitochondria.

In conclusion, mammalian mitochondrial ribosomal proteins, which translate only thirteen products housed in the inner membrane as oligomeric complexes, have a broader spectrum of functions most notably in apoptosis and disease. Yet, how is the balance maintained between these opposing processes? Phosphorylation is only one possible answer, which can be assessed directly by various biochemical and proteomic techniques. Though phosphorylation of mitochondrial ribosomes appears to be significant, other modifications such as acetylation may also play an important role in translation and other newly acquired functions.

## 5.5 References


Chintharlapalli, S.R., Jasti, M., Malladi, S., Parsa, K.V., Ballestero, R.P., and Gonzalez-Garcia, M. 2005. BMRP is a Bcl-2 binding protein that induces apoptosis. *J. Cell. Biochem.* **94:** 611-626.

Delage, L., Giege, P., Sakamoto, M., and Marechal-Drouard, L. 2007. Four paralogues of RPL12 are differentially associated to ribosome in plant mitochondria. *Biochimie* **89:** 658-668.

Deng, H., Jankovic, J., Guo, Y., Xie, W., and Le, W. 2005. Small interfering RNA targeting the PINK1 induces apoptosis in dopaminergic cells SH-SY5Y. *Biochem. Biophys. Res. Commun.* **337:** 1133-1138.

Helgstrand, M., Mandava, C.S., Mulder, F.A., Liljas, A., Sanyal, S., and Akke, M. 2007. The Ribosomal Stalk Binds to Translation Factors IF2, EF-Tu, EF-G and RF3 via a Conserved Region of the L12 C-terminal Domain. *J. Mol. Biol.* **365:** 468-479.

Holness, M.J., and Sugden, M.C. 2003. Regulation of pyruvate dehydrogenase complex activity by reversible phosphorylation. *Biochem. Soc. Trans.* **31:** 1143-1151.

Horbinski, C., and Chu, C.T. 2005. Kinase signaling cascades in the mitochondrion: a matter of life or death. *Free Radic. Biol. Med.* **38:** 2-11.

Ilag, L.L., Videler, H., McKay, A.R., Sobott, F., Fucini, P., Nierhaus, K.H., and Robinson, C.V. 2005. Heptameric (L12)6/L10 rather than canonical pentameric complexes are found by tandem MS of intact ribosomes from thermophilic bacteria. *Proc. Natl. Acad. Sci. U. S. A.* **102:** 8192-8197.

Kissil, J.L., Deiss, L.P., Bayewitch, M., Raveh, T., Khaspekov, G., and Kimchi, A. 1995. Isolation of DAP3, a novel mediator of interferon-gamma-induced cell death. *J. Biol. Chem.* **270:** 27932-27936.

Koc, E.C., Burkhart, W., Blackburn, K., Moseley, A., and Spremulli, L.L. 2001a. The small subunit of the mammalian mitochondrial ribosome: Identification of the full complement of ribosomal proteins present. *J. Biol. Chem.* **276:** 19363-19374.

Koc, E.C., Burkhart, W., Blackburn, K., Moyer, M.B., Schlatzer, D.M., Moseley, A., and Spremulli, L.L. 2001b. The large subunit of the mammalian mitochondrial ribosome. Analysis of the complement of ribosomal proteins present. *J. Biol. Chem.* **276:** 43958-43969.

Koc, E.C., Ranasinghe, A., Burkhart, W., Blackburn, K., Koc, H., Moseley, A., and L.L., S. 2001c. A new face on apoptosis: Death-associated protein 3 and PDCD9 are mitochondrial ribosomal proteins. *FEBS Lett.* **492:** 166-170.

Levshenkova, E.V., Ukraintsev, K.E., Orlova, V.V., Alibaeva, R.A., Kovriga, I.E., Zhugdernamzhilyn, O., and Frolova, E.I. 2004. The structure and specific features of the cDNA expression of the human gene MRPL37. *Bioorg. Khim.* **30:** 499-506.

Lyng, H., Brovig, R.S., Svendsrud, D.H., Holm, R., Kaalhus, O., Knutstad, K., Oksefjell, H., Sundfor, K., Kristensen, G.B., and Stokke, T. 2006. Gene expressions and copy numbers associated with metastatic phenotypes of uterine cervical cancer. *BMC Genomics* **7:** 268.

Macek, B., Gnad, F., Soufi, B., Kumar, C., Olsen, J.V., Mijakovic, I., and Mann, M. 2008. Phosphoproteome analysis of E. coli reveals evolutionary conservation of bacterial Ser/Thr/Tyr phosphorylation. *Mol. Cell. Proteomics* **7:** 299-307.

Mariani, L., Beaudry, C., McDonough, W.S., Hoelzinger, D.B., Kaczmarek, E., Ponce, F., Coons, S.W., Giese, A., Seiler, R.W., and Berens, M.E. 2001. Death-associated protein 3 (Dap-3) is overexpressed in invasive glioblastoma cells in vivo and in glioma cell lines with induced motility phenotype in vitro. *Clin. Cancer Res.* **7:** 2480-2489.

Marty, L., and Fort, P. 1996. A delayed-early response nuclear gene encoding MRPL12, the mitochondrial homologue to the bacterial translational regulator L7/L12 protein. *J. Biol. Chem.* **271:** 11468-11476.

Mikulik, K., and Janda, I. 1997. Protein kinase associated with ribosomes phosphorylates ribosomal proteins of Streptomyces collinus. *Biochem. Biophys. Res. Commun.* **238:** 370-376.

Miller, J.L., Koc, H., and Koc, E.C. 2008. Identification of phosphorylation sites in mammalian mitochondrial ribosomal protein DAP3. *Protein Sci.* **17:** 251-260.

Miyazaki, T., Shen, M., Fujikura, D., Tosa, N., Kon, S., Uede, T., and Reed, J.C. 2004. Functional role of death associated protein 3 (DAP3) in anoikis. *J. Biol. Chem.* **279:** 44667-44672.

Pridgeon, J.W., Olzmann, J. A., Chin, L.S., and Li, L. 2007. PINK1 protects against oxidative stress by phosphorylating mitochondrial chaperone TRAP1. *PLoS Biol.* **5:** e172.

Salvi, M., Brunati, A.M., and Toninello, A. 2005. Tyrosine phosphorylation in mitochondria: a new frontier in mitochondrial signaling. *Free Radic. Biol. Med.* **38:** 1267-1277.

Sasaki, H., Ide, N., Yukiue, H., Kobayashi, Y., Fukai, I., Yamakawa, Y., and Fujii, Y. 2004. Arg and DAP3 expression was correlated with human thymoma stage. *Clin. Exp. Metastasis* **21:** 507-513.

Soung, G.Y., Miller, J.L., Koc, H., and Koc, E.C. 2009. Comprehensive analysis of phosphorylation sites in *E. coli* ribosomal proteins. *(in revision)*.

Suzuki, T., Terasaki, M., Takemoto-Hori, C., Hanada, T., Ueda, T., Wada, A., and Watanabe, K. 2001a. Proteomic Analysis of the Mammalian Mitochondrial Ribosome. Identification of protein components in the 28S small subunit. *J. Biol. Chem.* **276:** 33181-33195.

Suzuki, T., Terasaki, M., Takemoto-Hori, C., Hanada, T., Ueda, T., Wada, A., and Watanabe, K. 2001b. Structural compensation for the deficit of rRNA with proteins in the mammalian mitochondrial ribosome. Systematic analysis of protein components of the large ribosomal subunit from mammalian mitochondria. *J. Biol. Chem.* **276:** 21724-21736.

Takeda, S., Iwai, A., Nakashima, M., Fujikura, D., Chiba, S., Li, H.M., Uehara, J., Kawaguchi, S., Kaya, M., Nagoya, S., et al. 2007. LKB1 is crucial for TRAIL-mediated apoptosis induction in osteosarcoma. *Anticancer Res.* **27:** 761-768.

Terasaki, M., Suzuki, T., Hanada, T., and Watanabe, K. 2004. Functional compatibility of elongation factors between mammalian mitochondrial and bacterial ribosomes: characterization of GTPase activity and translation elongation by hybrid ribosomes bearing heterologous L7/12 proteins. *J. Mol. Biol.* **336:** 331-342.

Traugh, J.A., and Traut, R.R. 1972. Phosphorylation of ribosomal proteins of Escherichia coli by protein kinase from rabbit skeletal muscle. *Biochemistry* **11:** 2503-2509.

Wang, Z., Cotney, J., and Shadel, G.S. 2007. Human mitochondrial ribosomal protein MRPL12 interacts directly with mitochondrial RNA polymerase to modulate mitochondrial gene expression. *J. Biol. Chem.* **282:** 12610-12618.

Weihofen, A., Thomas, K.J., Ostaszewski, B.L., Cookson, M.R., and Selkoe, D.J. 2009. Pink1 Forms a Multiprotein Complex with Miro and Milton, Linking Pink1 Function to Mitochondrial Trafficking. *Biochemistry* **48:** 2045-2052.

# VITA

## Jennifer Lynn Miller

## Education

- Ph.D. Biochemistry, Microbiology, and Molecular Biology, The Pennsylvania State University, PA, 2009
- B.Sc. Biology-Chemistry, Elmira College of New York, 2003

## Honors

- Recipient of the Braucher Award (Department of Biochemistry and Molecular Biology, The Pennsylvania State University), Summer 2004, 2005, and 2008
- Recipient of the Braddock Graduate Fellowship (Department of Biochemistry and Molecular Biology, The Pennsylvania State University), Fall 2003-Spring 2005

## Publications

- Miller, J.L., Koc, H., and Koc, E.C. (2008) Identification of phosphorylation sites in mammalian mitochondrial ribosomal protein DAP3. *Protein Sci.* 17**,** 251-260
- Soung, G.Y., Miller, J.L., Koc, H., and Koc, E.C. (2009) Comprehensive analysis of phosphorylation sites in *E. coli* ribosomal proteins. *(in revision)*
- Miller, J.L., Koc, H., and Koc, E.C. Role of *E. coli* ribosomal L7/L12 phosphorylation in translation. *(in preparation)*
- Miller, J.L., Koc, H., and Koc, E.C. Phosphorylated proteins of the mammalian mitochondrial ribosome: Implications in protein synthesis and apoptosis. *(in preparation)*

## Poster Presentations

- "Role of *E. coli* ribosomal L7/L12 phosphorylation in translation." Translational Control Meeting, Cold Spring Harbor, New York, 2008
- "Role of Post-Translational Modifications of a Mitochondrial Ribosomal Protein, MRP-S29, in Apoptosis." Translational Control Meeting, Cold Spring Harbor, New York, 2006
- "Identification of Phosphorylated Proteins of Mammalian Mitochondrial Ribosomes." ASMS, San Antonio, Texas, 2005